The Development of Invertebrate Host Models for Burkholderia spp. Infection Studies

Freeman, Zoe

Award date:
2013

Awarding institution:
University of Bath

The Development of Invertebrate Host Models for *Burkholderia* spp. Infection Studies

Zoë Nicole Freeman

A thesis submitted for the degree of Doctor of Philosophy

University of Bath

Department of Biology & Biochemistry

January 2013

Table of Contents

List of Figures

List of Tables

Acknowledgements

Many thanks go to my supervisor Dr Nick Waterfield, always a source of insightful ideas and boundless enthusiasm, and to my co-supervisor Dr Steve Dorus for helpful critique and encouragement since my undergraduate days.

As a newcomer to *Burkholderia* research, my work wouldn't have been possible without collaboration and help from other research groups. Professor Rick Titball's group from the University of Exeter have been invaluable; thanks collectively to Claudia Müller, Sariqa Wagley and Monika Bokori-Brown for all the strains and the advice, for the CL3 work, and to the whole group for adopting me at conferences! Thanks also to Izzy Norville at Dstl who kindly provided a mutant strain and molecular biology advice, and to Jason Kreisberg, Cat Ong and Patrick Tan at the Genome Institute of Singapore for sharing their fosmid-expression experiences with me.

Thank you to Maria Sanchez-Contreras for helping me to find my PhD feet, and to Christophe Fleury for his kind advice and always-interesting perspectives! Thanks go to Isabella Vlisidou for her endless technical knowledge and general wisdom, and to Chris Apark who tirelessly set up thousands of *Manduca* hatchlings for me. I am indebted to Alec Topham for his amazing skills with all things computational and, just as importantly, for always listening. And of course to all my office buddies in 3S 1.11 past and present: Jenny, Ciara, Steph, Freddie, Ruth, Fadaa, Mona and Mark – thank you for all the great times! Big thanks to Mike (especially for the proof-reading), Sara, Santiago and Jerry – muchas gracias for all the much-needed advice and cervecitas!

Finally, thank you to all my family and close friends who have vicariously shared the PhD experience along the way. Last but certainly not least, thanks especially to Chris – for more patience, support and hilarity than I can describe.

"I turned to the teeming small creatures that can be held between the thumb and forefinger: the little things that compose the foundation of our ecosystems; the little things, as I like to say, who run the world" (E.O. Wilson)

Declaration of work done in conjunction with others

The laboratory work described in Chapter 3 under ‘Dose response #3’ was devised and supervised by myself but due to a requirement for Containment Level 3 facilities it was carried out by appropriately trained personnel at the University of Exeter, as described in the corresponding methods section.

Notes on the structure of the thesis

Included in Appendix A is the transcript of a review paper written in the course of these studies and accepted for publication in PLoS Pathogens: "The KdpD/KdpE Two-Component System: Integrating K+ Homeostasis and Virulence". The subject of this review paper is related to the results described in Chapter 5.

Supplementary files are available on the DVD ‘e-Appendix’.

Abstract

Burkholderia pseudomallei (Bp) is the causative agent of melioidosis, an opportunistic but serious human disease endemic to Southeast Asia and Northern Australia. The 'Bp-group' includes Bp and the closely-related organisms *B. thailandensis* (Bt) and *B. oklahomensis* (Bo), all of which are usually soil-dwelling saprophytes, and *B. mallei* (Bm) which is an equine-host-adapted pathogen.

Bt is virulent in a number of invertebrate models but is generally non-pathogenic for mammals and is often used as a surrogate for the study of virulence mechanisms shared with Bp. Experiments to assess the potential of the Tobacco Hawkmoth *Manduca sexta* as a model host for Bp or Bt infection revealed surprising results. Bp, Bt and Bo were all lethal to *M. sexta* larvae. This is the first report of Bo virulence in an infection model. Additionally, the relative virulence of the three species was the reverse of that reported in humans and in larvae of the Greater Waxworm *Galleria mellonella*. Despite that, well-known hallmarks of Bp-group pathogenesis in mammalian hosts – intracellular survival and multiplication, actin remodelling and acute sepsis – were observed in *M. sexta* infection during a fluorescent confocal microscopy time-course study.

M. sexta feeding experiments with Bt and Bo indicated that cultures of these bacteria are also pathogenic via the oral route, which is likely to be relevant for natural insect-bacteria interactions. Cell-free supernatant of Bo was as harmful to larvae as complete culture, supporting previous suggestions that Bp-group bacteria produce toxins or paralytic agents that are active against invertebrates.

Finally, Rapid Virulence Annotation (RVA) was performed as a genome-wide screen for virulence determinants of Bp strain K96423, using three invertebrate bioassays with a recombinant expression library. In response to problems with the reproducibility of biologically active clones, a new statistical approach was devised which enabled quantitative identification of the most convincing RVA hits.

List of Abbreviations

ABC	adenosine tri-phosphate (ATP)-binding cassette
A. polyphaga	*Acanthamoeba polphaga*
aGOT	amoeba Gain of Toxicity
AMP	antimicrobial peptide
Ara+/-	arabinose positive/negative
ATP	adenosine tri-phosphate
Bcc / *B. cepacia* complex	*Burkholderia cepacia* complex
Bm / *B. mallei*	*Burkholderia mallei*
Bo / *B. oklahomensis*	*Burkholderia oklahomensis*
Bp / *B. pseudomallei*	*Burkholderia pseudomallei*
Bt / *B. thailandensis*	*Burkholderia thailandensis*
BLAST	Basic Local Alignment Search Tool
BPF	*Burkholderia pseudomallei* fosmid
BSA	bovine serum albumin
C. elegans	*Caenorhabditis elegans*
CDS	coding sequence
CFU	colony forming unit
CHBP	Cif homologue from *B. pseudomallei*
chr	chromosome
CL2 / CL3	containment level 2/3
CPS	capsular polysaccharide

DAPI	4’,6-diamidino-2-phenylindole
E. coli	*Escherichia coli*
g	gram
GIM	Grace’s insect medium
G. mellonella	*Galleria mellonella*
GFP	green fluorescent protein
GI	genomic island
GO	gene ontology
GOT	Gain of Toxicity
HC / HCs	haemocyte(s)
HK	histidine kinase
hr	hour
hrs_post_inj	hours post-injection
iGOT	insect Gain of Toxicity
KO	knock-out
L	litre
LB	Luria-Bertani
LD50	50% lethal dose
LPS	lipopolysaccharide
M. sexta	*Manduca sexta*
Mb	mega base pair
mg	milligram
mGOT	macrophage Gain of Toxicity
ml	millilitre

MLST	multi-locus sequence typing
MNGC	multi-nucleated giant cells
MTTD	median time to death
NGM	nematode growth media
nGOT	nematode Gain of Toxicity
NRPS	non-ribosomal peptide synthetase
Obs/Exp	observed/expected
OD_{600}	optical density (600nm)
PAMP	pathogen-associated molecular pattern
PAS	Page's amoebal saline
PBS	phosphate buffered saline
PCR	polymerase chain reaction
Pfa	paraformaldehyde
PKS	polyketide synthase
PO	phenoloxidase
PRR	pattern recognition receptor
Ps. syringae	*Pseudomonas syringae*
PYG	peptone-yeast-glucose
RPM	rotations per minute
RR	response regulator
RT-PCR	reverse-transcription polymerase chain reaction
RVA	rapid virulence annotation
SD	standard deviation

S.E./SE	standard error
SSR	simple sequence repeat
STM	signature-tagged mutagenesis
T3SS	type three secretion system
T6SS	type six secretion system
TAT	twin-arginine translocation
TraDIS sequencing	transposon directed insertion-site sequencing
TRITC	tetramethylrhodamine B isothiocyanate
w/v	weight per volume
w/w	weight per weight
µg	microgram
µl	microlitre

Chapter 1. General Introduction

The work described in this thesis investigates the use of invertebrates – amoebae, nematodes and, in particular, insects – as model hosts to study infection with bacterial species from the *Burkholderia* genus. This introductory chapter therefore discusses the *Burkholderia*, invertebrates as infection model hosts and finally background information with particular relevance to each of the three results chapters (Chapters 3-5).

1.1. The *Burkholderia* genus

Bacteria of the genus *Burkholderia* are motile Gram-negative bacilli and are members of the β-proteobacteria. They occupy diverse ecological niches with lifestyles ranging from obligate or opportunistic intracellular pathogens of animals (including humans) to plant-associated pathogens and even symbionts with potential benefits for agriculture and bioremediation (Compant *et al*. 2008).

The genus is best known for the human pathogens *Burkholderia pseudomallei* (Bp) and the *Burkholderia cepacia* complex (Bcc), which are phylogenetically distinct within the *Burkholderia*.

The Bcc group are usually environmental organisms but can cause opportunistic infections. The group is comprised of 17 phenotypically similar bacterial species that can exhibit pathogenic and beneficial effects on plants (Mahenthiralingam *et al*. 2008; Compant *et al*. 2008; Vial *et al*. 2011). In humans they can cause severe lung infections in immunodeficient patients, such as those with cystic fibrosis or chronic granulomatous disease. However, Bcc pathogens have been extensively studied elsewhere (for reviews see Mahenthiralingam *et al*. (2008) and Vial *et al*. (2011)). They do not fall within the scope of this work.

This study stems from interest in *Burkholderia pseudomallei* (Bp), the causative agent of the serious human disease melioidosis. Bp is a containment level 3 pathogen requiring specialist facilities for laboratory work. This study focuses on Bp and its closest relatives; *B. thailandensis* (Bt) is higly relevant for the study of Bp – despite the fact it is non-virulent to humans – because it shares extensive genetic similarity to Bp. It has therefore been used in many studies as a safe surrogate to investigate their shared or divergent biology.

Burkholderia phylogeny

The *Burkholderia* were originally classified as *Pseudomonas* species, as were several other bacterial species which have since been assigned to new genera (Tayeb *et al*. 2008). A phylogenetic analysis which sought to define the relatedness of those species found that based on combining analyses from three genes (16S rRNA, *rpoB and gyrB*) the *Burkholderia* clade was divided into four sub-groups: a group including *B. glathei* and *B. graminis*; the *B. plantarii-B. glumae-B. gladioli* group; the *B. cepacia* complex (Bcc); and the *B. pseudomallei-B. thailandensis* group (Tayeb *et al*. 2008).

Other phylogenetic analyses which include the species *B. mallei* and *B. oklahomensis* also group them into the same branch as Bp and Bt, as shown in Figure 1.1 (Glass, Steigerwalt, *et al*. 2006). In the absence of an established name for this group of four related species they will be referred to in this thesis as the 'Bp-group'.

Figure 1.1 Neighbour-joining phylogenetic tree of *Burkholderia* species. Based on 16S rRNA sequences, the tree shows the relationship between Bp-group species (*B. oklahomensis, B. pseudomallei, B. thailandensis* and *B. mallei*) and other *Burkholderia*. (Scale corresponds to 5% sequence dissimilarity). The abbreviations Bo, Bp, Bt and Bm are also shown. Image reproduced from Glass, Steigerwalt *et al*. (2006).

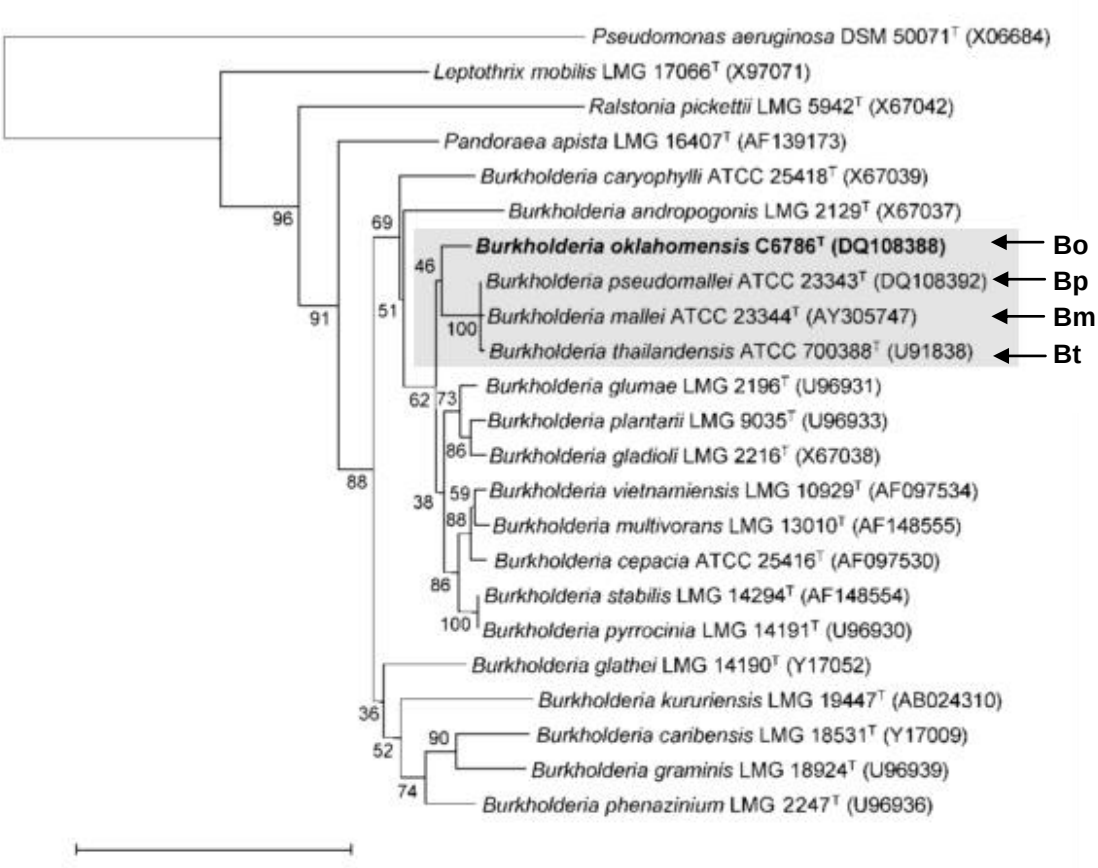

1.1.1. The *B. pseudomallei* (Bp)-group

The four member species of the Bp group show high genetic similarity but can be further divided by differences in lifestyle; *B. mallei* is an obligate intracellular pathogen whereas the three species studied in this thesis – *B. pseudomallei, B. thailandensis* and *B. oklahomensis* – are environmental saprophytes and opportunistic pathogens.

***B. mallei*: an obligate intracellular pathogen**

B. mallei (Bm) is the causative agent of glanders, an equine disease which was first described by Aristotle over 2,000 years ago. Bm is a highly evolved obligate pathogen with a narrow natural reservoir limited to horses, donkeys and mules (Nierman *et al*. 2004). Equine glanders presents as either an acute or chronic disease, with typical symptoms including an infectious and bloody nasal discharge, swelling of the lymph nodes, and ulcerated skin. The glanders infection can be transmitted to humans in contact with infected horses via ingestion or inhalation of infected material, although it is not reported to be transmissible from human-to-human. Bm has historically been used as a biological weapon (Galyov *et al*. 2010). Due to its high infectivity as an aerosol and the fact that glanders is incapacitating and often fatal in humans, it has been classed as a category B agent by the Centers for Disease Control and Prevention (Nierman *et al*. 2004). It was also included in the recently created 'Tier 1' disease agents or toxins considered by the US Federal Select Agent Program to be exceptional threats to security (Butler 2012).

***B. pseudomallei, B. thailandensis* and *B. oklahomensis*: environmental saprophytes**

Bp (previously known as *Pseudomonas pseudomallei*) is the causative agent of melioidosis, a 'glanders-like' disease of humans and other animals which was first described by Alfred Whitmore in Burma in 1911 (Whitmore 1913). Bp is also classed as a category B agent and a Tier 1 agent. *B. thailandensis* (Bt) and *B. oklahomensis* (Bo) were originally classed as non-virulent strains of Bp until they were recognised as separate species in 1998 and 2006 respectively (Brett *et al*. 1998; Glass, Steigerwalt *et al*. 2006). Unlike Bm, these three species are naturally soil-dwelling saprophytes, found in moist tropical soils and still waters such as rice paddies (Allwood *et al*. 2011).

The virulence, phenotypes and genetics of Bp-group species will be discussed further, as will the mechanisms of Bp and Bt pathogenicity as understood so far.

1.1.2. Bp-group species virulence and disease

Bp is well known to cause the potentially fatal human disease melioidosis which affects thousands of people in endemic areas each year, while Bt has been isolated from clinical infections in a small number of cases and Bo has been associated with human infection in just two documented cases.

B. pseudomallei (Bp)-associated disease: melioidosis

Melioidosis, the human disease caused by Bp, is primarily a disease of tropical regions. It is endemic to Southeast (SE) Asia and Northern Australia and is occasionally reported in travellers returning from such areas. The potential that the disease is an emerging global problem has been recognised, with melioidosis being reported in the Indian sub-continent, the Caribbean, and less conclusively in South Africa, the Middle East, and Central and South America (Dance 2000; Cheng *et al*. 2005). In Northeast Thailand, melioidosis accounts for 40% of all deaths from community-acquired septicaemia (Felgner *et al*. 2009). In 1996 it was estimated that 2,000-5,000 patients were presenting with melioidosis in Thailand alone (Dharakul & Songsivilai 1999).

Figure 1.2. Some of the varied clinical features of melioidosis, which often contribute to its misdiagnosis. The disease may be acute (often associated with septicaemia and dissemination to sites such as the lungs, liver or spleen), or chronic (often involving lung disease). Melioidosis can also re-activate many years after apparently successful treatment. Alternatively, exposure may not lead to disease; many children in endemic areas test positive for antibodies to Bp but are asymptomatic. Based upon a diagram from Wiersinga *et al* (2006)

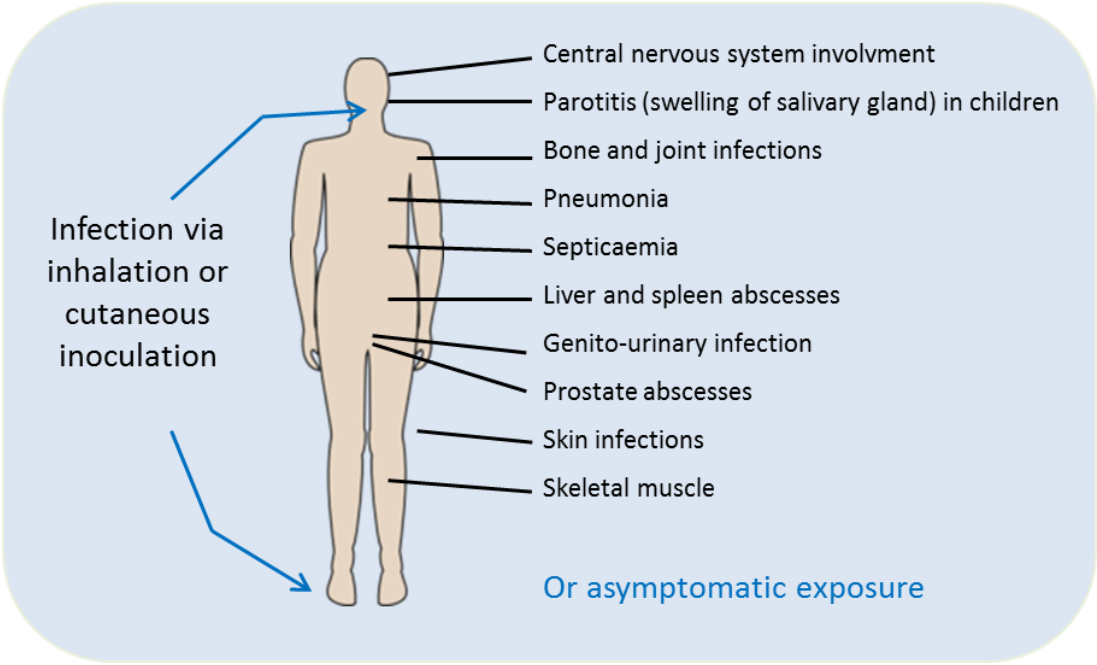

Melioidosis is severe and often fatal and diagnosis is often complicated by a range of different presenting symptoms, as shown in Figure 1.2. So much so in fact, that it has been nick-named ‘The Great Mimicker’. Typically there is septicaemic illness with bacterial

dissemination to distant sites, which might include the lungs, spleen, kidneys or prostate (Holden *et al*. 2004). Other presentations include swelling of the parotid salivary gland (usually in children), soft tissue lesions, infections of the genito-urinary tract, and even involvement of the central nervous system (Wiersinga *et al*. 2006).

Bp infection is opportunistic in nature. Infection is possible through inhalation of Bp-contaminated dust or near-drowning in contaminated water, but the most common route of infection is thought to be through exposure to broken skin (Dance 2000).

In a study in Northeast Thailand, 81% of melioidosis patients were rice farmers or their families (Suputtamongkol *et al*. 1994). Work in rice paddies is thought to pose a high risk of exposure to Bp via contaminated mud and water. In Australia, cases most often occur after heavy rainfall in the wet season. In over 90% of cases studied in Thailand, no specific exposure incident was known (Suputtamongkol *et al*. 1994); the incident may even have occurred years earlier, as another trait of Bp is its ability to remain dormant at unknown sites in the body, becoming reactivated later in life. Asymptomatic exposure to Bp is thought to be common in Thailand, where up to two-thirds of children have antibodies to Bp by the age of fourteen years (Wuthiekanun *et al*. 2006). Disease most often occurs in adults with an underlying immune-suppressing illness, especially diabetes mellitus, chronic renal disease or alcoholism, although the precise nature of the predisposition is still not well understood (Dance 2000). Melioidosis can be cured if treated promptly with antibiotics but due to the variety of symptoms it can elicit it is easily misdiagnosed. Without appropriate antibiotic treatment, mortality from septicaemic melioidosis is close to 90% (Stone 2007). There is currently no vaccine (Cuccui *et al*. 2007).

Bp is also a facultative pathogen of a diverse range of non-human animal species. Just as in humans, the infection can exhibit latency and a wide range of clinical symptoms in many species (Choy *et al*. 2000). Sheep and goats are particularly susceptible. Natural infections also occur in: horses, camels, alpacas, kangaroos, koalas, deer, cats, dogs monkeys, gorillas, dolphins, birds, and reptiles including crocodiles (Lee *et al*. 2010; Choy *et al*. 2000). Interestingly, some species such as rats are only susceptible when immunocompromised (Choy *et al*. 2000). Bovine melioidosis is rare, and porcine melioidosis is often limited to asymptomatic organ abscesses (Choy *et al*. 2000). In experimental infection models, Syrian golden hamsters are exquisitely sensitive to Bp infection (Brett *et al*. 1997). A range of mammalian models of melioidosis have been developed; these are discussed further later in relation to Chapter 3. In laboratory experiments Bp has been shown to be virulent against insects (Schell *et al*. 2008; Fisher *et al*. 2012; Wand *et al*. 2011) and tomato plants *Solanum lycopersicum* (Lee *et al*. 2010).

B. thailandensis (Bt)-associated disease

Bt is usually isolated in Southeast Asia, where a number of mammalian-avirulent 'Bp' strains were later confirmed by 16S sequencing and biochemical tests to be a distinct species (Brett *et al*. 1997; Brett *et al*. 1998; Smith *et al*. 1997). There are also two clinical isolates from the USA and one from a foal in France (Glass, Gee, *et al*. 2006). No strains have yet been isolated from the environment in the USA or France however.

Bt is generally referred to in the literature as avirulent to humans and other mammals. Human clinical isolates of Bt are rare and are usually associated with extreme circumstances – serious injuries that had been heavily contaminated with soil or incidents of near-drowning (Glass, Gee, *et al*. 2006). Bt was cultured from an amputated knee following a motorcycle accident in Thailand which, it is thought, must have been due to a very heavy inoculation from the soil (Lertpatanasuwan *et al*. 1999). There is one other similar report from Thailand. Of the two American clinical isolates, one was associated with a near-drowning incident of a young infant and one from a pleural wound of an elderly man (Glass, Gee, *et al*. 2006). In a study of over 1,000 patients with melioidosis Bt was never isolated (Smith *et al*. 1997); Bt does not cause melioidosis.

Bt exhibits greatly reduced virulence in the hamster model of infection that is so highly sensitive to Bp (Brett *et al*. 1997; Brett *et al*. 1998). In the BALB/c mouse the mean 50% lethal dose of Bt is 10^9 colony-forming units (CFU), versus 182 CFU of Bp (Smith *et al*. 1997). In cell-based assays Bt exhibits cytotoxity to mammalian (HeLa) cells to a greater extent than Bp does (Brett *et al*. 1997). Interestingly, Bt is pathogenic for the tomato plant *Solanum lycopersium* and for *Arabidopsis thaliana*, but not for rice plants (*Japonica nipponbare*) (Lee *et al*. 2010). Yet Bp and Bt are frequently isolated from rice paddies, so this may suggest the bacteria co-exist alongside rice plants in a non-pathogenic relationship. Bt has recently been discovered to be virulent to three insect species: the caterpillar *Galleria mellonella* (Wand *et al*. 2011), the Madagascar Hissing cockroach (Fisher *et al*. 2012), and the fruit fly *Drosophila melanogaster* (Pilátová & Dionne 2012).

B. oklahomensis (Bo)-associated disease

Originally known as the *Pseudomonas pseudomallei* 'Oklahoma strain', Bo C6786 was isolated in 1973 from an infected deep leg wound of a patient after a farming accident in Oklahoma, USA (McCormick *et al*. 1977; Glass, Steigerwalt, *et al*. 2006). The wound had been heavily contaminated with soil. Two environmental isolates matching C6786 were also found at the location. Another clinical isolate (E0147) was recovered in Georgia in 1977 from the wounded eye of a car accident victim, eight weeks after having been thrown into a clay embankment (Nussbaum *et al*. 1980). Both of these cases involved

extensive contamination of wound with soil and no other reports of Bo clinical infections exist. A guinea pig inoculated with Bo C6786 did not show any signs of infection (McCormick *et al*. 1977). The same was true for hamsters and mice inoculated with up to 10^7 CFU of Bo (DeShazer 2007). Therefore Bo has been considered avirulent.

1.1.3. Bp-group phenotypes and genomes

Phenotypes

The member speicies of the Bp-group share similar cellular morphologies and antigenicities (Lertpatanasuwan *et al*. 1999). The colony morphology differs however: on modified Ashdown's selective medium Bp colonies are 'rough and wrinkled with a dark purple pigmentation' and Bt colonies are 'smooth and glossy with a pink pigmentation' (Brett *et al*. 1997). The most reliable biochemical test for differentiation between Bp and Bt is for assimilation of L-arabinose: Bt is capable (Ara^+) whereas Bp is not (Ara^-) (Smith *et al*. 1997). The two species also show broadly different profiles of exoproduct secretion (protease, lipase, lecithinase, and siderophore), although there is also variation within each species (Brett *et al*. 1997). Bo differs from either Bp or Bt in its ability to produce gas from nitrate, although that also varies (Glass, Steigerwalt, *et al*. 2006). PCR-based genetic tests are used to differentiate Bp-group species (Price *et al*. 2012). Multi-locus sequence typing (MLST) shows that the Bo isolates are divergent from Bp (Godoy *et al*. 2003). Phylogenetically Bp, Bm and Bt are very closely related and Bo lies on a separate branch within the Bp-group (Glass, Steigerwalt, *et al*. 2006).

Genomes

Bp genome

The Bp sequence strain K96243 was isolated from a 34 year old female melioidosis patient in Thailand in 1996. The relatively large 7.2Mb genome consists of two circular chromosomes of 4.07Mb and 3.17Mb; chromosome 1 and 2, with 3,460 and 2,395 coding sequences (CDSs), respectively (Holden *et al*. 2004). As genes for central metabolism and essential functions are encoded on both replicons, they are both considered to be true chromosomes. Chromosome 1 encodes a higher proportion of core function CDSs for basic growth and survival whereas chromosome 2 encodes more accessory functions such as for adaptation, osmotic protection, iron acquisition, and secondary metabolism, suggesting it may be primarily responsible for the ability of Bp to survive in different niches. Chromosome 2 also has more CDSs which correspond to unknown "hypothetical" proteins or those with no database matches at all, i.e. there are currently many CDSs with no identified function (Holden *et al*. 2004).

However, a key feature of the Bp genome is that it is highly variable and dynamic (Wiersinga *et al*. 2012). 86% of the K96423 genome is present in all Bp strains but the remaining 14% varies among strain isolates (of which there are more than one hundred, with genome sequence data available for at least 19 strains). Horizontal acquisition of DNA has been intrinsic to the evolution of Bp. Genomic islands (GIs) are regions bearing unusual sequence hallmarks, such as atypical GC content or dinucleotide frequencies, which are likely to have been acquired horizontally. They are often associated with virulence- or survival-related genes (Sim *et al*. 2008). 6.1% of the Bp genome is found within 16 GIs (Nierman *et al*. 2004), and their distribution is highly variable between Bp strains (Holden *et al*. 2004). Bp sampled from different sites within the same melioidosis patient can even show considerable genetic diversity (Price *et al*. 2010).

Sim *et al* (2008) used whole genome microarrays of 94 Southeast Asian Bp strains (clinical, animal, and environmental isolates) to define the common core genome and the variable accessory genome. 86% of the K96243 reference genome was common to all strains tested, and 14% was variably present. The core genome included many genes for basic functions such as amino acid metabolism and contained most of the genes which are conserved among other *Burkholderia* species. Well known virulence determinants from other bacteria such as secretion systems, capsular polysaccharides, adhesins, fimbriae and pili are encoded in the Bp core genome. The accessory genome includes multiple GIs. Interestingly the human clinical isolates of Bp cluster together in a phylogenetic tree based on accessory gene content and were significantly more likely to harbour certain GIs than environmental isolates (Sim *et al*. 2008).

Bp can adapt to survive in diverse niches: soil, water and air, and in plants, mammals, invertebrates, birds and reptiles (Gan *et al*. 2002; Choy *et al*. 2000). In the environment the bacteria face changing biotic and abiotic challenges including temperature, humidity, and UV radiation, limited nutrients, predatory organisms, bacteriocides and phage infection (Sim *et al*. 2008). The large bipartite genome structure of Bp, with variable GIs and a repertoire of genes for diverse functions, is presumed to be what gives it the flexibility to cope with such pressures and to lead a dual existence as a soil coloniser and an effective pathogen of various species (Sim *et al*. 2008). It is thought that the adaptability of Bp is what enables it to cause multiple and variable disease manifestations in melioidosis, as well as chronic disease or relapse many years after treatment (Holden *et al*. 2004).

Bm genome

Bm diverged from a Bp-like ancestor and has undergone genomic deletions and rearrangements resulting in a genome that is 1.31 Mb smaller, lacking 16% of the Bp

chromosome 1 and 31% of chromosome 2 (Nierman *et al*. 2004; Holden *et al*. 2004). These differences are consistent with genome reduction associated with the lifestyle of Bm as an obligate mammalian parasite (Moore *et al*. 2004). The Bm, Bp and Bt genomes contain notably high numbers of simple sequence repeats (SSRs) – over 12,000 in Bm (Nierman *et al*. 2004). SSRs are associated with frameshift mutations and phase variation due to slipped-strand mispairing. SSRs were found in over two-thirds of Bm CDSs and some promoter regions. Examination of SSR loci from surface-expressed and putative virulence genes in Bm and Bp revealed considerable variation both between and within strains, suggesting that phase variation may occur in genes critical for infection (Nierman *et al*. 2004).

Bt genome

The Bt sequence strain E264 is 0.5Mb smaller than Bp K96423, with chromosomes of 3.8Mb and 2.9Mb (Yu *et al*. 2006). Unlike Bm, Bt shows extensive synteny with the gene order of Bp. Genomic comparisons between Bp K96423 and Bt E264 reveal that: Bp (and also Bm) has lost a gene cluster for arabinose assimilation which is suspected to play an anti-virulence regulatory role in Bt (Moore *et al*. 2004); Bt lacks a capsular polysaccharide (CPS) gene cluster which is present in Bp; there are some differences in presence of metabolic gene clusters; and virulence-related genes (especially type 3 secretion systems; T3SSs) are generally the most divergent at the amino acid level (Yu *et al*. 2006). Like Bp, Bt also contains multiple GIs which are variably present across different strains (Yu *et al*. 2006).

Bo genome

The Bo reference strain is C6786. Bo strains C6786 and E0147 have been draft-sequenced and exist as contig assemblies (Mukhopadhyay *et al*. 2010). MLST and 16S gene sequencing have been described (Glass, Steigerwalt, *et al*. 2006; Godoy *et al*. 2003). The relative DNA-DNA binding ratio of Bo C6786 to three other Bo isolates was over 90%, and to Bp ATCC 23343 or Bt E254 was less than 65% (Glass, Steigerwalt, *et al*. 2006). Nucleotide Basic Local Alignment Search Tool (BLASTN) searches of the two Bo strains did not identify loci with similarity to Bp gene clusters for CPS, T3SS-3 (Stevens *et al*. 2002) or type 6 secretion system 5 (T6SS-5) (Shalom *et al*. 2007). No detailed analysis of the Bo genome has yet been published.

1.1.4. The basis of Bp-group pathogenesis

The majority of research into Bp-group pathogenesis has focused on melioidosis, and some has focused primarily on glanders. Some studies have used Bm or Bt to provide insights into Bp pathogenesis. The molecular and cellular basis of Bp pathogenesis in

melioidosis and strategies employed by Bp for intracellular survival have been comprehensively reviewed (Lazar Adler *et al*. 2009; Allwood *et al*. 2011). Another review discusses molecular insights into pathogenesis of both Bp and Bm (Galyov *et al*. 2010). Bp virulence factors will also be discussed further later in relation to Chapter 5.

Bp bacteria possess many virulence factors that are common to other bacterial pathogens (Schell *et al*. 2008) including: three T3SSs (T3SS-1, T3SS-2, T3SS-3 / $T3SS_{Bsa}$) (Stevens *et al*. 2002); six T6SSs (T6SS-1 to T6SS-6); capsular polysaccharide (CPS) (Reckseidler-Zenteno *et al*. 2010); lipopolysaccharide / O-antigen (LPS); flagella (Inglis *et al*. 2003; Chua *et al*. 2003); and type IV pili and adhesins (Essex-Lopresti *et al*. 2005; Balder *et al*. 2010). There is conflicting evidence about the requirement of many of these factors (Allwood *et al*. 2011). Although many virulence factors are involved in Bp infection, there appears to be considerable redundancy as few have been identified as essential. The secretion systems (particularly T3SS-1, T3SS-3, T6SS-1 and T6SS-5) are thought to play critical roles in transporting effector molecules into target host cells (D'Cruze *et al*. 2011; Burtnick *et al*. 2011). A recently identified effector molecule (CHBP; Cif homologue from *B. pseudomallei*) is a potent inhibitor of eukaryotic ubiquitination, which ultimately leads to host cell cycle arrest (Cui *et al*. 2010).

Secreted factors include proteases, haemolysins, lipases, lecithinases, catalases, and phospholipase C (Holden *et al*. 2004; Ashdown & Koehler 1990; Balaji *et al*. 2004; Hautbergue & Wilson 2012). Thermolabile toxins have been detected (Heckly & Nigg 1958) and a lipid toxin complex has been suggested to exist, but not identified (Balaji *et al*. 2004). Recently the first lethal toxin of Bp has been identified and characterised – BLF1 (*Burkholderia* lethal factor 1) is lethal to mice and to macrophage cells (Cruz-Migoni *et al*. 2011; Hautbergue & Wilson 2012). The toxin specifically deamidates a glycine residue of eIF4A (eukaryotic initiation factor 4A), which extensively inhibits protein synthesis in mammalian cells (Hautbergue & Wilson 2012).

Intracellular survival allows bacteria to access nutrients while avoiding the host immune response, and is key to Bp virulence and pathogenicity (Allwood *et al*. 2011). The pattern of Bp pathogenesis, outlined in Figure 1.3, typically involves: bacterial attachment and uptake by phagocytes or invasion into non-phagocytic cells; phagosome vacuolar escape; intracellular survival and replication; and spread to other cells. Attachment to host cells involves pili (PilA) and the adhesins BoaA and BoaB (Essex-Lopresti *et al*. 2005). Entry into host cells includes the type 3 secretion system-3 (T3SS-3) and regulatory proteins IrlR and RpoS. T3SS-3 is also required for escape from endocytic vesicles, via membrane disruption (Allwood *et al*. 2011). Bp survives and replicates in the cytosol of the host cell, which appears to involve biosynthetic pathways for purines (PurM, PurN), histidine (HisF)

and paraminobenzoate (PabB) (Pilatz *et al*. 2006). Bp bacteria also leave the intracellular environment; in clinical and experimental melioidosis there is often a septicaemic infection of the blood in acute cases, or dissemination to other sites in the body in chronic infection.

Figure 1.3. The intracellular infection cycle of *B. pseudomallei*. The bacteria (green): A - adhere to and are phagocytosed by epithelial or phagocytic host cells; B – are internalised in an endocytic/phagosomal vacuole; C – escape from vacuoles into the cytosol where they evade destruction, replicate, and may utilise actin-mediated motility to move within or out of the host cell. D – Cell-cell fusion may occur, forming multi-nucleated giant cells (MNGCs); actin-mediated motility (represented by red filaments) may be involved in but is not essential for inter-cellular spread. Inter-cellular spread allows the bacteria to access more nutrients and to replicate while remaining inside the relatively protected intracellular niche. Finally, bacterial cellular escape follows host cell apoptosis or lysis. [Image based upon part of figure 1 from Allwood *et al* (2011)].

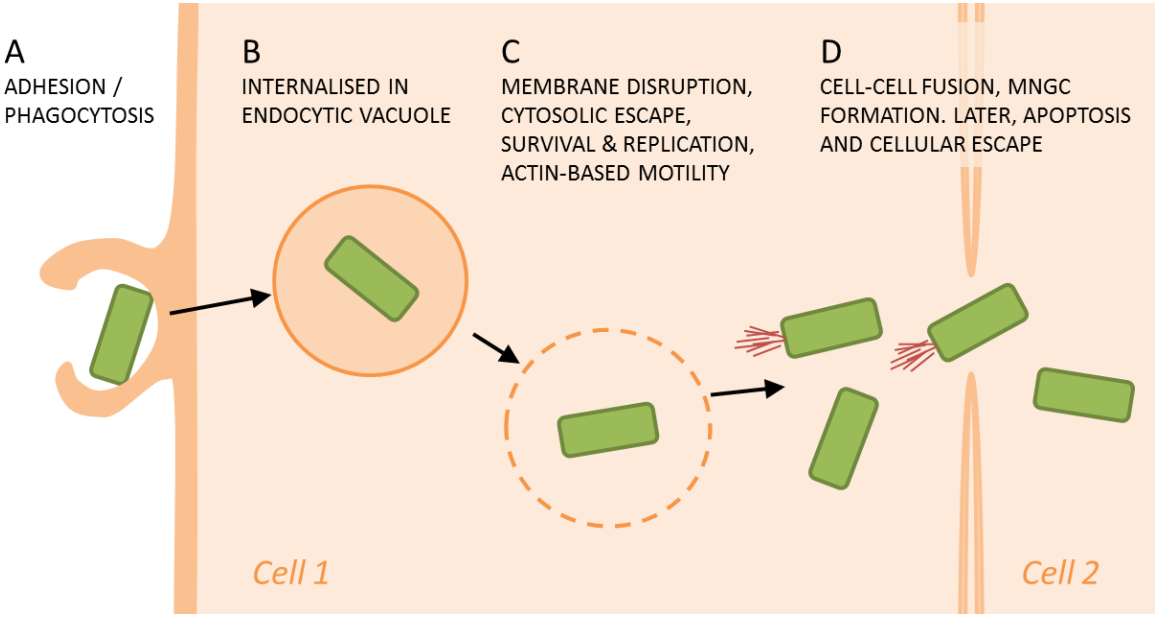

Characteristic hallmarks of Bp pathogenesis are the formation of actin tails for intracellular motility and multi-nucleated giant cells (MNGCs) for intercellular spread; these are discussed further later in relation to Chapter 4. Actin tails were previously thought to be used primarily for cell-to-cell spread of Bp bacteria but cell-to-cell fusion is now considered to be the primary mechanism for intercellular spreading (French *et al*. 2011). Actin-based motility has also been described for other bacteria including *Listeria* and *Shigella* but the activation mechanism of *Burkholderia* actin-based motility is unique (Stevens *et al*. 2006; Allwood *et al*. 2011). The BimA protein is known to be required for formation of actin tails (Stevens *et al*. 2005), and it has been suggested that the remodelling process requires a concerted effort of multiple factors including type 6 secretion system-1 (T6SS-1) (Burtnick *et al*. 2011; Allwood *et al*. 2011). The T6SS-1 protein Hcp1, the sigma factor RpoS, and the T3SS-3 protein BipB all play a role in stimulating fusion with a neighbouring host cell and the subsequent formation of MNGCs.

1.2. Invertebrate models for Bp-group pathogens

The majority of insights into Bp so far have come from clinical cases and mammalian infection models. In addition to mammalian infection models for the study of human pathogens, there are alternative models (also known as complementary, surrogate or mini-host models) (Casadevall 2005). These include invertebrate and plant infection models. They provide insights into comparative host responses, the evolution of pathogenicity, and bacterial virulence. Mechanisms of bacterial virulence and pathogenesis are often conserved across different hosts, so insights from invertebrate model hosts are often relevant to mammalian hosts (Casadevall 2005; Mahajan-Miklos *et al*. 2000). Invertebrate model hosts of microbial pathogens have been used widely since the discovery of an important parallel to mammalian immunity – that the Toll signalling pathway is essential for the *Drosophila melanogaster* (fruit fly) anti-microbial host response (Lemaitre *et al*. 1996).

1.2.1. Benefits of invertebrate infection models

Invertebrate model hosts provide a compelling alternative to mammalian infection models due to a number of advantages (Lionakis 2011). Invertebrates are ethically sound experimental models and an animal license is not required for their use. Under the 3Rs – the Replacement, Refinement and Reduction of 'protected' animals in research – invertebrates are considered a preferable replacement for vertebrates, which are protected under the Animals (Scientific Procedures) Act 1986 (Balls *et al*. 1995). In practical terms invertebrates are simple to work with, economical in terms of resources and space for their breeding or maintenance, and they also have rapid lifecycles compared to mammals. This means they are practical for undertaking high-throughput experiments that may not be feasible in mammalian hosts. As experimental tools many invertebrate host species have well-characterised physiologies and genomes, and relatively well-studied gene expression. Species including the fruit fly *Drosophila melanogaster* and the nematode worm *Caenorhabditis elegans* have tractable genetics and a considerable availability of characterised mutants (Lionakis 2011; Vlisidou *et al*. 2009; Marsh & May 2012). Other popular host models of microbial infection include: the soil-dwelling amoebae *Dictyostelium discoideum* and *Acanthamoeba* species; the greater wax worm *Galleria mellonella*; the tobacco hornworm *Manduca sexta*; the silkworm *Bombyx mori*; and the mosquito *Culex quinquefasciatus* (Lionakis 2011; King & Hillyer 2012; Waterfield *et al*. 2008; Harding *et al*. 2012; Vogel *et al*. 2011).

1.2.2. Basis for using invertebrate models for mammalian pathogens

Importantly, there is also a sound biological basis for the use of invertebrates to investigate pathogens of mammals, owing to commonalities in the innate immune systems and ecological and evolutionary relevance.

Innate immunity similarities

The innate immune response is the primary defence against invading organisms. Invertebrates lack an adaptive immune system in the true sense, but the innate immune systems of invertebrates and mammals share many common features, both mechanistically and genetically (Khush & Bruno Lemaitre 2000; Sadd & Schmid-Hempel 2006).

The innate immune response consists of humoral and cellular elements, which are inter-connected in their activities. In terms of humoral immunity, invertebrates produce a range of antimicrobial peptides (AMPs) which are analogous to vertebrate defensins (Kavanagh & Reeves 2004). Oxidative burst mechanisms and induction of lysozyme are also common to both. The insect phenoloxidase (PO) cascade leads to melanisation – the deposition of melanin to immobilise invading microbes – and it has been likened to the complement cascade of mammals; both are activated by pattern recognition receptors (PRRs) (Kavanagh & Reeves 2004). The cellular immune response includes phagocytosis, the process by which specialised cells engulf and kill invading microbes, which is common to both vertebrates and invertebrates. Mammalian phagocytes include neutrophils and macrophages, and invertebrate phagocytes are known as haemocytes. Haemocytes themselves include multiple sub-types, including plasmatocytes and granulocytes (Strand 2008). The mechanism of phagocytosis is the same in mammals and invertebrates – the phagocyte recognises and immobilises the invading microbe, which is then engulfed and sequestered within a phagosomal vacuole inside the cell. In mammalian macrophages, phago-lysosome fusion leads to increased acidity and a barrage of lytic enzymes and peptides which destroy the trapped microbes; similar effector molecules are found within insect-produced phagosomes (Strand 2008).

Evolutionary and ecological relevance

The evolutionary and ecological relevance relates to the fact that: (i) bacteria-invertebrate interactions are common in most environments (so experimental challenge has a natural basis); (ii) bacteria and invertebrates have co-evolved in a host-pathogen arms race over vast evolutionary timescales; and (iii) the commonalities between mammalian and

invertebrate immune systems means that the mechanisms bacteria have evolved to survive in invertebrates might confer an advantage in mammalian hosts.

Amoebae are essentially free-living phagocytes, engulfing environmental bacteria for nutrition. It has been proposed that environmental bacteriovores may act as training grounds for the evolution of bacterial traits which confer 'accidental' virulence to other hosts (Molmeret *et al*. 2005). For example, *Legionella pneumophila* is able to evade predation by amoebae and to survive in a protected niche within them. It has been discovered that *L. pneumophila* uses similar strategies to subvert amoebae and macrophages, leading to Legionnaire's disease in humans (Swanson & Hammer 2000). Both amoebae and nematodes consume large amounts of bacterial biomass. Insects too are likely to represent a natural environmental host for *Burkholderia* species. The extent to which *Burkholderia* associate with insects in natural environments, or what the typical outcomes of those associations are, has not been studied. The natural ecology of insects which feed on large quantities of plant material (including herbivorous caterpillars like *M. sexta*) means that they are highly likely to ingest environmental bacteria such as *Burkholderia* (Pauchet *et al*. 2010).

1.2.3. Invertebrate studies with members of the Bp-group

Bp-infection (experimental melioidosis) has been modelled in invertebrate hosts to varying extents. Over 60 years ago it was found that fleas and mosquitoes could transfer Bp infection from one guinea pig to another (Blanc & Baltazard 1949). Subsequent investigations of possible vectors of Bp included synanthropic flies (i.e. those that associate with or benefit from humans) in Malaysia (Sulaiman 2000), and two tick species (Kharbov *et al*. 1981). The collected flies were often found to harbour Bp, and after the tick species contracted Bp from infected rabbits the bacterium was culturable from the tick faeces. No further studies of natural Bp transmission vectors *per se* have been reported.

Soil-dwelling organisms potentially represent a vast environmental reservoir of *Burkholderia* bacteria. Therefore numerous studies have looked at Bp in environmental bacteriovores, with the majority of work having been conducted with the *C. elegans* nematode model (Day & Sifri 2012; Inglis *et al*. 2003).

Amoebae

The interaction of Bp with three *Acanthamoeba* species was first described after amoebae were recovered from the vicinity of a melioidosis outbreak in Australia (Inglis *et al*. 1999; Inglis *et al*. 2000). Bp strain NCTC 10276 was co-cultured with the amoebae and bacterial

endocytosis was observed in all three species. Further experiments with *A. astronyxis* (Figure 1.4) showed that Bp cells were adhering by one bacterial pole to the amoeba.

Figure 1.4. *Acanthamoeba astronyxis* amoeba. Confocal laser scanning micrograph from Inglis *et al* (2000), depicting adhesion of polar end of bacillus to *A. astronyxis* surface (white arrow) leading to inclusion in vacuole (white arrowhead).

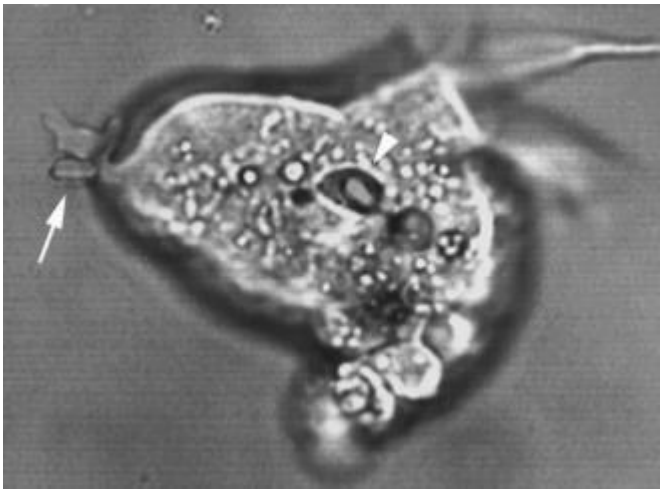

Attached bacteria were observed to rotate for a few seconds before engulfment, in a style of coiling phagocytosis that is also characteristic of *L. pneumophila* entry into either amoebae or macrophages (Bozue & Johnson 1996; Horwitz 1984). Vacuoles packed with bacteria were seen adjacent to or protruding through the external plasma membrane, and some were in the process of releasing bacteria, forming an external tuft of cells. In a few cases, single bacilli moved throughout the amoeba cytoplasm, uncontained by vacuoles. Viable bacteria were recovered from amoebae one hour after endocytosis and motile intracellular bacilli were observed 72 hours after co-culture began (Inglis *et al*. 2000). A subsequent study indicated that the bacterial flagellum was involved in entry of Bp into *A. astronyxis* (Inglis *et al*. 2003). It has been suggested that amoebae might represent a natural reservoir of Bp in the environment (Dance 2000). No investigations testing this theory have yet been published.

A recent study used the social amoeba *Dictyostelium discoideum* in two assays – one quantitative and one high-throughput (Hasselbring *et al*. 2011). The quantitative assay confirmed that levels of wild-type and mutant Bp and Bt resistance to *D. discoideum* predation (and survival within the amoeba) correlated well with results from other host models. 1,500 Bt strain DW503 transposon mutants were screened using the high-throughput assay; 13 genes were identified as involved in resistance to amoeba predation and their orthologues were inactivated in Bp strain DD503. Ten mutants exhibited reduced resistance to predation; these are discussed further in Chapter 5. Of those, several also showed reduced intra-macrophage survival or cytotoxicity and finally tests in a murine model confirmed that some mutants were indeed attenuated for the mammalian host,

particularly the mutants in T3SS and a sensor kinase gene *bpsl0127* (Hasselbring *et al*. 2011).

Nematodes

Burkholderia species known to kill nematodes include multiple strains of Bp, Bt strain E264, and three Bm strains (O'Quinn *et al*. 2001). Over a decade of research into the effects of Bp on *C. elegans* has recently been reviewed (Day & Sifri 2012). Initial studies confirmed that Bp and Bt were pathogenic to the nematode by the feeding route and that locomotion, feeding and egg-laying were affected (O'Quinn *et al*. 2001). An unknown neurotoxin or paralytic agent was hypothesised to have been responsible. Subsequently, it was shown that a 12 hour and 24 hour exposure to Bp killed 55% and 100% of the nematode population respectively, indicating that maximal killing requires prolonged association with the live bacteria (Gan *et al*. 2002). It was suggested that Bp must continuously produce toxins to kill *C. elegans*, as Bp does not accumulate within the gut of wild-type worms (Lee *et al*. 2011; Ooi *et al*. 2012), and filtrate assays caused significantly less nematode mortality than direct killing assays (Lee *et al*. 2011). Figure 1.5 shows *C. elegans* nematodes following feeding on green fluorescent protein (GFP)-expressing Bp cells.

Figure 1.5. *C. elegans* nematodes fed with GFP-expressing Bp, from Lee *et al* (2011). In the top image (wild-type nematode) GFP fluorescence is confined to the anterior gut and is very faint. In the bottom image a grinder-defective mutant nematode is used to demonstrate the level of GFP fluorescence from a fully colonised gut.

The rate of killing was also noted to be strain-specific and dependent on the type of growth media used in co-culture experiments (Lee *et al*. 2011). From the findings of O'Quinn (2001), Gan (2002) and Lee (2011) there is evidence both for and against the existence of a diffusible nematode-toxic factor from Bp. Recently Ooi *et al* (2012) looked at *C. elegans* gene expression during Bp infection. It was found that *pgp-5*, which encodes a toxin-exporting ATP-binding cassette (ABC) transporter, was highly induced in response to Bp exposure; a *pgp-5* RNAi knock-down worm was also more susceptible to

infection (Ooi *et al*. 2012). The available evidence so far supports a theory that Bp killing of *C. elegans* involves both intoxication and unknown active processes which require the presence of live bacteria (O'Quinn *et al*. 2001; Day & Sifri 2012).

Insects

Insect species are often associated with soil and plants and are therefore likely to encounter *Burkholderia* in the environment. Four recent publications describe insect models of Bp-group infection (Schell *et al*. 2008; Fisher *et al*. 2012; Pilátová & Dionne 2012; Wand *et al*. 2011).

Schell *et al* (2008) first infected *G. mellonella* wax moth larvae with Bm, Bp and Bt. They found that Bp and Bm were highly pathogenic for *G. mellonella*: injection of just ten Bp K96423 cells led to over 80% mortality within two days; Bm virulence was lower, with the same dose taking up to six days to kill 90% of larvae. Bt virulence was lower still, with 10^5 cells leading to 35% mortality in seven days, and no further work was conducted with Bt in that study. Both Bp and Bm caused insect paralysis around 12 hours prior to death, from which point the bacteria multiplied in number in the insect haemocoel by two logs, although there was no speculation as to whether this was due to intra- or extracellular replication. Four Bm mutants which are attenuated in mammalian models showed corresponding levels of attenuation in *G. mellonella*: a T3SS cluster mutant, a CPS mutant, a type II secretion mutant and an auxotrophic mutant (Schell *et al*. 2008). *In silico* genomic subtraction generated a set of 650 genes present in Bm ATCC 23344 and Bp, but absent from related non-pathogenic species (four environmental *Burkholderia* and one *Ralstonia* species). 70% of the virulome genes were also noted to be present in Bt. Inactivation of some of these 'Bm-Bp virulome' genes was followed by testing in *G. mellonella* infection assays. The most dramatic attenuation of Bm virulence was with a mutant of an AraC-type transcriptional regulator predicted to regulate a T6SS. Other attenuating mutants were in genes related to a putative insect-pathogenic toxin or secondary metabolite (with similarity to a *Photorhabdus luminescens* gene cluster), and a putative polyketide synthase (PKS).

Wand *et al* (2011) reported that a macrophage cell culture model and the *G. mellonella* insect model both reflect the relative virulence levels of Bp, Bt and Bo strains as observed in murine models. These are the only published results of Bo infection in insects so far, and the conclusion was that Bo strains were the least virulent *Burkholderia* tested. The researchers challenged *G. mellonella* larvae with 100 CFU of bacteria and recorded survival at 24 hours post-challenge. Strain-dependent differences were evident; Bp K96423 and Bp 576 caused 100% mortality but Bp 708a caused no deaths. Bo C6786 and Bo E0147 also caused no deaths. The American Bt strains CDC 272 and CDC 301

caused 100% mortality, the sequence strain E264 caused 50% mortality, and the Phuket strain caused 80% mortality. The number of bacteria in the haemocoel of some insects was enumerated at 20 hours post-challenge; bacterial numbers had increased since injection for all strains tested, although Bp 708a, Bt E264 and the Bo strains showed less of an increase relative to the others. Heat-killing rendered virulent Bt strains avirulent. At a challenge dose of 10^5 CFU Bo C6786 did cause 100% mortality within 24 hours, but Bo E0147 still did not (Wand *et al*. 2011).

A Madagascar hissing cockroach (*Gromphadorhina laevigata*) infection model was recently used to test Bp, Bm and Bt (Fisher *et al*. 2012). The cockroaches were highly susceptible to all three species; all exhibited a 50% lethal dose (LD_{50}) of less than 10 CFU per insect. This matches the Bp K96423 LD_{50} in the hamster model (Burtnick *et al*. 2011). Although the LD_{50} values were the same, Bm killed more slowly than either Bp or Bt, which is also the case in rodents (Galyov *et al*. 2010) and likely reflects the extent of Bm adaptation to the equine host. T6SS-1 (*Δhcp1*) mutants were attenuated in all three species, which is consistent with findings from mammalian models (Burtnick *et al*. 2011; Fisher *et al*. 2012). As insects lack adaptive immunity this result may indicate that the T6SS-1 plays a role in evading the innate immune response. Haemocytes sampled from Bp-infected cockroaches 48 hours post-infection contained numerous intracellular bacteria, indicating that Bp replicates within insect phagocytes. Some haemocytes had actually fused to form MNGCs; this is the first report of MNGC formation in a whole-organism animal model, and means that infected haemocytes can fuse in the insect's haemolymph (Fisher *et al*. 2012).

The fruit fly *D. melogaster* has also been tested as a model host for Bt (Pilátová & Dionne 2012). Bt E264 was highly virulent to *D. melanogaster* either by injection or by feeding; indeed this represents the first report of feeding Bp-group pathogens to an insect host. The study looked at fly survival and bacterial burden post-injection. 100% of flies injected with approximately 250 CFU died within 3.5 days post injection. Heat-killed bacteria did not cause any deaths. Bacterial burden in the fly rose slowly from 0-6 hours and then rapidly from 6-12 hours post-injection. Sterile Bt-conditioned medium was also lethal by injection, unless it was heat-treated, indicating that Bt secretes an exotoxin with activity against insects. Bt cells washed free of the conditioned medium were also lethal however. Bt mutants in T3SS-3 and T6SS-5, which are attenuated in murine models, did not show significantly different virulence compared to wild-type Bt in the fly model (Pilátová & Dionne 2012). After transfer onto Bt-laced food, at 24 hours the flies were apparently healthy but by 48 hours there was 50% mortality. Survivors at 48 hours which were transferred to control food still later died from the infection. Flies fed green fluorescent protein (GFP)-labelled Bt were dissected and imaged, and were observed to have

distended gut crops full of bacteria. Bacteria were not detected outside the gut (Pilátová & Dionne 2012).

qRT-PCR was performed to analyse expression of host antimicrobial peptides (AMPs) (Pilátová & Dionne 2012). During the Bt infection all six of the tested AMPS were strongly induced. In addition, a rhodamine-based probe for phagocytosis was used and confirmed that haemocyte function was apparently normal at approximately 24 hours prior to fly death. Pilátová *et al* also reported a temperature effect on Bt infection in the fly, whereby median fly survival time increased from 2 days when maintained at 25°C to 20 days at 18°C. At the lower temperature the bacterial numbers increased only slowly but shifting the temperature to 25°C caused host death within one or two days.

1.3. Background to specific chapters of this study

Invertebrate models including amoebae, nematodes and insects have been invaluable in the study of numerous bacterial pathogens. The *Manduca sexta* larva in particular is a well-characterised insect host which offers some beneficial differences compared to other invertebrate models of infection. Until recently there was negligible published evidence regarding the virulence of Bp-group pathogens in invertebrates; the publications discussed over the previous pages demonstrate a growing recognition of the potential value of these hosts for *Burkholderia* research.

The aims of Chapter 3 were to confirm (or otherwise) the reported insect-virulence of Bt using the *M. sexta* host, and to place it in context by also comparing the virulence of Bp and Bo in *M. sexta*.

The aim of Chapter 4 was to take advantage of the ease with which insect blood (haemolymph) samples can be collected from *M. sexta* to perform a time-course analysis of Bt infection *in vivo*. This would illuminate the progression of *Burkholderia* infection and help to characterise the *M. sexta* infection model, with a view to further development.

Finally the aim of Chapter 5 was to screen a genome-wide Bp recombinant library against three invertebrate models (amoebae, nematodes and insects) in order to identify genomic regions containing putative virulence factors. This Rapid Virulence Annotation technique would allow the investigation of Bp virulence: (i) using an assumption-free approach; (ii) at containment level 2; and (iii) in practical, accessible and ethically sound host species. Putative virulence-related loci would then be confirmed and characterised further.

1.3.1. Chapter 3 - *Burkholderia* infection assays in *Manduca sexta*

Host models of infection are an invaluable tool for the study of bacterial pathogens. Infection in a good model host mirrors that seen in the host of interest (e.g. humans) in terms of the level of virulence, the mechanisms of pathogenesis, and/or the similar attenuating effects of mutations in key genes. Therefore they provide a safe and suitable way to evaluate virulence of related species, potential attenuating mutations, or the protective effects of vaccine candidates.

Model hosts of Burkholderia

Mammalian models

As discussed in the general introduction, Bp presents a considerable threat to human health. Several studies have used animal (mostly mammalian) infection models for Bp with a view to investigating melioidosis. Some data has come from guinea pig and goat models (Miller *et al*. 1948; Narita *et al*. 1982; Soffler *et al*. 2012), and recently a non-human primate model of acute melioidosis via inhalational infection has been developed using the marmoset, *Callithrix jacchus* (Nelson *et al*. 2011). However by far the most-established Bp models are mice, Syrian hamsters and infant diabetic rats, with the majority of recent work using BALB/c and C57BL6 mouse strains (Titball *et al*. 2008). Healthy rats are resistant to Bp infection but infant diabetic rats are susceptible, which mirrors the occurrence of human melioidosis, for which diabetes and other immune-compromising conditions are a pre-disposing factor (Wiersinga *et al*. 2012). Bt and Bo infection have also been tested in the mouse and hamster models (DeShazer 2007). However, there is a high level of variability in the results from those three small mammal models: the susceptibility to infection and the pathogenesis of disease can vary greatly depending on the model used. Even within the same model, the route of infection, the dose, and the particular strain of *Burkholderia* can lead to varied results (Titball *et al*. 2008). For example some Bp mutant strains that are attenuated in mice are fully virulent in the hamster model, indicating an unknown difference in the host-pathogen interaction between the two hosts (Chua *et al*. 2003; Titball *et al*. 2008). Certain characteristics in each model reflect particular aspects of human melioidosis, but it is not certain whether which (if any) of them reflects the human disease best. As such, the current thinking is that the best approach may be to use multiple different animals to model different aspects of melioidosis (Titball *et al*. 2008). Therefore there is still a need to investigate and characterise novel models of *Burkholderia* infection. Table 1.1 indicates the virulence of Bp-group pathogens in human clinical cases and in various experimental mammalian hosts.

Table 1.1 Virulence of *Burkholderia* species in human clinical cases and experimental mammalian models. Cell colour denotes virulence (red), attenuation or contrasting results (orange), reported avirulence (green), or no data (blank). Table continued overleaf.

		Bp	**Bm**	**Bt**	**Bo**
Human		Virulent: Environmental, can infect humans (usually immuno-compromised, e.g. diabetic). Mortality rate 40% in Thailand, 14% in Australia (Wiersinga *et al*. 2012)	Virulent: persists in equine hosts but can pass to humans. 50% mortality rate with antibiotic therapy (Balder *et al*. 2010)	Generally avirulent: Environmental, some clinical isolates from soil-contaminated wounds, one from near-drowning (Glass, Gee, *et al*. 2006)	Generally avirulent: Environmental, two clinical isolates from soil-contaminated wounds (Glass, Steigerwalt, *et al*. 2006)
Mouse	**BALB/c**	Virulent: Intraperitoneal median lethal doses (MLD) 14 - 5750 CFU. Intranasal MLD 5-20 CFU. Model for acute melioidosis (Titball *et al*. 2008; Smith *et al*. 1997)	Virulent (Fritz *et al*. 2000; Lever *et al*. 2003; DeShazer *et al*. 2001)	Highly attenuated or avirulent: intraperitoneal MLD >10^7 CFU. Intranasal MLD >10^4 CFU. Bt CDC 272 avirulent (Titball *et al*. 2008; DeShazer 2007)	Avirulent: intraperitoneal MLD >10^7 CFU (DeShazer 2007)
	C57BL6	Virulent: host is much more resistant than BALB/c mice (intraperitoneal). Used to model chronic melioidosis (Titball *et al*. 2008; Ulett *et al*. 2005; Leakey *et al*. 1998; Conejero *et al*. 2011)			
Rat		Virulent: by intra-tracheal route. Only infant diabetic rats susceptible intra-peritoneally (Van Schaik *et al*. 2008; DeShazer 2007; Woods *et al*. 1993; Brett & Woods 1996)	Avirulent (Fritz *et al*. 2000)		
Hamster		Virulent: host is highly susceptible. Used to model acute melioidosis (DeShazer 2007; Warawa & Woods 2005; Tuanyok *et al*. 2006)	Virulent (Galyov *et al*. 2010; Fritz *et al*. 1999; Ulrich & Deshazer 2004; DeShazer *et al*. 2001)	Most strains virulent at >10^5 CFU. Bt CDC 272 avirulent (Brett *et al*. 1997; DeShazer 2007)	Avirulent (no data presented) (DeShazer 2007)
Guinea pig		Virulent: Used for many early experiments to characterise Bp (Miller *et al*. 1948; Whitmore 1913)	Virulent: Used for many early experiments to characterise Bm. Variable host susceptibility (Miller *et al*. 1948; Whitmore 1913; Fritz *et al*. 2000)		Avirulent (no data presented) (DeShazer 2007)

		Bp	Bm	Bt	Bo
Horse			Virulent (Lopez *et al*. 2003)		
Pig		Virulent at very high dosage, causing chronic infection (Najdenski *et al*. 2004)			
Goat		Virulent: model not used since 1982 (Narita *et al*. 1982)			
Non-human primates	**Rhesus macaque**	Virulent (Yeager *et al*. 2012; W. R. Miller *et al*. 1948)			
	African Green Monkey	Virulent (Yeager *et al*. 2012)			
	Hamadryas baboon	Virulent (Manzeniuk *et al*. 1999)			
	Gorilla	Virulent: host is highly susceptible (Yap *et al*. 1995)			

Invertebrate models

Invertebrate models of Bp and Bt have increasingly been developed and adopted, particularly within the last two years (Schell *et al*. 2008; Wand *et al*. 2011; Hasselbring *et al*. 2011; Ooi *et al*. 2012; Fisher *et al*. 2012; O'Quinn *et al*. 2001; Gan *et al*. 2002; Pilátová & Dionne 2012). Table 10 indicates the virulence of Bp-group pathogens in various experimental non-mammalian hosts. Amoebae including several *Acanthamoeba* species and the social amoeba *Dictyostelium discoideum* are susceptible to infection and intracellular replication by Bp (Inglis *et al*. 2000; Hasselbring *et al*. 2011). Similarly, the nematode *C. elegans* is susceptible to *Burkholderia* species including Bp, Bt, and Bm (O'Quinn *et al*. 2001). Some studies have probed the mechanisms by which Bp causes pathogenesis in the nematode (Ooi *et al*. 2012; Lee *et al*. 2011; O'Quinn *et al*. 2001; Gan *et al*. 2002).

Insect species from the lepidopteran, coleopteran and dipteran orders are also susceptible to infection following injection with *Burkholderia*. Bp has been shown to be virulent in the wax worm (the larva of *Galleria mellonella*) and the Madagascar hissing cockroach *Gromphadorhina laevigata* (Schell *et al*. 2008; Wand *et al*. 2011). Bt was also tested and exhibited virulence in those models, as well as in the fruit fly *Drosophila melanogaster* (Pilátová & Dionne 2012). Bm is also virulent in *G. mellonella* and in the cockroach (Wand *et al*. 2011; Fisher *et al*. 2012). Bo has only been tested for insect virulence in *G. mellonella*, and was not found to be virulent (Wand *et al*. 2011).

To date, the most widely used *Burkholderia* insect model has been the *G. mellonella* larva. As discussed in the main introduction, there are numerous reasons to support the use of insect models as a proxy for or in addition to mammalian infection models. These include mechanistic and genetic similarities in the insect and mammalian innate immune systems, and practical issues including reduced regulatory restrictions. In addition, there are fewer ethical issues surrounding the use of invertebrates and indeed their use represents a step towards the replacement, refinement and reduction (3Rs) of 'protected' animals in research (Balls *et al*. 1995). Table 1.2 indicates the virulence of Bp-group pathogens in various experimental non-mammalian hosts.

Table 1.2. Virulence of *Burkholderia* species in experimental non-mammalian models. Cell colour denotes virulence (red), attenuation or contrasting results (orange), avirulence (green), or no data (blank). Purple cells denote possible symbiosis or vector relationships. Table continued overleaf.

			Bp	**Bm**	**Bt**	**Bo**
Invertebrates	**Amoeba**	***Acanthamoeba* spp.**	A possible symbiotic relationship with limited damage to host or Bp (Inglis *et al*. 2000)			
		Dictyostelium discoideum	Resistant to predation, able to survive intracellularly (Hasselbring *et al*. 2011)	Resistant to predation, able to survive intracellularly (Hasselbring *et al*. 2011)		
	Nematode	***C. elegans***	Virulent (Ooi *et al*. 2012; Lee *et al*. 2011; Gan *et al*. 2002; O'Quinn *et al*. 2001)	Conflicting reports: virulent (Gan *et al*. 2002), avirulent (O'Quinn *et al*. 2001)	Virulent (Gan *et al*. 2002; O'Quinn *et al*. 2001)	
	Insect	**Fruit fly**			Virulent (Pilátová & Dionne 2012)	
		***G. mellonella* wax worm**	Virulent: except strain 708a (Schell *et al*. 2008; Wand *et al*. 2011)	Virulent (Schell *et al*. 2008)	Virulent: but attenuated compared to Bp. ~35% killed by >10^5 CFU (Schell *et al*. 2008; Wand *et al*. 2011)	Attenuated compared to Bt (Wand *et al*. 2011)
		Cockroach	Virulent: 50% lethal dose (LD50) <10 CFU (Fisher *et al*. 2012)	Virulent: LD50 <10 CFU. Killed more slowly than Bp or Bt (Fisher *et al*. 2012)	Virulent: LD50 <10 CFU (Fisher *et al*. 2012)	
		Flea	Virulence unknown: but able to transmit Bp to guinea pigs (Blanc & Baltazard 1949)			
		Mosquito	Virulence unknown: but able to transmit Bp to guinea pigs (Blanc & Baltazard 1949)			

			Bp	Bm	Bt	Bo
	Arachnid	**Tick**	Virulence unknown: but able to contract Bp from infected rabbits (Kharbov *et al*. 1981)			
Plants and Fungi	**Plants**	**Tomato plant**	Virulent (Lee *et al*. 2010)		Virulent (Lee *et al*. 2010)	
		Rice	Avirulent (Lee *et al*. 2010)		Avirulent (Lee *et al*. 2010)	
		A. thaliana	Avirulent (Lee *et al*. 2010)		Avirulent (Lee *et al*. 2010)	
	Fungal spores	***G. decipiens***	Virulence unknown: colonises germinating spores (A. Levy *et al*. 2003)			

Rationale behind Manduca sexta as a potential model host for Burkholderia

A substantial body of work has successfully used lepidopteran larvae to model bacterial infections, and the lepidopteran immune system has been studied for over 50 years now (Stephens 1962). As discussed in the main introduction, data from these models cover all aspects of their biology including the host-pathogen response. This considerable existing knowledge complements the practical advantages offered by these hosts.

Ecological relevance

As *Burkholderia* are environmental bacteria occupying a range of habitats and lifestyles, there are also interesting evolutionary and ecological reasons to investigate the outcomes of their interactions with invertebrates, as discussed in the main introduction. *Burkholderia* are well known for their close associations with plants, as are invertebrates. Studies have revealed that Bp uses flagellum-mediated phagocytosis to enter amoebae (Inglis *et al*. 2003), that Bp and Bt kill *C. elegans* probably via a combination of toxin release and active mechanisms (Day & Sifri 2012), and that Bp-group pathogens are virulent in several insect species (Fisher *et al*. 2012; Wand *et al*. 2011; Schell *et al*. 2008; Pilátová & Dionne 2012).

Advantages over the *Galleria mellonella* infection model

Despite the relatively wide use of the *G. mellonella* lepidopteran model, the *Manduca sexta* model offers some significant advantages. For a start, *M. sexta* is more physiologically tractable due to its larger overall size, numerous haemocytes, and greater volume of haemolymph. With last instar *M. sexta* larvae reaching weights of 10-12 g, haemolymph volumes up to or in excess of 1 ml can be collected from each larva, containing approximately one million haemocytes (Kanost *et al*. 2004). *G. mellonella* last instar larvae, by comparison, weigh around 250 mg and yield correspondingly lower blood volumes (Ramarao *et al*. 2012). Bacteria-infected *M. sexta* larvae often survive for longer than *G. mellonella* equivalents. Unpublished results (Waterfield lab) suggest that differences in virulence between various *Bacillus cereus* strains and also of different *Staphylococcus aureus* mutants can be masked in *G. mellonella* due to rapid “septicaemia” infection dynamics. These differences become apparent when using the larger and more resilient *M. sexta* host to compare the same strains. The slower infection kinetic probably reflects the larger size of the organism and its corresponding availability of resources. There could also be important differences between the immune systems of the two lepidopteran hosts which are as yet unknown.

It should be noted that *G. mellonella* larvae are usually purchased from external suppliers (for fishing bait or reptile food) and as such their growth conditions and health are

unknown and cannot be controlled by the researcher. Conversely, at Bath a staged *M. sexta* colony is maintained in-house under tightly-controlled environmental and hygiene conditions. Light, heat and humidity are regulated, as is the artificial *Manduca* diet which is supplemented with antibiotics and formaldehyde to prevent unwanted microbial contamination of the colony. The *M. sexta* are monitored daily as they develop from hatchlings (neonates) through to later larval instars and finally pupae and moths. The ability to produce experimental cohorts all of the exactly the same age and developmental stage is also a distinct advantage for infection and immunity studies. Furthermore this colony has been in-bred and maintained since 1981 which means the individuals will be genetically highly homogenous.

Another consideration is that *G. mellonella* are supplied at the wanderer stage of development, i.e. after they cease feeding. While that is convenient for short-term storage of the insects, a disadvantage is that in order to infect these larvae orally they must be force-fed – a process which is anecdotally unreliable. *M. sexta* larvae can be easily used for feeding assays by simply lacing the normal diet with bacteria or toxin samples. Young neonate stage larvae are thought to be best suited to use in feeding assays as even potent *Photorhabdus* insecticidal toxins exhibit little or no oral toxicity in older (e.g. fifth instar) larvae (Waterfield *et al*. 2001; Waterfield *et al*. 2005). This presumably relates to the immaturity of the neonate gut compared to later developmental stages, by which time the gut has become a frontline for antimicrobial defence (Pauchet *et al*. 2010).

Finally, while a *G. mellonella* transcriptome has recently been published (Vogel *et al*. 2011), there is currently a greater availability of research tools for *M. sexta*. These include transcriptomes relating to immunity (Zou *et al*. 2008), the antennae (Grosse-Wilde *et al*. 2011), and the larval midgut which is critical for detoxification and defence mechanisms (Pauchet *et al*. 2010). There is a complete sequenced mitochondrial genome (Cameron & Whiting 2008). The genome of *M. sexta* itself has been fully sequenced by the Tobacco Hornworm Genome Project (https://www.hgsc.bcm.edu/content/tobacco-hornworm-genome-project), available at: http://www.ncbi.nlm.nih.gov/assembly/382238/.

Further background to Chapter 3

To test the validity of the *M. sexta* model for *Burkholderia* infection, several strains were tested by injection and by feeding to larvae.

Assessing *Burkholderia* virulence in *Manduca sexta*

Bt E264 is the fully sequenced Bt type strain and was originally an environmental isolate (Brett *et al*. 1998). Bp K96423 is fully sequenced and is among the most studied of the Bp strains. It was a clinical isolate from Thailand (Holden *et al*. 2004). The Bt strains CDC

2721121 and CDC 3015869 (abbreviated elsewhere to CDC 272 and CDC 301) are atypical Bt strains in several regards (Glass, Gee, *et al*. 2006).

Bt is usually described as avirulent in humans but CDC 272 and CDC 301 are rare clinical isolates from humans. Both were also isolated in the USA, whereas most Bt strains are isolated in Southeast Asia or Northern Australia. Bt CDC 301 is considered the most convincing case for human infection with Bt, isolated from an infant after a near-drowning incident. Bt CDC 272 was isolated from a pleural wound in an elderly man. Interestingly, a genomic approach using either multi-locus sequence typing (MLST) or array-based comparative genomic hybridisation (aCGH) clusters both these strains into a phylogenetic sub-group distinct from the ancestral Bt population. Although the two are phylogenetically very closely related, Bt CDC 301 encodes and expresses a Bp-like capsular polysaccharide (CPS) gene cluster which is absent from almost all characterised Bt strains including CDC 272 (Sim *et al*. 2010). One other strain in the Bt outlier group, Bt E555, also possesses this 'Bp-likeCPS' gene cluster. Experimental evidence from Bt E555 with and without deletion of the Bp-likeCPS cluster indicated that the CPS is required for intracellular survival in RAW macrophages (Sim *et al*. 2010). This importance has not borne out in mammalian models though; relative to Bt E264, Bp-likeCPS strains did not display greater virulence in mouse or hamster models (Sim *et al*. 2010). In *C. elegans* Bt E555 was slower to kill than E264 was, but a CPS KO E555 strain was further attenuated, suggesting that the CPS cluster is somehow involved in nematode killing. It has therefore been proposed that the acquisition of the Bp-likeCPS by Bt strains may have conferred a selective advantage not in terms of mammalian infection but in terms of surviving environmental challenges (Sim *et al*. 2010).

Bo was discovered following isolation from human clinical infections yet, like Bt, Bo is usually described as avirulent to humans and other tested mammals. Only two strains exist – Bo C6786 and Bo E0147 – which were both recovered from severe injuries that were extensively contaminated with soil (Glass, Steigerwalt, *et al*. 2006; McCormick *et al*. 1977; Nussbaum *et al*. 1980).

Testing attenuated Bt mutants in *Manduca sexta*

Mutant Bt strains which have been demonstrated to be attenuated in other infection models can also be compared in the *M. sexta* model in order to confirm whether it shows the same attenuation effect. Two mutant strains were available: a *surA* mutant and a Twin-Arginine Transport (TAT) system mutant.

In *E. coli* the SurA protein is a well characterised parvulin; that is, it exhibits peptidyl-prolyl isomerase (PPIase) activity (which catalyses the isomerisation of proline peptide bonds) and it is also a chaperone protein, aiding the correct folding and assembly of outer

membrane proteins such as OmpA (www.uniprot.org). It is also required for pilus construction (Watts & Hunstad 2008). SurA has recently also been implicated in the virulence of *E. coli*, *Salmonella* and *Shigella* species (Behrens-Kneip 2010). Homologues were identified in Bp K96423 and Bt E264 (Norville 2011). A non-polar deletion mutant of the Bt E264 *surA* gene (Bt Δ*surA*) resulted in attenuated virulence in the *G. mellonella* model; challenge of 10^2 or 10^3 CFU resulted in a significantly increased time to death compared to wild-type (Norville 2011). Cell line assays with J774.A macrophages and A549 epithelial cells also showed significantly reduced intracellular growth at 24 hours post-infection. The reduction in virulence is believed to be due to pleiotropic effects on the outer membrane, reducing overall fitness and virulence under certain stresses (I. Norville, unpublished).

The TAT pathway enables the transport of fully folded proteins across membranes. In bacteria TAT systems are prevalent in the cytoplasmic membrane and many proteins transported by them are involved in important homeostasis and pathogenesis functions (Sargent 2007; Stevenson *et al*. 2007). In Bp, factors transported via the TAT system include the haemolytic virulence factor phospholipase C. The enzyme is transported via TAT into the periplasm ready for export out of the cell via the type II secretion system (Vasil *et al*. 2012). A conditional mutant of the Bt E264 TAT system (Bt *prhA:tatA)* was reported to show attenuation in *G. mellonella* (S. Wagley, unpublished). In this conditional mutant the TAT system is under the control of a rhamnose-inducible promoter: when grown in the presence of rhamnose the system is active; when rhamnose is substituted with glucose the system is inactivated. It can therefore be used as an experimental tool.

Feeding *Burkholderia* to *Manduca sexta*

Finally, the effect of *Burkholderia* infection via the digestive route can be investigated, taking advantage of the ability to feed *M. sexta*. Until very recently the *Burkholderia* invertebrate infection models all used direct injection as the infection route. However, the most common natural route of *Burkholderia* infection is more likely to be via the digestive tract following ingestion of contaminated plants or detritus. Therefore it was of interest to investigate the effect of feeding Bt and Bo strains to *M. sexta* larvae. At the time that this work was conducted no results had been published regarding the effects of infecting insects with *Burkholderia* via the oral route. Very recently, a *Drosophila melanogaster* model has been used for this purpose (Pilátová & Dionne 2012) and the results will be compared in the discussion.

1.3.2. Chapter 4 - *In vivo* time-course of *Burkholderia* insect infection and pathogenesis

Dose response virulence assays indicate which strains are more virulent relative to others in terms of how quickly (or whether) morbidity or mortality occurs, as judged by external signs. For more insight into mechanisms of bacterial pathogenesis, two types of experimental systems are typically used: *in vitro* cell culture models and *in vivo* infection of whole organisms.

Monolayer cell cultures provide many useful insights, with fewer additional variables complicating the interpretation of results. Most discoveries regarding the cellular and molecular pathogenesis of Bp have come from such models, particularly RAW 264.7 cells (mouse leukaemic monocyte macrophages) or J774A.1 cells (BALB/c mouse monocyte macrophages). However, homogeneous cell culture models cannot reflect the full complexity of *in vivo* infection. The complete effects of the immune response and inter-linked pathways are lost. Therefore whole organism models are an invaluable supplement to cell culture models, and *vice versa*.

In whole-organism models, samples may be taken for analysis during the infection (e.g. blood samples) or *post-mortem* (e.g. dissection and examination of organs). Examining the location and number of bacteria, pathological effects on cells and tissues, or gene expression from bacteria or host all help to complete the picture of pathogenesis. For instance, as already discussed, *Burkholderia* pathogenesis hallmarks can include actin-remodelling, multi-nucleated giant cell (MNGC) formation, and apoptosis of host cells. With cellular labelling or staining, these physical hallmarks are visible under the microscope.

Case study: a murine Bp infection time-course

Despite growing knowledge regarding Bp pathogenicity at the molecular level, it has been noted that there still remains a paucity of information about how Bp actually interacts with a host to elicit melioidosis symptoms (Chin *et al*. 2010). To address this need Chin *et al* examined the status of bacterial load and host leukocytes at time-points during a BALB/c mouse model of acute melioidosis. Parallel host gene expression profiling revealed that a range of innate immune mechanisms were activated within 24 hours of infection. At 16, 24 and 42 hours after infection with Bp D286 ($1.1x10^3$ CFU) the bacterial load was evaluated in the spleen and liver, both of which contained increasingly high numbers of Bp (10^3-10^5 CFU/organ). Viable Bp cells were also detected in the blood (10^2-10^3 CFU/ml), indicating acute septicaemic melioidosis. Changes in the proportions of different types of leukocytes were observed, with the ratio of neutrophils to lymphocytes increasing throughout the

infection. The increase in number of neutrophils indicated the involvement of the innate immune response (Chin *et al*. 2010).

Case study: Bp pathogenesis in a cockroach model

Invertebrates possess phagocytic cells known as haemocytes (HCs). A recent cockroach model of Bp infection used haemolymph samples taken at the point when the insects were judged to be near to death (up to a maximum of 48 hours post-infection) (Fisher *et al*. 2012). For the first time, it was reported that HCs from the haemolymph of infected insects harboured numerous intracellular Bp bacteria and that some had formed MNGCs despite being non-adherent in the insect's open circulatory system. Bacteria were also observed extracellularly in the haemolymph, though it was noted that it was unclear whether they were alive or dead, or just released from lysed cells. The authors suggested that Bp survives in an intracellular niche within the cockroach; infected HCs fuse with other HCs to enable continued bacterial replication, and eventually the bacterial load in the cells and haemolymph may overwhelm the insect (Fisher *et al*. 2012).

Visible signs of Burkholderia cellular pathogenesis

Actin remodelling

Bp-group pathogens exhibit an ability to remodel the actin of a host cell (Stevens *et al*. 2006). Actin-based motility is achieved when the bacterium recruits host actin monomers to build a 'tail'-like projection; the bacterium remains at the extreme end of the actin tail (also known as comet tails), effectively being propelled within or out of a host cell (see panel B of Figure 1.6).

Figure 1.6. Characteristic MNGCs and actin tails are visible in infected RAW 264.7 murine macrophage culture. Panel A: MNGCs are evident as multiple blue-stained nuclei within single large cells. Panel B: Many actin tails (red) propel *B. pseudomallei* bacteria (green) around macrophage cells (nuclei stained blue). Images reproduced from Galyov (2010).

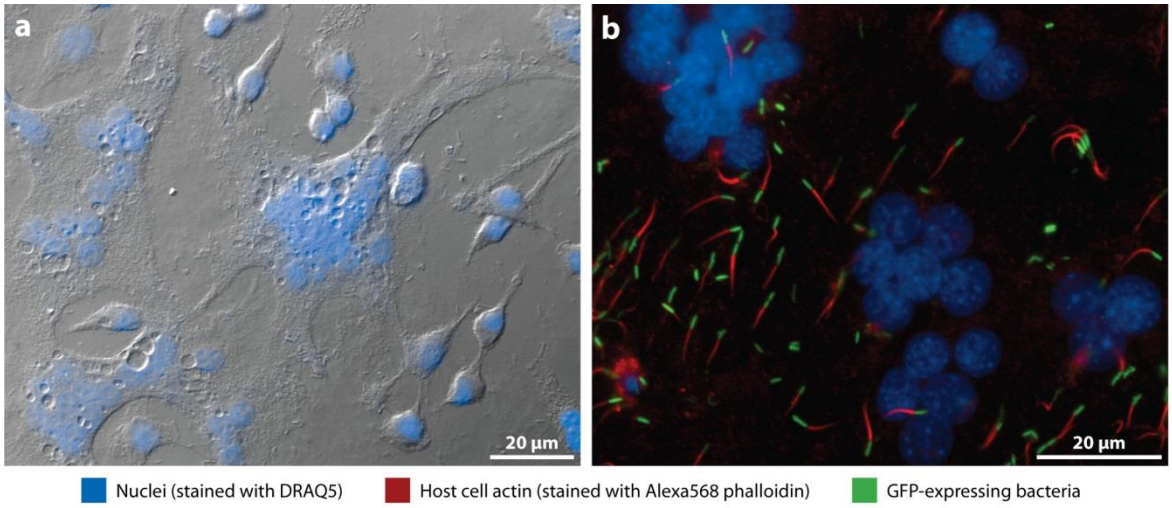

Actin-based motility was believed to be the mechanism by which Bp primarily spreads from one host cell to another, until it was found that actin remodelling-defective mutants were able to spread to other cells (French *et al*. 2011). It is now accepted that optimal intercellular spread involves a combination of cell fusion and actin-based motility (Galyov *et al*. 2010). The T6SS-1 appears to be involved in that process, perhaps with unknown 'fusogenic' factors (French *et al*. 2011). Motility within the cell increases the likelihood of contact between the bacteria and the host cell membrane, which can lead to cell-cell fusion. Studies in HEK293 human embryonic kidney cells revealed an interesting difference between the motility of Bp and Bt. Bp requires actin-based motility for intracellular propulsion but Bt has no absolute requirement for either actin polymerisation or membrane protrusion as it possesses a secondary flagellar system which enables rapid intracellular motility (French *et al*. 2011). Nonetheless, actin remodelling is a distinctive characteristic of *Burkholderia* infection and formation of actin tails is a sign of bacterial pathogenesis within the host.

Multi-Nucleated Giant Cells (MNGCs)

Cell fusion leads to the formation of MNGCs (also seen in Figure 1.6), which occur in clinical melioidosis infections and have been demonstrated to occur *in vitro* in phagocytic and non-phagocytic cell lines (Kespichayawattana *et al*. 2000). Bp, Bm and Bt are all able to induce MNGCs (Boddey *et al*. 2007; Burtnick *et al*. 2011; Harley *et al*. 1998; Pilatz *et al*. 2006; Suparak *et al*. 2005; Utaisincharoen *et al*. 2001). The exact role of MNGCs in melioidosis or glanders is not fully understood but they must enable the bacteria to access more nutrients and space for replication without leaving the safety of the cell, and thereby avoiding the immune system (Galyov *et al*. 2010).

MNGC formation by Bp has been discovered to be linked to a type VI secretion system (T6SS-1) – in particular to a surface-associated component, Hcp1 (Pilatz *et al*. 2006; Burtnick *et al*. 2011; French *et al*. 2011). A Bp *hcp1* mutant strain was able to multiply to high numbers in the cytosol of RAW 264.7 cell monolayers but no fusion with adjacent cells occurred (Burtnick *et al*. 2011). Interestingly, Burtnick *et al* noted that no MNGCs were observed in their hamster model of melioidosis at 48 hours post-infection. They suggested that the rapidity of death in the hamster (an acute model of melioidosis) may limit the possibilities for identifying MNGCs in infected tissues (Burtnick *et al*. 2011), yet as described above, MNGCs have been reported within 48 hours post-infection in a cockroach model (Fisher *et al*. 2012).

Apoptosis / cell death

Apoptosis of host cells has been observed during Bp and Bt infection of either phagocytic or non-phagocytic cell lines – single cells and MNGCs both show condensed or

fragmented nuclei characteristic of apoptosis (Kespichayawattana *et al*. 2000; Burtnick *et al*. 2011). Kespichayawattana *et al* (2000) reported their findings for 'virulent Ara^{-}' and 'non-virulent Ara^{+}' strains, which are now known to be Bp and Bt species respectively (Smith *et al*. 1997; Brett *et al*. 1998; Kespichayawattana *et al*. 2000); Bp infection resulted in approximately double the proportion of apoptotic J774A.1 cells at six hours (43%) compared to Bt (23%). Figure 1.7 shows bright condensed nuclei in the remnants of a large MNGC (Burtnick *et al*. 2011).

Figure 1.7. RAW 264.7 cells infected with Bp show signs of cell death: these multi-nucleated cells show extensive cell damage and some bright nuclei. Scale = 20 μm. Image reproduced from Burtnick *et al* (2010).

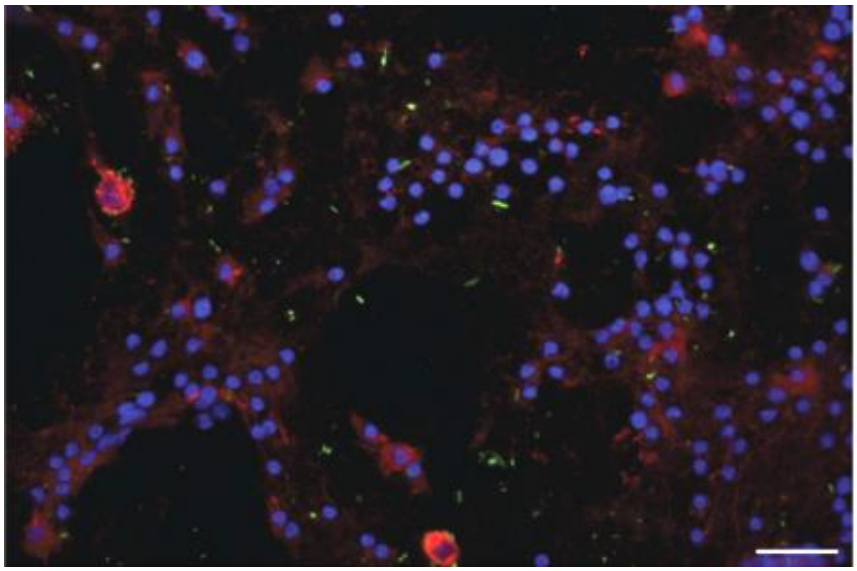

In the first identification of a Bp factor that mediates apoptosis of host cells Suparak *et al*. (2005) found that MNGC formation and apoptosis are linked to a T3SS translocator protein, BipB. A polar deletion mutant of *bipB* was attenuated in a mouse model. It also resulted in reduced MNGC formation, cell-to-cell spreading and apoptosis in J774A.1 cells (Suparak *et al*. 2005). It is likely that a T3SS-secreted effector mediates the effects. In the *bipB* mutant the BopE T3SS effector was still secreted but other factors may have been affected by the polar mutation. For example a T3SS effector (CHBP: cycle inhibiting factor in Bp) was recently discovered to cause macrophage-specific apoptosis (Yao *et al*. 2012). Dowling *et al* (2010) reported that crude lysate from *E. coli* expressing 15kb of Bp genome caused MNGC formation and apoptosis in J774-2 macrophage-like cells (Dowling *et al*. 2010). Within that region were putative toxin encoding genes (*bpsl0590-91*), although the effect was not confirmed to be due to those genes.

Manduca sexta cellular immunity

The cellular immune response of *M. sexta* to bacterial infection has been extensively studied. Cellular defences including phagocytosis, nodule formation and encapsulation

around invading organisms are mediated by HCs (Strand 2008). Insect HCs are heterogeneous populations; different subtypes exhibit different cell morphologies and functions. Two main populations most relevant for the immune response against microbial pathogens are plasmatocytes and granulocytes (or granular cells), which constitute up to 95% of all HCs in lepidopteran larvae (Nardi *et al*. 2003). Granulocytes are the most abundant HC type in *M. sexta* and function as professional phagocytes, akin to mammalian neutrophils. Plasmatocytes are responsible for forming capsules around foreign bodies that are too large to be engulfed, such as nematodes (Strand 2008). *M. sexta* hyperphagocytic (HP) cells resemble large granulocytes and can each engulf up to 500 bacteria (Dean *et al*. 2004). Although they only account for 1% of the circulating HC population, in experimental assays HP cells are reported to sequester the majority of heat-killed bacteria (Strand 2008). In terms of morphology, granulocytes and plasmatocytes are rounded when circulating in the haemolymph and spread when bound to foreign surfaces (e.g. microscope slides). As shown in Figure 1.8, granulocytes and HP cells spread symmetrically (panel A) whereas plasmatocytes spread asymmetrically and more extensively (panel B).

Figure 1.8. Confocal microscopic images of *Manduca sexta* haemocytes (Strand 2008). Panel A: Small granulocytes and larger, spreading plasmatocytes (PL = plasmatocytes, GR = granulocytes). Panel B: An aggregate of haemocytes including several hyperphagocytic cells (containing dense masses of *E. coli*, coloured light grey). Images reproduced from Strand *et al*., (2008).

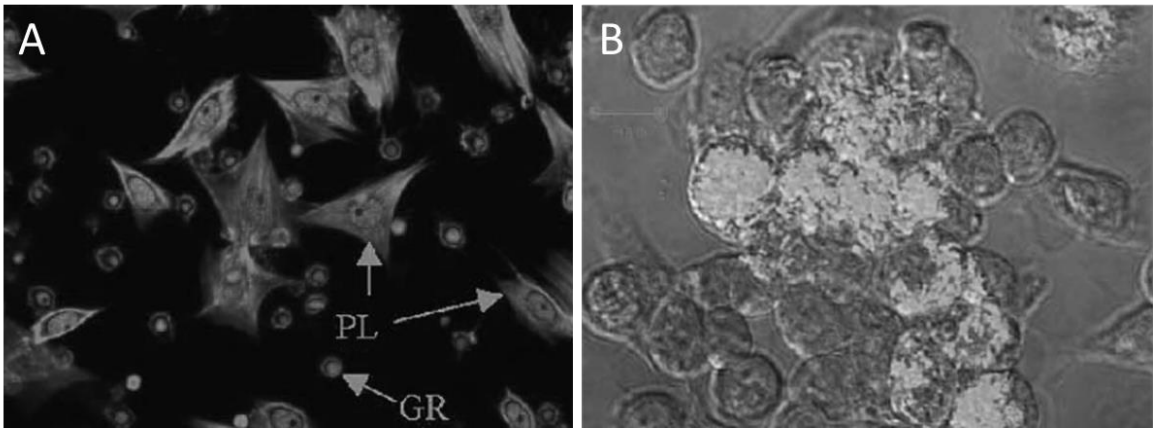

1.3.3. Chapter 5 - Rapid Virulence Annotation of *Burkholderia pseudomallei*

Rapid Virulence Annotation (RVA) is a technique developed by Waterfield *et al* (2008) to identify virulence factors of bacterial pathogens. The technique is an assumption-free approach; instead of targeting specific loci predicted to have an effect, RVA uses heterologous expression of relatively small genome fragments in an *E. coli* host strain. The cosmid- or fosmid-bearing *E. coli* clones are tested in a range of bioassays to look for any "gain of toxicity" (GOT) compared to the non-recombinant *E. coli* host strain. This means that quite subtle effects (or effects which are complemented by other genes in a complete genome) can be identified, whereas they may go unnoticed in approaches which mutate single genes (the effects of which may be masked by redundancy of virulence factors). In order to assess the whole genome, a large library of clones is used. The clone library is produced by shearing genomic DNA of the pathogen and ligating fragments of a certain size range into a fosmid vector. With a sufficiently large library the clones' inserts overlap to cover the pathogen genome with several-fold redundancy.

Rather than just one bioassay, RVA uses multiple model hosts from diverse taxa. The original RVA (of *Photorhabdus asymbiotica*) used four hosts: amoebae, nematodes, insects and a mammalian macrophage cell line, coining the terms aGOT, nGOT, iGOT and mGOT respectively. There are several reasons behind this selection of hosts. All are relatively inexpensive in terms of cost and space requirements, and have short life cycles. Three are whole organisms, which allows for effects to be studied in context with relevant host interactions in place. The fourth, although only a cell line, added a direct relevance to mammalian hosts. The different models give insights into different infection routes: direct inoculation and "blood"-borne infection in the insect; via the digestive route in the nematode; via engulfment by the amoebae (which has direct parallels to the engulfment of bacteria by professional phagocytes such as macrophages); and direct application of crude cellular lysates to the macrophage cell line. Finally, comparing positive 'hits' between the various GOT models gives insights into host-specific factors versus those with a less restricted general role in virulence.

Previous RVA analyses

Successful RVA screening results have previously been published for the insect pathogen and emerging human pathogen *P. asymbiotica* (Waterfield *et al*. 2008), and RVA-style analyses have also been applied to its close relative *P. luminescens* (unpublished). Both *Photorhabdus* species exist in symbiotic relationships with Heterorhabditid nematode hosts; the bacteria are vectored into an insect by the nematode whereupon they rapidly kill the insect by lethal septicaemia. Unlike *P. luminescens*, *P. asymbiotica* has

increasingly been recognised as a causative agent of invasive soft tissue infections and disseminated bacteraemia in humans (Gerrard *et al* 2006). As a result of the RVA study, 21 discrete regions of the *P. asymbiotica* genome were identified as containing virulence determinants. These regions were identified by the clustering and overlapping of the inserts from GOT positive clones. Particular loci were narrowed down further based on the region of minimum genetic overlap between overlapping positives. The results successfully confirmed known virulence-related genes such as the toxin *mcf1* (*makes caterpillars floppy*). Other factors included seven putative secretion systems, three operons for pili/fimbriae, TC (Toxin-Complex) insecticidal toxins, and ten polyketide synthases and non-ribosomal peptide synthetases (PKSs/NRPSs) (Waterfield *et al*. 2008). PKSs and NRPSs produce secondary metabolites including toxins, siderophores, pigments, antibiotics and immune-suppressants. Virulence-related genes encoding these types of small molecules are of particular interest as potential antibiotic or anti-virulence targets. Among RVA-style results from *P. luminescens* was the identification of a putative lipase *pdl1* which was recently reported to enhance secretion of TC toxins (Yang *et al*. 2012). Three *Pseudomonas syringae* pathovars were also probed with RVA using invertebrate hosts, leading to the identification of genes for a type 6 secretion system (T6SS), a TC toxin and flagellar proteins amongst others as being important for *Ps. syringae* virulence against invertebrates (Dorati 2011).

The basis and methodology of RVA

The rationale behind RVA is that *E. coli* laboratory strains such as K12 (from which the host strain for the clone library is derived) are harmless to the invertebrate hosts. In fact the amoebae and nematodes readily feed upon these *E. coli*. The insect immune system can efficiently cope with *E. coli* injected into the haemocoel, as is discussed in Chapter 4. Therefore if the addition of a small region of pathogen DNA causes an *E. coli* clone to have a harmful effect upon the insect or to resist predation by the amoebae or nematodes, then this gain of toxicity can be attributed to the effects of the insert DNA. End sequencing of the library allows knowledge of which genomic fragment is contained within the insert to be derived. A positive screening result can therefore be linked to a particular region of the pathogen's genome.

The fosmid library used for this Bp RVA was constructed at the Sanger Institute for Prof. Rick Titball (University of Exeter) and consists of *E. coli* bearing approximately 35-40 kb inserts from the Bp K96423 genome. The three invertebrate model hosts are the free-living amoeba *Acanthamoeba polyphaga*, the nematode *Caenorhabditis elegans* and the larva of the lepidopteran insect *Manduca sexta*. How toxicity is assessed depends on the nature of the GOT screen. The insect (iGOT) screen involves direct injection of bacterial

culture into the haemocoel and larvae are subsequently assessed for signs of morbidity such as slow development, reduced feeding, melanisation or death. The amoeba (aGOT) and nematode (nGOT) assays present the bacterial mat as a food source to approximately one-thousand amoebae or ten adult nematodes, and the time taken for the mat to be consumed is monitored. A delay in feeding suggests the presence of toxic or repellent factors. RVA screens are relatively high-throughput so each clone is tested once initially. Positive-scoring clones are then re-tested with replicates. Finally the genomic loci corresponding to positive clones are calculated and loci found in multiple overlapping positive clones are shortlisted for further investigation. A typical next step is then to mutate a positive clone with transposon insertions across the full insert region and re-test the mutants to pin-point the precise gene(s) responsible for the GOT phenotype.

Although the term 'toxicity' is used, a positive result from GOT assays could also be due to host reactions. For instance, in iGOT a strong immune reaction will give the appearance of insect illness (e.g. melanisation or slow development) but could be caused by an immunogenic factor which has no direct role in virulence. In aGOT and nGOT there can be multiple explanations for slow consumption of bacteria. True toxic factors could kill or paralyse the host or prevent their reproduction, or could have an "anti-predation" repellent effect which prevents consumption in the first place. In another scenario the hosts do consume the bacteria to some extent but a growth advantage has been conferred to the bacteria that allows them to out-grow the rate of consumption. Nonetheless, positive hits from any of these scenarios could give informative insights into bacterial virulence and the host-pathogen interaction.

Why apply RVA to Bp?

As already discussed, Bp is an opportunistic human pathogen of considerable clinical importance and represents a potential terrorist bio-threat. Much effort has gone into understanding its pathogenesis and numerous virulence factors have been identified. However, with researchers using different Bp strains and different model hosts, studies have often given contradictory results as to the importance of various factors. The picture of Bp virulence is therefore still confusing and further efforts are needed to improve our understanding of this important pathogen. The status of Bp as a containment level 3 (CL3) pathogen certainly limits the ease with which it can be investigated, and for that reason Bt is often used as a proxy for Bp. A major benefit of the recombinant fosmid library system is that it allows the genome of Bp strain K96243 to be investigated under CL2 laboratory conditions.

Furthermore, the use of invertebrate models for Bp is appropriate due to the bacterium's soil-dwelling saprophytic lifestyle. The extent to which Bp associates with organisms such

as amoebae and nematodes in the environment has not been thoroughly studied but they are certain to encounter one another frequently. It is highly likely that they are engaged in co-evolutionary arms races. These invertebrate models are also suited to the RVA analysis of Bp because they are all susceptible to infection by the bacterium; according to published findings (Inglis *et al*. 2000; Gan *et al*. 2002; Ooi *et al*. 2012) and as discussed in Chapter 3, *M. sexta* larvae, *A. polyphaga* and *C. elegans* are all killed by (or at least cannot predate) Bp.

Previous invertebrate models for Bp virulence factor discovery

Previous approaches for the identification of Bp virulence factors have taken advantage of invertebrate hosts. Genes of Bp strain KHW were mutated by transposon insertion and the mutants were tested in the *C. elegans* system (Gan *et al*. 2002). Of 3,400 mutants, 39 exhibited reduced lethality towards the nematode; after eliminating mutants in which the reduced killing phenotype was due to debilitation of the bacteria, five attenuated mutants remained. The mutants had insertions in genes for hypothetical proteins, an amino acid transporter and a sugar ABC transporter. The virulence of those mutants was comparable between a BALB/c mouse model and the *C. elegans* killing assay, validating the clinical relevance of the nematode model as an alternative host for virulence factor discovery. The study reported that their transposon mutant screen did not reach genetic saturation of the Bp KHW genome and that therefore there may be more potential virulence genes to be discovered. Another approach used the *G. mellonella* insect model together with comparative genomics between *Burkholderia* species to identify novel virulence genes of Bm (Schell *et al*. 2008). *In silico* genomic subtraction identified a set of 650 genes (termed the 'Bm-Bp virulome') which were present in Bp and Bm (both opportunistic human pathogens) but absent from non-human-pathogenic *Burkholderia* species. Genes thought likely to encode novel virulence factors were selected, inactivated, tested in *G. mellonella*, and verified in a hamster model.

Top-down approaches are often used for investigating microbial virulence, focusing on particular putative virulence factors based on gene homology and known roles in other species. The transposon insertion library method used by Gan *et al* (2002) for virulence factor discovery is similar to the RVA method in terms of using an assumption-free, bottom-up approach to reveal possibly unexpected determinants of virulence. Unlike that study, the RVA would use a different strain of Bp (K96243 *versus* KHW) and multiple invertebrate hosts. In addition it would not be possible to work with a Bp transposon mutant library in the laboratory facilities available at the University of Bath, but the recombinant fosmid library allows the investigation of this important pathogen at CL2.

Potential pitfalls of RVA

Every experimental system also has its disadvantages. Although the recombinant expression system is advantageous in allowing subtle effects and the effects of discrete loci to be detected, it is potentially also a weakness. The biosynthesis and transport of proteins is exquisitely coordinated in native bacterial systems at all levels: regulation of transcription, translation, post-translational modification, and localisation to appropriate cellular compartments or secretion to the outside of the cell. Numerous inputs and genetic checkpoints influence the control of these processes and the recombinant expression system removes these normal levels of regulation. This could be either beneficial or detrimental to the discovery of virulence determinants. Regulation of gene transcription in the recombinant system has a level of unpredictability, for example in the combined effects of native and fosmid promoters or the lack of transcriptional activator proteins. Problems may also occur at the level of protein translation if the *E. coli* host lacks tRNAs in adequate proportions to translate a transcript with a significantly different codon bias. Once translated, other important factors are whether the protein will be located in the appropriate cellular location, correctly folded, or successfully secreted. It should be noted however that RVA is not intended to model a pathogen's virulence comprehensively or exactly, but rather to provide a 'rough and ready' shortlist of genomic regions for further study.

What discoveries might be expected from Bp RVA?

Despite the fact the approach is assumption-free, a few predictions can be made about what Bp RVA results might reveal. For a start, it is likely there will be some false-positives – due to larvae which were simply less healthy, or bacterial mats which were fed upon by more bacteriovores than average, for example. False-positives should be excluded during the re-testing round. True-positive hits – clones which make larvae less healthy or which somehow resist bacteriovore predation – can fall into several categories. Some may be true virulence factors, detrimental to the host either directly or by enabling the bacteria to evade host responses (which might be considered 'offensive' and 'defensive' virulence factors, respectively). These could include previously identified virulence factors or unexpected novel factors. Other GOT positives may be due to side-effects of aberrant gene expression in the recombinant system; over- or under-regulation of genes which usually play no role in virulence might have pleiotropic effects on the bacterium or host. Finally, clones may be detrimental to the host if they are particularly immunogenic; either the immune response itself (e.g. melanisation) will cause the clone to be scored positive, or the immune response may divert resources away from normal feeding and development, again leading to a false-positive identification. However, immunogenic

factors are integral in the host-pathogen interaction and can therefore be considered virulence determinants themselves.

Considering the results of the *P. asymbiotica* RVA and the importance of expressing proteins and other molecules in the right locations, perhaps the types of factors most likely to be identified are those which: can export themselves (autotransporters); can be exported by *E. coli* secretion systems; or those encoded in close proximity to their transport genes so that a fosmid insert can include all necessary genes. Alternatively an accumulation of a toxin inside a bacterial cell could also allow for a large 'dose' to be delivered to the ingesting host or cell. Small 'stand-alone' exotoxin genes are more likely to be cloned intact within any one clone, while large genes such as many that encode NRPS systems are less likely to be cloned intact within the 40kb of a fosmid. Also, factors specific to other taxa – mammalian or plant hosts for example – should not be identified in the invertebrate screens, but general virulence factors (such as non-specific proteases or lipases) or those specific to the models used should be.

Chapter 2. Methods and Materials

Invertebrate host organisms and *Burkholderia* and *Escherichia coli* bacteria were used throughout the study. Species, strains, and culture and maintenance details are listed in section 2.1. Details of methods and materials relating to specific results chapters are given in sections 2.2 – 2.4.

2.1. General methods and materials

2.1.1. Invertebrate species and maintenance

Three distinct classes of invertebrates were used as model hosts for bacterial infection and Gain of Toxicity (GOT) experiments: insect larvae, amoebae and nematodes (Table 2.1).

Table 2.1 Invertebrate species used in this study

Species		Notes	Source
Manduca sexta	Kingdom: Animalia Family: Arthropoda Class: Insecta Order: Lepidoptera	Tobacco Hawkmoth. Insect larva used at fifth-instar stage for injection assays. Used at neonate stage for feeding assays	In-house colony, University of Bath
Galleria mellonella	Kingdom: Animalia Family: Arthropoda Class: Insecta Order: Lepidoptera	Greater Waxworm. Insect larva used at fifth-instar stage for injection assays	Livefoods UK
Acanthamoeba polyphaga	Kingdom: Amoebozoa Phylum: Amoebozoa Family: Acanthamoebidae	Free-living amoeba. Used for amoeba feeding assays	Cultured in-house, University of Bath
Caenorhabditis elegans	Kingdom: Animalia Phylum: Nematoda Class: Secernentea Order: Rhabditida	Nematode worm. Bristol N2 strain. Used for nematode feeding assays	Cultured in-house, University of Bath

Insect maintenance

A *Manduca sexta* colony was maintained in controlled conditions (25 °C, 80% humidity) and on an artificial diet as detailed in Table 2.2, according to Reynolds, Nottingham, & Stephens (1985). *Galleria mellonella* larvae were purchased in batches from Livefoods Ltd and stored at 4 °C with no requirement for feeding.

Table 2.2. Details of *Manduca sexta* diet

Media	Uses	Composition
***Manduca* diet**	*M. sexta* maintenance and feeding and infection assays	Per cake (Reynolds *et al*. 1985): 99.1% (v/v) dH_20, 0.22 (v/v) corn oil, 0.22% (v/v) linseed oil, 0.45% (v/v) formaldehyde (final 6mM), 18.81% (w/v) premix, 1.26% (w/v) agar, 0.01% (w/v) chlortetracycline (final 234mM), 0.01% (w/v) Vandersant vitamins, 0.45% (w/v) ascorbic acid (final 25mM). Store at 4 °C. Premix (w/w): 43.99% wheatgerm, 20.53% casein, 17.60% sucrose, 8.80% dried active yeast, 5.87% Wesson's salt, 0.58% choline chloride, 1.17% cholesterol, 0.58% methyl paraben, 0.88% sorbic acid
Antibiotic-free *Manduca* diet	*M. sexta* feeding assays	Recipe as for complete diet (above) minus formaldehyde and chlortetracycline.

Amoeba maintenance

Acanthamoeba polyphaga amoebae were maintained in 25cm^2 tissue culture flasks of peptone–yeast–glucose (PYG) broth (Table 2.3) at 22-25°C, and sub-cultured twice weekly (Rowbotham, 1980).

Table 2.3. Details of amoeba media

Media	Uses	Composition
Page's Amoebal Saline (PAS)	Minimal media, basis for PYG media	PAS 1 stock: in dH_2O, 410.66 mM NaCl, 3.25 mM $MgSO4.7H_2O$, 1.75mM $CaCl_2.6H_2O$, in dH_2O PAS 2 stock: in dH_2O, 200 mM Na_2HPO_4, 200 mM KH_2PO_4 PAS working solution: in dH_2O, 0.5% (v/v) PAS 1 stock, 0.5% (v/v) PAS 2 stock. Autoclave at 121 °C. (Final: 2.05 mM NaCl, 0.016 mM $MgSO4.7H_2O$, 0.009 mM $CaCl_2.6H_2O$, 1 mM Na_2HPO_4, 1 mM KH_2PO_4).
Peptone-Yeast-Glucose (PYG) broth	Complete media for *A. polyphaga* maintenance and feeding	In PAS working solution: 1.5% (w/v) proteose peptone (Oxoid L85), 100 mM D-glucose, 0.25% (w/v) yeast extract (Oxoid L21). Autoclave at 110 °C.
PYG agar	Amoeba assays	In PAS working solution: 0.75% (w/v) proteose peptone (Oxoid L85), 50 mM D-glucose, 0.125% (w/v) yeast extract (Oxoid L21), 1.5% (w/v) agar. Autoclave at 110 °C. Plus 25 µg/ml chloramphenicol for fosmid selection.

Nematode maintenance

Caenorhabditis elegans worms were maintained on Nematode Growth Medium (NGM) agar at room temperature, using *E. coli* OP50 as a feeding strain (200µl spread per plate) and transferred weekly to fresh plates (Table 2.4).

Table 2.4. Details of nematode media

Media	Uses	Composition
Nematode Growth Medium (NGM) agar	*C. elegans* maintenance and feeding (with *E. coli* OP50 bacteria), nematode feeding assays	In dH_2O: 50 mM NaCl, 0.25% (w/v) peptone, 1.7% (w/v) agar. Autoclave at 121 °C for 15 min. When approx. 50 °C, add: cholesterol (final 5 µg/ml), 25 mM KH_2PO_4, 1mM $MgSO_4$, 1mM $CaCl_2$. For feeding: 200µl *E. coli* OP50 onto dry plates, incubated at 37 °C overnight. For nGOT assays, add 25 µg/ml chloramphenicol.

2.1.2. Bacterial strains and culture methods

E. coli strains were used as host strains for expression of the *B. pseudomallei* fosmid library, as well as controls in infection experiments, and for cloning (Table 2.5).

Table 2.5. *Escherichia coli* strains and associated plasmids used in this study

***E. coli* strain**	**Uses**	**Notes / genotype**	**Selection**	**Source**
Epi300™ / pCC1FOS™	Fosmid expression strain for Rapid Virulence Annotation (RVA) screening. Control in invertebrate models	*F- mcrA Δ(mrr-hsdRMS-mcrBC) Φ80dlacZΔM15 ΔlacX74 recA1 endA1 araD139 Δ(ara, leu)7697 galU galK λ- rpsL (StrR) nupG trfA tonA*	25 µg/ml chlor-amphenicol	Epicentre; M. Holden, Sanger Institute
Ec100 / pWEB	Control in invertebrate models and in RVA (prior to receipt of Epi300 strain)	*F- mcrA Δ(mrr-hsdRMS-mcrBC) Φ80dlacZΔM15 ΔlacX74 recA1 endA1 araD139 Δ(ara, leu)7697 galU galK λ- rpsL (StrR) nupG.* With pWEB plasmid.	50 µg/ml ampicillin & 50 µg/ml kanamycin	Epicentre
Ec100 Mcf	Toxic control for *M. sexta* injections	*E. coli* Ec100 expressing the Mcf1(Makes caterpillars floppy) toxin from *Photorhabdus asymbiotica*	50 µg/ml ampicillin & 50 µg/ml kanamycin	Epicentre / Waterfield laboratory
Ec100 GFP	Fluorescent confocal microscopy	Green-fluorescent *E. coli*, chromosomally labelled	-	Waterfield laboratory
OP50	Strain for feeding *C. elegans*	Uracil-requiring *E. coli* mutant; grows thinly on nematode growth agar, therefore nematodes can be visualised	-	Waterfield laboratory
EZ Competent cells	Sub-cloning strain for deletion or over-expression constructs	*[F'::Tn10(Tcr) proA+B+ lacIqZΔM15] recA1 end A1 hsdR17 (rK12– mK12+) lac glnV44 thi-1 gyrA96 relA1*	-	Qiagen
DH5α λpir	Transformation of deletion construct	*F- endA1 thi-1 recA1 relA1 gyrA96 Φ80lacZΔM15 Δ(lacZYA-argF) U169 hsdR17 (rk- mk+) λ pir*	-	Biomedal (Grant *et al.* 1990)

***E. coli* strain**	**Uses**	**Notes / genotype**	**Selection**	**Source**
S17-1 λpir	Intended for conjugation of deletion construct	*TpR SmR recA thi pro hsdR- M+RP4: 2-Tn7 λ pir*	-	Biomedal (Simon *et al.* 1983)
DH5α λpir / pBHR4-groS-RFP	Intended for over-expression of *kdpDE* KO genes	DH5α λpir strain bearing a broad host range vector, expressing red fluorescent protein from the strong groS promoter. Cm^R	50 µg/ml chlor-amphenicol	Claudia Müller, University of Exeter (Wand *et al*. 2011)

B. thailandensis and *B. oklahomensis* strains were handled at containment level 2 (CL2). On my behalf, *B. pseudomallei* was grown and manipulated by appropriately trained workers using containment level 3 (CL3) facilities at the University of Exeter. *Burkholderia* strains used in this study are listed in Table 2.6.

Table 2.6. *Burkholderia* species and strains used in this study

***Burkholderia* species / strain**	**Comments**	**Selection**	**Source**
***B. pseudomallei* K96423**	Clinical isolate; type strain; Gen^R. The fosmid library consisted of Epi300 cells containing ~35kb regions of this genome	-	Prof. Rick Titball, University of Exeter
***B. thailandensis* E264**	Environmental isolate; type strain; genomic sequence completed; Gen^R	-	Prof. Rick Titball, University of Exeter
B. thailandensis* E264 *ΔtatA	Conditional mutant of the Twin Arginine Translocation system (*prhAB::tatA*). Supplement media with rhamnose to activate or glucose to inactivate TAT system	(To activate / inactivate TAT) 0.2% (w/v) rhamnose or glucose	Sariqa Wagley, University of Exeter
B. thailandensis* E264 *ΔsurA	Unmarked deletion mutant of Survival protein A (*surA*) gene (*ΔBTH_I0576*); Gen^R	-	Isobel Norville, Dstl, Porton Down
***B. thailandensis* E264 GFP**	Enhanced Green Fluorescent Protein (eGFP)-expressing strain. Constitutive expression from GroES promoter	50 µg/ml chloramphenicol	Claudia Müller and Monika Bokori-Brown, University of Exeter
***B. thailandensis* CDC 2721121**	Clinical isolate from a human wound, USA. Also referred to as CDC 272	-	Claudia Müller, University of Exeter

***Burkholderia* species / strain**	**Comments**	**Selection**	**Source**
***B. thailandensis* CDC 3015869**	Clinical isolate from human blood following an automobile accident, USA. Also referred to as CDC 301	-	Claudia Müller, University of Exeter
***B. oklahomensis* C6786**	Clinical isolate from a human wound, identical to environmental isolates at the same site, USA	-	Claudia Müller, University of Exeter
***B. oklahomensis* E0147**	Clinical isolate from human conjunctiva following an automobile accident, USA	-	Claudia Müller, University of Exeter

2.1.3. Bacterial culture media

Bacteria were grown on Luria Bertani (LB) agar plates or shaking in LB broth (200-250rpm) at 37 °C overnight, unless otherwise stated. Stocks were stored long-term in 20% glycerol at -80 °C. Culture media used in this study are listed in Table 2.7. Media was supplemented with antibiotic selection as necessary (refer to Tables 2.5-2.6).

Table 2.7. Bacterial culture media used in the study

Medium	**Use**	**Composition**
Luria Bertani (LB) broth	Bacterial growth	In dH_2O: 2% (w/v) pre-formulated LB powder mix (Sigma). Autoclave at 121 °C. (Final: 1% (w/v) tryptone peptone, 0.5% (w/v) yeast extract, 85.5 mM NaCl).
LB agar	Bacterial growth and isolation	In dH_2O: 2% (w/v) pre-formulated LB powder mix (Sigma, as above). 1.5% (w/v) agar. Autoclave at 121 °C.
Skimmed milk agar (3% w/v)	Testing for proteolysis	Solution 1: In dH_2O, 4% (w/v) LB powder, 3% (w/v) agar. Solution 2: In dH_2O, 6% (w/v) skimmed milk powder. Autoclave both solutions at 110°C for 15 min, cool to approximately 50 °C then gently mix equal volumes together. (Final: 3% (w/v) skimmed milk, 2% (w/v) LB powder, 1.5% (w/v) agar)
LB broth or agar with rhamnose (0.2% w/v)	To maintain *B. thailandensis* conditional *prhAB::tatA* mutant with promoter on	As for LB broth and LB agar compositions (above) plus 0.2% (w/v) rhamnose (12.18 mM). Autoclave at 110 °C.
LB broth or agar with glucose (0.2% w/v)	To maintain *B. thailandensis* conditional *prhAB::tatA* mutant with promoter off	As for LB broth and LB agar compositions (above) plus 0.2% (w/v) glucose (11.10 mM). Autoclave at 110 °C.

2.2. Chapter 3 methods – *Burkholderia* infection assays in *Manduca sexta*

2.2.1. Confirmation of Bt virulence against invertebrate hosts

Caenorhabditis elegans infection assay

A simple assay was used to confirm a lethal effect of our Bt E264 stock on nematodes. 200µl of Bt E264 culture was spread into a rectangle on NGM agar plates (*n* = 3). The same was done using *E. coli* OP50, as for normal *C. elegans* maintenance. The bacterial lawns were grown overnight at 37°C. Adult *C. elegans* were washed in PBS to remove remaining OP50 cells and seeded onto the lawns, *n* = 10 nematodes per plate. The plates were assessed daily for one week to assess nematode activity.

Acanthamoeba polyphaga dose response assay

A simple dose response assay was used to confirm a lethal effect of our Bt E264 stock on *A. polyphaga* amoebae. Bt E264 and *E. coli* Epi300 were grown overnight and adjusted to OD_{600} 0.5, then serially diluted 1:2. 10µl of cultures at OD_{600} 0.5, 0.25, 0.125, 0.0625 and 0.0313 was spotted onto PYG nutrient agar or PAS minimal media agar. Bacterial mats were grown overnight at 37°C. An *A. polyphaga* suspension was adjusted to $2x10^5$ cells per ml and serially diluted 1:2 to $2.5x10^4$ cells per ml. 10µl drops of the four amoeba dilutions (or 10µl PYG liquid media) were spotted into the corner of wells with bacterial mats at the centre. Mats were assessed daily for up to 13 days, noting the days at which mat consumption began and ended.

Initial dose response assay in Manduca sexta

M. sexta larvae were infected using a range of doses of different *Burkholderia* species, initially by injection directly into the haemocoel with subsequent assessment of larva health and mortality. Where mortalities reach 50% or greater, median time to death (MTTD) values were calculated, providing a simple comparative value between species, strains or doses.

Dose response #1: First, to confirm a lethal effect of our Bt E264 stock on *M. sexta* high doses of Bt E264 based on OD_{600} values were tested (*n* = 3 larvae per condition). Bacterial liquid cultures were grown overnight (37 °C, 225-250 rpm) and adjusted to OD_{600} 0.5, followed by 1:2 serial dilutions to approximately OD_{600} 0.0313. *E. coli* Epi300 was used as a non-pathogenic control (*n* = 3) and LB medium was also injected as a control. Bacterial inoculum samples were spread on LB plates and incubated at 37 C to enumerate CFUs.

Larvae were reared as described in section 2.1.1. Fresh fifth-instar larvae were anaesthetised on ice for 10 minutes, surface-sterilised with 70% ethanol, and injected using sterile insulin needles. 100 µl of bacterial culture was injected between the 2nd and 3rd last segment on the side of each larva. Larvae were supplied with *Manduca* diet, incubated at 25 °C, and scored daily until they either died or reached the pre-pupation 'wanderer' stage of development. At that point they were euthanised by freezing at -20 °C. Larva health was assessed by visual appearance and by response to physical stimulus (prodding or lifting up with tweezers).

2.2.2. Manduca sexta as a Burkholderia infection model

Burkholderia dose responses were subsequently carried out in *M. sexta* over four more experiments, using the same basic methodology with a greater serial dilution factor and more replicate larvae.

Bacterial liquid cultures were grown overnight (37 °C, 225-250 rpm) and adjusted to OD_{600} values as described for each experiment, then serially diluted in 0.9% (w/v) NaCl as appropriate. Estimated doses between 10^5 – 10^1 CFU were injected into *M. sexta* larvae (100 µl from cultures of 10^6-10^2 colony forming units (CFU) per ml). Five to ten replicate larvae were used per condition tested. Diluted samples were also spread on LB plates to enumerate CFUs.

Dose response #2 tested a wider and lower range of Bt E264 doses compared to the initial dose response #1. Initial OD_{600} adjustment was to 0.25, followed by 1:10 serial dilutions to 10^5-10^1 CFU (*n* = *5*).

Dose response #3: Having confirmed a dose-responsive lethal effect of Bt E264 in *M. sexta*, dose response #3 tested Bp K96423 (10^5-10^1 CFU; *n* = 8). This work was carried out in CL3 facilities at the University of Exeter by appropriately trained personnel (Claudia Müller and Sariqa Wagley). Heat-killed Bp K96423 was used as a negative control, as was *E. coli* Epi300 (both equivalent to 10^5 CFU).

Dose response #4 compared the effect of Bt E264 to that of two other Bt strains (CDC 272 and CDC 301) and two Bo strains (C6786 and E0147) to investigate whether virulence in *M. sexta* would reflect the relative virulence levels seen in other model species. Initial OD_{600} adjustment was to between 0.20-0.25, followed by 1:10 serial dilutions to 10^4-10^2 CFU (*n* = 10).

Dose response #5 repeated testing of the three Bt and two Bo strains at a 10^4 CFU intended dose; *n* = 10. Initial OD_{600} adjustment was to between 0.20-0.25, followed by 1:10 serial dilution to 10^4 CFU (*n* = 10).

Summaries of larva survival are shown in the results. Detailed notes on larva health are included in e-Appendix 3a.

Statistical analysis:
For statistical analyses the experimental data were grouped into log doses according to the actual CFU counts (rather than the estimated doses). The statistical package SPSS was used to perform Kaplan-Meier Survival Analysis. This produced survival curves, Median Time to Death (MTTD) values (also referred to as median survival times), and log-rank (Mantel-Cox) significance values (which indicate whether two sets of survival data are significantly different). [Settings: Time = hours post-injection; Status = 0 if survived, 1 if died; Factor = different treatment groups; analysed pairwise over strata.] Complete SPSS outputs are available in e-Appendix 3b.

2.2.3. Assessing attenuation of Bt E264 mutants

Two mutant strains of Bt E264 were tested: a deletion mutant in the *surA* gene (*ΔsurA*), and a conditional mutant of the Twin Arginine Translocation (TAT) system.

ΔsurA dose response: Bt E264 and the Δ*surA* mutant were compared at 10^6-10^4 CFU doses (*n* = 10 larvae). Note that this initial Δ*surA* test incubated the injected larvae at 37°C to replicate the conditions which had been used for *G. mellonella* tests (at Dstl Porton Down; personal correspondence with I. Norville). This was followed up by more detailed tests at doses 10^3-10^1 CFU (*n* = 10 larvae), repeated in three independent experiments, and incubating larvae at 25°C as for all other tests.

Conditional expression of the Bt TAT mutant: The Bt E264 TAT mutant (Bt E264 prhA:tatA) was conditional upon sugar supplementation in the LB medium. To activate expression of the TAT system, as in wild-type E264, the strain was grown in LB with 0.5% (w/v) rhamnose. To inactivate it the strain was grown in LB with 0.5% (w/v) glucose. The mutant growth rate was known to be reduced when the TAT system was inactivated (S. Wagley, personal communication).

TAT #1: A dose response from 10^5-10^2 CFU was tested using Bt E264 or the conditional mutant, each grown in LB with either rhamnose or glucose. Larvae were scored daily for 6 days, *n* = 8.

TAT #2: A second TAT dose response was performed which also tested the wild-type and mutant strain grown in LB alone. Doses of 10^6, 10^4 and 10^2 CFU were tested. Larvae were scored daily for 7 days, $n = 8$.

2.2.4. Virulence in *Galleria mellonella* at 25 °C versus 37 °C

Temperature is known to greatly affect bacterial growth and even virulence. Most of the experiments in this study maintained infected larvae at 25 °C. This is the ideal temperature for *M. sexta* maintenance and is also comparable to soil temperature in tropical regions where Bp and Bt are endemic. However, human body temperature (37 °C) is relevant to human infection and was used by Wand *et al* (2011). To investigate the effect of the post-injection incubation temperature on virulence, *G. mellonella* larvae were injected with *Burkholderia* strains: Bt E264, Bt CDC 272, Bt CDC 301, Bo C6786 and Bo E0147. *E. coli* Epi300 and 0.9% (w/v) NaCl were used as controls. Bacterial cultures were prepared as described for *M. sexta* injections. Larvae were used straight from storage at 4 °C, surface-sterilised with 70% ethanol, and injected with 10 µl of diluted culture to give doses of approximately 10^2 CFU. The larvae ($n = 10$) were subsequently maintained at 25 °C or 37 °C for four days and assessed daily for movement and response to stimulus.

2.2.5. *Manduca sexta* feeding assay

Manduca diet was prepared without antibiotics (see Chapter 2 – Materials and Methods) to avoid detrimental effects on the bacteria which would be added. The food was cut into uniform sizes with a sterilised borer (15mm diameter by approximately 5mm high). Liquid samples (bacteria or controls) were added onto the food pieces and allowed to soak in before adding larvae and sealing into lidded pots. For fifth-instar feeding, one recently moulted fifth instar larva was added per food block. For neonate feeding, two *M. sexta* larvae hatched from eggs the same day (neonates) were added per food block. Neonates were weighed on day 7 or 8 and each condition used 10-20 replicate larvae. Neonates or fifth-instars were monitored daily for mortality.

The samples applied to the food blocks were derived from Bt E264, Bo C6786, and *E. coli* Epi300. Bacterial liquid cultures were grown overnight (37 °C, 225-250 rpm) and applied directly to food blocks or treated to retrieve supernatant, to heat-kill supernatant or to wash cells, as described for each experiment below. LB was added to food blocks as a negative control; to confirm there was no contamination in the medium the LB was also incubated at 37 °C overnight with the bacterial cultures. No contamination was present.

Experiment #1: In the first instance, ten neonates were fed food laced with 100µl of either an overnight culture of Bt E264 or LB. Neonates were weighed on day 8.

Experiment #2: In the following experiment the dosage volume was increased to 200µl per food block in order to cover all exposed surfaces of the food. An *E. coli* Epi300 control was also used. All bacteria were adjusted to OD_{600} 0.1 before addition. Ten neonates were used per condition. Weights were not recorded.

Experiment #3: Using undiluted overnight cultures again, with 200µl volumes. 'Cell-reduced culture' samples were included (see Table 2.8); this sample was mostly supernatant but some cells were still present as it was not filtered. Samples were spread on LB plates and incubated at 37 °C; the cell-reduced culture did exhibit bacterial growth, although to a lesser extent than the whole-culture lawn (colonies were not separated enough to enumerate CFUs). Twenty neonates were used per condition. Day 8 weights were recorded. Fifth instar larvae were also tested: food blocks were 20x10x10mm, 400µl samples were added per block, five larvae per condition. Fifth instar larvae were euthanised (-20°C) on day 5 when they reached the wanderer stage of development.

Table 2.8. Conditions for feeding assay #3. Epi300 = *E. coli* Epi300

Condition	**(Bt E264, Epi300) Undiluted overnight culture treated as follows:**
Culture	200µl directly added per block
Cell-reduced culture	Centrifuged (5 minutes at 10,000G) to pellet cells, supernatant carefully retrieved. Spin repeated and supernatant carefully retrieved. 200µl added to blocks

Experiment #4: See Table 2.9 for sample preparation. Bo C6786 was added as an extra sample. In this experiment supernatant samples were filtered (0.2 µm) to achieve cell-free supernatant; this was confirmed by spreading samples on LB plates and incubating at 37 °C. Washed cells and heat-treated supernatant were also tested. This experiment was set up on two sequential days so that bacteria could be tested which had been incubated: (i) for 16 hours as before ('1 night'), and (ii) for 40 hours ('2 nights'). This was because some *Photorhabdus* toxins are known to be produced more strongly after extended incubation (Yang *et al*. 2012). Another improvement was to decrease the supernatant addition volumes to reflect the removal of the cellular component. Twenty neonates were used per condition. Day 7 weights were recorded. The neonates which were available to use in the first batch (for 1-night-incubated samples) appeared to be less healthy than usual (pale colour and less movement). The 2nd batch (used for 2-night-incubated samples) showed normal health.

Table 2.9. Conditions for feeding assay #4. Epi300 = *E. coli* Epi300

Condition	**(Bt E264, Bo C6786, Epi300) Undiluted overnight culture treated as follows:**
Culture	200µl directly added per block
Cell-free supernatant	200µl per block centrifuged (5 minutes at 7,000G) to pellet cells for washing (below). Supernatant retrieved and centrifuged (15 minutes at 20,000G), then filtered (0.2 µm). Cell-free volumes (equivalent to cell-replete 200µl) were calculated and added to blocks
Heat-killed supernatant	As for supernatant: after filtration step, 10 minutes in an 80 °C heat block. Cell-free volumes (equivalent to cell-replete 200µl) added to blocks
Washed cells	Cells pelleted from the supernatant (above) were washed in LB, centrifuged again (5 minutes at 7,000G), and re-suspended in LB to the original volumes. 200µl added to blocks

Statistical analysis: The significance of average weight differences between groups was calculated using the two-tailed T-test statistic for unequal variances. (The data were first assessed for equality of variances).

2.3. Chapter 4 methods – *In vivo* time-course of *Burkholderia* insect infection and pathogenesis

These experiments investigated the progression of infection within the insect model after injection. Haemolymph samples taken from infected larvae were viewed using fluorescent confocal microscopy. Images were assessed for bacterial and haemocyte cell numbers and cellular hallmarks of *Burkholderia* infection. Haemolymph samples were also assessed for haemocyte number and viability using a kit for flow cytometry.

2.3.1. Comparative virulence of Bt E264 wild-type and GFP strains

Green fluorescent protein (GFP)-labelled strains of Bt E264 and *E. coli* Ec100 were to be used for microscopy. Therefore the relative virulence of labelled and wild-type strains was investigated using injections into *M. sexta* fifth-instar larvae.

Bacteria and larvae were prepared and larvae were injected with bacteria as described for dose responses #4 and #5 in Chapter 3: initial OD_{600} adjustment was to between 0.20-0.25, followed by 1:10 serial dilutions. First, estimated doses of 10^2-10^4 CFU were tested (n = 10). Estimated doses of 10^4 CFU were repeated in a second experiment (n = 10).

Statistical analysis:
The statistical package SPSS was used to perform Kaplan-Meier Survival Analysis on the data from each dose. This produced survival curves, Median Time to Death (MTTD) values (referred to in the software output as median survival times), and log-rank (Mantel-Cox) significance values (which indicate whether two sets of survival data are significantly different). [SPSS settings: Time = hours post-injection; Status = 0 if survived, 1 if died; Factor = different treatment groups; analyse pairwise over strata.] Analysis for the estimated 10^4 CFU dose was performed for each set of data (each n = 10) and for the combined data (n = 20). Complete SPSS output is available in e-Appendix 4a.

2.3.2. Visualisation of haemocytes and bacteria

Injections and haemolymph collection at time-points

GFP-labelled Bt E264 or GFP-labelled *E. coli* Ec100 were used. Overnight cultures of bacteria were adjusted to OD_{600} 0.20-0.25 and injected into fifth-instar *M. sexta* larvae as described in Chapter 3. Larvae were injected with 50µl doses, equating to approximately 10^6 CFU. A batch of six replicate larvae was used per condition.

Injected larvae (or un-injected control larvae) were bled at certain time-points to collect haemocytes and bacteria. After chilling on ice for 10 minutes, the larvae were surface sterilised with 70% ethanol and the dorsal horn was cut at its mid-point with sterilised dissection scissors. Larvae were gently squeezed and haemolymph was collected into ice-cold micro-centrifuge tubes. Sample dilutions were plated onto LB agar plates and incubated at 37 °C for enumeration of bacterial colony forming units (CFU).

Experiment #1: Initial assessment of infection

Initial images were captured from samples collected at 5, 24, 30, 36 and 48 hours post-injection with Bt E264 GFP or *E. coli* Ec100 GFP. Samples were also used from an un-injected batch of six insects at 24 hours 'post-injection'. Filamentous actin was stained with TRITC-phalloidin. Staining (without DAPI) and microscopy were performed as described below.

Experiment #2: Time-course microscopy

For the time-course study the time-points were altered to provide more data from within the first 24 hours and triplicate batches of insects were used per time-point, with ten images captured per batch. The solutions used are detailed in Chapter 2. Haemocytes were double-stained with TRITC-phalloidin (filamentous actin) and DAPI (nuclei) as described. The time-points were at 0 hours (within 45 minutes of injection), and 3, 6, 12, 18, 24 and 30 hours post-injection. The images were all studied manually in order to assess bacterial and haemocyte numbers and health, and to look for hallmarks of *Burkholderia* pathogenesis such as actin tail formation or MNGCs.

In summary:

Haemolymph of six larvae pooled per microscope slide
Ten fields of view imaged and analysed per microscope slide
Three independent replicate slides produced per time-point
= 30 fields of view imaged and analysed per time-point

Staining and microscopy

Collection of haemolymph

Haemolymph samples were centrifuged for 5 minutes at 1200 rpm to a fluffy pellet. Very loose pellets were spun for a further 2 minutes. As much supernatant was removed as possible without disturbing the pellet and tubes were topped up to 500µl with ice-cold Grace's Insect Medium (GIM) to wash. Following centrifugation for 5 minutes at 1000-1500 rpm, supernatant was again gently removed and tubes were topped up to 1ml with

ice-cold GIM. For each set of 6 larvae, the contents were gently re-suspended and pooled.

Cells were allowed to attach to 13 mm cover slips in wells of a 24-well plate: 500µl of the cell suspension was added per cover slip and left to attach for 30-45 minutes at room temperature, protected from light. Liquid was then aspirated and wells were washed gently with 500µl of room temperature GIM. In a fume hood, GIM was removed and replaced with fixative (500µl 4% (w/v) paraformaldehyde (Pfa) in PBS). Plates were stored at 4 °C for 1-16 hours.

Fluorescent staining and mounting

Solutions used in fluorescent confocal microscopy to analyse *M. sexta* haemocytes are described in Table 2.10.

Table 2.10. Reagents used for microscopy procedures

Reagent	Preparation	Source
Grace's Insect Medium (GIM)	With L-glutamine and sodium bicarbonate, liquid, sterile-filtered, suitable for insect cell culture	Sigma
1X Phosphate buffered saline (PBS)	Pre-formulated tablets dissolved 1 per 100ml as per supplier guidelines. Autoclaved at 121 °C	Sigma
4% (w/v) paraformaldehyde (Pfa)	100mls PBS heated to 40-50°C, 4g Pfa, one drop NaOH. Stored at -20°C. Aliquots thawed on day of use	Sigma
0.1% (v/v) Triton X-100 in PBS	100µl Triton X-100 added to 100ml PBS, mixed well. Sterile-filtered	Sigma
0.5% (w/v) Bovine Serum Albumin (BSA) in PBS	0.5g BSA dissolved in 100ml PBS. Sterile-filtered	Sigma
1µg/ml TRITC-phalloidin solution in PBS	Stock solution: 1mg dissolved in 1ml DMSO Working solution: 1:100 - 1:1000 dilution from stock into PBS	Sigma
1 µg/ml 4',6-diamidino-2-phenylindole (DAPI) in PBS	Stock solution: 2mg dissolved in 1ml dH_2O Working solution: 1:2000 dilution from stock into PBS	Sigma
Mowiol mounting medium	6g glycerol plus 2.4g Mowiol 4-88, stirred. Add 6ml dH_2O, incubate at room temperature for 2 hrs. Add 12ml 0.2M Tris (pH 8.5), heat to 53 °C until dissolved. Centrifuge at 5000 rpm for 20 mins. Store aliquots at -20°C.	Sigma

See the materials and methods section for complete details of solutions used. The following solutions were freshly prepared: 0.1% (v/v) Triton X-100, 0.5% (w/v) Bovine Serum Albumin (BSA), 1 µg/ml 4',6-diamidino-2-phenylindole (DAPI) in PBS, and

tetramethylrhodamine B isothiocyanate (TRITC)-phalloidin in PBS. TRITC-phalloidin final concentrations ranged from 0.5-5.0 µg/ml (conditions were optimised for different dye batches).

Samples and fluorescent dyes were protected from light as far as possible at all steps. Care was taken to wash cells gently. Wells were washed 3 times with PBS in the fume hood. Cells were permeabilised with Triton X-100 in PBS for 5 minutes, and washed a further 3 times with PBS. Non-specific binding sites were blocked with BSA in PBS for 30 mins, and wells were washed 2 times with PBS. Cellular filamentous (F)-actin was then stained with TRITC-phalloidin diluted in PBS (from 40 minutes to 4 hours; conditions were optimised for different dye batches). Wells were washed 3 times with PBS and then stained with DAPI (final concentration) for 15-20 minutes. Finally wells were washed 5 times with PBS.

Small drops of Mowiol mounting medium were prepared on clean slides. Coverslips were dipped once into dH_2O and their edges carefully blotted onto tissue, before being placed cell-side down onto the Mowiol. Slides were incubated in the dark at room temperature overnight to dry, and then stored at 4 °C.

Microscopy and analysis

A Zeiss LSM 510 META confocal microscope was used, with a Plan-Apochromat 63X/1.4 Oil Ph3 lens. Red, green and blue (543nm, 405nm, and 488nm) channels were used, as well as white light.

For the initial assessment (experiment #1): dependent on the required image quality, scan number was 1 or 2, frame size was 512 or 1024, and zoom was typically 1X – 3X. Z-stacks were captured in order to be able to visualise bacteria at all planes: on the surface of the slide, or within or on top of haemocytes. Some single-plane images were also captured.

For the time-course (experiment #2): scan number was 1, frame size was 512, and zoom was 2X. Z-stacks were captured. Single-plane images were only used if all bacteria were verified as visible in one focal plane (i.e. on the surface of the slide) and no amoebae were in the field of view.

Images were processed using LSM Image Browser (Carl Zeiss Ltd.). For the time-course images Z-stacks were each made into 3D projections and assessed by eye to count:

Number of extracellular bacteria
Number of intracellular bacteria
Number of bacteria associated with the surface of a haemocyte

Total number of haemocytes

And to qualitatively assess:

Whether cell debris was present
If actin remodelling was apparent
If multinuclear giant cells (MNGCs) were present

Statistical analyses

The data were used to calculate average values and standard errors of the following parameters:

Number of haemocytes
Total number of bacteria
Number and proportion of extracellular bacteria (excluding surface-attached)
Number and proportion of intracellular bacteria

n = 30 for each time-point with ten images from each of the three replicate batches. Significance of the data from Bt-infected samples compared to the equivalent data from *E. coli* -infected samples was tested using T-tests for unequal variances.

Whether the following signs of pathogenesis were observed in any images from each time-point was noted: evidence of cell death or cellular debris; actin remodelling; or MNGCs.

2.3.3. ViaCount haemocyte quantification

Cytometry was used to assess the number and viability of *M. sexta* haemocytes, using Guava ViaCount Reagent (Millipore). Insects were injected as described for the microscopy with Bt E264, Bt E264 GFP, *E. coli* Ec100, or *E. coli* Ec100 GFP. Control insects were injected with saline (0.9% w/v NaCl) or were not injected at all.

At 24 hours post-injection the larvae were bled into ice-cold micro-centrifuge tubes as described for the microscopy method. Samples were diluted 1:2 with ice-cold GIM to reduce cell clumping or melanisation, then treated with ViaCount reagent according to manufacturer's guidelines (1:20 sample-to-reagent mixed gently, five minutes incubation at room temperature). Readings were taken using a Guava EasyCyte™ cytometer (Millipore) and the ViaCount Assay program. Following the readings, the software's analysis gates were set using equivalent samples from non-injected larvae as a baseline control to identify healthy cell populations.

Haemolymph was pooled from a batch of six replicate larvae for each condition. Each reading measured 1,000 events (insect cells). Bacteria are too small to be counted as cells and instead they should register as debris. Three readings were taken per condition per experiment. Two independent replicate experiments were performed.

Statistical analyses

The ViaCount data (n = 6) were plotted as averages (± standard error): for percentage of cells live, dead or apoptotic; and for cell concentration. Data for the viable percentage of cells and for cell concentration were tested for significant differences between conditions using two-tailed T-tests for unequal variances.

2.4. Chapter 5 methods – Rapid Virulence Annotation of *Burkholderia pseudomallei*

A library of *E. coli* clones bearing fosmids with inserts from the Bp K96243 genome had been prepared by the Sanger Centre for genome sequencing purposes. The library was subsequently used for RVA, i.e. parallel screening of the clones against the invertebrates *M. sexta*, *A. polyphaga* and *C. elegans*.

2.4.1. Analysis of the *B. pseudomallei* fosmid (BPF) library

The *B. pseudomallei* K96243 genomic library was constructed by the Sanger Centre using the CopyControl™ Fosmid Library Production Kit by Epicentre. Epi300™-T1^{R} *E. coli* was the host strain for the pCC1FOS™ fosmid vector. 3,552 individual fosmid-containing clones were arrayed into 37 96-well plates (referred to as BPF (Bp Fosmid) plates) and stored at -80°C. End-sequencing of the BPF library clones was also performed at the Sanger Centre.

Assessing coverage

Using the end-sequences, fosmid sizes and locations were determined by Batch-BLASTN comparison of each end against the published *B. pseudomallei* K96243 genome. Where multiple best matches were returned for an end-sequence, these were curated manually to select the most likely locations. Where only one end could be located, the average fosmid insert size was used to predict an estimated location for the opposite end. In instances where the location of only one end was known, corresponding ends were calculated at 38,878 bp away. This conservative value is based on the mean plus 1 standard deviation; while it may underestimate the true length of some inserts, in theory this value should be equal to or greater than the length of 68.2% of the inserts (based on a normal distribution).

Using all clones with coordinates, a coverage map was generated using Microsoft Excel: the mid-point base pair coordinate of each clone was plotted along the x-axis, each with horizontal error bars representing the average insert length.

Testing for protein expression from RVA clones

As Bp has an unusual codon bias it was important to discern whether the BPF clones (*E. coli* clones containing fosmids with Bp DNA) were able to express Bp proteins. In the first instance, expression was assessed using fosmid clones bearing a protein which would produce a visually identifiable phenotype. The Bp metalloprotease MprA, encoded by *bpss1993*, has previously been transgenically expressed in *E. coli* from 2-4kb inserts (Lee

and Liu, 2000). BPF clones containing *bpss1993* were identified based on their insert end-sequences; eight were grown up in LB with or without CopyControl™ Auto-Induction solution (Epicentre) to up-regulate copy number. These were streaked onto 3% (w/v) milk agar plates with 25 µg/ml chloramphenicol. Plates were incubated at 37 °C. Epi300 *E. coli* and Bt E264 were used (without antibiotic) as negative and positive controls for proteolysis, respectively.

2.4.2. RVA assays and re-testing

RVA GOT assays were based on methods previously published by Waterfield *et al* (2008), as described below. Bacterial and invertebrate maintenance methods and media are described in the Methods and Materials chapter.

Amoeba Gain of Toxicity (aGOT) screen

aGOT screens were performed on Peptone Yeast Glucose (PYG) agar in 25-well plates with 1ml of agar per well. To prepare the bacterial clones, BPF library plates stored at -80 °C were sub-cultured into 96-well plates of LB broth with 25 µg/ml chloramphenicol and incubated at 37 °C overnight shaking at 225-250rpm. 10 µl drops of grown bacteria were added to the centres of the agar wells, allowed to dry, and incubated at 37 °C overnight to form bacterial mats. Epi300 *E. coli* (the fosmid strain) was not initially available so Ec100 *E. coli* with plasmid pWEB (a closely related expression strain from the same supplier) was used as a control.

To prepare the amoebae, stationary phase (approximately 10-day-old) cultures of *A. polyphaga* were adjusted to $2x10^5$ cells per ml using a haemocytometer, and a 10 µl drop was applied to one corner of each agar well (Figure 2.1). Drops were allowed to dry and plates were sealed with parafilm to prevent dessication. Assay plates were incubated at 22-25 °C and scored daily until bacterial mats were consumed, up to a maximum of 2 weeks. Mats of Ec100 were used as a comparative control.

Figure 2.1. Illustration of the aGOT or iGOT assay well. In the centre of each well is the bacterial mat. Amoebae or nematodes are added to the top right corner (shown in the left-most well). The progression from left to right shows the typical pattern of consumption by amoebae.

Toxicity was assessed qualitatively according to any delay in consumption of the bacterial mat. Amoeba screens were scored from 0-5 according to the extent to which the bacterial mat was consumed, whereby:

5 = mat intact
4 = one-quarter eaten
3 = half eaten
2 = one-quarter remaining
1 = less than one-quarter remaining
0 = totally consumed

Examples of scores 1-4 are shown in Figure 2.2. Fosmids which were consumed slowly (relative to the majority from the same batch) were counted as positive GOT hits. Positive hits were to be re-tested in the same manner with 10 replicate mats.

Figure 2.2. Photo showing examples of scores for amoeba (aGOT) or nematode (nGOT) feeding assays. Bacterial mats in the centre of each well are scored qualitatively according to how much of the mat remains each day, from 0 (totally consumed) to 5 (mat intact).

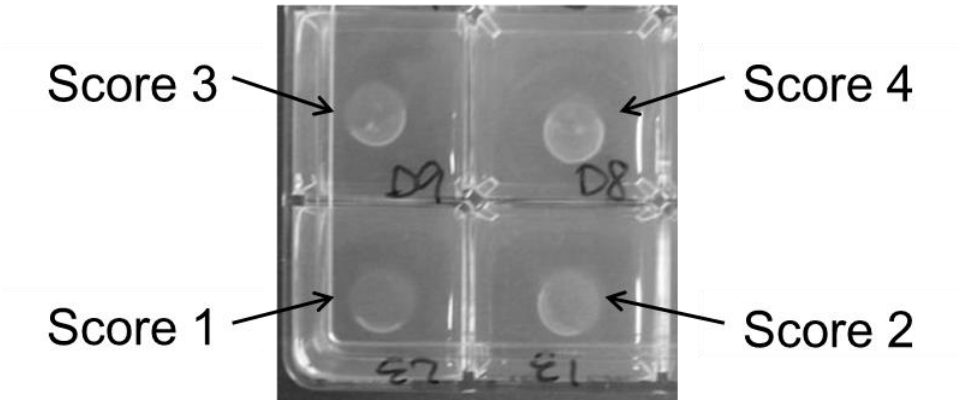

Nematode Gain of Toxicity (nGOT) screen

nGOT screens were performed on nematode growth media (NGM) agar in 25-well plates with 1ml of agar per well. BPF clones were prepared as described for aGOT.

To prepare the nematodes, adult worms were washed off maintenance plates with phosphate buffered saline (PBS) and the suspension was adjusted to 10 adult nematodes per 10µl drop. Drops were allowed to dry and plates were sealed with parafilm to prevent dessication.

As for aGOT, assay plates were incubated at 22-25°C and scored daily until bacterial mats were consumed, up to a maximum of 2 weeks. Mats of *E. coli* Ec100 were used as a comparative control. Toxicity was assessed qualitatively according to delay in

consumption of the bacterial mat. The same scoring system was used as that for aGOT. Fosmids which were consumed slowly (relative to the majority from the same batch) were counted as positive GOT hits. Positive hits were to be re-tested in the same manner with 10 replicate mats.

Insect Gain of Toxicity (iGOT) screen

iGOT screens were performed by injection of clones into *M. sexta* caterpillars (Figure 2.3). BPF library plates stored at -80 °C were sub-cultured into plates or universal tubes with 5 mL tubes of LB broth plus 25 µg/ml chloramphenicol. These were incubated overnight at 37 °C, shaking at 225-250rpm. The grown bacterial culture was used directly in iGOT assays.

Figure 2.3. A healthy *Manduca sexta* larva at the fifth-instar stage of development

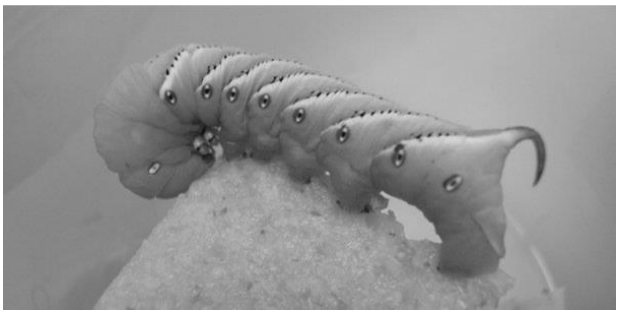

Larvae were reared as described in the Methods and Materials chapter (Chapter 2). Fresh fifth-instar larvae were anaesthetised on ice for 10 minutes, surface-sterilised with 70% ethanol, and injected using sterile insulin needles. A 100 µl dose of bacterial culture was injected into the haemocoel between the 2nd and 3rd last segment on each larva's side (one clone injected per larva). Larvae were then supplied with *Manduca* diet, incubated at 25 °C, and scored daily for signs of morbidity or mortality. *E. coli* Ec100 negative controls were also set up for each batch of fosmids tested. The health of caterpillars injected with this was used as a comparative negative control. As a positive control, larvae were injected with an *E. coli* Ec100 strain expressing the lethal Mcf1 (Makes Caterpillars Floppy) toxin from *Photorhabdus asymbiotica* ('Ec100 Mcf') (Waterfield *et al*. 2003).

Larvae were maintained and scored daily until they either died or reached the pre-pupation 'wanderer' stage of development, at which point they were euthanised by freezing at -20 °C.

Larvae were assessed by visual appearance and by response to physical stimulus (prodding or lifting with blunt tweezers). Notes were recorded regarding the amount of food eaten and the condition of faeces, if unusual. Scores were judged relative to the Ec100-injected controls, and ranged from 0 to 4 including half-scores (e.g. 2.5, 3.5 etc):

0 = No greater effect than that seen in typical negative controls

1 = A slight effect which could be temporary or perhaps not due to the injection, e.g. a slightly smaller size, a pale colour but otherwise active, slow response, little eating on day 1

2 = The larva was relatively healthy but there was a noticeable effect on development, or development was normal but there are indications of illness, e.g. a small size, not eating after day 1, some diarrhoea, melanisation, extremely pale or with a pinkish colouration, slightly shrunken appearance

3 = The larva was alive but obviously unwell or moribund, e.g. obviously shrunken / very small, severe diarrhoea, floppy, severe melanisation

4 = Dead. Notes were taken on the appearance/phenotypes of any dead larvae.

Fosmids which scored 4 were 'best' positives. Scores of 3 or 3.5 were 'higher possible' positives, scores of 2.5 were 'lower possible' positives, and some lower-scoring fosmids with interesting phenotypes such as unusual colouration were 'phenotype' positives. All fosmids scoring 2.5 or above were re-tested in 10 replicate larvae, and some phenotype positives were also retested.

Non-statistical analysis of RVA results

A genome coverage map plotting only 'hit' fosmids (according to their end-sequences) was created to assess visually whether the GOT positives clustered to any genomic regions in particular.

2.4.3. Statistical analysis of RVA results

Subsequently a statistical method was devised to determine whether the distribution of hits was any different to that expected by chance, taking into consideration the coverage of the genome in the fosmid library. Gene coding sequences (CDSs) were used as the data units: if a clone was a positive hit then every CDS within its insert would acquire one hit. A script was used to calculate which CDSs are located within each fosmid (written by A. Topham using C# and Visual C#2010). The input was a file containing all fosmid start and stop coordinates (from end-sequencing results) and a file containing all *B. pseudomallei* K96243 CDS start and stop base pair coordinates (from published annotations available via www.sanger.ac.uk).

The action of the script is outlined briefly:

Look at each row of a list of fosmids, one at a time;

For each fosmid, look at each row in a list of all the Bp CDSs;

For each CDS, if its chromosome matches the fosmid's chromosome,

AND its Stop bp >= the fosmid's Start bp,

AND its Start bp <= the fosmid's Stop bp,

Then that CDS is recorded as present within that fosmid;

Look at next CDS, and repeat.

The output recorded all CDSs within each fosmid. CDSs which straddled fosmid coordinate boundaries were included to compensate for the fact that some fosmids had only estimated coordinates at one end, and therefore to risk including false-positives rather than risk excluding true ones.

Re-determining library coverage

The script outputs were entered into a Microsoft Access database, and the data were interrogated to return counts of how many times each particular CDS was represented in fosmids, using data only from clones which had successfully grown and been tested in GOT screens. (961 clones could not be tested in one or more screens. In total 57,228 CDS representations were tested in aGOT and nGOT, and 57,170 in iGOT.) This formed the 'Coverage' data, i.e. the number of times each CDS was represented in testing.

Determining 'expected' hit values

GOT assay results were also interrogated to determine how many times each CDS had been hit in each screen. This formed the 'Observed Hit' data. The total number of hits and the total number of tested CDS representations was noted for each GOT screen and used to calculate average 'Hit Rates' (total hits / total representations). 'Expected Hit' values were calculated by multiplying each CDS's Coverage value by the average Hit Rate for that GOT screen.

Descriptive statistics of the data

The statistical analysis software SPSS was used to analyse the RVA data. First the GOT Coverage data and Observed Hit data were tested for their fit to the normal distribution, using a One-Sample Kolmogorov-Smirnov test. None of the distributions were normal, so non-parametric statistics were used for subsequent analyses. Correlation analyses were performed using Spearman's rho statistic.

Determining observed-to-expected hit values

Observed-to-Expected (Obs/Exp) Hit Ratios were calculated for the CDSs (using Observed Hit values divided by Expected Hit values). These values were used to identify CDSs which had been hit significantly more than the average (median) ratio among hits. This should highlight the most statistically convincing positives. To identify significantly 'over-hit' CDSs, the distribution of the ratios was analysed. CDSs which had received no actual hits were excluded from this analysis because they skewed the distribution towards zero and were not relevant for the purpose.

Obs/Exp Hit Ratios were calculated. iGOT hits were analysed as a whole (all hits) but also by progressively eliminating hit types (best, higher-possible, lower-possible, and phenotype). The qualitatively weakest hit categories were removed one at a time so that from one analysis the 'phenotype hits' were excluded, from the next both the phenotype and lower-possible hits were excluded, and finally only the 'best hits' remained. This was performed in order to assess whether similar results were seen among the different hit types.

Identifying a refined subset of hit CDSs

The data were analysed using SPSS's 'Ratio Statistic' to find the median values (with 95% or 99.9% confidence intervals) for each GOT screen's hits. [Despite its name the Ratio Statistic does not compute the desired output simply by entering Observed Hits as numerator and Expected Hits as denominator. Instead the calculated Obs/Exp Ratios must be entered as the numerator with the integer 1 as denominator].

Mapping refined hit regions

Using the upper-boundary values of the confidence intervals, CDSs with below average ratios were eliminated and the remainder were identified and mapped. In cases where two refined-hit CDSs flanked a relatively small 'non-significant' region (<10 kb between the start coordinates of the two CDSs), the entire region was included for the purposes of mapping. This was done in order to simplify visualising the significant regions, and was considered appropriate on the basis that: (i) around 30 CDSs are simultaneously counted as hit when a fosmid is positive, and there was uncertainty of some end-sequence data, so the results may not be accurate enough to specify single genes; and (ii) effects are likely to often be due to the activity of multiple genes in concert.

Summarising functional annotations of hits

Gene Ontology (GO) information was used to look for patterns in the functions of the refined hit genes. Biological Process GO data was originally downloaded from JCVI

[http://pathema.jcvi.org]. Many CDSs lacked GO annotations, so annotations from the Bp genome files (for the Artemis genome browser) were also used. The Artemis annotations include some additional functions and many similarities to known genes.

2.4.4. Relation to known and putative Bp virulence factors

The published literature was searched in order to collate a list of known and putative genes linked to Bp virulence. The Access database was used to cross-reference the list with the RVA refined hit genes. Genomic island data was cross-referenced in the same way (Holden *et al*. 2004). Particular attention was paid to genes that were also identified by the 'mGOT'-style macrophage assay using the same BPF library (and BAC clones) (Dowling *et al*. 2010).

2.4.5. Follow-up 1: Final re-resting of key positive hits

A selection of positive GOT hits were re-tested in insect larvae to determine if the effects were reproducible. Fosmids were selected on the basis of their hits in GOT screens and relevance to virulence factors cited in *Burkholderia* literature (Table 2.11). Some aGOT or nGOT hits were also re-tested in insect larvae, on the basis that: their published links to virulence could be relevant in the insect host; and the aGOT or nGOT assays showed problems with consistency between replicates during the earlier re-testing.

Table 2.11. BPF fosmids re-tested in insect hosts

Fosmid	Region of interest	CDSs of interest	Rationale for re-test
29d10	*kdpDE* and *kdpFABC* operons	*bspl1170-1175*	aGOT hit. KdpDE has links to virulence in many bacteria as reviewed in Appendix A (review article in press). Comparing 29d10 to 32e10 may reveal whether presence of the ATPase structural genes is necessary for a virulence-related effect
32e10	*kdpDE* (lacking *kdpFA*)	*bpsl1174-5*	
19e10	CHBP cyclomodulin gene	*bpss1385*	iGOT hit. CHBP is involved in host ubiquitination interference and immune evasion (Cui *et al*. 2010; Felgner *et al*. 2009; Jubelin *et al*. 2009; Yao *et al*. 2009). The fosmid also encodes a phospholipase D.
02e09	T6SS-6 operon	*bpsl3096-3108*	iGOT hit. Encodes a complete T6SS-6 operon
33e06	*irlRS* and sugar ABC transporter operon	*bpss0139-42*	iGOT and nGOT hits. Contains the Invasion-related locus regulatory genes (IrlRS) and adjacent ABC sugar transport operon which is up-regulated in macrophages (Chieng *et al*. 2012; Jones *et al*. 1997)

Both *M. sexta* and *G. mellonella* larvae were used as hosts. *M. sexta* injections were as described for iGOT. *G. mellonella* were injected with 10 µl, as described for chapter 4. For each fosmid clone, cultures were tested following growth either with or without auto-induction solution. 10 replicates were used in each case and the larvae were assessed daily for four days.

2.4.6. Follow-up 2: Preliminary fosmid RT-PCR results

RT-PCR was used to assess whether transcription of particular *Burkholderia* genes was occurring (and could be detected) in BPF fosmid clones. Genes selected for RT-PCR (shown in Table 2.12) were chosen on the basis of RVA results, known roles in virulence and non-virulence housekeeping roles.

Bp gene targets were in an *E. coli* background (Bp fosmids), so all primer pairs were checked for similarity to *E. coli* genomes and only the best pairs were used (those

predicted to have no *E. coli* matches or if unavoidable, where possible non-specific products would be of very different sizes to the expected Bp amplicon). BPF fosmid clones were prepared by culturing in LB overnight, plus or minus CopyControl™ Auto-Induction solution to increase copy number.

Table 2.12. Targets for RT-PCR (RVA targets in Bp/Ec fosmids)

Target	Bp CDS	BPF clone	GOT hit	Notes
MprA	*bpss1993*	05b11	nGOT	Evidence suggests this protein is expressed in fosmids
KdpD	*bpsl 1174*	29d10	aGOT	Sensor kinase of two-component system with links to virulence in many species
TC toxin	*bpsl 0590*	08d10		An 'mGOT'-style macrophage hit. TC toxins are known for links to invertebrate virulence
BylA	*bpss1269*	01d07	nGOT	Also an 'mGOT'-style macrophage hit. NRPS/PKS secondary metabolism
BimA	*bpss1492*	19b08	aGOT	Involved in actin mobility. Usually expressed intracellularly
BipD	*bpss1529*	08h02	nGOT	Part of the T3SS, involved in cellular invasion and escape
Pyoverdine/ ornibactin/ luxE NRPS	*bpsl 1777*	14d04	nGOT	Small molecule / NRPS secondary metabolism
CHBP cyclomodulin	*bpss1385*	19e10	iGOT	Up-regulated in macrophages, role in host actin and ubiquitination processes

Samples were taken from overnight grown bacterial cultures: RNA was preserved using RNAlater and stored at -20 °C. RNA was purified using the RNeasy Mini Kit (Qiagen) following the protocol for Animal Cells Using Spin Technology (for cells grown in suspension). Homogenisation with a blunt needle was not required as re-suspension by pipetting was sufficient. The optional on-column DNase digestion step was included (RNase-free DNase I; NEB). After problems with DNA contamination, samples were DNase digested a second time following Appendix C of the Qiagen MinElute Cleanup handbook but extending the incubation time to 1 hour:

≤87.5 µl RNA solution (contaminated with genomic DNA)
10 µl Buffer RDD
2.5 µl DNase I stock solution
Volume made up to 100 µl with RNase-free water

Purified samples were quantified using a Qubit® RNA BR Assay Kit (Invitrogen) and stored at -20 °C (-70 °C for longer term). RT-PCR was performed using the Access RT-PCR Kit (Promega). This method completes both the RT and PCR reactions in one tube; one target is amplified (i.e. with one set of specific PCR primers) per tube. The reaction mix was as follows:

Nuclease-free water (to final 50 µl)
10 µl reaction buffer (5X)
1 µl dNTP mix (10mM each dNTP)
Forward primer (50 pmol)
Reverse primer (50 pmol)
2 µl MgSO4 (25 mM)
1 µl AMV reverse transcriptase* (5u / µl)
1 µl Tfl DNA polymerase (5u / µl)
RNA template (25 ng)
Total 50 µl

*Control reactions omitting the reverse transcriptase enzyme were included to detect any DNA contamination. Reaction samples were visualised by gel electrophoresis (1.5% TAE agarose gels).

Thermo-cycling conditions:

45 °C	45 min	reverse transcription	
94 °C	2 min	RT inactivation, denaturation	
94 °C	30 sec	denaturation	40 cycles
** °C	1 min	annealing	
68 °C	2 min	extension	
68 °C	7 min	final extension	
4 °C	∞	soak	

**Annealing temperatures are shown in Table 2.13. The first seven cycles used touch-down annealing temperatures, decreasing 1 °C per cycle until the calculated annealing temperature, which was used for the remaining 33 cycles.

Table 2.13. Primers for fosmid RT-PCR

Target	Primer sequence (5'-3')	Calculated annealing temp. (°C)	Touch-down temp. range (°C)	Size (bp)
MprA	BpMprA_fwd GAGCAATGGGGCTACTTCAA BpMprA_rev CTCGGGATATCGGAGATGAA	51.3	57 - 50	173
KdpD	BpKdpD_fwd GACGTCTACACGAGCGTCAA BpKdpD_rev GCCATGTAGACCTTGCCTTC	53.4	59 – 53, 61 - 54	188
TC toxin	BpTcTox_fwd AAGACGTTCCTGTCGTTCGT BpTcTox_rev GCCGATGTTCAGGAAGTTGT	51.3	57 - 50	240
BylA	BpBylA_fwd GCTGTGGGAAAACTTGCTGT BpBylA_rev TGATTGAAGACGCTCGACAC	51.3	57 - 50	150
BimA	BpBimA_fwd GCGTGTAACCGAGGACGTAG BpBimA_rev ATGGTCCTTCGGACCTTTTC	51.3	57 - 50	234
BipD	BpBipD_fwd GGACTACATCTCGGCCAAAG BpBipD_rev ATCAGCTTGTCCGGATTGAT	49.3	55 - 48	201
Pyoverdine/ ornibactin/ *luxE* NRPS	BpNRPS_fwd GGAGCTGTCGTCGTTCTACC BpNRPS_rev GGATATGTCGAACGCATGG	51.3	57 - 50	247
CHBP cyclomodulin	BpCHBP_fwd AACAACGTCGGAAAAACTGG BpCHBP_rev TGAAATGATCGGCGTTATCA	47.2	53 - 46	183

2.4.7. Follow-up 3: Investigating *Burkholderia kdpD*

Attempts to construct a knock out (KO) strain

Several attempts were made to construct vectors for the generation of deletion mutations in the *kdpDE* operon of Bt E264, Bt CDC 272 or Bt CDC 301. Techniques used in the KO attempts and the strategies used are described below.

Genomic DNA extractions: Bacterial genomic DNA (gDNA) extraction was performed using the DNeasy® Blood & Tissue Handbook (Qiagen) according to manufacturer's instructions. From overnight cultures of the Bt strains, 500 µl was pelleted and processed according to the "cultured cells" sub-section of the kit protocol. A proteinase K step was

incubated for 3 hours. Purified gDNA samples were run on a 0.8% TAE gel and quantified using Qubit® BR DNA Assay (Invitrogen).

Polymerase Chain Reaction (PCR): For approach #1 Pfu high-fidelity polymerase was used (Promega). A typical reaction mixture was:

5 µl Pfu polymerase buffer (10X)
1 µl forward primer (25 pmol/µl)
1 µl reverse primer (25 pmol/µl)
1 µl dNTPs mix (10 mM)
1 µl genomic DNA (100 ng)
0.5 µl Pfu polymerase (2-3 units/µl)
40.5 µl distilled water
50 µl total

Typical thermo-cycling conditions for Pfu polymerase:

95°C	1 min	denaturation	
95°C	1 min	denaturation	30 cycles
X °C	30 sec	annealing	
72°C	2 min per kb	extension	
72°C	10 min	final extension	
4°C	∞	soak	

For approaches based on #2 Phusion™ proof-reading polymerase was used (New England Biolabs). A typical reaction mixture was:

4 µl GC polymerase buffer (5X)
1 µl forward primer (25 pmol/µl)
1 µl reverse primer (25 pmol/µl)
0.4 µl dNTPs mix (10 mM)
0.4 µl DMSO
0.5 µl genomic DNA (100 ng)
0.2 µl Pfu polymerase (2-3 units/µl)
12.5 µl distilled water
20 µl total

Typical thermo-cycling conditions for Phusion polymerase:

98°C	30 sec	denaturation	
98°C	10 sec	denaturation	35 cycles
X °C	25 sec	annealing	
72°C	20 sec per kb	extension	
72°C	10 min	final extension	
4°C	∞	soak	

Agarose gel electrophoresis: For gel electrophoresis of PCR products gels were prepared with 1% or 1.5% (w/v) agarose in 1X TAE buffer, with ethidium bromide. Gels were typically run at 100V for 30-60 minutes.

Restriction digestions: Restriction enzymes (New England BioLabs) were used according to the manufacturer's guidelines, typically in total reaction volumes of 20-45 µl. Vector DNA was digested for 2-3 hours and insert (PCR product) DNA was digested for 3-6 hours. Cut DNA was purified after each digestion reaction.

DNA purification methods:

Different DNA purification methods are detailed in Table 2.14.

Table 2.14. Methods used for DNA purification

DNA type / source	Method
Bacterial genomic DNA	DNeasy Blood and Tissue Kit (QIAGEN); according to manufacturer's instructions
Plasmid DNA	Plasmid Spin Mini-prep Kit (QIAGEN); according to manufacturer's instructions
PCR reactions	PCR Purification Kit (QIAGEN); according to manufacturer's instructions
DNA of particular sizes	Gel electrophoresis followed by gel extraction kit (QIAGEN); according to manufacturer's instructions

KO approach #1: Based on a method successfully used at Dstl Porton Down (Norville 2011) to KO genes in Bt, whereby the two flanking regions of the gene to be knocked out are amplified by PCR and each cloned into separate cloning vectors. Each flank is then digested, the two flanks are ligated together, and the joined construct is re-ligated back into a vector, which is transformed into electrocompetent *E. coli*. This allows multiple steps where the PCR or ligation products can be confirmed by PCR or sequencing.

- Primer design: Primers were designed to amplify ~500bp regions upstream and downstream of the target gene, including the start (left flank) and stop (right flank) codons, with appropriate restriction sites designed into the primers (See Table 2.15 for sequences).
- Generation of an unmarked deletion construct: Each flank was amplified by PCR and cleaned up. PCR products were quantified using Qubit® dsDNA assays (Invitrogen).

This approach was not completed past this point but the next steps would have been to:

- Add A-overhangs and clone each product into separate pDrive cloning vectors. Transform each into EZ competent *E. coli* (Qiagen), pick colonies and confirm sequences of each. Digest each flank and clean-up. Ligate cut flanks together. Ligate the joined construct into pDrive vector. Transform into EZ competent cells. Confirm by PCR and sequencing.
- Create pDM4-LFRF deletion construct
- Transform the construct into DH5α cells
- Transform into S17-1 λpir cells (conjugation strain)
- Conjugate pDM4 into Bt E264
- Sucrose counter-selection for loss of suicide plasmid

Table 2.15. Primers for *kdpD* KO in Bt: approach #1

Primer	Sequence (5'-3')	Annealing temp. for Pfu polymerase (°C)	Restriction site
KdpD LF_F:	ACTAGTACTCAATCTCGCGCTCGAC	64.6	SpeI
KdpD LF_R:	ATAGATCTTCTTGTCGAGAAGCTGGTCA	63.7	BglII
KdpD RF_F:	TAAGATCTCCGTATCCAACGAACATCC	63.4	BglII
KdpD RF_R:	ACTAGTACTTCACGACCGGCGATTC	64.6	SpeI

KO approach #2: Based on a method successfully used at the University of Exeter, this approach is simplified in terms of cloning and ligation steps. Instead of putting each PCR flank into a separate vector (as with approach #1) the two purified PCR products resemble each other at the 3' end and are used as a mixed template for a crossover PCR. The crossover product is cloned into the pDM4 plasmid. Additional Bt strains (CDC 272 and CDC 301) were also used as those strains reportedly have a higher KO success rate (unpublished; personal correspondence). All three Bt strains were 100% identical in the nucleotide region relevant for the KO primers.

- Primer design: Primers were designed to give 600bp flanking fragments (including the start and stop codon of *kdpD*, respectively) which would complement each other. A hexameric restriction site was included in the overlapping region (which can be used for restriction analysis) and two different sites at the ends were suitable for cloning into the pDM4 vector. One site used (XbaI) is dam-methylation sensitive but the methylation sequence was confirmed as absent. See Table 2.16 for sequences.

Table 2.16. Primers for *kdpD* KO in Bt: approach #2

Primer	**Sequence (5'-3')**	**Annealing temp. for Phusion polymerase (°C)**	**Restriction site**
Bt_D#1-fw:	CC ACT AGT CGT ACA ACG CGG CGG GCT C	72	SpeI
Bt_D#2-rv:	GTC GGT TCA TCT AGA CAT GCG AGG CCG AAG TCT CCG G		XbaI
Bt_D#3-fw:	CCT CGC ATG TCT AGA TGA ACC GAC CGT CAC CGT CGT	72	XbaI
Bt_D#4-rv:	G CCC GGG GCC ATG TAG ATT CGC AGG TAG T		XmaI

- PCR amplification: See Figure 2.4. Upstream and downstream fragments were amplified by PCR using primers 1&2 and 3&4, respectively, and genomic DNA of target organism as template. The crossover PCR used ten-fold-diluted PCR products from the 1st PCR as a template and the outside primers 1&4, which should give a 1.2 kb PCR fragment.

Figure 2.4. PCR approach for gene deletion (image courtesy of C. Müller, University of Exeter)

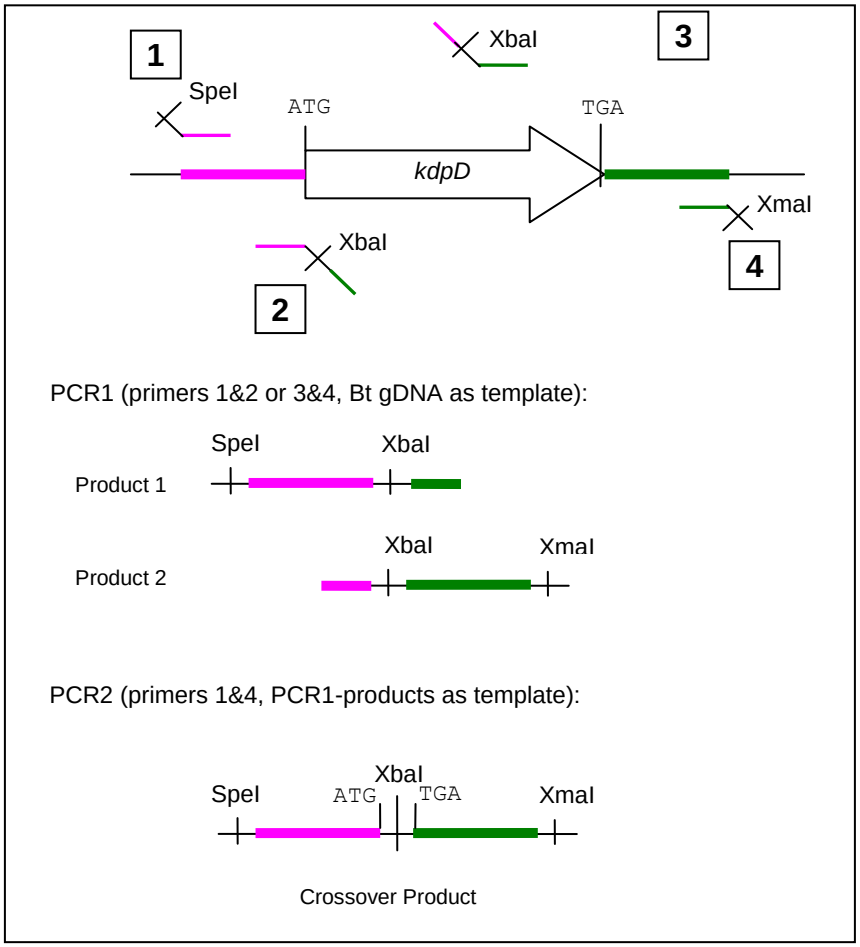

This approach was not completed past this point but the next steps would have been to:

- Digest the pDM4 plasmid and recombinant PCR product with appropriate enzymes (SpeI and XmaI) and ligate the fragments together using T4 DNA ligase. Transform *E. coli* DH5α λpir with the ligation mix and select for Cm^R clones. Check the resulting plasmids by PCR and restriction digest pattern or sequencing, and transfer correct plasmids into *E. coli* S17 λpir by electroporation.
- Conjugation to integrate suicide plasmid construct into chromosome
- Sucrose counter-selection for loss of suicide plasmid
- Confirm mutant by PCR and sequencing

KO approach #2.1: This used the same approach as #2 but with new primers. The left flank primers were re-designed to lower the annealing temperature (Table 2.17). The right flank XmaI site (GGGCCC) was replaced with a SacI site (GAGCTC) to attempt to reduce perceived difficulties with primer structures and to lower the annealing temperature closer to that of Bt_D#1-fw.

Table 2.17. Primers for *kdpD* KO in Bt: approach #2.1

Primer	Sequence (5'-3')	Annealing temp. for Phusion polymerase (°C)	Restriction site
Bt_D#1-fw:	CC ACT AGT AAC GTG CTG AAA CTC AAT CT	70	SpeI
Bt_D#2-rv:	GAT AC TCT AGA CAG CAT CGC ATA GGT CTT		XbaI
Bt_D#3-fw:	ATG CTG TCT AGA GTA TCC AAC GAA CAT CC	72	XbaI
Bt_D#4-rv:	G GAG CTC TCA GAT GCA CGA CCT C		SacI

KO approach #2.2: This used the same approach as #2 but with new primers again (Table 2.18). The size of the flanking regions was increased to ~800bp following advice that 600bp would not be long enough either side of the deletion to easily allow double cross-over into the chromosome.

Table 2.18. Primers for *kdpD* KO in Bt: approach #2.2

Primer	Sequence (5'-3')	Annealing temp. for Phusion polymerase (°C)	Restriction site
BtD_LF1:	CC ACT AGT CAT CGA GAA GGA CGG CAAG	66	SpeI
BtD_LF2:	TAC GGG TCT AGA GAG CAG CAT CGC ATA GGT CTT	66	XbaI
BtD_RF3:	CTG CTC TCT AGA CCC GTA TCC AAC GAA CAT CC	66	XbaI
BtD_RF4:	G GAG CTC ATG ACG AGC GGA AAT TGG AG	66	SacI

Attempts to over-express kdpDE

In order to try a different molecular approach, attempts were also made to over-express *kdpDE* using a *groS* promoter. The plasmid pBHR4-groS-RFP expresses RFP (red fluorescent protein) under the control of the *groS* promoter. The RFP gene would be replaced with the Bt *kdpDE* genes and the plasmid would be transformed into *E. coli* DH5α.

- **Primer design:** Primers were designed to amplify both the *kdpD* and *kdpE* genes from Bt in case proximity of the two proteins is necessary for *kdpE* activation (Table 2.19). A SpeI site was engineered adjacent to the start of *kdpD* in the forward primer so that the insert would be close to the *groS* promoter. (The primer was particularly long because a second site was also included which may have

been used for a TOPO cloning method, which was not used). The reverse primer was 154-173 bp downstream of the *kdpE* stop site.

Table 2.19. Primers for *kdpDE* over-expression construct

Primer	Sequence (5'-3')	Annealing temp. for Phusion polymerase (°C)	Restriction site
BtDE comp Fw:	AAGTGGTACCAGGAGGTAACTAGTATGAATCGTCC CGATCCTG	65	SpeI
BtDE comp Rv:	AATAGGATCCGAATGACGACGAACGACGAT	65	BamHI

- **PCR of *kdpDE* from Bt:** Phusion polymerase was used as described above to amplify the 3.97kb region from Bt gDNA. For the annealing step a gradient from 62 – 72 °C was used. Reactions were analysed on 1.5% TAE gels; 71.8°C was selected as the optimal annealing temperature and PCR was repeated. The corresponding band was excised and cleaned up using a gel extraction kit (Qiagen).
- **Digestion of vector and insert:** pBHR4-groS-RFP DNA was purified using a Plasmid Spin Mini-prep Kit (Qiagen). The purified vector and *kdpDE* insert were digested with SpeI-HF and BamHI-HF enzymes (NEB) at 37 °C for 2 hours and 6 hours respectively. The cut insert was purified on a PCR purification column (Qiagen). The cut vector was run on a gel to confirm two separate fragments were seen and to excise and gel-extract the 5.65 kb band. Samples of purified vector and insert were run on a gel to compare DNA concentration.
- **Ligation and transformation:** T4 DNA ligase (NEB) was used for ligation of sticky-ended DNA fragments, with a vector (µg) : insert (µg) ratio of approximately 1:3 in a total reaction volume of 20 µl. Following manufacturer's instructions, reaction components were assembled on ice, mixed well prior to ligase addition, and then mixed gently. Alongside vector-insert ligation reactions, a control reaction lacking insert DNA was also set up to check for re-ligation of the vector backbone. Reactions were incubated at room temperature for 2 hours, and immediately transformed into competent cells. EZ Competent Cells (Qiagen) were used for heat-shock transformation of ligated cloning constructs. One 50 µl aliquot of cells was thawed on ice per transformation, and 1 µl of ligation reaction was added. Cells were gently mixed by flicking, and incubated for 5 minutes on ice, then 30 seconds in a 42 °C water bath, and then back on ice for 2 minutes. 250µl SOC media was added per tube, and tubes were incubated shaking at 37 °C for 30

minutes. 100 µl and 200 µl samples were spread onto LB plates with 50 mg/mL chloramphenicol (or no selection for a control), and incubated at 37 °C overnight.

No transformants were seen but the next step would have been to prepare plasmid DNA from transformants and confirm by restriction mapping or sequencing.

Preliminary RT-PCR of fosmid kdpD in response to host

RT-PCR of the *kdpD* gene was performed on two fosmids: fosmid 29d10 which contains the two complete operons for the Kdp potassium ATPase (*kdpFABC* and *kdpDE)*, and fosmid 32e10 which is incomplete in the structural operon (lacking *kdpFA)*.

To discover whether the *kdpD/kdpE* genes were differentially transcribed after injection into the insect host, RT-PCR of the *kdpD* target was performed using RNA samples collected before and after exposure. The same cultures from which the RNA samples were prepared (inoculum samples) were also used to inject *M. sexta* larvae (4 larvae per condition). 30 minutes post-injection the larvae were bled and RNA was prepared from the pooled haemolymph. RNA samples were processed and DNase digested twice as described earlier. RT-PCR of the *kdpD* gene was performed as described earlier.

Chapter 3. *Burkholderia* infection assays in *Manduca sexta*

3.1. Chapter summary

The major aim of the work described in this chapter was to investigate the virulence of several *Burkholderia* species and strains in *M. sexta* by injection directly into the haemocoel or by feeding. It was observed that *B. pseudomallei* (Bp) and *B. thailandensis* (Bt) were virulent by injection, which agrees with reported virulence in *Galleria mellonella*. Unexpectedly, *B. oklahomensis* (Bo) strains were also virulent, which has not been reported from any animal infection models so far. In fact the relative virulence of Bp, Bt and Bo was reversed in *M. sexta* compared to reports from mammalian or other insect models, with Bo strains being amongst the most virulent. Infections were repeated in *G. mellonella* maintained at both 37 °C and 25 °C to determine whether that observation reflects differences in the host systems or is primarily related to temperature. The results indicated that there may be host-specific differences, but were not conclusive and further investigation will be required.

No previous publications have reported feeding Bp, Bt or Bo to lepidopteran hosts. Bt and Bo were virulent to *M. sexta* neonates via the oral route of infection, although variability was observed between experiments with Bt. Based on the ability of cell-free Bo supernatant to kill the larvae or prevent normal growth our findings support previous suggestions that *Burkholderia* secrete diffusible toxic or paralytic agents which are active against invertebrates.

3.2. Introduction

Until recently there was negligible published evidence regarding the virulence of Bp-group pathogens in invertebrates. Host models of infection are an invaluable tool for the study of bacterial pathogens. Infection in a good model host mirrors that seen in the host of interest (e.g. humans) in terms of the level of virulence, the mechanisms of pathogenesis, and/or the similar attenuating effects of mutations in key genes. Therefore they provide a safe and suitable way to evaluate virulence of related species, potential attenuating mutations, or the protective effects of vaccine candidates.

The aims of the work described in this chapter were to: (i) investigate the virulence of several *Burkholderia* species and strains in *M. sexta*; (ii) test the virulence of mutant

strains which display attenuation in other hosts; and (iii) challenge *M. sexta* with *Burkholderia* orally to investigate a more ecologically plausible route of infection.

Aim: Assessing *Burkholderia* virulence in *Manduca sexta*

Following preliminary tests in *M. sexta* with the Bt type strain E264, dose response injection assays were also performed with Bp K96423, two other Bt strains and two Bo strains. These same strains of Bp, Bt, Bo have previously been tested in *G. mellonella* and the results were reported to generally compare well in that model with the virulence observed in BALB/c mouse models, as shown in Table 3.1 (Wand *et al*. 2011; Titball *et al*. 2008; DeShazer 2007). In those models Bp was the most virulent species and Bo was the least. These results will be compared to those from *M. sexta* regarding the relative virulence of these same species and strains.

Table 3.1. Comparative virulence of *Burkholderia* strains in the *G. mellonella* model versus the mouse. Median Lethal Dose (MLD) or % survivors were reported from BALB/c mice after intra-peritoneal injections (Titball *et al*. 2008; DeShazer 2007). *G. mellonella* were injected with 10^2 colony forming units (CFU; 10µl at 10^4 CFU /ml); % survivors and growth of bacteria in the insects are shown (Wand *et al*. 2011). Strains are ranked in order of observed virulence in those studies.

Isolate	Virulence in mouse (Titball 2008; DeShazer 2007)	Ranked virulence in mouse	Virulence in *G. mellonella* (10^2 CFU dose: 10^4 CFU /ml) (Wand 2011)		Ranked virulence in *G. mellonella*
			Larvae surviving to 24hrs post-injection	Bacteria in haemocoel at 20hrs post-injection	
B. pseudomallei					
K96243	MLD = 262 CFU	1	0 %	~$6x10^6$ CFU /ml	1
B. thailandensis					
E264	10% survivors at 10^7 CFU	2	50 %	~$4x10^5$ CFU /ml	4
CDC 301	80% survivors at 10^7 CFU	3	0 %	~$2x10^6$ CFU /ml	=2
CDC 272	100% survivors at 10^7 CFU	4	0 %	~$3x10^6$ CFU /ml	=2
B. oklahomensis					
C6786	100% survivors at 10^7 CFU	=5	100 %	~$2x10^4$ CFU /ml	=5
E0147	100% survivors at 10^7 CFU	=5	100 %	~$3x10^4$ CFU /ml	=5

Aim: Testing attenuated Bt mutants in *Manduca sexta*

Mutant Bt strains which have been demonstrated to be attenuated in other infection models were also tested in the *M. sexta* model in order to confirm whether the same attenuating effects were seen. Two mutant strains were available: a *surA* mutant and a

Twin-Arginine Transport (TAT) system mutant, which are both discussed in the main introduction. Briefly, both mutants had been seen to be attenuated in the *Galleria mellonella* model (I. Norville and S. Wagley respectively, unpublished results).

Aim: Feeding *Burkholderia* to *Manduca sexta*

Finally, the effect of *Burkholderia* infection via the digestive route will be investigated, as ingestion of contaminated plant material is likely to be the most common route of insect infection with *Burkholderia* in the natural environment. Bt E264 and Bo C6786 were fed to *M. sexta* larvae and the results were compared to the effects of feeding Epi300 *E. coli* or LB controls.

3.3. Results

3.3.1. Confirmation of *Burkholderia* pathogenicity to invertebrate hosts

The first step was to confirm that Bt E264 (and by extrapolation, Bp K96423) was pathogenic to the invertebrate model hosts used in Rapid Virulence Annotation (RVA; the subject of Chapter 5). RVA detects an increase in toxicity/pathogenicity/virulence (or repellent factors) in otherwise harmless *E. coli* clones expressing portions of the genome of a pathogenic bacterium. Therefore, pathogenicity of the whole bacterium in *M. sexta,* and the ability to survive or avoid predation by *Caenorhabdus elegans* and *Acanthamoeba polyphaga,* is a pre-requisite for RVA testing. Bp K96423 was to be the subject of RVA but on the basis of their genetic similarity and the lower containment requirement Bt E264 was used for these preliminary tests instead.

Caenorhabditis elegans pathogenicity / predation avoidance

As expected (based on published results, discussed in the introduction), Bt E264 was lethal to *C. elegans*. Plates were maintained at room temperature. Control plates with *E. coli* OP50 were fully consumed by 3 days after seeding with nematodes, and the worms were seen to be active on every day assessed. However, on plates with Bt E264 no nematode activity was seen even 1 day after seeding. The Bt lawn was thick and not all nematodes were visible; those that were visible were motionless. By day 7 the mats had still not been consumed and no nematode movement (or tracks across the plates) had been observed. Therefore the nematodes were not consuming or were not surviving consumption of Bt E264.

Acanthamoeba polyphaga pathogenicity / predation avoidance

Plates were maintained at room temperature. Control plates seeded with *E. coli* were readily fed upon by the amoebae: on PAS minimal medium all the *E. coli* mats were fully consumed by the amoebae by day 4; on PYG nutrient medium there was a very slight *E. coli* dose response effect (see Table 3.2), with the most amoebae ($2x10^5$ per ml) eating the least bacteria (OD_{600} 0.0313) by day 5, and the least amoebae eating the most bacteria by day 6. However, the Bt E264 mats were not consumed at all on either agar type or with any amoeba concentration, even by day 13. Therefore the amoebae were not consuming or were not surviving consumption of Bt E264.

Table 3.2. Rate of *A. polyphaga* feeding upon *E. coli* Epi300 mats on PYG agar (showing 'day started'-'day completed'). The amoebae fed readily upon the *E. coli* controls. Results for Bt E264 are not shown as the mats were not consumed within 13 days' testing, indicating that Bt E264 is not consumed or is harmful to *A. polyphaga*.

		***E. coli* Epi300 (OD_{600})**				
		0.5	**0.25**	**0.125**	**0.0625**	**0.0313**
***A. polyphaga* (cells per ml)**	**$2.0x10^5$**	Day 5-6	Day 5-6	Day 4-5	Day 4-6	Day 4-5
	$1.0x10^5$	Day 5-6	Day 4-5	Day 4-5	Day 4-5	Day 4-5
	$5.0x10^4$	Day 5-6	Day 5-5	Day 5-5	Day 4-6	Day 4-5
	$2.5x10^4$	Day 5-6	Day 5-6	Day 5-6	Day 5-6	Day 5-5
	PYG only	Not eaten	Not eaten	Not eaten	Not eaten	Not eaten

Manduca sexta pathogenicity (experiment #1)

Initial experiments to look at the pathogenicity of Bt E264 in *M. sexta* used low numbers of insects (n = 3) simply to determine whether the bacterium was pathogenic and, if so, to roughly gauge the dynamics of the infection. Insects were maintained at 25 °C pre- and post-injection. A series of OD_{600} cell densities was initially tested as inoculum. Table 3.3 shows the results.

Table 3.3. Results of initial Bt E264 injections in *Manduca sexta.* Epi300 = *E. coli* Epi300. O/n culture = overnight culture. P = paralysis. D = death. Bt E264 was lethal at all doses tested, with a dose responsive effect. A paralysis phase preceded death.

	OD_{600}	CFU	Replicate	20 hr	24 hr	48 hr	120 hr
Bt E264	O/n culture	$1.53x10^8$	1	P	D		
			2	P	D		
			3	P	D		
	0.250	$1.46x10^7$	1	OK	P	D	
			2	OK	P	D	
			3	OK	P	D	
	0.125	$8.40x10^6$	1	OK	P	D	
			2	OK	P	D	
			3	OK	P	D	
	0.063	$4.95x10^6$	1	OK	P	D	
			2	OK	P	D	
			3	OK	OK	D	
	0.031	$1.90x10^6$	1	OK	OK	D	
			2	OK	OK	D	
			3	OK	OK	D	
Epi300	0.250	$3.59x10^7$	1	OK	OK	OK	OK
			2	OK	OK	OK	OK
			3	OK	OK	OK	OK
LB only			1	OK	OK	OK	OK

White cell = insect alive and well. Light grey, P = alive and paralysed. Dark grey, D = dead.

All *E. coli* and LB-injected controls remained healthy at 120 hours post-injection. Undiluted overnight culture of Bt E264 killed all three larvae by 24 hours and the diluted samples all killed by 48 hours. The progression from an outwardly healthy appearance to death included a paralysis phase where movement was extremely limited or involved uncoordinated spasms. With the undiluted overnight culture the progression from paralysis to death was rapid (<4 hours). In summary, Bt E264 was lethal to *M. sexta* at all doses tested, with a dose responsive effect. A paralysis phase preceded death.

3.3.2. *Manduca sexta* as a *Burkholderia* infection model

Unless otherwise stated, all *Manduca sexta* were maintained at 25 °C before and after injection with bacteria (which was incubated overnight at 37 °C).

Dose response #2: Bt E264

Having established that Bt E264 was pathogenic to *M. sexta*, a wider and lower range of doses was tested.

Table 3.4 shows the survival of insects injected with different doses, over six days. The dose responsive effect was more apparent with this wider range of doses compared to dose response #1. Subsequent Bt injections used greater numbers of insects, and replicates, for improved reliability and statistical significance.

Table 3.4. Numbers of larvae surviving Bt E264 infection (*n* = 5) over six days.Epi300 = *E. coli* Epi300. Various doses were tested and a dose responsive effect was observed in the time to death.

Strain	CFUs injected (in 100µl)	Day 1 24 hrs	Day 2 48 hrs	Day 3 72 hrs	Day 4 96 hrs	Day 5 120 hrs	Day 6 144 hrs
Bt E264	$2.30x10^1$	5	5	5	5		1
	$2.20x10^2$	5	5	5	0		
	$1.90x10^3$	5	5	3	1		0
	$2.20x10^4$	5	5	0			
	$2.00x10^5$	5	0				
Epi300	$3.80x10^5$	5	5	5	5		5

Hatched cells indicate no data available. Light grey = <100% alive. Dark grey = 0% alive.

Figure 3.1 depicts the calculated median times to death (MTTDs) for the different doses. The 10^3 CFU dose shows a standard error (SE) of the median because the point at which half of the insects died (2.5 insects) lies between 72-96 hours; at the other doses the SE was zero because ≥2.5 of the insects had died by the same day. The dose responsive effect is evident. MTTDs ranged from 48-144 hours post-injection.

Figure 3.1. Median Time to Death (MTTD) for different Bt E264 doses. Error bars show SE of the median.

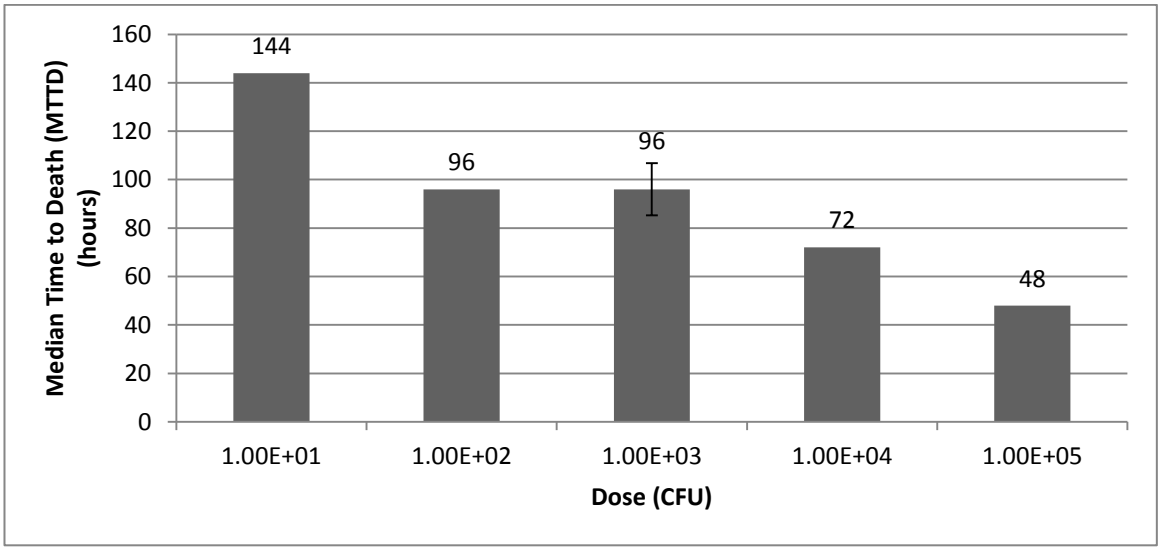

Figure 3.2 is a Kaplan-Meier survival curve for the Bt E264 doses; the curves start at 1.0 and drop down the *y*-axis (cumulative survival) as the insects die; the point at which the curve ends indicates the number of surviving insects at the end of the assessment. In cases where insects survive the Kaplan-Meier survival curve line displays a small cross, which is described in the key as a 'censored' case. Confirming what was shown in figure 10, Bt E264 shows a dose-responsive lethal effect; the curves drop off sooner at higher doses and at the lowest dose the cumulative survival is 0.2 (one insect survived).

Figure 3.2. Kaplan-Meier survival curve for Bt E264 doses injected into *M. sexta*. The curves start at 1.0 (all alive) and drop down the y-axis (cumulative survival) as the insects die. The point at which the curve ends indicates the number of surviving insects at the end of the assessment. In cases where insects survive, the curve line displays a small cross which is described in the key as a 'censored' case. Survival curves drop quickly to zero at high doses of Bt E264. At 10^1 CFU Bt E264 one insect (0.2 of the total) survives to 140 hours post-injection.

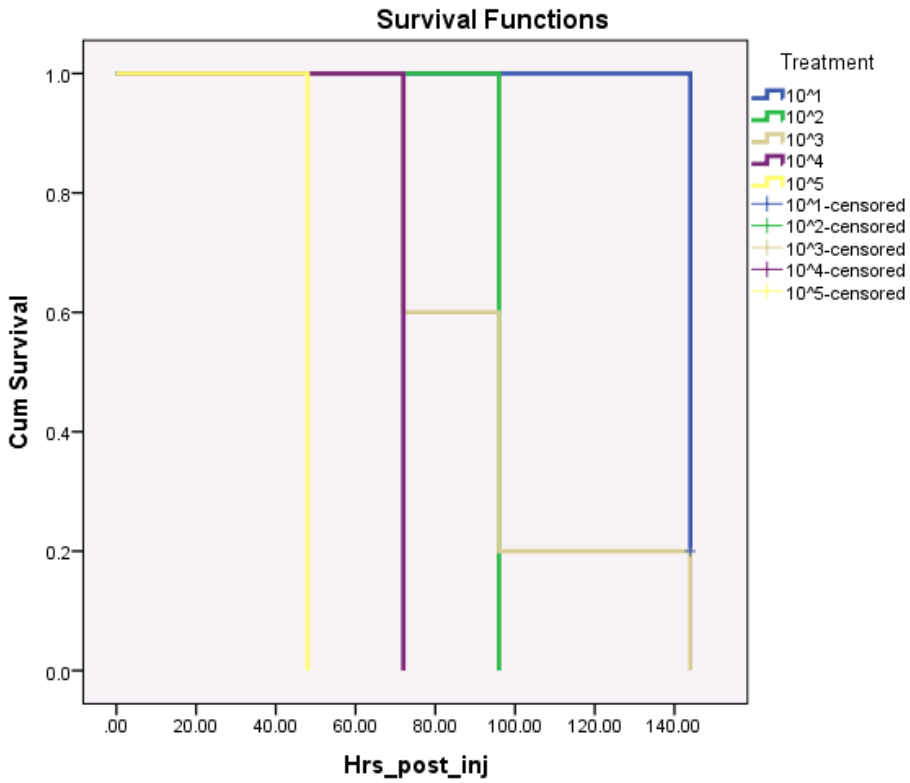

As shown in Table 3.5 log-rank (Mantel-Cox) tests performed as part of the Kaplan-Meier analysis revealed that the 10^3 CFU dose gave a statistically similar larva-survival profile to the 10^2 CFU dose ($p = 0.649$) but the differences between all other combinations of doses were significant ($p \leq 0.05$).

Table 3.5. Log-rank (Mantel-Cox) pairwise comparisons between Bt E264 doses. NS = not significantly different, * $p \leq 0.05$, ** $p \leq 0.01$, *** $p \leq 0.001$

Bt E264 dose	Bt E+01	Bt E+02	Bt E+03	Bt E+04	Bt E+05
Bt E+01		**	*	**	**
Bt E+02	**		NS	**	**
Bt E+03	*	NS		*	**
Bt E+04	**	**	*		**
Bt E+05	**	**	**	**	

Dose response #3: Bp K96423

Following the initial Bt E264 experiments, *M. sexta* larvae were injected with Bp K96423 in appropriate containment facilities. This served to confirm whether Bp K96423 was in fact virulent to *M. sexta* and therefore suitable for RVA testing (in chapter 5), rather than relying on extrapolation based on the virulence of Bt E264.

Figures 3.3-3.5 show representative photographs of Bp-infected larvae or controls.

Figure 3.3. Representative larvae injected with controls, on day 6 post-injection. Both are healthy wanderer stage larvae.

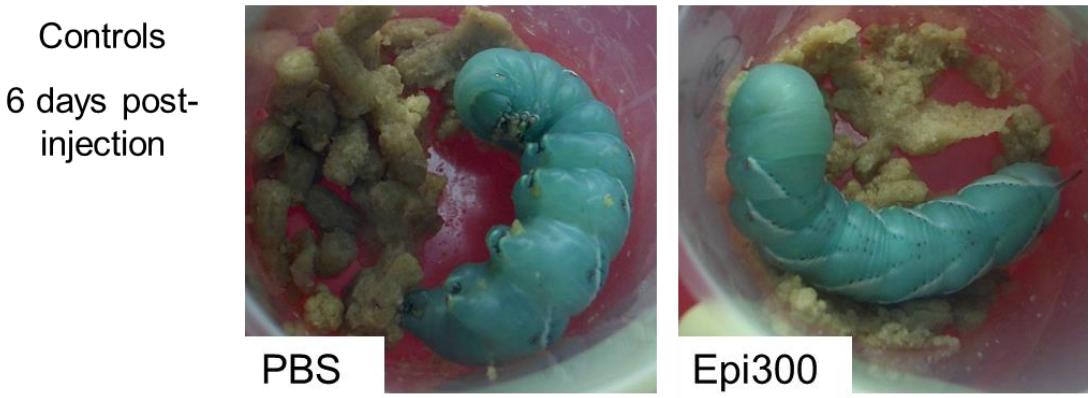

Figure 3.4. *M. sexta* larvae injected with Bp K96423 (various doses or heat-killed cells), on day 3 post-injection. These larvae were representative of those that succumbed to Bp infection, which was not the case for all larvae. A positively-correlated dose-responsive effect on insect morbidity is evident. With 20 live CFU or 200,000 heat-killed CFU the larva is healthy. With 20,000 live CFU the larva is small and slightly shrunken larva. With 200,000 live CFU the larvae is dead, with a shrunken appearance, discolouration, and little evidence of having eaten.

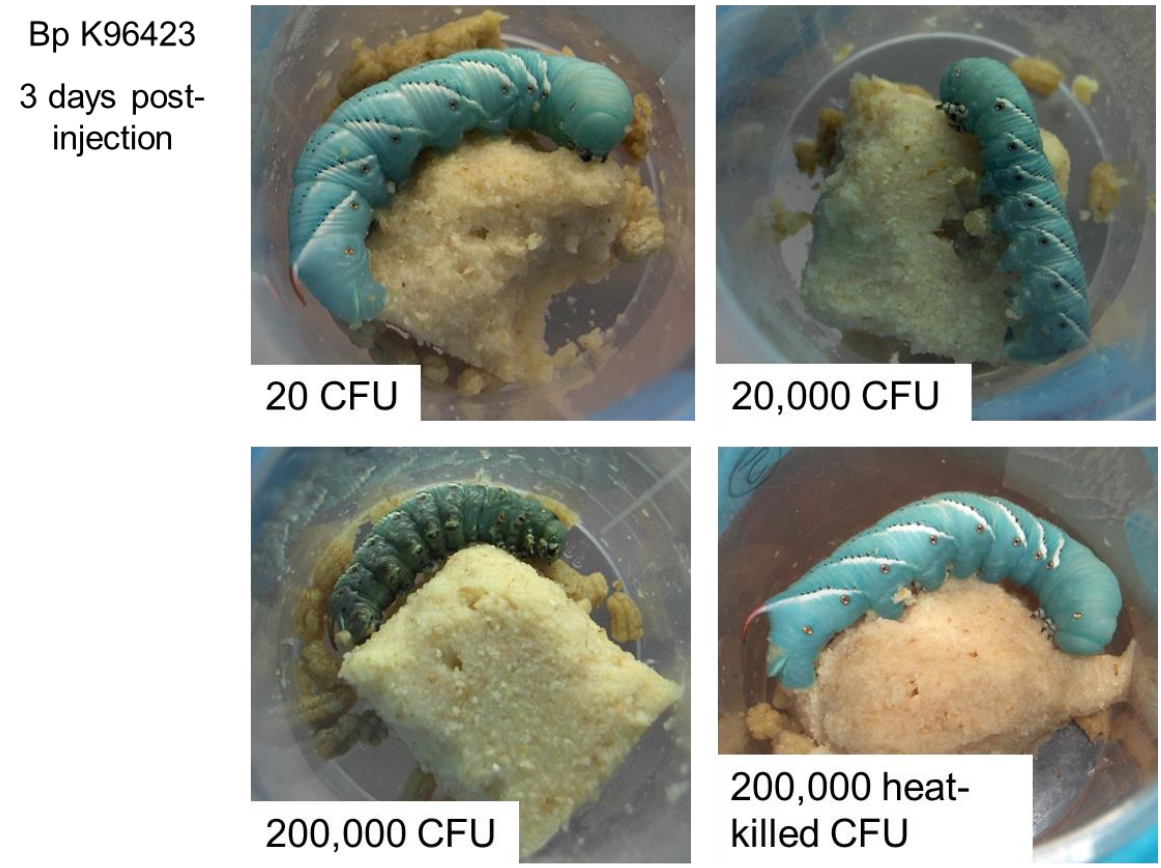

Figure 3.5. *M. sexta* larvae injected with Bp K96423 did not all succumb to infection. At day 6 post-injection these larvae show examples of differing states of health from the same dose of Bp. 20 CFU: (left) dead larva, developed to approximately wanderer stage; (right) healthy wanderer larva. 200 CFU: (left) dead wanderer larva; (right) healthy wanderer larva. 2,000 CFU: (left) healthy larva showing signs of melanocytic nodulation immune response (black spots visible in the enlarged image); (right) dead larva.

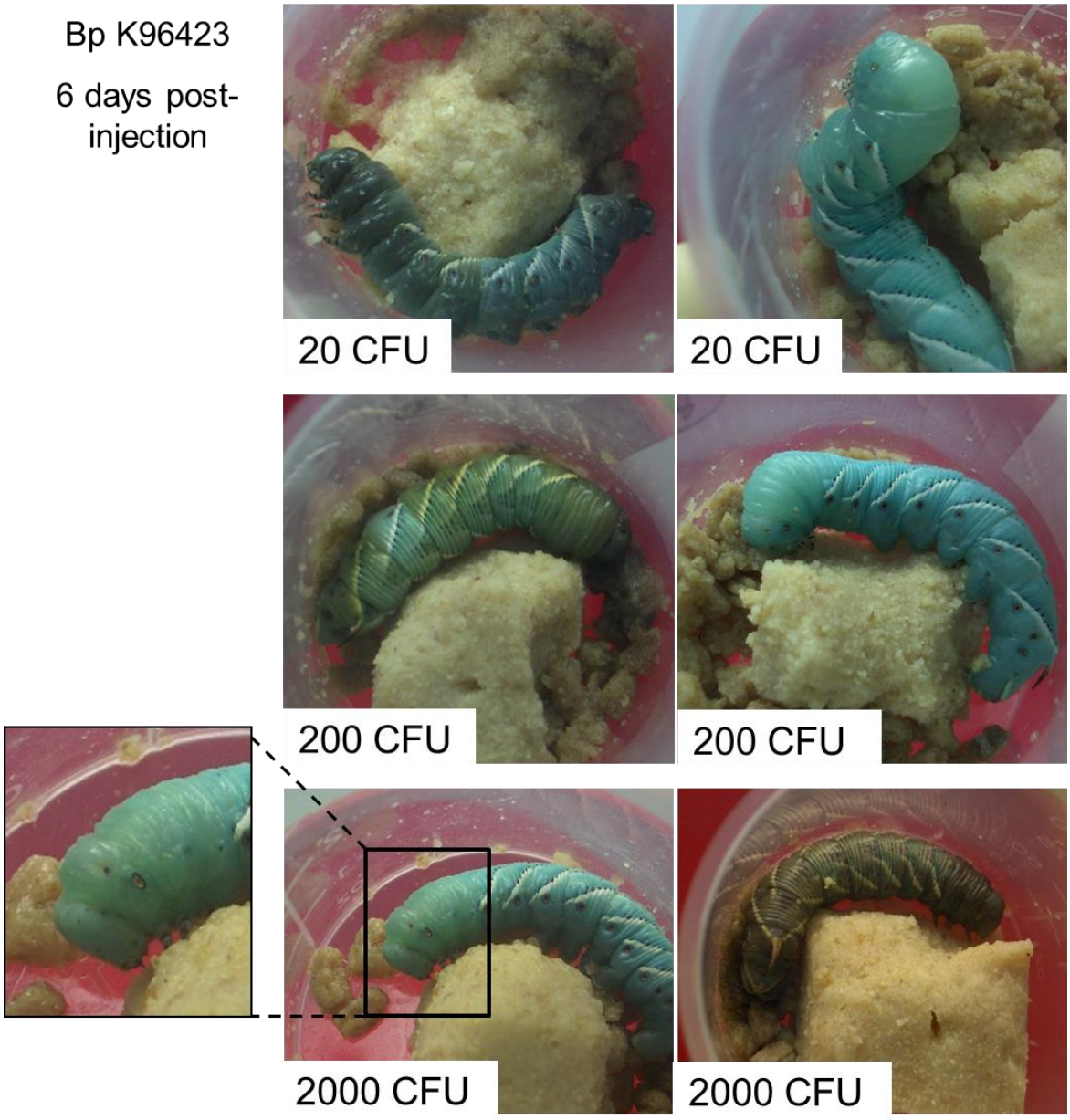

Table 3.6 shows the survival of insects injected with different doses, over seven days.

Table 3.6. Numbers of larvae surviving Bp K96423 infection (*n* = 8) over seven days.Epi300 = *E. coli* Epi300. Various doses were tested and a dose responsive effect seemed to occur, although data was missing on two days when several insects died.

Strain	CFUs injected (in 100µl)	Day 0 0 hrs	Day 1 24 hrs	Day 2 48 hrs	Day 3 72 hrs	Day 4 96 hrs	Day 5 120 hrs	Day 6 144 hrs	Day 7 168 hrs
Bp K96423	$2.00x10^1$	8	8	8	8			6	5
	$2.00x10^2$	8	8	8	8			6	6
	$2.00x10^3$	8	7	7	7			4	4
	$2.00x10^4$	8	8	8	8			0	0
	$2.00x10^5$	8	8	8	1			0	0
Heat killed Bp	$2.00x10^5$	8	8	8	8			8	8
Epi300	$2.00x10^5$	8	8	8	8			8	8
PBS		8	8	8	8			8	8

Hatched cells indicate no data available. Light grey = <100% alive. Dark grey = 0% alive.

A dose responsive lethality was evident, as it had been with Bt E264, although the time to death was noticeably longer. The median time to death (MTTD) for larvae injected with Bp was 72 hours at a 10^5 CFU dose. The MTTD was calculated as 144 hours at a 10^4 or 10^3 CFU dose; however, those MTTDs are not reliably useful because the deaths may have occurred during day 4 or 5 when no data was collected. MTTDs could not be calculated for the lower doses because more than half of the larvae survived beyond the seven days.

Figure 3.6 is a Kaplan-Meier survival curve for the Bp K96423 doses, confirming the dose-responsive lethal effect.

Figure 3.6. Kaplan-Meier survival curve for Bp K96423 doses. The curves start at 1.0 (all alive) and drop down the y-axis (cumulative survival) as the insects die. The point at which the curve ends indicates the number of surviving insects at the end of the assessment. In cases where insects survive, the curve line displays a small cross which is described in the key as a 'censored' case. Survival curves fell to zero at the two highest doses of Bp K96423. Several insects survived at the lower doses and with the controls. H.K. = heat-killed Bp K96423. Epi300 = *E. coli* Epi300.

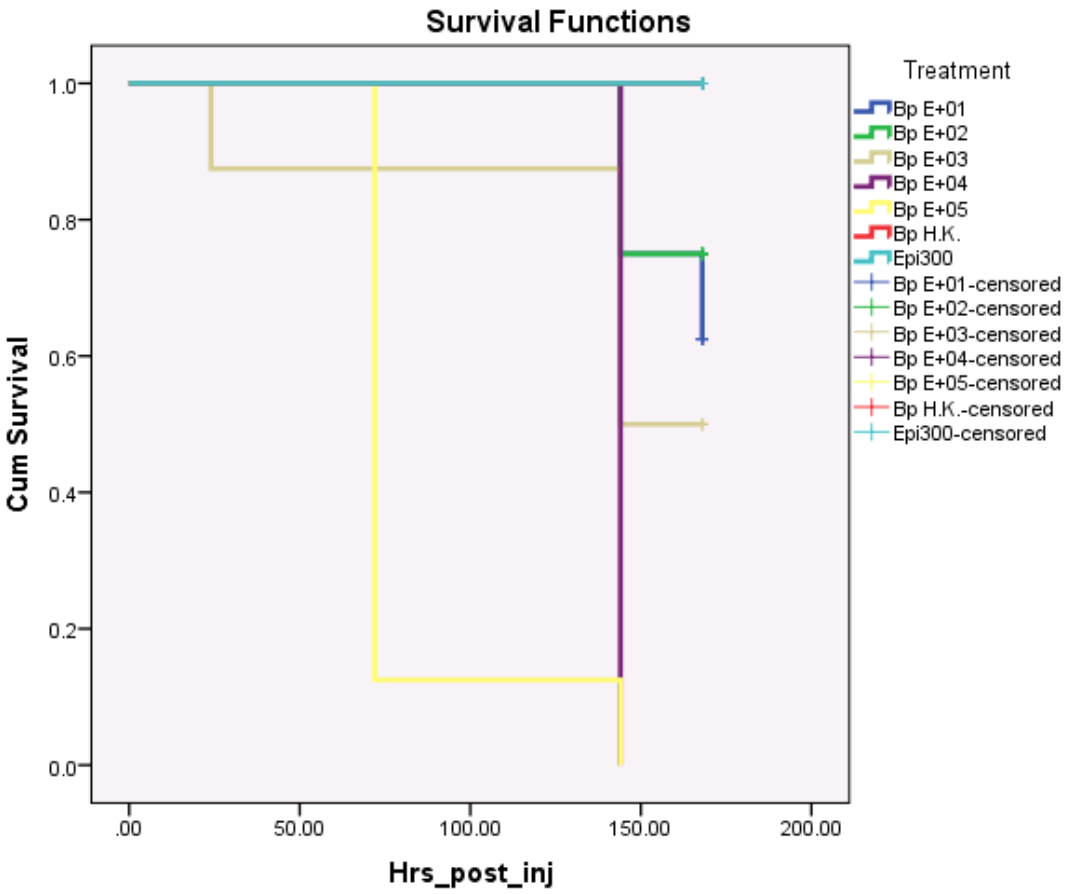

Shown in Table 3.7, log-rank (Mantel-Cox) tests performed as part of the Kaplan-Meier analysis of Bp K96423 injections revealed that: the highest dose generated a survival curve significantly different from all the other doses; the lower doses were significantly different from the higher doses; yet there were similar profiles between some doses that were only one log different.

Table 3.7. Log-rank (Mantel-Cox) pairwise comparisons between Bp K96423 doses. NS = not significantly different, * $p \leq 0.05$, ** $p \leq 0.01$, *** $p \leq 0.001$

Bp K96243 dose	**Bp E+01**	**Bp E+02**	**Bp E+03**	**Bp E+04**	**Bp E+05**
Bp E+01		NS	NS	**	***
Bp E+02	NS		NS	**	***
Bp E+03	NS	NS		NS	**
Bp E+04	**	**	NS		***
Bp E+05	***	***	**	***	

Like Bt E264, Bp K96423 showed a dose-responsive lethal effect: at 10^5 CFU the MTTD was 72 hours. At 10^4 or 10^3 CFU doses the MTTD was not reliable but was between 96-144 hours. At the lower doses more than half of the larvae survived beyond the seven days. The controls all showed 100% survival throughout the experiment, including the heat-killed Bp cells at the highest concentration tested (equivalent to 10^5 CFU). Importantly, the Bp K96423 appeared to be less virulent than Bt E264 to *M. sexta.*

In summary, Bp strain K96423 was less virulent than Bt strain E264 in *Manduca sexta*. Table 3.8 compares the *M. sexta* MTTD values calculated for Bp K96423 and Bt E264 at equivalent doses. As well as having longer MTTDs, fewer larvae succumbed to disease with Bp: up to 50% of the larvae given doses below 10^4 CFU remained healthy throughout the seven days. With Bt only one larva (20%) survived throughout the six days, and only at the lowest dose tested (10^1 CFU).

Table 3.8. Median Times to Death for *M. sexta* larvae injected with equivalent doses of Bt E246 (*n* = 5) or Bp K96423 (*n* = 8). *MTTDs were not calculable for 10^1 or 10^2 CFU doses of Bp because more than half the larvae survived beyond 168 hours. MTTDs for 10^3 and 10^4 CFU Bp were calculated as 144 hours but data were missing; the true MTTD values are in the range of 96-144 hours.

Dose (CFU)	MTTD (hours)	
	Bt E264	Bp K96423
10^1	144	*
10^2	96	*
10^3	96	96-144*
10^4	72	96-144*
10^5	48	72

Dose response #4 and repeat #5: Bt and Bo strains

For greater reliability and statistical significance, further experiments were conducted with Bt E264 with more replicates. Out of interest, a selection of other containment level 2 *Burkholderia* strains were also assessed in parallel – two other Bt strains (Bt CDC 272 and Bt CDC 301) and two *B. oklahomensis* (Bo) strains (Bo C6786 and Bo E0147). These strains were all previously tested in mice and *Galleria mellonella* (Wand *et al*. 2011) and are therefore useful for comparison in the *M. sexta* model. The natural history of the strains is discussed in the introductory chapter.

M. sexta injections were performed with Bt and Bo strains. Dose response #4 tested a range of doses, as shown in Table 3.9.

Table 3.9. Dose response #4: Numbers of larvae surviving various Bt and Bo infections (*n* = 10) over seven days, 10^4-10^1 CFU doses. Epi300 = *E. coli* Epi300.

Strain	Calculated dose (CFU per 100µl)	No. alive (/10) at timepoints																				
		Day:	1			2			3			4			5			6			7		
		Hour:	18	24	28	42	48	52	66	72	76	90	96	100	114	120	124	138	144	148	162	168	172
Bt E264	0.43x10^4		10	10	10	10	10	10	9	5	3	0											
	0.43x10^3		10	10	10	10	10	10	10	9	8	2	1		0								
	0.43x10^2		10	10	10	10	10	10	10	10	10	10	10		6	6	4	0					
Bt CDC 272	1.50x10^4		10	10	10	10	10	10	10	10	10	10	10		10	10	10	10	W				
	1.50x10^3		10	10	10	10	10	10	10	10	10	10	10		10	10	10	10	W				
	1.50x10^2		10	10	10	10	10	10	10	10	10	10	10		10	10	10	10	10	10	10	W	
Bt CDC 301	0.69x10^4		10	10	10	10	10	10	0														
	0.69x10^3		10	10	10	10	10	10	1	0													
	0.69x10^2		10	10	10	10	10	10	9	3	1	0											
Bo C6786	1.41x10^4		10	10	10	7	0																
	1.41x10^3		10	10	10	10	10	10	0														
	1.41x10^2		10	10	10	10	10	10	9	6	2	0											
Bo E0147	0.33x10^4		10	10	10	10	10	7	0														
	0.33x10^3		10	10	10	10	10	10	2	0													
	0.33x10^2		10	10	10	10	10	10	10	9	7	1	0										
Epi300	0.77x10^4		10	10	10	10	10	10	10	10	10	10	10		10	10	10	10	W				

Hatched cells indicate no data available. Light grey = <100% alive. Dark grey = 0% alive. W = wanderer stage, euthanised

The experiment showed a dose-responsive lethal effect for Bt CDC 301, Bo C6786, Bo E0147, and Bt E264 as before. However, Bt CDC 272 did not show any effect on the larvae, which all developed to the wanderer stage.

Dose repeat #5 focused on and repeated the 10^4 CFU dose, as shown in Table 3.10. When the ~10^4 dose of each strain was repeated in dose repeat #5, Bt CDC 272 did kill all larvae, yet at a considerably slower rate than the other strains.

Table 3.10. Dose repeat #5: Numbers of larvae surviving various Bt and Bo infections (*n* = 10) over seven days,10^3-10^4 CFU doses. Epi300 = *E. coli* Epi300.

Strain	Calculated dose (CFU per 100µl)	No. alive (/10) at timepoints																				
		Day:	1			2			3			4			5			6			7		
		Hour:	18	24	28	42	48	52	66	72	76	90	96	100	114	120	124	138	144	148	162	168	172
Bt E264	0.49x10^4		10	10	10	10	10	10	3	2	1	0											
Bt CDC 272	0.71x10^4		10	10	10	10	10	10	10	10	10	9	9	9	5	4	4	0					
Bt CDC 301	1.44x10^4		10	10	10	10	10	3	0														
Bo C6786	0.77x10^4		10	10	10	9	1	0															
Bo E0147	0.24x10^4		10	10	10	10	10	9	0														
Epi300	1.10x10^4		10	10	10	10	10	10	10	10	10	10	10	10	10	10	10	10	w				

Light grey = <100% alive. Dark grey = 0% alive. W = wanderer stage, euthanised

For statistical analyses the data from dose response #4 and dose repeat #5 were combined and grouped into log doses according to the actual CFU counts. Bp K96423 data was also compared. Bo E0147 CFU numbers were nearly one log lower than expected, so no data was available for the 10^4 dose (i.e. they were used for 10^3). The same was the case for the Bt E264 data; data from dose response experiment #2 were analysed for the Bt E264 10^4 dose. Bt CDC 301 had slightly low CFU numbers but they were closer to 10^4 than 10^3, so were retained in the 10^4 data set.

Therefore the 10^3 and 10^2 dose comparisons were the most reliable and complete data sets for between-species comparison of virulence, but the 10^4 dose comparison is still informative. These data are analysed below, by dose.

10^2 CFU dose

MTTDs for the 10^2 CFU doses are shown in Figure 3.7, with standard errors of the median.

Figure 3.7. Median Time to Death (MTTD) for Bt, Bo and Bp strains at 10^2 CFU doses. Error bars show SE of the median. No MTTDs were calculable for Bp K96423 or Bt CDC 272 because less than 50% of the larvae died at 10^2 CFU

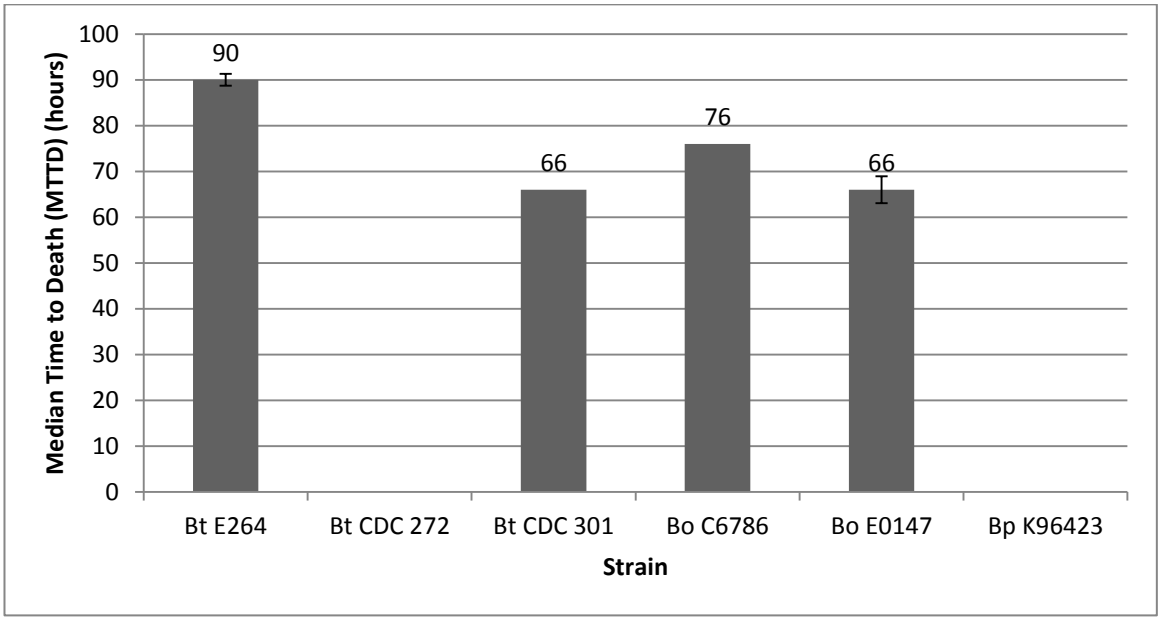

The Kaplan-Meier survival curves for the 10^2 CFU doses are shown in Figure 3.8.

Figure 3.8. Kaplan-Meier survival curve for 10^2 doses. 'CDC 2' = CDC 272, 'CDC 3' = CDC 301, 'K96' = K96423. The curves start at 1.0 (all alive) and drop down the y-axis (cumulative survival) as the insects die. The point at which the curve ends indicates the number of surviving insects at the end of the assessment. In cases where insects survive, the curve line displays a small cross which is described in the key as a 'censored' case. Several insects survived with Bp K96423 and all survived with Bt CDC 272. The other strains killed all larvae.

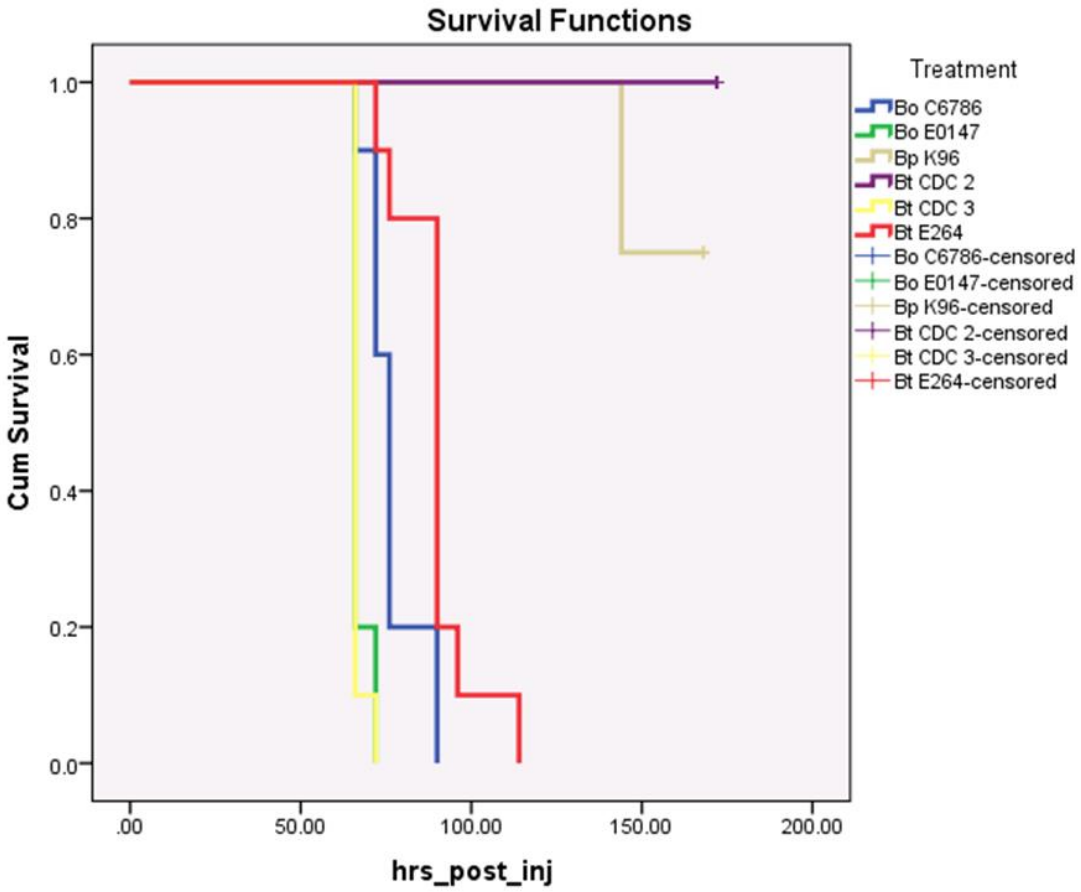

Log-rank (Mantel-Cox) pairwise comparisons performed as part of the Kaplan-Meier analysis of Bp/Bt/Bo 10^2 CFU injections revealed that:

- Bo C6786 was significantly different from all other strains ($p \leq 0.007$)
- Bt E264 was significantly different from all other strains ($p \leq 0.007$)
- Bo E0147 and Bt CDC 301 were similar ($p = 0.542$) but different from all other strains ($p \leq 0.001$)
- Bp K96423 and Bt CDC 272 were similar ($p = 0.103$) but different from all other strains ($p = 0.000$)

10^3 CFU dose

At a 10^3 CFU dose, in one experiment Bt CDC 272 killed no larvae. In the second it killed all 10. Therefore it was possible to calculate an overall MTTD, although this value should be used with caution. This value (MTTD = 138 hours) places Bt CDC 272 slightly ahead of Bp K96423 in terms of virulence (Bp MTTD = 144 hours). 10^3 CFU MTTDs are shown in Figure 3.9, with standard errors of the median.

Figure 3.9. Median Time to Death (MTTD) for Bt, Bo and Bp strains at 10^3 CFU doses. Error bars show SE of the median.

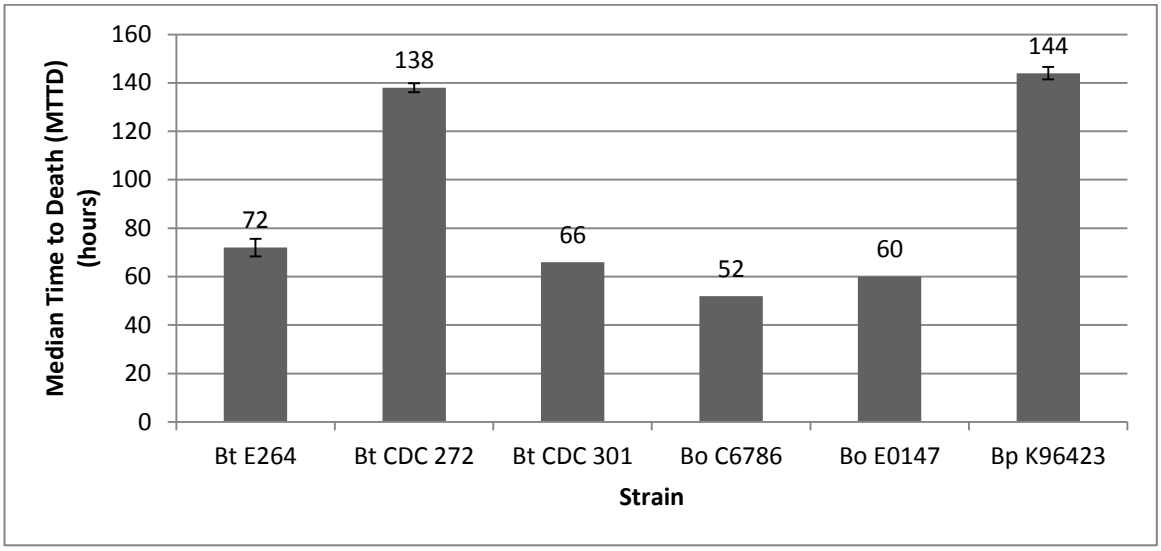

The Kaplan-Meier survival curve for the 10^3 CFU doses is shown in Figure 3.10.

Figure 3.10. Kaplan-Meier survival curve for 10^3 doses. 'CDC 2' = CDC 272, 'CDC 3' = CDC 301, 'K96' = K96423. The curves start at 1.0 (all alive) and drop down the y-axis (cumulative survival) as the insects die. The point at which the curve ends indicates the number of surviving insects at the end of the assessment. In cases where insects survive, the curve line displays a small cross which is described in the key as a 'censored' case. Several insects survived with Bp K96423 and Bt CDC 272, and all survived with the *E. coli* control. The other strains killed all larvae.

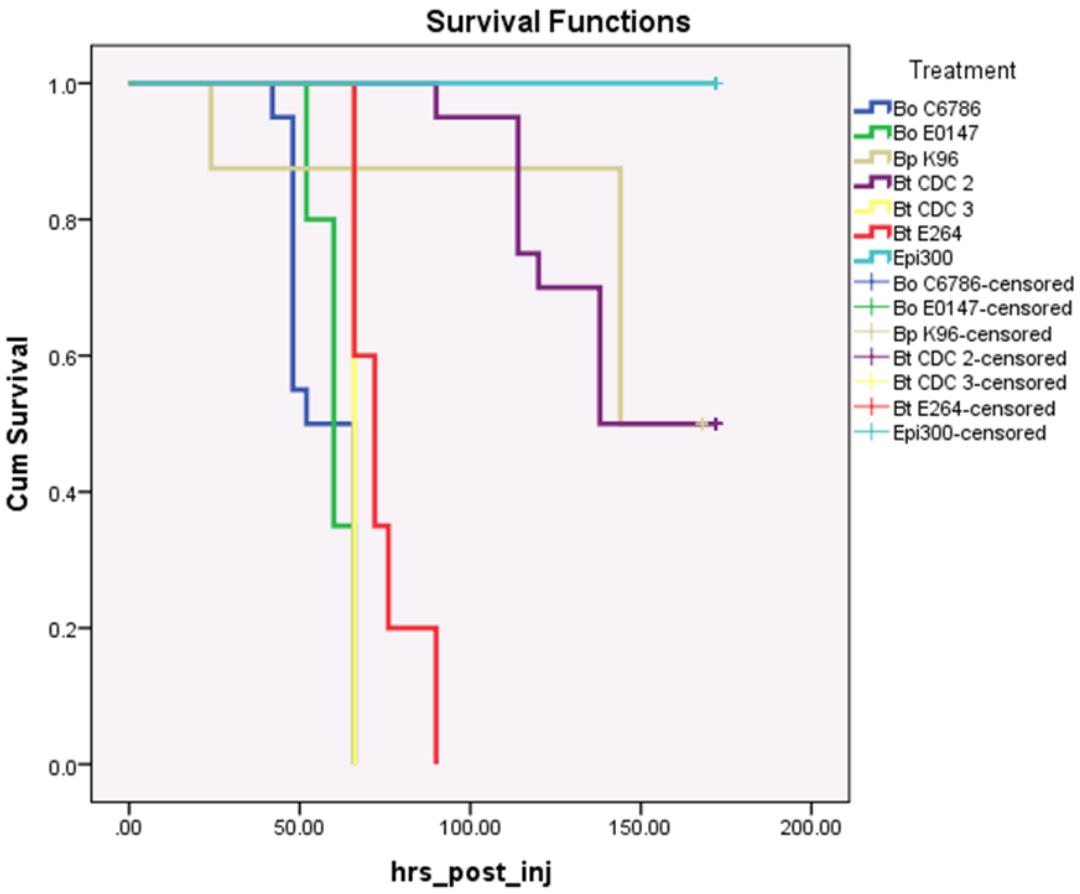

Log-rank (Mantel-Cox) pairwise comparisons performed as part of the Kaplan-Meier analysis of Bp/Bt/Bo 10^3 CFU injections revealed that:

- The two Bo strains were similar to each other (p = 0.860) but significantly different from all other strains ($p \leq 0.008$)
- Bp K96423 was similar to Bt CDC 272 (p = 0.757) but significantly different from all other strains ($p \leq 0.014$)
- Bt CDC 301, Bt E264 and *E. coli* Epi300 were all significantly different from other strains ($p \leq 0.014$).

10^4 CFU dose

10^4 CFU dose MTTDs are shown in Figure 3.11, with standard errors of the median. No data was available for Bo E0147 at 10^4 CFU doses. More than half of the Bt CDC 272 larvae survived so no MTTD could be calculated.

Figure 3.11. Median Time to Death (MTTD) for Bt, Bo and Bp strains at 10^4 CFU doses. Error bars show SE of the median. No data was available for Bo E0147 at 104 CFU doses. All of the Bt CDC 272 larvae survived at this dose so no MTTD could be calculated.

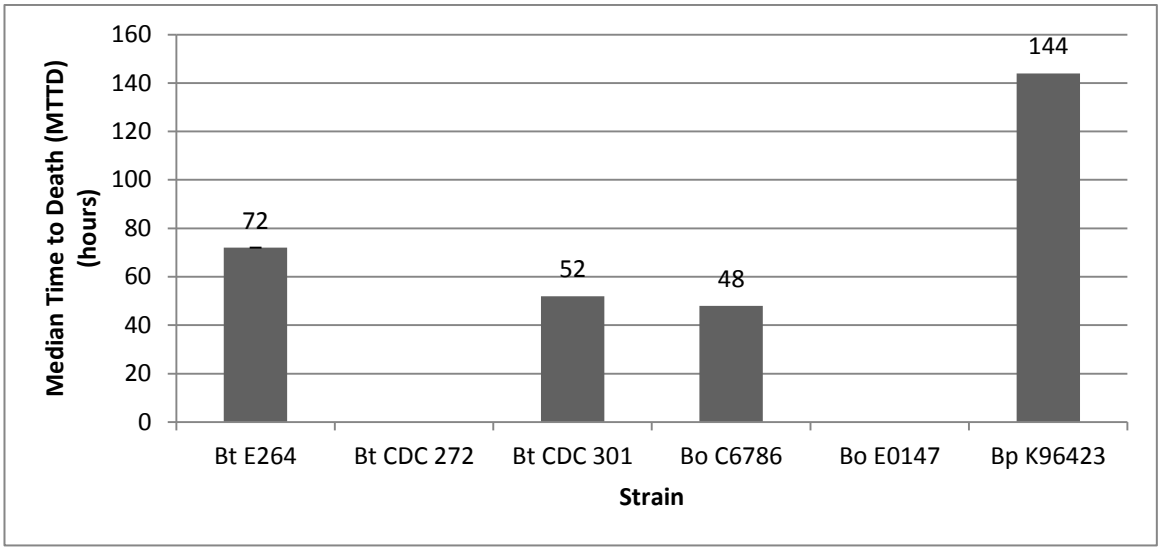

The Kaplan-Meier survival curve for the 10^4 CFU doses is shown in Figure 3.12.

Figure 3.12. Kaplan-Meier survival curve for 10^4 doses. 'CDC 2' = CDC 272, 'CDC 3' = CDC 301, 'K96' = K96423. The curves start at 1.0 (all alive) and drop down the y-axis (cumulative survival) as the insects die. The point at which the curve ends indicates the number of surviving insects at the end of the assessment. In cases where insects survive, the curve line displays a small cross which is described in the key as a 'censored' case. All insects survived with Bt CDC 272 and with the *E. coli* control. The other strains killed all larvae, although Bp K96423 was considerably slower to kill.

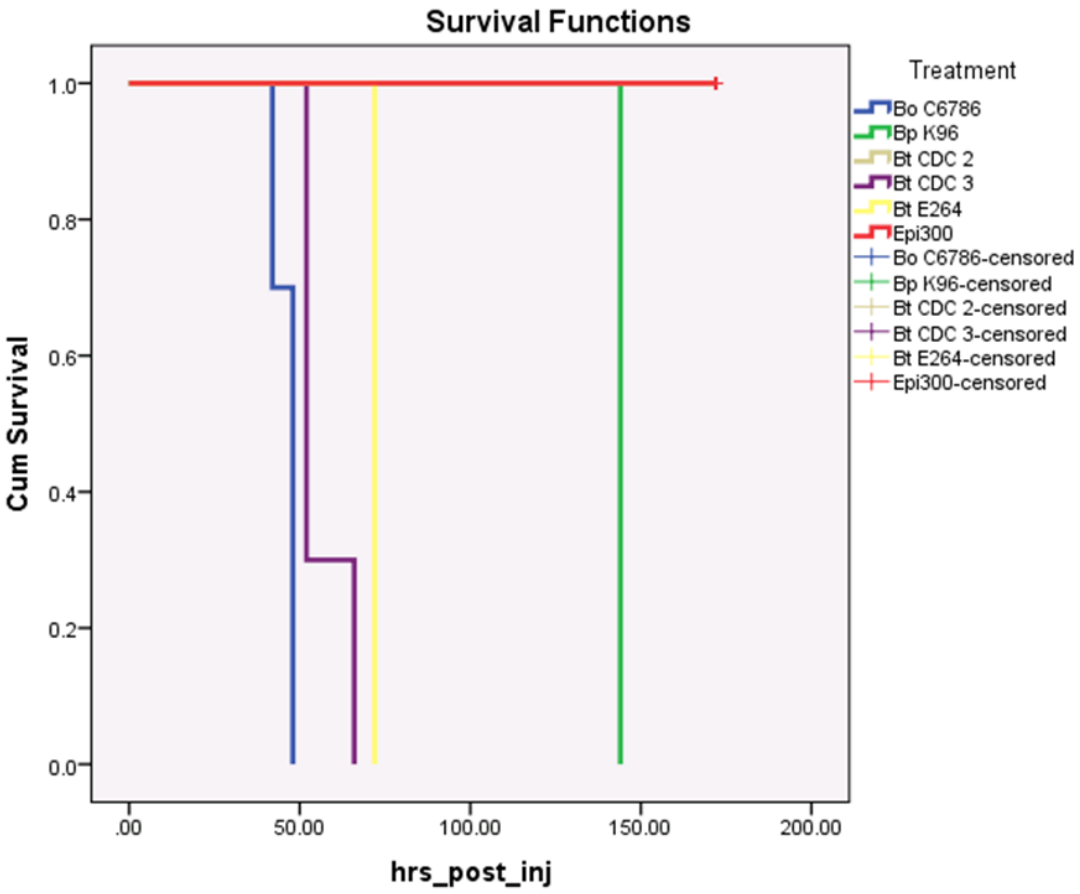

Log-rank (Mantel-Cox) pairwise comparisons performed as part of the Kaplan-Meier analysis of Bp/Bt/Bo injections revealed that at 10^4 CFU the survival curve of every *Burkholderia* strain tested was significantly different from every other ($p \leq 0.001$).

Table 3.11 summarises the MTTD values for Bt and Bo in the dose response #4 and dose repeat #5 experiments.

Table 3.11. Median Time to Death (MTTD) values for Bt and Bo strains. *n* = 10.

Strain	Calculated dose (CFU per 100µl)		MTTD (hrs)
	Dose response #4	Dose repeat #5	
Bt E264	$2.2x10^{4*}$		**72**
	$4.3x10^{3}$	$4.9x10^{3}$	**72**
	$4.3x10^{2}$		**90**
Bt CDC 272	$1.5x10^{4}$	$0.71x10^{4}$	**-**
	$1.5x10^{3}$		**138****
	$1.5x10^{2}$		**-**
Bt CDC 301	$0.69x10^{4}$	$1.44x10^{4}$	**52**
	$0.69x10^{3}$		**66**
	$0.69x10^{2}$		**66**
Bo C6786	$1.41x10^{4}$	$0.77x10^{4}$	**48**
	$1.41x10^{3}$		**52**
	$1.41x10^{2}$		**76**
Bo E0147	NT		NT
	$3.3x10^{3}$	$2.4x10^{3}$	**60**
	$3.3x10^{2}$		**66**

A dash denotes cases where death was not observed. NT = not tested
*Bt E264 10^{4} dose data is based on dose response #2
** Bt CDC 272 MTTD is based on 100% death in one experiment and 0% death in another, so should be used with caution

Combined with the data from Bp K96423, Table 3.12 summarises the relative virulence at different doses of all the Bp-group bacteria tested in *M. sexta.*

Table 3.12. Relative virulence in *M. sexta* of Bp, Bt and Bo strains, based on MTTD values. *n* = 10 except for Bp K96423 where *n* = 8

	Doses and strain MTTDs					
	10^4 CFU		**10^3 CFU**		**10^2 CFU**	
MOST VIRULENT	Bo C6786	48hrs	Bo C6786	52hrs	= Bt CDC 301	66hrs
	Bt CDC 301	52hrs	Bo E0147	60hrs	= Bo E0147	66hrs
	*		Bt CDC 301	66hrs	Bo C6786	76hrs
	Bt E264	72hrs	Bt E264	72hrs	Bt E264	90hrs
LEAST VIRULENT	Bp K96423	96-144hrs	Bt CDC 272	138hrs	Bp K96423	**
	Bt CDC 272	**	Bp K96423	96-144hrs	Bt CDC 272	**

= denotes tied places
*No data for Bo E0147 at 10^4 CFU
**No MTTD value

In summary, differences were observed in the virulence of different *Burkholderia* strains, both within and between species. In general the pattern of virulence was the same at the different doses tested, with Bp K96423 and Bt CDC 272 being the least virulent in the insect host, and most virulent strains being the Bo strains and Bt CDC 301. These results were in contrast to those published from the *G. mellonella* larva model, where Bp K96423 was the most virulent strain and Bt CDC 272 was also highly virulent (Wand *et al.* 2011).

3.3.3. Virulence in *Galleria mellonella* at 25 °C versus 37 °C

In addressing the differences seen in the results of *Burkholderia* insect infection compared to those of Wand *et al*. (2011), it was apparent that a major difference in methodology was the temperature at which the larvae were maintained post-injection. Therefore in this experiment larvae were injected with the same strains (at 10^2 CFU doses) and maintained at either 25 °C (as before) or 37 °C (as by Wand *et al*).

It was decided to use *G. mellonella* larvae for this purpose, as previous experience of keeping infected *M. sexta* at 37 °C had resulted in even *E. coli* control-injected larvae dying in considerable numbers (although other authors have reported success using *M. sexta* at 37 °C (Fleming *et al*. 2006)).

Table 3.13 shows the results of Bt and Bo infections in *G. mellonella* larvae maintained at 25 °C (top) and 37 °C (bottom).

Table 3.13. Numbers of *G. mellonella* larvae surviving various Bt and Bo infections (*n* = 10) over four days, 10^1-10^2 CFU doses. Showing results of larvae incubated at 25 °C (top) and 37 °C (bottom). Median Time to Death (MTTD) values were calculated by Kaplan-Meier survival analysis. Epi300 = *E. coli* Epi300. Infection dynamics were faster at 37 °C, with little discrimination between several strains.

***G. mellonella* 25 °C**	**Calculated dose (CFU per 10µl)**	**No. alive (/10) at time-points**						**MTTD (hrs)**
		Day:	**0**	**1**	**2**	**3**	**4**	
		Hour:	***0***	***24***	***48***	***72***	***96***	
Bt E264	0.49x10^2		10	10	10	1	0	**72**
Bt CDC 272	0.71x10^2		10	10	9	9	6	*****
Bt CDC 301	1.44x10^2		10	10	9	0		**72**
Bo C6786	0.77x10^2		10	9	9	0		**72**
Bo E0147	0.24x10^2		10	10	10	0		**72**
Epi300	1.10x10^2		10	10	10	10	10	*****
NaCl			10	10	10	10	10	*****

***G. mellonella* 37 °C**	**Calculated dose (CFU per 10µl)**	**No. alive (/10) at time-points**						**MTTD (hrs)**
		Day:	**0**	**1**	**2**	**3**	**4**	
		Hour:	***0***	***24***	***48***	***72***	***96***	
Bt E264	0.49x10^2		10	10	0			**48**
Bt CDC 272	0.71x10^2		10	8	7	7	7	*****
Bt CDC 301	1.44x10^2		10	3	0			**24**
Bo C6786	0.77x10^2		10	10	0			**48**
Bo E0147	0.24x10^2		10	10	0			**48**
Epi300	1.10x10^2		10	8	7	7	7	*
NaCl			10	10	10	10	10	*

Light grey = <100% alive. Dark grey = 0% alive. * No MTTD values as >50% survived

Bt CDC 272 failed to kill all *G. mellonella* larvae at either temperature, just as was observed in the *M. sexta* model at 25 °C. This supports the results from this study instead of the results of Wand *et al* (2011).

At 25 °C all the other *Burkholderia* strains had MTTD values of 72 hours post-injection. At 37 °C most MTTD values were reduced to 48 hours and Bt CDC 301 was reduced to just 24 hours; however, it should be noted that the calculated dose was the highest for that strain. At 37 °C some *E. coli* -injected control larvae also died.

Raising the maintenance temperature to 37 °C increased the rate of disease progression but the overall pattern of relative virulence in *G. mellonella* was not changed. This suggests that the relative virulence of these strains is not temperature-dependent. Wand *et al* (2011) reported that in *G. mellonella* at 37 °C Bt CDC 272 was the most virulent Bt or Bo strain tested; yet in the same conditions it was found here to be the least virulent.

Wand *et al* (2011) also reported that the Bo strains were less virulent than Bt strains. With the exception of Bt CDC 272, this was found to be the same in this *G. mellonella* study, at either temperature. This general pattern which was conserved in the *G. mellonella* results is in contrast to that seen in the *M. sexta* results, wherein the Bo strains were generally the most virulent.

In summary, Bt CDC 272 showed strikingly different results between Wand *et al* (2011) and this study. With that exception, in *G. mellonella* Bt strains were generally more virulent than Bo strains regardless of maintenance temperature. In *M. sexta* however, Bo strains were generally the most virulent. Therefore the relative virulence of these Bt and Bo strains appeared to be host-species-dependent.

3.3.4. Attenuation of Bt E264 mutants in *Manduca sexta*

To further investigate the suitability of *M. sexta* as a model host for *Burkholderia* infection, mutants were also tested which were reported to be attenuated in the established model *G. mellonella*. The *ΔsurA* deletion mutant and TAT (*prhA:tatA*) conditional mutant are discussed in the introductory chapter.

Bt E264 ΔsurA

The *ΔsurA* deletion mutant was reported to be attenuated in the *G. mellonella* insect model (I. Norville, unpublished results) and was therefore compared for attenuation in the *M. sexta* model. High doses of wild-type Bt E264 or the Δ*surA* mutant were tested first (10^6-10^4 CFU), with larvae maintained at 37°C post-injection to match the method used at Dstl for *G. mellonella* (I. Norville, unpublished results). Results are shown in Table 3.14.

Table 3.14. Numbers of larvae surviving infection with wild-type or Δ*surA* Bt E264 (*n* = 10) over two days, 10^6-10^4 CFU doses. Note that larvae were incubated at 37°C. Epi300 = *E. coli* Epi300

Strain	**Calculated dose (CFU per 100µl):**	**No. Alive (/10) at time-points**			
		Day:	**Day 0**	**Day 1**	**Day 2**
		Hour:	***0***	***24***	***48***
NaCl			10	10	10
Epi300	$2.22x10^6$		10	10	10
	$2.22x10^5$		10	10	10
	$2.22x10^4$		10	10	10
Bt E264 WT	$1.31x10^6$		10	0	
	$1.31x10^5$		10	0	
	$1.31x10^4$		10	0	
Bt ΔsurA	$1.64x10^6$		10	0	
	$1.64x10^5$		10	1	0
	$1.64x10^4$		10	1	0

Light grey = <100% alive. Dark grey = 0% alive.

E. coli -injected controls all survived as expected. At 10^6 CFU no difference was evident between the wild-type Bt E264 and the mutant. At 10^5 and 10^4 CFU 10% of the larvae injected with the mutant strain survived for longer.

To reveal greater differentiation this was followed up by tests at lower doses (10^1-10^3 CFU), with larvae incubated at 25°C as for the other *M. sexta* dose responses. This low dose test (n = 10, 25°C incubation) was repeated in three independent experiments; combined results are shown in Table 3.15.

Table 3.15. Numbers of *M. sexta* surviving infection with wild-type or Δ*surA* Bt E264 (*n* = 30) over two days; combined data from three replicate experiments at 10^3-10^1 CFU doses. Larvae incubated at 25°C as usual. Epi300 = *E. coli* Epi300. WT = wild-type. Larvae injected with the mutant strain survived slightly longer than the wild-type equivalents.

Strain	**Calculated average dose (CFU per 100µl, across replicate experiments)**	**No. alive (/30) at time-points**						
		Days:	**Day 0**		**Day 1**		**Day 2**	
	Ave.	**Hours:**	***0***	***18***	***24***	***32***	***42***	***48***
NaCl			30	30	30	30	30	30
Epi300	**3.50 x10^3**		30	30	30	30	30	30
Bt E264 WT	**1.93 x10^3**		30	30	27	0		
	1.93 x10^2		30	30	30	4	0	
	1.93 x10^1		30	30	30	18	1	0
Bt *ΔsurA*	**2.63 x10^3**		30	30	30	5	0	
	2.63 x10^2		30	30	30	28	0	
	2.63 x10^1		30	30	30	30	8	1
Light grey = <100% alive. Dark grey = 0% alive.								

Figure 3.13 shows MTTD values for larvae injected with different doses of wild-type and Δ*surA* mutant Bt E264, with standard errors of the median. The mutant strain was attenuated in terms of MTTD at the 10^2 CFU dose.

Figure 3.13. Median Time to Death (MTTD) for wild-type or Δ*surA* Bt E264 at different doses (*n* = 30 over three replicate experiments). Error bars show SE of the median. The *ΔsurA* mutant strain was attenuated at 10^2 CFU.

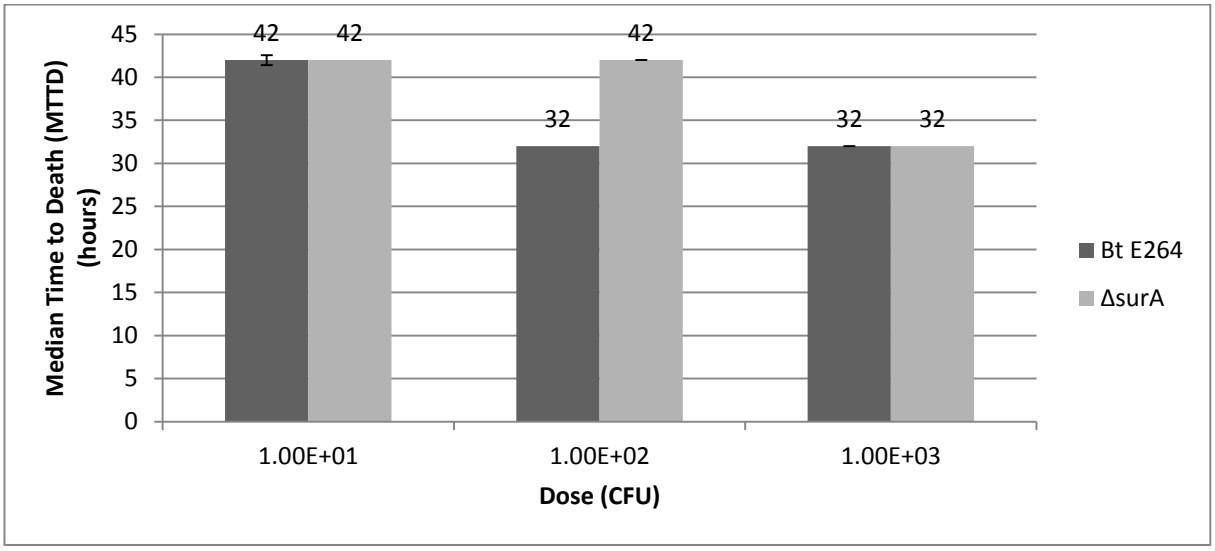

Although median time-to-death (MTTD) values have been used for comparing the strain virulence, the mean time-to-death values (Figure 3.14) shows a little more variation between strains, which may be informative in this case.

Figure 3.14. Mean time to death for wild-type or Δ*surA* Bt E264 at different doses. Error bars show SE of the mean. At each dose mean time to death is greater for the mutant strain, indicating attenuation of virulence. At the 10^3 CFU dose the difference is slight.

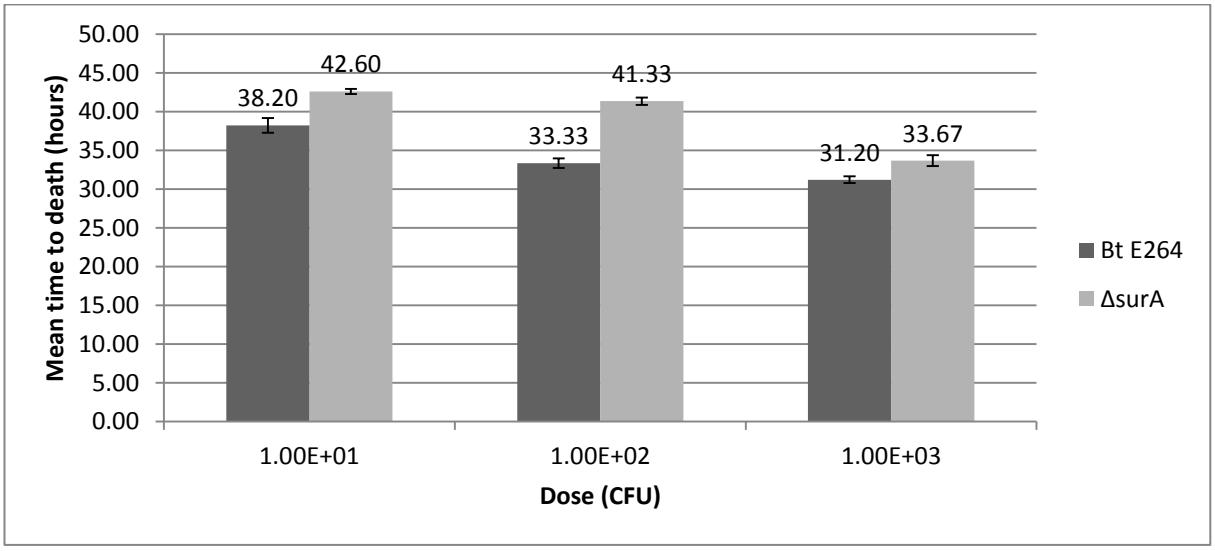

Figure 3.15 is the Kaplan-Meier survival curve for insects injected with wild-type or *ΔsurA* Bt E264.

Figure 3.15. Kaplan-Meier survival curve for wild-type or Δ*surA* Bt E264 doses. BtE = Bt E264 wild-type. surA = Bt E264 *ΔsurA.* The curves start at 1.0 (all alive) and drop down the y-axis (cumulative survival) as the insects die. The point at which the curve ends indicates the number of surviving insects at the end of the assessment. In cases where insects survive, the curve line displays a small cross which is described in the key as a 'censored' case.

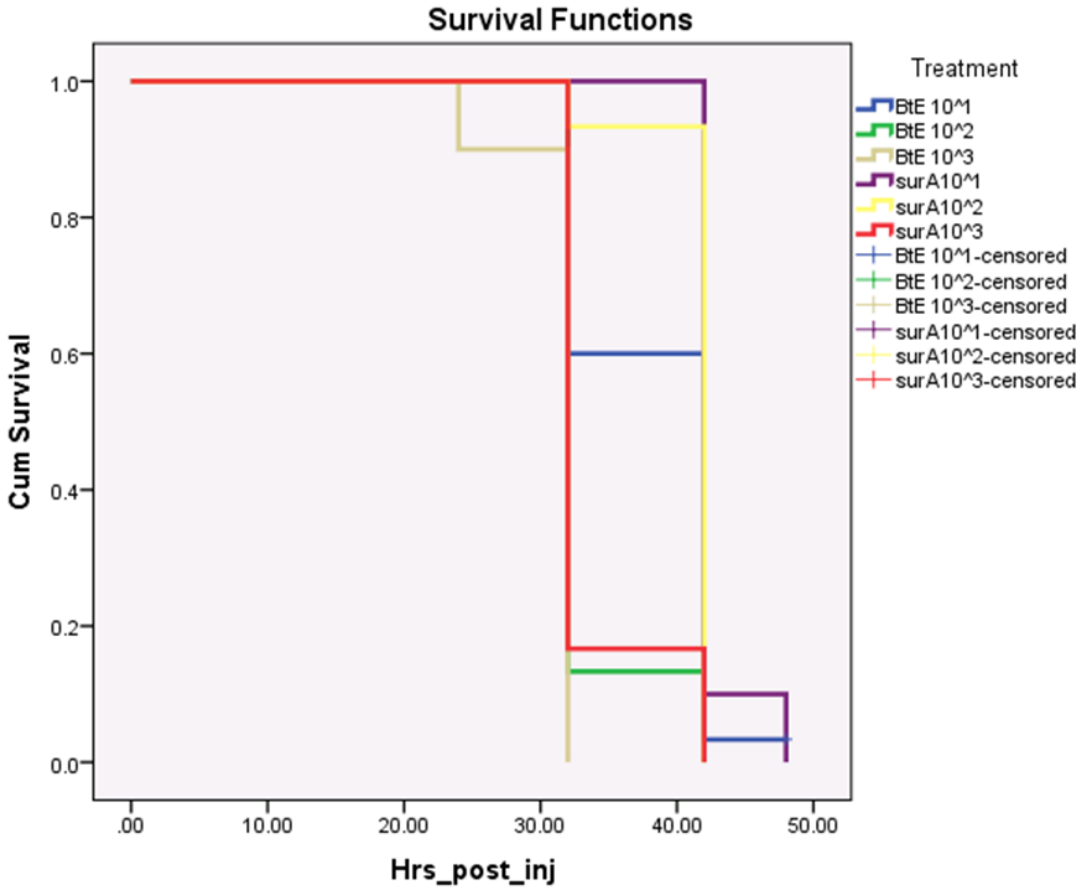

According to log rank (Mantel-Cox) pairwise significance calculations shown in Table 3.16, the difference between wild-type and *ΔsurA* virulence was significant at equivalent doses ($p \leq 0.005$).

Table 3.16. Log-rank (Mantel-Cox) pairwise comparisons between *M. sexta* survival profiles when injected with wild-type or *ΔsurA* Bt E264. NS = not significantly different, * $p \leq 0.05$, ** $p \leq 0.01$, *** $p \leq 0.001$. The survival was significantly different at each equivalent dose.

Dose	ΔsurA10^1	ΔsurA10^2	ΔsurA10^3
BtE 10^1	**	NS	***
BtE 10^2	***	***	NS
BtE 10^3	***	***	**

Bt E264 Δ*surA* was also tested alongside the other Bt and Bo strains in dose response #4 and dose repeat #5 (*n* = 10 in each case) so that data could be used for direct comparisons (i.e. using larvae from the same batch and including a 10^4 CFU dose). MTTD values are summarised in Table 3.17. This time the MTTD values were considerably greater; all larvae still died but survived for a longer time period.

Table 3.17. MTTD values for *M. sexta* injected with Bt E264 *ΔsurA* compared to values for the Bt and Bo strains already discussed. Data is combined from dose response #4 and dose repeat #5.

Strain	**Calculated dose (CFU per 100µl)**		**MTTD (hrs)**
	Dose response #4	**Dose repeat #5**	
Bt E264	$2.2x10^{4*}$		72
	$4.3x10^3$	$4.9x10^3$	72
	$4.3x10^2$		90
Bt CDC 272	$1.5x10^4$	$0.71x10^4$	-
	$1.5x10^3$		138**
	$1.5x10^2$		-
Bt CDC 301	$0.69x10^4$	$1.44x10^4$	52
	$0.69x10^3$		66
	$0.69x10^2$		66
Bo C6786	$1.41x10^4$	$0.77x10^4$	48
	$1.41x10^3$		52
	$1.41x10^2$		76
Bo E0147	NT		NT
	$3.3x10^3$	$2.4x10^3$	60
	$3.3x10^2$		66
Bt E264 *ΔsurA*	$1.09x10^4$	$0.89\ x10^4$	72
	$1.09x10^3$		76
	$1.09x10^2$		124

A dash denotes cases where death was not observed. NT = not tested
* Bt E264 10^4 dose data is based on dose response #2
** Bt CDC 272 MTTD is based on 100% death in one experiment and 0% death in another, so should be used with caution

Table 3.18 summarises the relative virulence of the Bp-group bacteria, as previously shown in Table 3.12, now including the Bt E264 *ΔsurA* mutant.

Table 3.18. Bt E264 *ΔsurA* relative virulence compared to other strains, based on MTTD values

	Doses and strain MTTDs					
	10^4 CFU		**10^3 CFU**		**10^2 CFU**	
MOST VIRULENT ⇩ LEAST VIRULENT	Bo C6786	48hrs	Bo C6786	52hrs	= Bt CDC 301	66hrs
	*		Bo E0147	60hrs	= Bo E0147	66hrs
	Bt CDC 301	52hrs	Bt CDC 301	66hrs	Bo C6786	76hrs
	= Bt E264	72hrs	Bt E264	72hrs	Bt E264	90hrs
	= Bt E264 *ΔsurA*	**72hrs**	**Bt E264 *ΔsurA***	**76hrs**	**Bt E264 *ΔsurA***	**124hrs**
	Bp K96423	96-144hrs	Bt CDC 272	138hrs	Bp K96423	**
	Bt CDC 272	**	Bp K96423	96-144hrs	Bt CDC 272	**

= denotes tied places
*Bo E0147 not tested at 10^4 CFU
**No MTTD values as >50% survived

In summary, the Bt E264 *ΔsurA* mutant which was reported to be attenuated in the established *G. mellonella* host model (I. Norville, unpublished results) was also seen to be attenuated in *M. sexta*, most notably at a 10^2 CFU dose. According to MTTD values the strain is less virulent than the Bt E264 wild-type strain but still more virulent than Bt CDC 272 or Bp K96423.

Bt E264 TAT (prhA:tatA) mutant

The second mutant strain tested was a Bt E264 twin-arginine transport (TAT) system conditional mutant which was also attenuated in *G. mellonella* (S. Wagley, unpublished results). Larvae were maintained at 25 °C. Table 3.19 shows the results of *M. sexta* injection with the Bt E264 TAT system mutant in a TAT-active state (media supplemented with rhamnose) or a TAT-deficient state (media supplemented with glucose).

Table 3.19. Numbers of larvae surviving infection with wild-type or conditional TAT mutant E264 (*n* = 8) over six days,10^6-10^2 CFU doses. LB medium was supplemented with rhamnose to give normal TAT system expression or glucose to inactivate the system in the mutant strain. Wild-type Bt E264 was grown in identical conditions to the mutant strain for comparison. Epi300 = *E. coli* Epi300

TAT #1	Calculated average dose (CFU per 100µl)	Number alive (/8) at timepoints					
		Day 1	Day 2	Day 3	Day 4	Day 5	Day 6
		24 hr	48 hr	72 hr	96 hr	120 hr	144 hr
Bt E264 rhamnose	$1.14x10^6$	8	8	0			
	$1.14x10^5$	8	8	2	0		
	$1.14x10^4$	8	8	8	0		
	$1.14x10^3$	8	8	8	3	0	
	$1.14x10^2$	8	8	8	7	3	0
Bt E264 glucose	$0.80x10^6$	8	8	0			
	$0.80x10^5$	8	8	5	0		
	$0.80x10^4$	8	8	7	1	0	
	$0.80x10^3$	8	8	8	1	1	0
	$0.80x10^2$	8	8	8	6	2	1
Bt TAT rhamnose	$1.31x10^6$	8	8	0			
	$1.31x10^5$	8	8	5	0		
	$1.31x10^4$	8	8	8	4	1	1
	$1.31x10^3$	8	8	8	8	7	6
	$1.31x10^2$	8	8	8	8	8	8
Bt TAT glucose	~~10^6~~	/	/	/	/	/	/
	$1.50x10^5$	8	8	0			
	$1.50x10^4$	8	8	3	0		
	$1.50x10^3$	8	8	8	0	0	
	$1.50x10^2$	8	8	8	2	1	1
	$1.50x10^1$	8	8	8	8	5	3
Epi300	$0.86x10^6$	8	8	8	8	8	8
PBS		8	8	8	8	8	8
Light grey = <100% alive. Dark grey = 0% alive. / = no data.							

Figure 3.16 shows TAT #1 MTTD values for larvae injected with different doses of wild-type and TAT mutant Bt E264 grown in the presence of rhamnose or glucose, with standard errors of the median.

Figure 3.16. TAT #1: Median Time to Death (MTTD) for wild-type or TAT-mutant Bt E264 at different doses (*n* = 8). Error bars show SE of the median. The TAT mutant should have wild-type-like ('WT-like') TAT expression when grown in the presence of rhamnose and an inactive TAT system when grown in the presence of glucose. The different sugars were not expected to affect the virulence of wild-type Bt E264. No MTTD values were calculated for 'TAT rhamnose' at 10^4 or 10^5 CFU because more than half of the larvae survived. It appears that the condition in which the TAT system should be inactive has amongst the shortest MTTD values, suggesting it was actually more virulent.

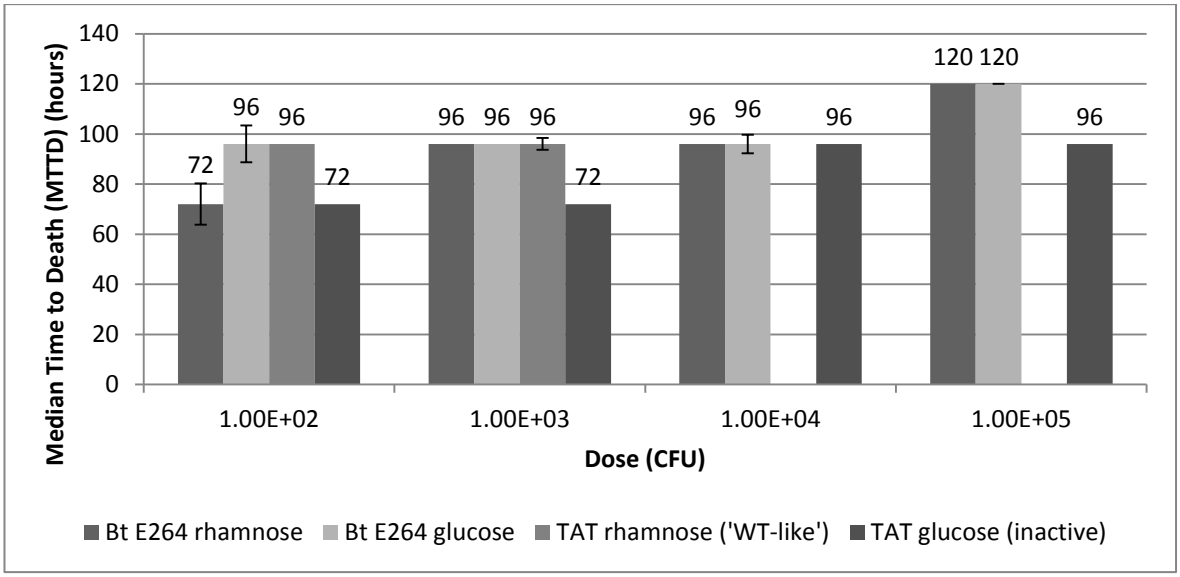

Figure 3.17 shows representative photos of *M. sexta* larvae at three days post-injection with the Bt E264 TAT conditional mutant. The two sugar-supplemented conditions are shown, at two dosages.

Figure 3.17. Representative larvae at 3 days post-injection with two doses of the Bt E264 TAT conditional mutant. With rhamnose the TAT system is active, as in wild-type Bt E264. The inactive TAT (with glucose) was expected to be attenuated in *M. sexta* infection but actually killed more quickly.

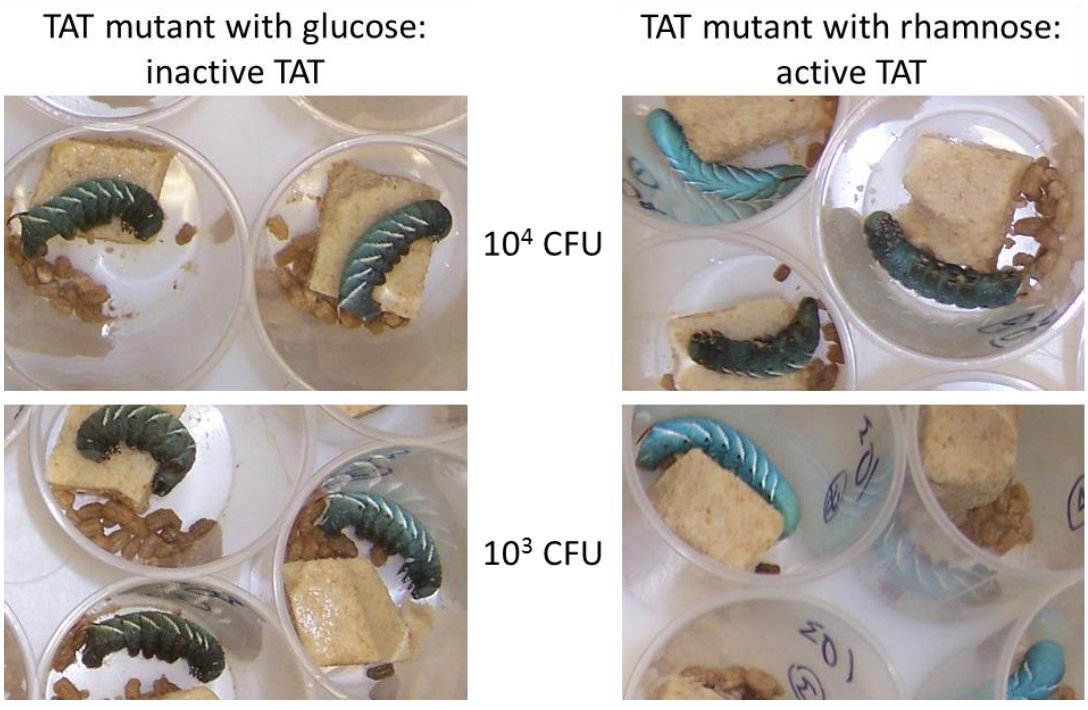

Figure 3.18 shows the Kaplan-Meier survival curve for the TAT #1 injections at 10^4 CFU.

Figure 3.18. TAT #1: Kaplan-Meier survival curve for wild-type or TAT conditional mutant Bt E264 at 10^4 CFU doses. Growth with rhamnose ('rh') should give the mutant a wild-type TAT phenotype. Growth with glucose ('gl') inactivates the TAT system. The curves start at 1.0 (all alive) and drop down the y-axis (cumulative survival) as the insects die. The point at which the curve ends indicates the number of surviving insects at the end of the assessment. In cases where insects survive, the curve line displays a small cross and is described in the key as a 'censored' case.

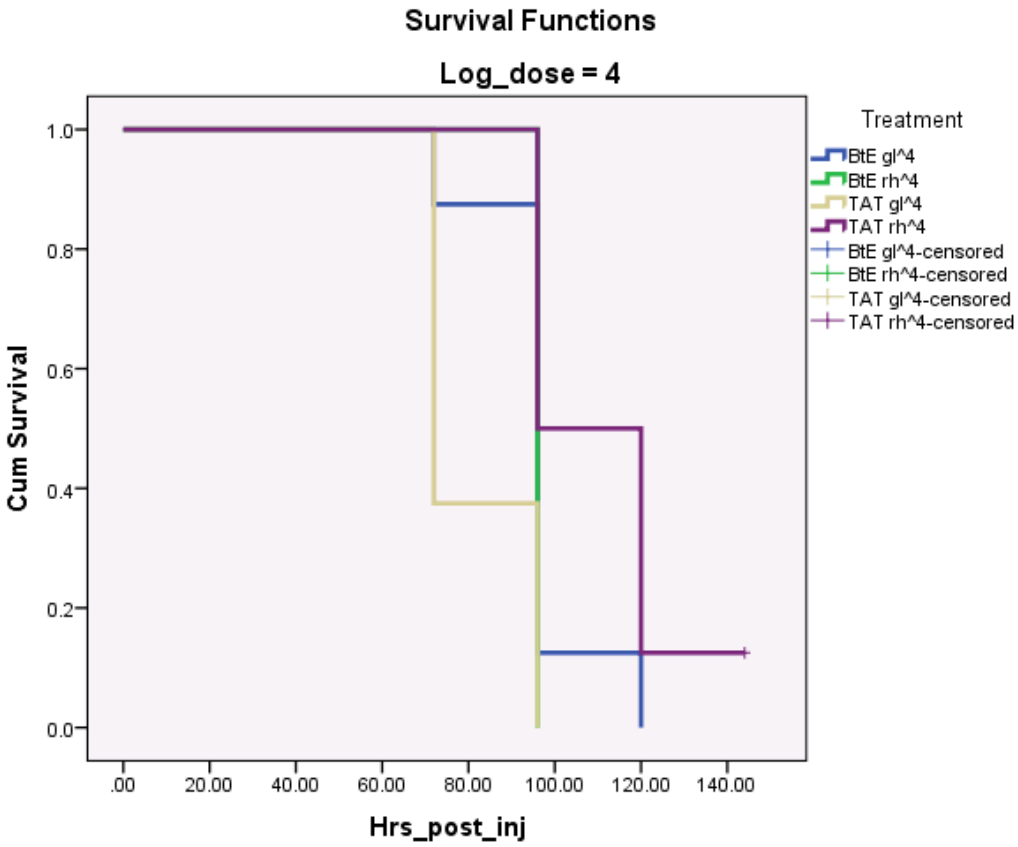

Log-rank (Mantel-Cox) pairwise comparisons performed as part of the Kaplan-Meier analysis revealed that:

- None of the pairwise comparisons between wild-type Bt E264 grown with rhamnose or with glucose were significant, i.e. there was no significant difference in Bt E264 virulence as a result of the media used (*p*-values = 0.143 – 0.962).
- Most of the *p*-values comparing actual wild-type Bt E264 and the 'wild-type-like' TAT phenotype were significant, meaning that there was a significant difference in virulence between them (10^2-10^4 CFU dose: *p*-values = 0.000 – 0.025). Therefore the rhamnose-induced expression of the TAT system did not appear to fully match wild-type; some larvae injected with TAT (rhamnose) did not die whereas all Bt E264-injected larvae did.

- Comparing the active (rhamnose-induced) and inactive (glucose) states of the TAT mutant showed that there was a significant difference in virulence, as all *p*-values were highly significant. However, the observed effect was the opposite of the expected effect; at 10^5, 10^4 and 10^2 CFU the TAT-inactive mutant killed more rapidly than the wild-type E264 or 'wild-type'-like TAT.

As the results were unexpected, a second TAT dose response was performed (TAT #2) this time also using the wild-type and mutant strains grown in LB alone to better understand whether the presence of sugar in the inoculum was affecting the bacteria-host interaction (Table 3.20). A greater range of doses was used in order to differentiate effects more clearly; 10^2, 10^4 and 10^6 CFU.

Table 3.20. Numbers of larvae surviving infection with wild-type or conditional TAT mutant E264 (*n* = 8) over seven days, with 10^6, 10^4 and 10^2 CFU doses. LB medium was supplemented with rhamnose to give normal TAT system expression or glucose to inactivate the system in the mutant strain. As a control un-supplemented LB was also used. Wild-type Bt E264 was grown in identical conditions to the mutant strain for comparison.

TAT #2	**Calculated average dose (CFU per 100µl)**	**Number alive (/8) at timepoints**						
		Day 1	**Day 2**	**Day 3**	**Day 4**	**Day 5**	**Day 6**	**Day 7**
		24 hr	**48 hr**	**72 hr**	**96 hr**	**120 hr**	**144 hr**	**168 hr**
Bt E264 LB	$1.16x10^6$	8	8	0				
	$1.16x10^4$	8	8	5	0			
	$1.16x10^2$	8	8	8	3	2	0	
Bt E264 rhamnose	$0.74x10^6$	8	8	0				
	$0.74x10^4$	8	8	5	2	0		
	$0.74x10^2$	8	8	8	6	4	2	0
Bt E264 glucose	$0.99x10^6$	8	8	0				
	$0.99x10^4$	8	8	1	0			
	$0.99x10^2$	8	8	8	3	0		
Bt TAT LB	est: $0.61x10^6$	8	8	8	7	0		
	est: $0.61x10^4$	8	8	8	8	8	8	4
	est: $0.61x10^2$	8	8	8	8	8	8	8
Bt TAT rhamnose	est: $0.61x10^6$	8	8	0				
	est: $0.61x10^4$	8	8	8	5	2	2	1
	est: $0.61x10^2$	8	8	8	8	6	5	3
Bt TAT glucose	$0.61x10^6$	8	8	0				
	$0.61x10^4$	8	8	5	1	0		
	$0.61x10^2$	8	8	8	7	5	1	1

Light grey = <100% alive. Dark grey = 0% alive. 'est' = CFUs could not be calculated; estimates are based on Bt TAT glucose figure and similar OD_{600} values

Figure 3.19 shows TAT #2 MTTD values for larvae injected with different doses of wild-type and TAT mutant Bt E264 grown in the presence or absence of rhamnose or glucose, with standard errors of the median.

Figure 3.19. TAT #2: Median Time to Death (MTTD) for wild-type or TAT mutant Bt E264 at different doses (*n* = 8). Error bars show SE of the median. The TAT mutant should have wild-type-like TAT expression when grown in the presence of rhamnose and an inactive TAT system when grown in the presence of glucose. Both strains were also grown in LB without sugar supplements as a control. No MTTD value was calculable for 'TAT LB' at 10^6 CFU because more than half of the larvae survived. In the absence of sugar supplement the mutant strain was attenuated, probably due to lowered bacterial fitness. However, once again the mutant with glucose (inactive TAT) was more virulent than that with glucose (supposedly wild-type-like).

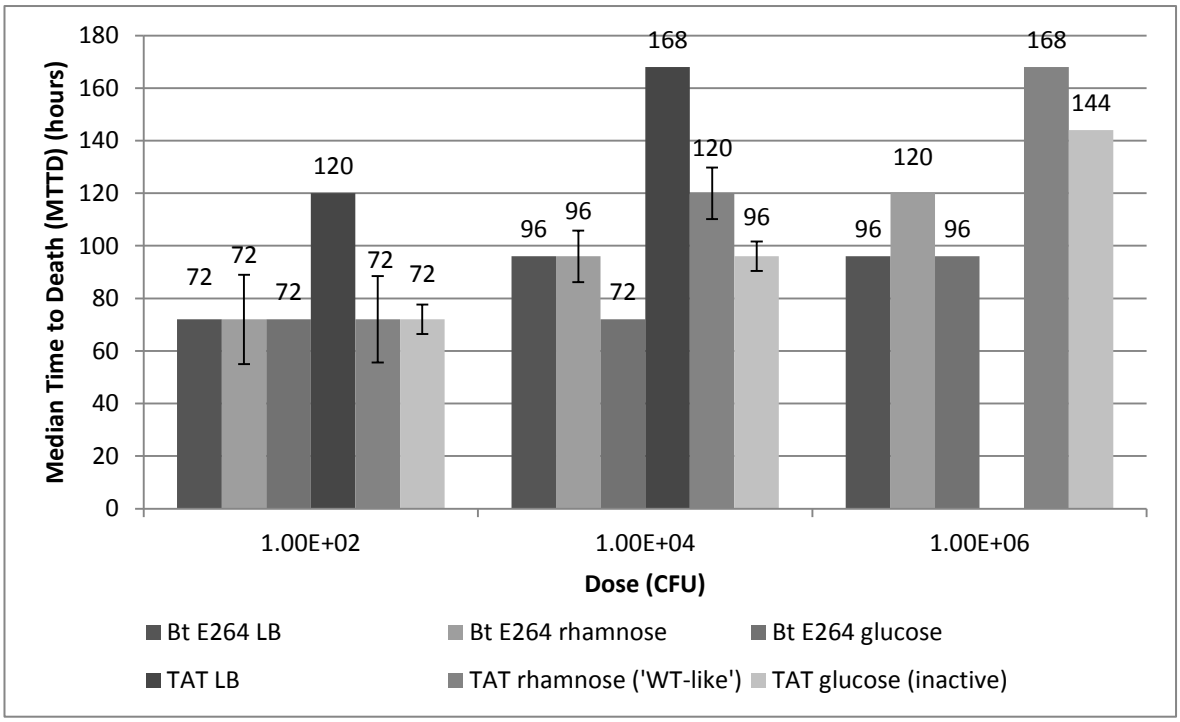

Once again the TAT mutant with rhamnose was attenuated compared to an inactive TAT system with glucose (at 10^4 and 10^6 CFU doses). Another surprising result was that when the TAT mutant was grown with LB alone its virulence was even more attenuated. This suggests that the mutant has a lower fitness and that the presence of the different sugars in the inoculum may have complicated the outcome of the infections, for example by providing an extra energy source.

In summary, the TAT-inactivated mutant did not show the same attenuating effect in the *M. sexta* model as in the *G. mellonella* model (S. Wagley, unpublished results). An additional level of complication is involved when conditional mutants are controlled by supplementation of the media with metabolites such as sugars. Fortunately the chromosomal Δ*surA* mutant had shown attenuation, supporting the validity of the *M. sexta* model for Bt infection.

3.3.5. Burkholderia exhibit oral pathogenicity or toxicity to *Manduca sexta*

Another aspect of *Burkholderia* virulence which was of interest to study was the possibility that they may be pathogenic to *M. sexta* larvae via the oral route. This follows from the fact that *Burkholderia* are predominantly environmental organisms and saprophytes in particular, and that insects ingest a large amount of plant material and detritus.

Experiments #1-3 were initial assessments of the effect on *M. sexta* neonates of ingesting Bt E264, with ingestion of LB or Epi300 *E. coli* as controls. In assessing the effect on larvae, two measurements were informative: the proportion and the weight of surviving insects, as either death or reduced weight may be indicative of a pathogenic or toxic effect.

Experiment #1: There was a clear difference in mortality between LB and Bt E264-fed neonates; by day eight of the feeding assay 9 out of 10 control neonates were alive, compared to 3 out of 10 Bt E264-fed neonates (Table 3.21). However, the average weight of the surviving larvae was 0.139g for the LB control group and 0.135g for the Bt E264 group (Figure 3.20 and Table 3.21); there was no significant difference (T-test for unequal variances, $p = 0.833$).

Figure 3.20. Average day 8 weights of surviving neonates (experiment #1). Error bars = SE

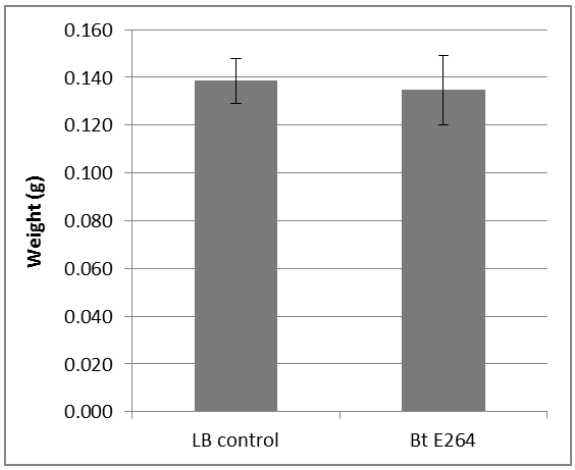

Table 3.21. Survival of fed neonates to day 8 (experiment #1)

	LB control	Bt E264 culture
Survival to Day 8	90 %	30 %

Table 3.21 shows the complete results for experiment #1.

Table 3.21. Day 8 weights of surviving neonates (experiment #1). D = neonate died

Neonate	LB control (g)	Bt E264 culture (g)
1.	0.129	0.146
2.	0.126	0.152
3.	0.085	0.106
4.	0.163	D
5.	0.140	D
6.	0.139	D
7.	0.187	D
8.	0.128	D
9.	0.150	D
10.	D	D
AVERAGE	**0.139**	**0.135**
SE	**0.009**	**0.014**

Experiment #2: As a considerable number of neonates that had been fed Bt E264 had died, experiment #2 used diluted cultures. However, when the bacteria were adjusted to OD_{600} 0.1 all of the neonates survived to day eight and no differences were seen between Bt E264, *E. coli* Epi300 and LB (data not shown). Therefore further experiments reverted to using undiluted overnight culture samples. The 200 µl addition volume was kept.

Experiment #3: Reverting back to undiluted overnight cultures, this experiment tested the effect of feeding on both fifth istar and neonate larvae. In a crude attempt to produce a supernatant-only sample, cells were centrifuged to pellets and the supernatant was harvested; however, as the samples were not filtered a small amount of viable bacterial cells remained. Therefore these are referred to as ‘reduced-cell’ cultures.

Fith instars: From the fifth-instar group all the larvae remained healthy. By day 2 they had consumed the bacteria-laced food blocks and were given normal antibiotic-free food. By day 5 none had died and all seemed healthy. In summary, Bt E264 had no harmful effect on fifth-instar stage *M. sexta*

Neonates: The neonate results were quite different, as summarised in Table 3.22. The Bt-fed neonates (fed either complete or reduced-cell Bt E264 culture) showed increased mortality compared to the *E. coli* controls.

Table 3.22. Survival of fed neonates to day 8 (experiment #3).

		LB control	Epi300 culture	Epi300 reduced-cell culture	Bt E264 culture	Bt E264 reduced-cell culture
Survival to Day 8	***n***	10	20	20	16	17
	%	100 %	100 %	100 %	80 %	85 %

The Bt-fed survivors also showed reduced weight in comparison to the controls, as shown in Figure 3.21. Interestingly, the weight of surviving larvae which were fed reduced-cell Bt culture was considerably lower than those fed complete Bt culture.

Figure 3.21. Average day 8 weights of surviving neonates (experiment #3). In this experiment the 'reduced-cell' culture samples contained relatively few bacteria (not quantified). Error bars = SE.

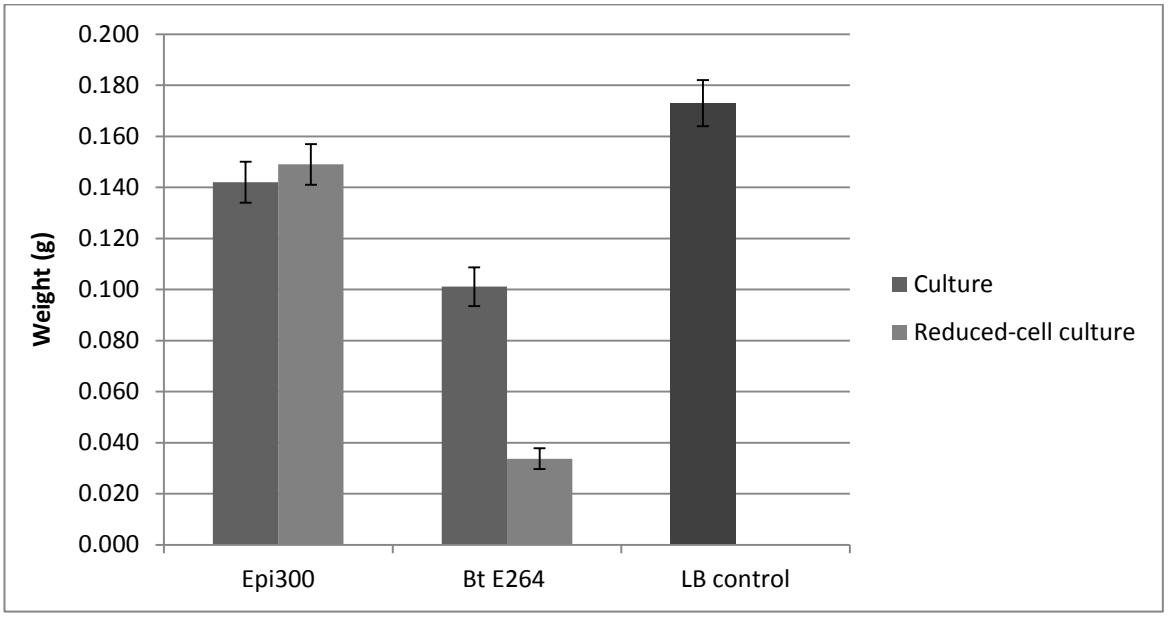

This effect may perhaps be explained if: a low number of cells allows the Bt to achieve a 'stealthy' infection and avoid immune detection before establishing an acute 'attack'; or if a loosely surface-attached toxin is released into the medium (and thereby made available/active) during the centrifugation step to remove cells. Table 3.23 shows the complete results for experiment #3.

Table 3.23. Day 8 weights of surviving neonates (experiment #3). Epi300 = *E. coli* Epi300. In this experiment reduced-cell culture samples contained fewer bacteria (not quantified).

Neonate	LB control (g)	Epi300 culture (g)	Epi300 reduced-cell culture (g)	Bt E264 culture (g)	Bt E264 reduced-cell culture (g)
1.	0.205	0.166	0.158	0.124	0.022
2.	0.171	0.145	0.14	0.135	0.021
3.	0.154	0.144	0.188	0.087	0.025
4.	0.162	0.193	0.198	0.083	0.02
5.	0.17	0.141	0.183	0.189	0.022
6.	0.178	0.106	0.135	0.067	0.028
7.	0.151	0.172	0.202	0.081	0.052
8.	0.136	0.187	0.173	0.082	0.036
9.	0.229	0.156	0.114	0.098	0.023
10.	0.177	0.161	0.171	0.113	0.072
11.		0.134	0.123	0.093	0.021
12.		0.154	0.202	0.085	0.048
13.		0.157	0.149	0.126	0.023
14.		0.158	0.135	0.085	0.024
15.		0.123	0.144	0.079	0.067
16.		0.144	0.126	0.091	0.047
17.		0.041	0.082	D	0.023
18.		0.178	0.074	D	D
19.		0.109	0.135	D	D
20.		0.08	0.139	D	D
AVERAGE	**0.173**	**0.142**	**0.149**	**0.101**	**0.032**
SIG.		**0.015 ***	**0.047 ***	**0.000 *****	**0.000 *****
n	**10**	**20**	**20**	**16**	**17**
SE	**0.009**	**0.008**	**0.008**	**0.008**	**0.004**

D = neonate died. SIG. = significance of difference compared to LB average (T-test, unequal variances) *p=0.05, **p=0.01, ***p=0.001.

Figure 3.22 depicts neonate larvae from experiment #3, eight days after beginning to feed on the bacteria-laced diet. The size differences are apparent: LB and Epi300-fed controls are healthy and relatively large; Bt E264-fed larvae are somewhat smaller when fed complete culture or considerably smaller when fed centrifuged culture with low numbers of cells.

Figure 3.22. Day 8 neonates after feeding on bacteria or LB control (experiment #3). In this experiment the reduced-cell culture samples (labelled 'supernatant') contained fewer bacteria (not quantified).

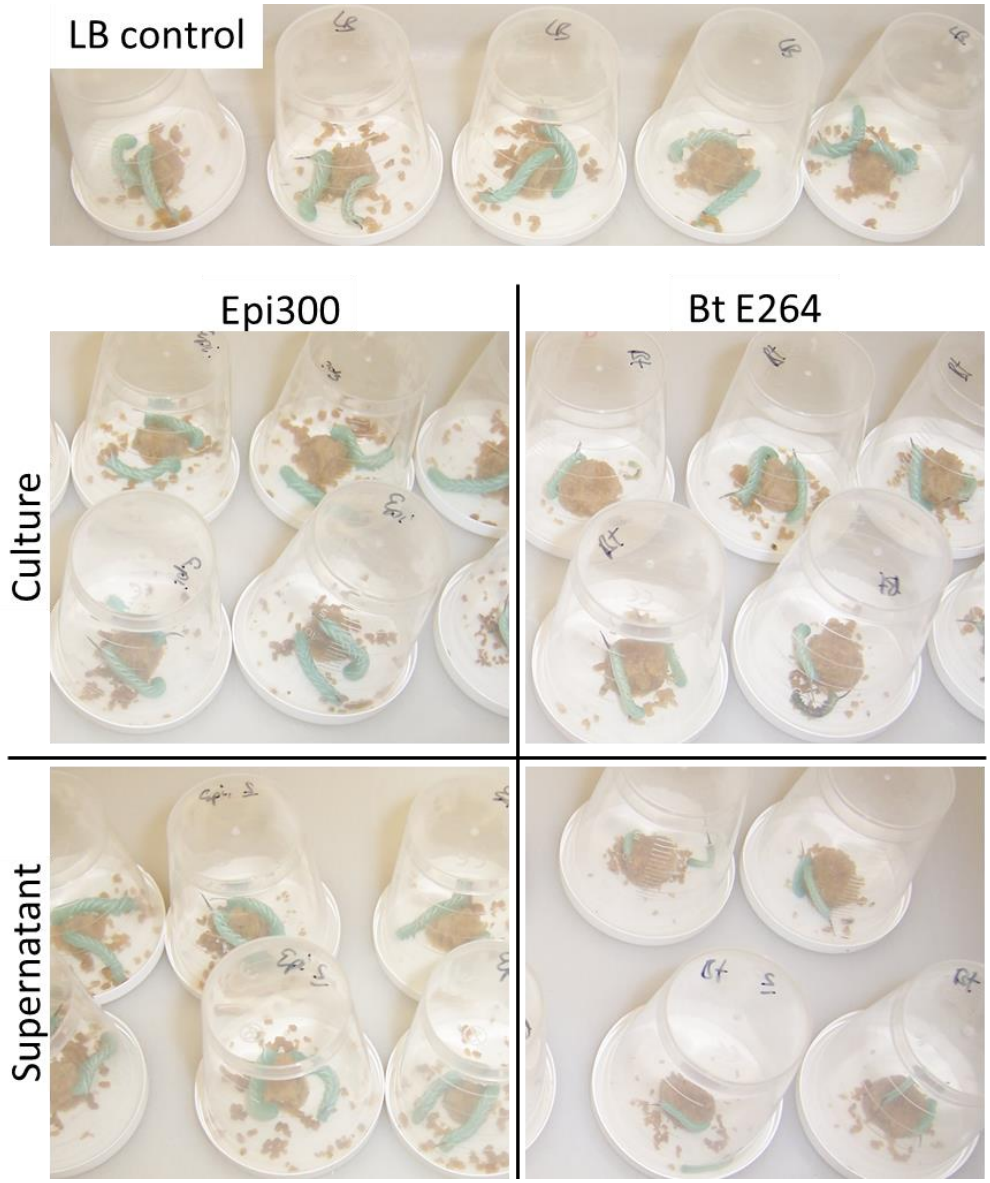

Reduced-cell culture samples were intended as a crude supernatant but they were not truly sterile, so a filtration step was added for the next experiment.

Experiment 4: Experiment #4 was performed in order to repeat experiment #3 but with a properly sterile supernatant and a heat-treated supernatant. Additonally, the experiments were performed over two days so that exponential phase (16 hour) and stationary phase (40 hour) cultures could be compared, and a Bo strain (Bo C6786) was tested in parallel.

A number of food blocks dried out during the course of this experiment due to poor seals on the container pots: those larvae were removed from the data set. Table 3.24 and Figures 3.23-3.24 summarise the survival of neonates fed bacteria and controls which had been incubated for 1 or 2 nights.

Table 3.24. Survival of fed neonates to day 7 (experiment #4). Epi300 = *E. coli* Epi300. 1-night = 16 hours, 2-night = 40 hours. All larvae fed 1-night incubated cultures

		Survival to Day 7			
		1-night incubation		2-night incubation	
		n	%	*n*	%
LB control		17 / 18	94.4	16 / 16	100
Epi300	**Culture**	14 / 14	100	12 / 12	100
	Washed cells	15 / 18	83.3	18 / 18	100
	Supernatant	18 / 18	100	13 / 14	92.3
	Heat-treated supernatant	16 / 16	100	18 / 18	100
Bt E264	**Culture**	11 / 14	78.6	13 / 16	81.3
	Washed cells	13 / 16	81.3	17 / 18	94.4
	Supernatant	13 / 14	92.3	12 / 13	92.3
	Heat-treated supernatant	16 / 16	100	14 / 16	87.5
Bo C6876	**Culture**	16 / 20	80.0	14 / 19	73.7
	Washed cells	13 / 14	92.3	8 / 16	50.0
	Supernatant	14 / 18	77.8	20 / 20	100
	Heat-treated supernatant	10 / 10	100	16 / 17	94.1

Figure 3.23. Experiment #4: Survival of neonate larvae fed upon 1-night-incubated samples. The larvae fed Bt and Bo whole culture or cell-free supernatant showed lower survival than equivalent *E. coli* controls.

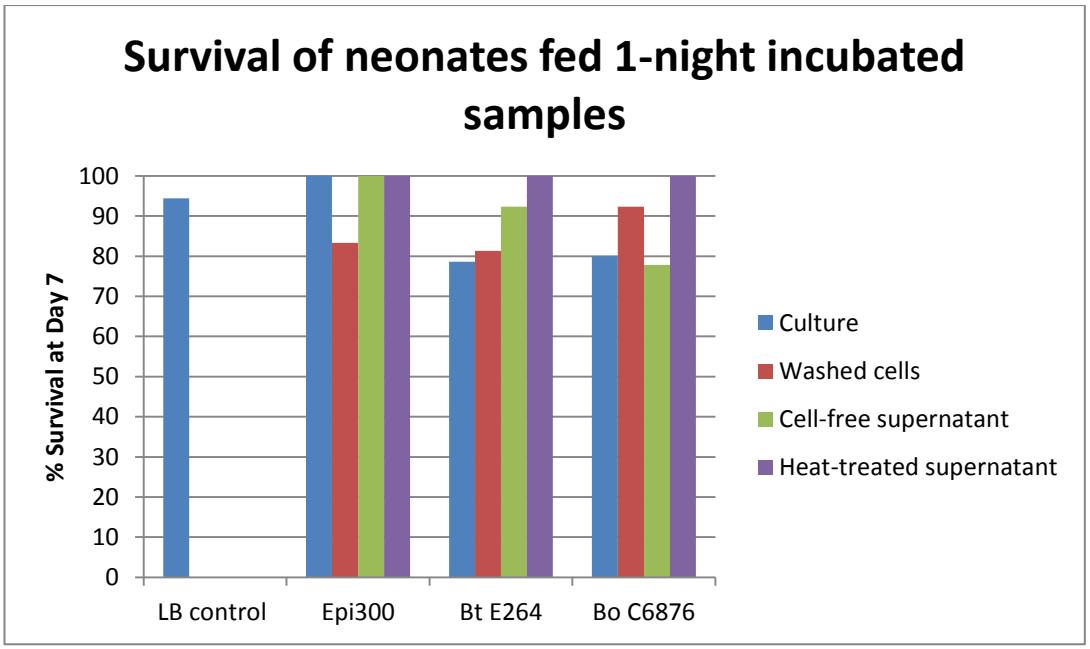

Figure 3.24. Experiment #4: Survival of neonate larvae fed upon 2-night-incubated samples. The larvae fed with each Bt sample showed lower survival than their *E. coli* couterparts. The most striking result is the reduction in survival when fed Bo washed (supernatant-free) cells.

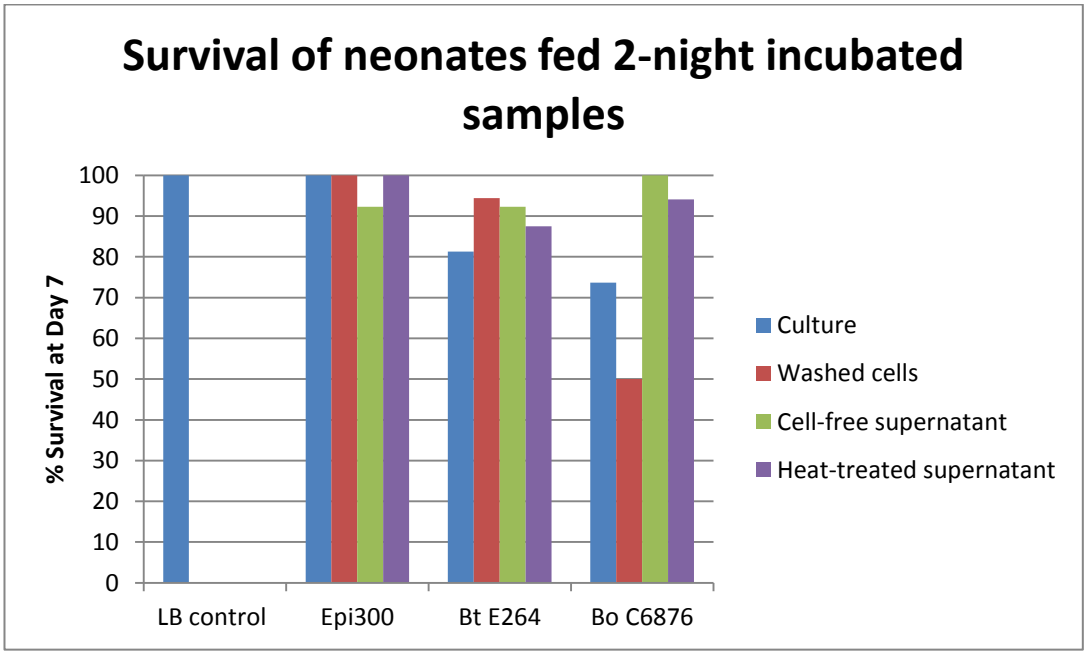

In terms of survival rates, most samples were similar at between 70-100%. The larvae fed Bt and Bo whole culture or cell-free supernatant showed lower survival than equivalent *E. coli* controls. When fed the 2-night incubated (stationary phase) samples, the most striking result was the reduction in survival when fed Bo washed (supernatant-free) cells. This suggests that removal of supernatant also removes a protective factor for the insect host; perhaps a highly antigenic bacterial protein becomes exposed which causes an immune

over-reaction, or perhaps factors in the supernatant prime the insect immune system and allow it to cope better.

Turning to weight instead of survival, the effectsof Bt E264 and Bo C6786 samples on neonate growth are evident in the photos in Figure 3.25.

Figure 3.25. Day 7 neonates after feeding on bacteria or LB control: 2-night-incubated (experiment #4)

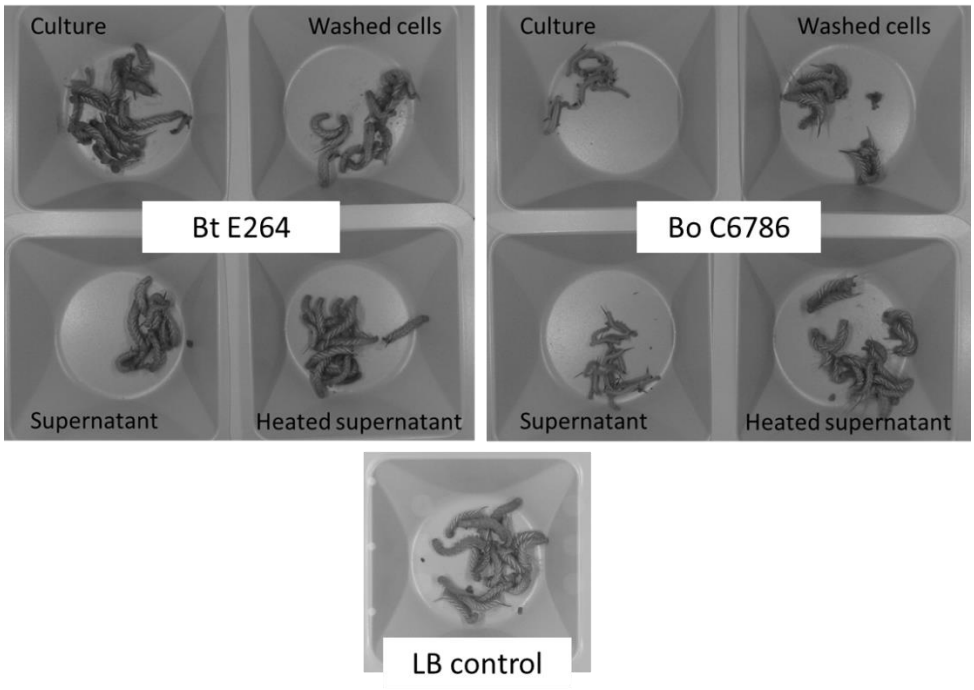

The following Figures 3.26-3.27 summarise the weights of surviving neonates which had been fed bacteria and controls which had been incubated for 1 or 2 nights. Compared to experiment #3, the effects of Bt on neonate weight were less apparent. Bo however showed striking results. Surviving larvae which had been fed Bo whole culture or Bo cell-free supernatant showed greatly reduced weight compared to their counterparts including Bt. The fact that neonates fed heat-treated Bo supernatant were a ‘normal’ weight implies that the factor responsible for the toxic or pathogenic effect is proteinaceous and is released into the supernatant, either naturally or as a result of centrifugation.

Figure 3.26. Experiment #4: Average day 7 weights of surviving neonates fed 1-night (16 hour)-incubated cultures. Error bars = SE. Surviving larvae fed Bo culture or Bo cell-free supernatant showed greatly reduced weight compared to their counterparts, including Bt.

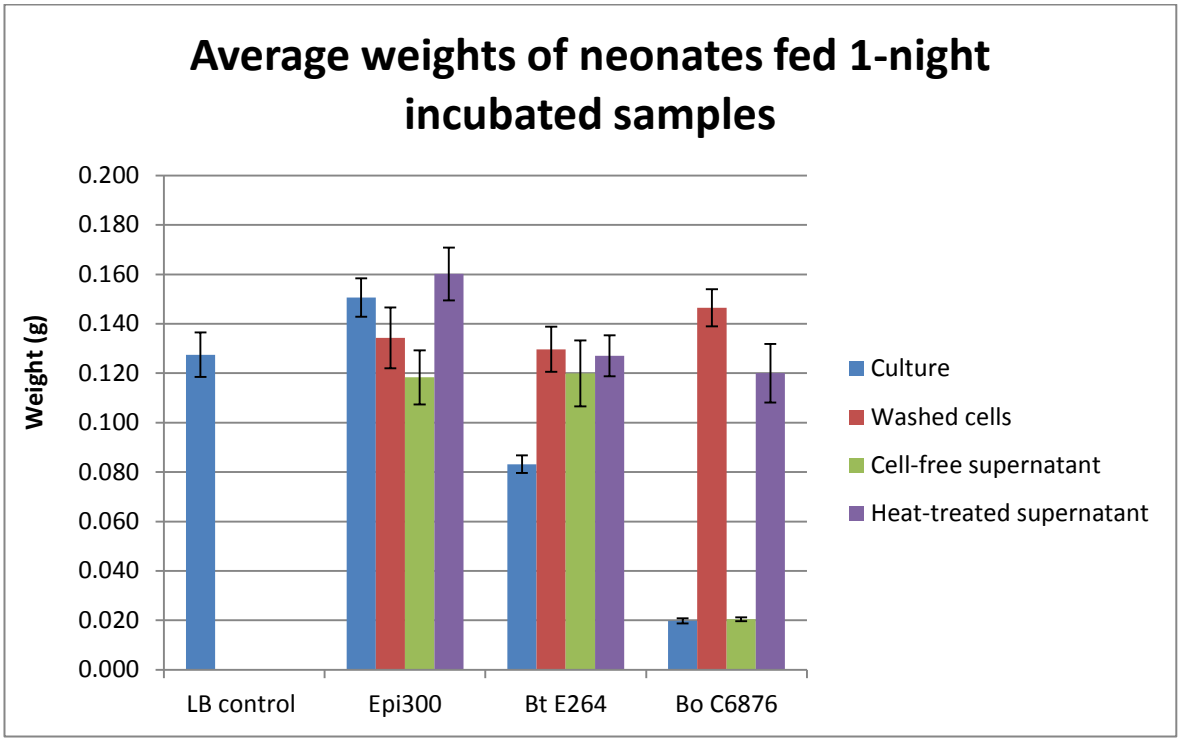

Figure 3.27. Experiment #4: Average day 7 weights of surviving neonates fed 2-night (40 hour)-incubated cultures.Error bars = SE. Surviving larvae fed Bo culture or Bo cell-free supernatant showed greatly reduced weight compared to their counterparts, including Bt.

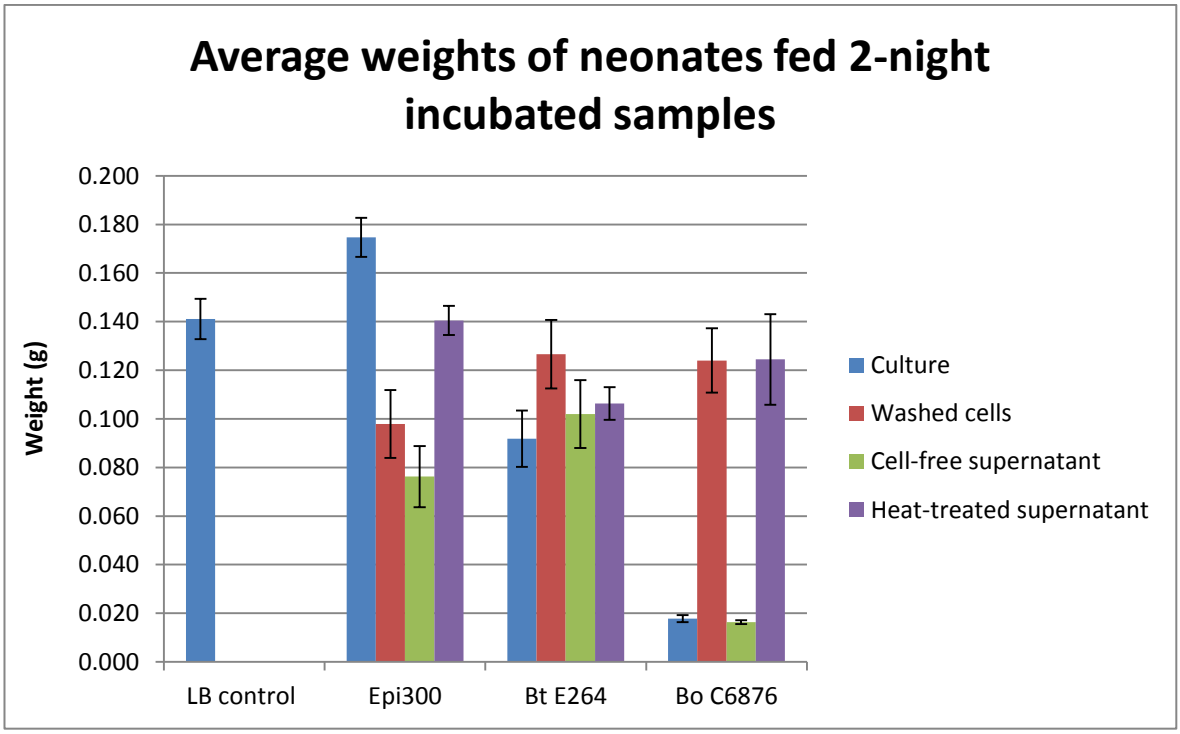

Tables 3.25 and 3.26 contain the data and calculated *p*-values for the 1-night and 2-night-incubated samples, respectively.

Table 3.25. Day 7 weights of surviving neonates: 1-night incubation (experiment #4). Epi300 = E. coli Epi300

Neo-nate	LB (g)	Epi300 (g)				Bt E264 (g)				Bo C6876 (g)			
		Culture	Washed cells	Supernatant	Heat-treated supernatant	Culture	Washed cells	Supernatant	Heat-treated supernatant	Culture	Washed cells	Supernatant	Heat-treated supernatant
1.	0.111	0.182	0.098	0.068	0.193	0.092	0.137	0.098	0.135	0.013	0.136	0.022	0.058
2.	0.121	0.132	0.159	0.046	0.196	0.078	0.137	0.103	0.136	0.015	0.150	0.022	0.155
3.	0.110	0.135	0.088	0.101	0.218	0.064	0.117	0.095	0.086	0.021	0.159	0.022	0.122
4.	0.074	0.190	0.086	0.125	0.144	0.070	0.122	0.154	0.144	0.022	0.106	0.020	0.065
5.	0.177	0.145	0.153	0.062	0.202	0.085	0.124	0.137	0.095	0.012	0.119	0.024	0.151
6.	0.150	0.185	0.228	0.054	0.190	0.088	0.107	0.193	0.088	0.021	0.133	0.022	0.154
7.	0.133	0.116	0.130	0.111	0.211	0.077	0.065	0.158	0.169	0.018	0.138	0.021	0.099
8.	0.124	0.124	0.093	0.128	0.141	0.072	0.209	0.179	0.149	0.026	0.201	0.021	0.112
9.	0.081	0.154	0.118	0.113	0.176	0.092	0.114	0.146	0.144	0.022	0.150	0.016	0.121
10.	0.114	0.159	0.190	0.117	0.130	0.096	0.165	0.122	0.167	0.017	0.173	0.025	0.163
11.	0.146	0.169	0.210	0.193	0.166	0.101	0.179	0.098	0.154	0.020	0.171	0.015	F
12.	0.106	0.185	0.192	0.185	0.157	D	0.099	0.050	0.058	0.017	0.162	0.018	F
13.	0.081	0.135	0.141	0.166	0.137	D	0.109	0.026	0.113	0.026	0.172	0.018	F
14.	0.189	0.097	0.081	0.107	0.147	D	D	D	0.130	0.024	D	0.020	F
15.	0.208	F	0.088	0.205	0.087	F	D	F	0.163	0.019	F	D	F
16.	0.123	F	D	0.138	0.068	F	D	F	0.101	0.024	F	D	F
17.	0.119	F	D	0.089	F	F	F	F	F	D	F	D	F
18.	D	F	D	0.122	F	F	F	F	F	D	F	D	F
19.	F	F	F	F	F	F	F	F	F	D	F	F	F
20.	F	F	F	F	F	F	F	F	F	D	F	F	F
MEAN (g)	**0.127**	**0.151**	**0.134**	**0.118**	**0.160**	**0.083**	**0.130**	**0.120**	**0.127**	**0.020**	**0.147**	**0.020**	**0.120**
SIG. vs LB		0.062	0.549	0.525	0.026 *	0.000 ***	0.881	0.645	0.970	0.000 ***	0.045 *	0.000 ***	0.621
SIG. vs Epi						0.000 ***	0.654	0.928	0.020 *	0.000 ***	0.332	0.000 ***	0.020 *
SIG. vs Bt										0.000 ***	0.328	0.000 ***	0.435
n	**17**	**14**	**15**	**18**	**16**	**11**	**17**	**13**	**16**	**16**	**13**	**14**	**10**
SE.	0.009	0.008	0.012	0.011	0.011	0.004	0.009	0.013	0.008	0.001	0.008	0.001	0.012

D = neonate died. F = food dried out, excluded from data. SIG. = significance of difference compared to LB average, equivalent Epi300 average, or equivalent Bt E264 average (T-test, unequal variances) *p≤0.05, **p≤0.01, ***p≤0.001.

Table 3.26. Day 7 weights of surviving neonates: 2-night incubation (experiment #4). Epi300 = *E. coli* Epi300

Neo-nate	LB (g)	Epi300 (g)				Bt E264 (g)				Bo C6876 (g)			
		Culture	Washed cells	Supernatant	Heat-treated supernatant	Culture	Washed cells	Supernatant	Heat-treated supernatant	Culture	Washed cells	Supernatant	Heat-treated supernatant
1.	0.134	0.159	0.047	0.054	0.149	0.112	0.138	0.166	0.092	0.023	0.190	0.024	0.225
2.	0.122	0.197	0.050	0.174	0.195	0.092	0.157	0.130	0.073	0.022	0.077	0.022	0.182
3.	0.208	0.182	0.150	0.146	0.098	0.059	0.052	0.166	0.144	0.020	0.097	0.018	0.182
4.	0.147	0.191	0.174	0.083	0.157	0.088	0.171	0.160	0.098	0.017	0.116	0.013	0.178
5.	0.075	0.209	0.078	0.028	0.146	0.081	0.163	0.074	0.105	0.014	0.168	0.017	0.071
6.	0.138	0.185	0.035	0.023	0.151	0.052	0.168	0.020	0.081	0.015	0.110	0.020	0.077
7.	0.174	0.175	0.174	0.062	0.131	0.149	0.111	0.084	0.146	0.014	0.128	0.011	0.183
8.	0.172	0.187	0.164	0.059	0.119	0.140	0.174	0.130	0.111	0.016	0.106	0.010	0.055
9.	0.148	0.120	0.151	0.102	0.140	0.087	0.155	0.084	0.113	0.013	D	0.019	0.058
10.	0.114	0.122	0.138	0.110	0.149	0.159	0.182	0.099	0.133	0.018	D	0.019	0.011
11.	0.161	0.191	0.098	0.051	0.173	0.091	0.184	0.052	0.034	0.032	D	0.013	0.109
12.	0.185	0.178	0.120	0.045	0.137	0.006	0.117	0.059	0.033	0.013	D	0.020	0.083
13.	0.110	F	0.189	0.054	0.158	0.078	0.020	D	0.174	0.018	D	0.013	0.150
14.	0.132	F	0.048	D	0.164	D	0.195	F	0.151	0.014	D	0.012	0.140
15.	0.112	F	0.060	F	0.072	D	0.085	F	D	D	D	0.015	0.141
16.	0.126	F	0.022	F	0.073	D	0.038	F	D	D	D	0.015	0.146
17.	F	F	0.022	F	0.169	F	0.042	F	F	D	F	0.016	D
18.	F	F	0.042	F	0.147	F	D	F	F	D	F	0.015	F
19.	F	F	F	F	F	F	F	F	F	D	F	0.018	F
20.	F	F	F	F	F	F	F	F	F	F	F	0.017	F
MEAN (g)	**0.141**	**0.175**	**0.098**	**0.076**	**0.140**	**0.092**	**0.127**	**0.102**	**0.106**	**0.018**	**0.124**	**0.016**	**0.124**
SIG. vs LB		0.008 **	0.013 *	0.000 ***	0.952	0.002 **	0.383	0.026 *	0.020 *	0.000 ***	0.294	0.000 ***	0.340
SIG. vs Epi						0.000 ***	0.158	0.183	0.019 *	0.000 ***	0.190	0.000 ***	0.351
SIG. vs Bt										0.000 ***	0.895	0.000 ***	0.341
n	**16**	**12**	**18**	**13**	**18**	**13**	**17**	**12**	**14**	**14**	**8**	**20**	**16**
SE.	0.008	0.008	0.014	0.013	0.006	0.012	0.014	0.014	0.007	0.001	0.013	0.001	0.019

D = neonate died. F = food dried out, excluded from data. SIG. = significance of difference compared to LB average, equivalent Epi300 average, or equivalent Bt E264 average (T-test, unequal variances) *p≤0.05, **p≤0.01, ***p≤0.001.

The *p*-values from the 1-night exponential phase samples (Table 3.25) indicate that: Epi300 samples had little effect on the neonates' growth compared to LB except that heat-treated supernatant seemed to confer some nutrition; Bt E264 culture resulted in significantly reduced weight gain compared to LB or Epi300; and Bo C6786 samples resulted in weight gain that was significantly even less than Bt E264 culture or supernatant.

The *p*-values from the 2-night stationary phase samples (Table 3.26) indicate that: Epi300 culture was nutritious whereas Epi300 washed cells or supernatant led to reduced weight; Bt E264 culture again resulted in significantly reduced weight gain compared to LB or Epi300; and Bo C6786 samples again resulted in weight gain that was significantly less than even Bt E264 culture or supernatant.

Table 3.27 summarises the percentage difference in mean neonate weight after feeding with 1-night-incubated versus 2-night-incubated bacteria. As noted in the method details, the neonates which were used for the first batch (1-night-incubated samples) appeared to be less healthy than usual, so it is unsurprising that the 2nd batch showed a 10.7% greater weight even in the LB control group.

Table 3.27. Comparison of Day 7 weights of surviving neonates fed 2-night incubated (stationary phase) *versus* 1-night incubated (exponential phase) bacterial or control samples. Epi300 = *E. coli* Epi300. Control larvae weighed 10.7% more in the 2nd batch, indicating the difference in general health of the larvae used on the two consecutive days.

	LB	Epi300				Bt E264				Bo C6876			
		Culture	Washed cells	Supernatant	Heat-treated supernatant	Culture	Washed cells	Supernatant	Heat-treated supernatant	Culture	Washed cells	Supernatant	Heat-treated supernatant
1-night incubation (g)	0.127	0.151	0.134	0.118	0.160	0.083	0.130	0.120	0.127	0.020	0.147	0.020	0.120
2-night incubation (g)	0.141	0.175	0.098	0.076	0.140	0.092	0.127	0.102	0.106	0.018	0.124	0.016	0.124
% difference	+10.7	+16.0	-27.1	-35.6	-12.3	+10.4	-2.4	-14.9	-16.3	-10.2	-15.4	-20.0	+3.7

Figure 3.28 therefore shows the percentage differences after accounting for the difference in the LB control.

Figure 3.28. Chart showing the % difference in average Day 7 weights of surviving neonates (fed 2-night incubated *versus* 1-night incubated samples) minus the % difference seen in the LB control group. A negative change indicates that neonates fed 2-night incubated samples weighed less, i.e. were less healthy, than those fed the equivalent 1-night incubated samples.

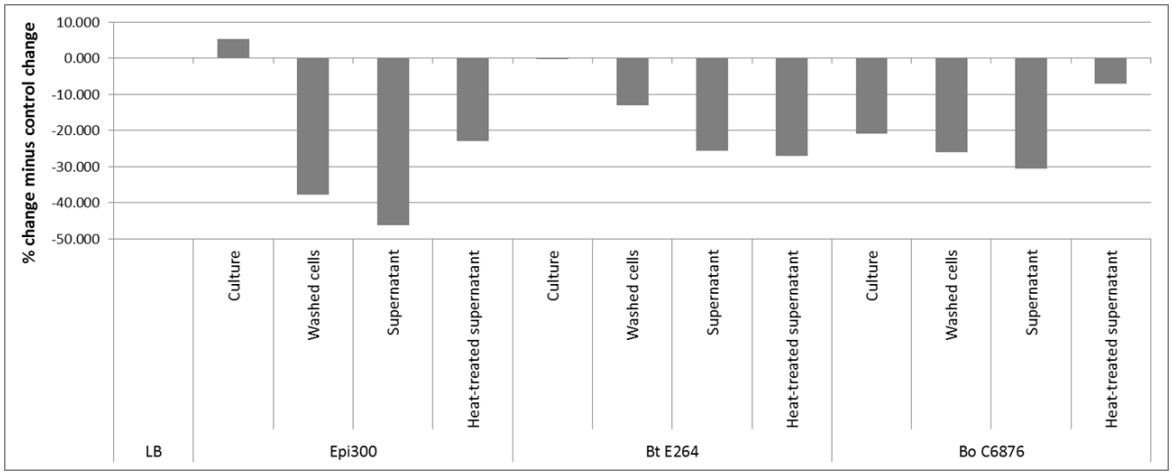

For most samples the stationary-phase samples were more harmful or less nutritious to neonates compared to exponential-phase samples. However, that effect was no greater for the Bt and Bo samples than the Epi300 *E. coli* samples, which indicates that unlike some *Photorhabdus* toxins the harmful factors produced by Bt or Bo are not up-regulated in stationary phase compared to exponential phase.

Several points summarise the feeding experiments. When fed Bt E264 cultures, *M. sexta* neonates were variably killed or their growth was reduced. When fed Bo C6786 culture or cell-free supernatant, neonates showed greatly reduced growth. Mortality and morbidity (indicated by reduced growth) can be caused by infection or by toxic factors, or both. Bo washed cells led to 50% mortality. Infection may play a role but the fact that Bo cell-free supernatant caused morbidity indicates that a toxic factor is involved. The Bt results varied in the different experiments; in experiment #3 the reduced-cell culture (non-sterile supernatant) resulted in greatly reduced weight, but in experiment #4 the effect of cell-free supernatant was no greater than that of Epi300 *E. coli*. In both cases however, Bt E264 whole culture caused significantly greater morbidity than Epi300.

The results overall show that Bt and Bo are pathogenic to *M. sexta* neonates by the oral route, and indicate that a soluble toxic factor(s) are involved to some extent.

3.4. Discussion

3.4.1. Burkholderia virulence in Manduca sexta

The initial experiments with *C. elegans* and *A. polyphaga* confirmed that our stock of Bt E264 was indeed pathogenic to these invertebrates or able to evade predation as other studies have reported it to be (Ooi *et al*. 2012; Inglis *et al*. 2000). Neither host organism succeeded in consuming the bacterial mats. *C. elegans* were motionless and no offspring were hatched. Injecting Bt E264 into *M. sexta* larvae for the first time confirmed that, like *G. mellonella*, *M. sexta* is susceptible to Bt infection. In fact, effects of pathogenesis were seen rapidly; with a direct injection of overnight culture the larvae exhibited signs of paralysis by 20 hours and were dead by 24 hours post-injection. Paralysis prior to death has previously been reported for Bp or Bt infection in nematodes and *G. mellonella* (O'Quinn *et al*. 2001; Kim *et al*. 2005; Gan *et al*. 2002; Schell *et al*. 2008; Wand *et al*. 2011).

Bt E264 shows a dose-responsive lethal effect

Further tests with Bt E264 confirmed that the rate of disease progression was positively correlated with bacterial dose, with median times to death (MTTDs) ranging from 48 hours at a dose of 10^5 CFU to 144 hours at 10 CFU.

In Manduca sexta Bp K96423 is less virulent than Bt E264

Surprisingly, when the Bp type strain K96423 was tested in *M. sexta* it was clearly less virulent than Bt E264. At 10^5 CFU the MTTD was 72 hours and at 10 CFU more than half of the larvae survived the course of the experiment (7 days post-injection). It was not feasible to maintain larvae beyond that time; beyond wanderer stage they begin to pupate and it could be hazardous and impractical to keep infected moths. As was the case with Bt E264, the larvae showed signs of paralysis prior to death. It is not clear whether the paralysis (judged by larvae showing an extremely limited response to stimuli) is due to a direct effect on the motor system or is a side-effect of limited resources and energy while fighting the bacterial infection. The fact that melanocytic spots were visible on several larvae (infected with either Bt or Bp) indicated that their immune systems had actively defended against bacteria.

Reversal of relative Bp-group virulence in M. sexta

When including Bt strains and the two Bo strains, it seems that in general the degree of *Burkholderia* virulence in *M. sexta* is inversely related to the degree of virulence in mammals. Both the Bo strains were more virulent than Bt E263, and Bp was less so. It

can be reasoned that greater virulence in a mammalian host comes at the expense of virulence in un-related host taxa such as insects, or in the environment, and *vice versa*. Thereby, although Bp is highly virulent in mammals it is much less so in *M. sexta*, and the mammalian-avirulent Bo strains display dramatic virulence in this insect. Indeed, in *C. elegans* Bt E264 was more virulent than Bp strains were (O'Quinn *et al*. 2001). However, this theory is not supported by contrasting results reported for the *G. mellonella* model. As illustrated in Figure 3.29, in most respects the *G. mellonella* findings from Wand *et al* correlated well with virulence in mammalians (Wand *et al*. 2011).

Figure 3.29. The relative virulence of several *Burkholderia* strains in the mouse *Mus musculus* (Titball *et al*. 2008; DeShazer 2007), in *G. mellonella* (Wand *et al*. 2011), and in *M. sexta* (this study). Bp = *B. pseudomallei*, Bt = *B. thailandensis*, Bo = *B. oklahomensis*. In the mouse Bp is highly virulent, most Bt strains are virulent, Bt CDC 272 and Bo strains are avirulent. In *G. mellonella* according to Wand *et al* Bp and Bt strains are virulent and Bo is avirulent. In *M. sexta* results (this study) Bo strains and Bt CDC 301 were the most virulent followed by Bt E264, and Bt CDC 272 and Bp exhibited relatively low virulence.

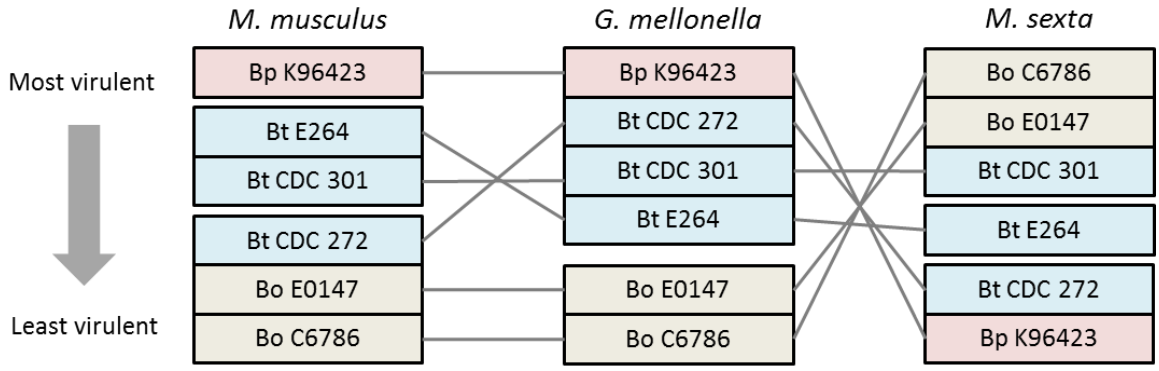

One notable exception relates to the virulence of Bt CDC 272. In hamsters and mice most Bt strains (including Bt E264 and Bt CDC 301) exhibit some virulence, but the Bt strain CDC 272 is avirulent (DeShazer 2007; Wand *et al*. 2011). Wand *et al* reported that in *G. mellonella* Bt CDC 272 was more virulent than E264. In *M. sexta* however, Bt CDC 272 showed low virulence, either killing as slowly as Bp K96423 or not at all. In this case the *M. sexta* results reflect observations from mammalian models; the variant strain CDC 272 is attenuated compared to most Bt strains.

Bt CDC 272 and CDC 301 are phylogenetically closely related but CDC 301 expresses a Bp-like CPS which is absent from CDC 272. As CDC 272 was at least as virulent as CDC 301 in the *G. mellonella* model Wand *et al* (2011) reasoned that the CPS cluster is not required for virulence in insects. Our findings show that those results were not necessarily representative of all insects. Although the CPS cluster is not required for virulence of Bt E264 and other Asian strains, it may well be important for the virulence of the American variant strains. Its presence might explain the greatly increased virulence of CDC 301 compared to its close relative CDC 272, in *M. sexta* at least.

Virulence in Galleria mellonella at 25 °C versus 37 °C

It was apparent that the results from *G. mellonella* (Wand *et al*. 2011) and *M. sexta* (this study) were quite different, and one crucial difference between the models was the temperature at which the larvae were maintained post-injection: *G. mellonella* at 37 °C and *M. sexta* at 25 °C. In order to assess whether the reversal of *Burkholderia* virulence is a consequence of the incubation temperature it would be ideal to repeat the *M. sexta* virulence assay with larvae maintained at both temperatures after injection. One limitation of the *M. sexta* model is that the health of the larvae may be compromised when maintained at 37°C; although other authors have reported success using *M. sexta* for infection studies at 37 °C (Fleming *et al*. 2006), in a previous study in this laboratory larva mortality at 37 °C was 30% when injected with PBS alone and 60% when injected with *E. coli* Epi300 (unpublished, Waterfield lab). For that reason, the comparative virulence of the same strains at 25°C and 37°C was investigated in this study using *G. mellonella* larvae only (summarised in Figure 3.30).

Figure 3.30. The relative virulence of several *Burkholderia* strains in *G. mellonella* maintained at 37 °C in a previous study (Wand *et al*. 2011) and at 37 °C and 25 °C in this study. The *M. sexta* results at 25 °C from this study are also compared. Bt = *B. thailandensis*, Bo = *B. oklahomensis*.

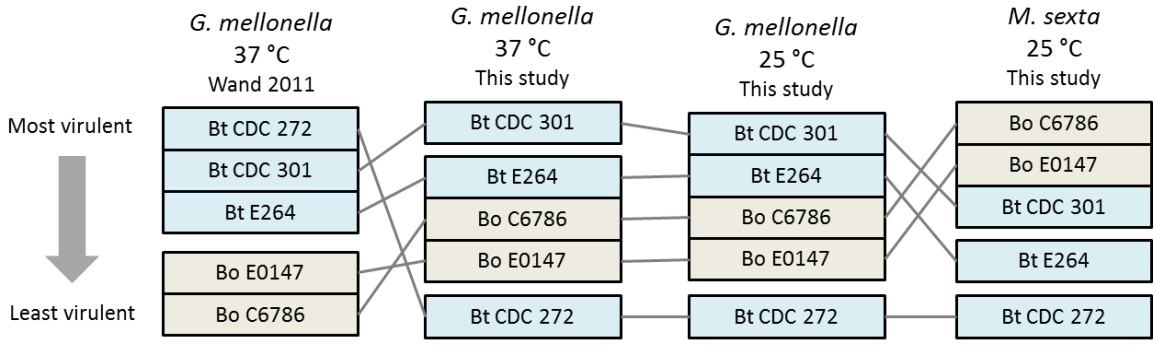

Our findings at 37°C again differed from those of Wand *et al*; Bt CDC 272 was still found to be attenuated (less than half the larvae died), and the Bo strains were as virulent as Bt E264 (MTTD = 48 hours). Bt CDC 301 was the most virulent strain (MTTD = 24 hours).

At 25°C our *G. mellonella* results were broadly the same as at 37°C. Bt CDC 272 was attenuated and the Bo strains were virulent. However, all four virulent strains had the same MTTD values (72 hours); shorter intervals between scoring would help to resolve whether there is any difference in virulence. Nonetheless, the difference must have been only slight. Notably the Bo strains and Bt E264 were found to have comparable virulence in *G. mellonella* at either temperature. In *M. sexta* the Bo strains were considerably more virulent than Bt E264, with MTTD values being 20-24 hours shorter.

The strains used came from the same source as those used by Wand *et al* (Titball lab, University of Exeter). It is not clear why the Bo strains were avirulent in their *G. mellonella* assay and virulent in ours, and why the opposite was true for Bt CDC 272. The further differences observed in *M. sexta* could related to: (i) unknown differences in the precise host-pathogen interactions; (ii) a longer time required to overcome the larger host which enables differences in MTTD to be resolved more accurately; (iii) a combination of both.

G. mellonella belongs to the Pyralidae family which is considered to be an ancient clade within the Lepidoptera. Therefore its immune system is thought to be basal and perhaps more relevant to mammalian innate immunity than the more evolved and specialised system of *M. sexta* (Vogel *et al*. 2011). The fact remains that there is still a lot to learn from these models in order to fully characterise and understand their immune mechanisms, differences and similarities. Additionally, our *G. mellonella* 37 °C and 25 °C MTTD values did not show a great deal of resolution between the virulence of the different strains as they were based on 24 hour intervals, so further investigation would be warranted to confirm to what extent temperature plays a part. The higher incubation temperature clearly affects the rate of disease progression, probably due to increased bacterial growth, reduced *M. sexta* health, or both.

3.4.2. Assessment of Bt E264 mutants in *Manduca sexta*

Two E264 mutants were tested that had been constructed by other research groups and found by them to be attenuated in the *G. mellonella* model (Norville 2011; Wagley, unpublished results).

ΔsurA mutant

In the first assay the Δ*surA* -infected *M. sexta* larvae were incubated at 37°C to replicate the conditions of the *G. mellonella* assay performed at Dstl. A slight attenuation was observed. To make the work comparable to the rest of our *Burkholderia* dose response assays, the next experiment, with lower doses, was incubated at 25°C. It was performed in triplicate experiments, giving n = 30 for each condition tested. At 10^2 CFU there was a 10 hour difference in MTTD, with the Δ*surA* strain being slower to kill. The calculated p-values indicated that survival curves were significantly different but for E264 and Δ*surA* at both 10^3 and 10 CFU doses the MTTD values were the same. Although the MTTD statistic has been used throughout this study to compare virulence, it is interesting to note that when the mean (as opposed to median) time to death is calculated there is a more pronounced attenuation of Δ*surA*, especially at the 10^3 CFU dose. When Δ*surA* was tested once again, this time alongside the other *Burkholderia* strains at doses 10^2-10^4, the MTTD values were considerably greater, with 10^3 CFU now having MTTD 76 hours (as

opposed to 36 hours in the triplicate experiment). This variation may be due to using different 'batches' of larvae; the health of the colony may naturally fluctuate slightly and the experiments were separated by several weeks. Combining all the results, Bt E264 Δ*surA* ranks just below the wild-type E264 strain in terms of *Burkholderia* virulence in *M. sexta*. Therefore, even this attenuated Bt strain was still more virulent to *M. sexta* than Bp K96423 or the Bt variant strain CDC 272.

TAT mutant

The E264 TAT mutant (prhA:tatA) yielded less straightforward results. The first experiment used the mutant and the E264 wild-type strain grown in LB containing either rhamnose (to maintain TAT activity) or glucose (to inactivate TAT in the conditional mutant). Results from three of the conditions looked fairly similar but surprisingly the mutant grown in rhamnose, reported to have wild-type-like activity in *G. mellonella*, was significantly less virulent. It was known that the mutant grows more slowly in LB with glucose but that was not the case for LB with rhamnose, suggesting that the general health of the bacterium was probably not the cause of this unexpected effect. It was also noticed that several of the larvae in the TAT experiments exhibited a dark blue tinge, which was unusual. Although they would be at a low concentration after diluting the inoculum to e.g. 10^3 CFU per ml, the presence of sugars may have affected the host physiology and response.

In order to investigate this theory the next experiment also tested the two strains after growth in LB alone. The TAT mutant grew slowly in LB without sugar, indicating that the system was probably inactive (although confirmation of this would require further experimental investigation). Bt E264 killed within 72-96 hours (MTTD) after growth in LB alone or with glucose; with rhamnose there was a slightly longer MTTD (72-120 hours). Directly compared to the E264 strain in LB, the MTTDs of the TAT mutant grown in LB were much longer (120-168 hours, and less than 50% dead at 10^2 CFU). This suggests that the TAT mutant is indeed attenuated. Whether that is due to a direct effect on virulence or simply reduced growth is not clear but seeing as growth in complete media was reduced it is reasonable to assume that growth in the host is also reduced. When either glucose or rhamnose was present in the LB the TAT mutant still killed more slowly at 10^2 CFU than wild-type, but more quickly than the mutant without any sugar. It is conceivable that the sugar helps the weakened bacterial mutant during the infection, as an energy source for example. Rhamnose is a pathogen-associated molecular pattern (PAMP) – for example, it forms part of the mycobacterial cell membrane (Ma *et al*. 2001). It may therefore 'distract' the *M. sexta* immune system from the Bt cells, acting as a competitive inhibitor to some degree. Importantly, glucose has been observed to enhance

Bp biofilm formation, which is likely to aid survival within a host (Ramli *et al*. 2012). Nutrients including sugars are also known to affect *Burkholderia* secondary metabolite production and quorum signals (Keum *et al*. 2009). The effects only seemed to be beneficial to the weakened TAT mutant strain; the wild-type E264 showed little difference in overall virulence with or without the different sugars present.

The sugar-related effect with the Bt E264 TAT mutant was apparently not observed in the wax worm model: *G. mellonella* challenged with 10^4 CFU Bt E264 or TAT mutant grown in rhamnose (active TAT) all died by 18 hours post-challenge, whereas those injected with TAT mutant grown in glucose (inactive TAT) all survived beyond 20 hours with 85% dead by 24 hours (S. Wagley, unpublished). The TAT mutant has since been assessed in zebrafish (*Danio rerio*) embryos as well; fish challenged with active TAT strains (Bt E264 or TAT mutant grown in rhamnose) showed 40% and 30% survival, whereas fish challenged with inactive TAT (mutant grown in glucose) showed 80% survival (S. Wagley, unpublished).

The aim behind testing known attenuated mutants in *M. sexta* was to discover whether this host is potentially useful for evaluating mutants in the future. Three conclusions can be drawn: (i) the Δ*surA* mutant did show attenuation, therefore supporting the potential use of the *M. sexta* model for mutant characterisation; (ii) conditional mutants controlled by sugar concentration are not suitable for testing in this model as sugar-control cannot be sustained inside the host and sugar appears to affect the outcome of host-pathogen interactions; and (iii) as seen earlier with Bo strains, attenuation in *G. mellonella* is not necessarily a predictor of attenuation in *M. sexta*.

3.4.3. *Burkholderia* exhibit oral pathogenicity or toxicity to *Manduca sexta*

Bt E264 was fed to *M. sexta* neonates in four experiments. In the first, only three of ten neonates survived to day eight, compared to nine of ten from the control group fed LB-laced food. Of the three survivors the day 8 weight was not significantly different from the control group. Therefore in that experiment the outcome of ingestion of Bt was ‘all or nothing’ – either the neonates died or they showed no ill effects. In most cases the dead larvae were found away from the food block, and they were very small. They may have starved as a result of a ‘choice’ not to consume Bt, or perhaps due to an inability to continue eating caused by consumption of the bacteria (e.g. paralysis).

As so many Bt-fed neonates had died, the next experiment used bacterial cultures diluted to OD_{600} 0.1, but then no difference was seen in terms of mortality or size compared to the

control group. Either the effect was not potent enough or the appropriate bacterial genes were not expressed at lower cell density.

Returning to undiluted overnight cultures, Bt was also fed to older fifth-instar larvae. The fifth-instars fully consumed the whole bacteria-laced food blocks by day two, which were then replaced with fresh bacteria-free and antibiotic-free diet. None of the larvae showed any signs of illness. It would be interesting to test whether, had they continued to be fed only on Bt-laced diet, a detrimental effect would eventually be observed; nematode studies show that prolonged contact with the bacteria is required for full pathogenesis of *C. elegans* (Ooi *et al*. 2012; Day & Sifri 2012). But the lack of effect on fifth-instar *M. sexta* was not unexpected, as feeding experiments within the Waterfield lab using *Photorhabdus* and *Yersinia* Toxin Complex (TC) toxins have shown that neonates are more susceptible to oral toxicity than the later developmental stages. This could relate to the immaturity of the neonate gut immune barriers or to the greater dose received relative to the size of the larva.

The neonate results did show again that Bt had a detrimental effect. This time however the mortality was less severe (80% survival as opposed to 30%) but the weight of surviving larvae was significantly reduced compared to LB-fed controls. This is in contrast to the previous 'all or nothing' result. The Bt was fed either as whole culture (as before) or as a 'reduced-cell culture' (non-sterile supernatant). The neonates fed reduced-cell culture were significantly smaller than the whole-culture-fed group, indicating that the centrifugation process used to remove cells had increased the toxicity of the sample. Perhaps loosely attached proteins or polysaccharides could be sheared off into the supernatant during centrifugation steps. For example, lipopolysaccharide (LPS) and lipooligosaccharide (LOS) endotoxins are important for virulence of many Gram negative bacteria and are associated with the outside of the cell. Furthermore, insecticidal TC toxins are variably cell-surface attached or secreted away from the cell, and homologues do exist in *Burkholderia* (Yang *et al*. 2012; Waterfield *et al*. 2001). Alternatively, perhaps the presence of fewer Bt cells may have led to a less vigorous host immune response or toxin excretory response, while a component of the conditioned medium still exerted an effect which ceased neonate feeding.

The final experiment separated different components of the cultures more carefully. As well as whole culture, the neonates were fed: cells which had been washed free of supernatant; cell-free filtered supernatant; and heat-denatured cell-free filtered supernatant. An additional variable that was tested was the effect of incubating the bacterial cultures for an extra 24 hours prior to the treatments. This was in order to

discover whether any effect might be more potent after stationary phase, as *Photorhabdus* TC toxins are expressed at stationary phase (Yang *et al*. 2012).

Out of interest this last experiment also compared the effects of a Bo strain (C6786), which exhibited striking effects. Comparing the day seven weights of surviving neonates revealed that this time Bt E264 culture and supernatant did not show the detrimental effects seen previously, but Bo C6786 did. Bo whole culture and supernatant were significantly toxic to the neonates, while washed cells and heat-denatured supernatant were not. This indicates that Bo supernatant can show a deleterious effect on *M. sexta* neonate health and the orally toxic factor was heat-inactivated, suggesting it is likely to be proteinaceous.

As discussed in the main introduction, Bp and Bt have been suggested to kill *C. elegans* nematodes in part through the activity of an unknown toxin or paralytic agent (O'Quinn *et al*. 2001), which may be soluble and heat labile (Gan *et al*. 2002). In contrast, one publication argued that a diffusible toxin was not present or at least was not effective (Lee *et al*. 2011), on the basis of the fact that nematode killing required prolonged contact with the bacteria. More recently, a comprehensive study has demonstrated that upon exposure to Bp: nematode pharyngeal pumping and defecation rates are reduced (which may be mediated by either the nematode or by bacterial factors); and a nematode detoxification transporter is up-regulated (Ooi *et al*. 2012). The *M. sexta* feeding results indicate that a diffusible toxic factor is produced by Bo. The Bt results from the last experiment (with cell-free supernatant) do not support the same conclusion but this would certainly warrant repeating.

As discussed earlier in this chapter and in the main introduction (Chapter 1), Bp-group species are known to produce several toxic factors. The BLF1 toxin of Bp is the only confirmed lethal toxin so far (Cruz-Migoni *et al*. 2011; Hautbergue & Wilson 2012). Unknown toxic factors from Bp and Bt are reportedly active against *C. elegans* (O'Quinn *et al*. 2001; Ooi *et al*. 2012; Balaji *et al*. 2004; Day & Sifri 2012), and *D. melanogaster* (Pilátová & Dionne 2012). The activity of Bo supernatant against *M. sexta* could conceivably be due to a related factor. Alternatively, Bp-group bacteria possess several polyketide synthases and non-ribosomal peptide synthetases (PKS/NRPSs), which may synthesise cytotoxic peptides (Biggins *et al*. 2012; Schell *et al*. 2008). T6SS Hcp proteins are also suggested to be toxic (Burtnick *et al*. 2011). CPS, LPS and other surface O-polysaccharides are additional putative virulence factors (Sim *et al*. 2008); it is possible that endotoxins such as these could have been sheared off during sample centrifugation.

Comparing results from *Burkholderia* samples which had been incubated before feeding for 40 hours ('two nights') *versus* 16 hours ('one night') did not show any particular

changes in the patterns of day seven weights. This confirms that the orally toxic factor produced by Bo was neither over-expressed at stationary phase nor any more active over time. The average weights for each group with the one-night and two-night incubated bacteria could not be directly compared in a T-test because the neonates used on the two subsequent days were of quite different sizes to begin with, simply due to variation in day-to-day health of the colony. Ideally every neonate would be weighed before feeding as well as after, but the precision of the scales is problematic at such low weights. One solution might be to calculate the average weight of a group before feeding by weighing all (e.g. twenty) neonates together. Accounting for the percentage weight change seen in the control groups between day one and day two, the largest negative changes were in *E. coli* Epi300 constituents, so the effect is probably due to a general toxicity from dead bacterial cells and lysates rather than a *Burkholderia* specific toxic effect. Interestingly the *E. coli* Epi300 whole culture (cells and supernatant together) gave the neonates a slight growth advantage compared to its 1-night grown culture. Bt E264 culture grown for 2 nights showed no different effect from the 1-night grown culture.

One important observation from the feeding assays is that the effect of Bt E264 culture varies from one experiment to another. Sometimes the result was high mortality but with survivors showing general good health. Sometimes most neonates survived but with very poor weight gain due to very little feeding activity. In some cases the toxic effect was observed from supernatant more than from whole culture, and in others it was only seen with whole culture (and to a lesser extent). What was consistent was that some detrimental effect was always seen from undiluted Bt E264 culture. In the experiment where the effect of Bt was limited to the whole culture only, Bo C6786 showed the same results that Bt E264 had shown previously; a highly deleterious effect on weight gain associated with the whole culture or the supernatant. It is noteworthy that a similarly variable result of a *Burkholderia* strain was observed in the dose response injections, where Bt CDC 272 failed to kill any larvae in one experiment and then killed all (but slowly) in a subsequent one. Some Bp-infected larvae died while others survived, apparently unharmed. Additionally, the MTTD value for Δ*surA* varied from 36 hours in one experiment to 76 hours in another, and the results of Bt CDC 272 and Bo virulence assays in *G. mellonella* were different in this study compared to that by Wand *et al* (Wand *et al*. 2011). The observed variability is likely to be due to subtle differences in individual host-pathogen interactions and/or natural variation within populations of *Burkholderia* cells, for example due to phase variation effects. Phase variation has been demonstrated to play a role in Bcc niche adaptation, with stable variants arising spontaneously and demonstrating differential expression of virulence factors (Vial *et al*. 2010). It has been suggested that this process enables the Bcc strain *B. ambifaria* to adapt to the very different

environments of the rhizosphere or the immunosuppressed lung of cystic fibrosis patients. Simple sequence repeats (SSRs) are often sites of slipped-strand mispairing, a mechanism which is linked to phase variation (Torres-Cruz & Van der Woude 2003) and the genomes of Bp and Bm (and most likely other *Burkholderia*) contain many thousands of SSRs, particularly in genes for surface- or secreted proteins (Song *et al*. 2009).

Toxin-antitoxin (TA) modules have been identified in Bp and Bt strains (and may exist in Bo strains): their function in *Burkholderia* is being investigated but in *E. coli* TA modules are linked to formation of persister cells (Butt *et al*. 2012). Persister cells are phenotypic variants within a population which are in a dormant state. As melioidosis is able to take the form of chronic or latent infections, it has been reasoned that these TA modules may lead to *Burkholderia* persister cell formation. Some Bp TA toxins expressed in *E. coli* did cause growth to cease, and their cognate antitoxins successfully restored growth. Therefore natural variation can occur within *Burkholderia* populations, and this probably contributes to the contrasting results which are quite often reported from different studies using the same strains.

3.4.4. Potential value of *Manduca sexta* as a model host for *Burkholderia*

The virulence of *Burkholderia* species in the wax worm *G. mellonella* apparently reflects their virulence in the mouse model quite well (Wand *et al*. 2011). This suggests that *G. mellonella* is potentially a good surrogate host for further study of *Burkholderia* pathogenesis, virulence factors, or vaccine candidates. Surprisingly, compared to this other lepidopteran host, *M. sexta* showed distinctly different results with a reversal of relative virulence. On one level this is discouraging in terms of the usefulness of *M. sexta* for the long-term aim of modelling melioidosis. However, even between different mammalian models there is considerable variability in the relative pathogenicity of different Bp strains. A review of mammalian models of Bp infection (Titball *et al*. 2008) emphasised that the disease pathogenesis differs between mice, hamsters and diabetic infant rat models. All reflect human melioidosis in different ways, so it is currently accepted that it may be necessary to use multiple different animal hosts to effectively model different aspects of melioidosis infection (Titball *et al*. 2008). *M. sexta* still has numerous practical advantages over *G. mellonella* as described earlier and therefore its usefulness for studying Bp should not be discounted. Although Bp was less virulent than Bt or Bo strains: (i) it was still virulent, killing up to half of the infected larvae; (ii) the fact that the larvae survived for at least three days (and in some cases beyond seven days) could be useful for investigating mechanisms relating to host defence or chronic or latent infection; (iii) only Bp K96423 was tested and as Bp strains are known to vary

considerably in their virulence in mammals it would be interesting to assess more strains in *M. sexta*.

The recent release of the *M. sexta* genome will undoubtedly lead to more genetic and molecular tools and an increased understanding of this insect; with this in mind it could be highly informative to examine the difference between Bp K96423 infection in *M. sexta* versus *G. mellonella*. Discovering what aspects of the bacteria-host interaction greatly reduce the virulence of this formidable pathogen in one insect compared to another could hold the key to developing effective anti-virulence therapeutics or identifying ways to bolster the host immune defences.

An interesting and unexpected finding of this study is that Bo strains which were considered avirulent in animals did show virulence in *G. mellonella* (contrary to a previous report) and indeed showed greater virulence in *M. sexta* than Bt or Bp strains. This reversal of *Burkholderia* virulence is very interesting from an ecological and evolutionary perspective, for example in terms of understanding generalism *versus* specialism and niche adaptation within the *Burkholderia*. Additionally the extent and relevance of *Burkholderia*-insect interactions in nature has not been studied and would be interesting from either a purely entomological standpoint or applied to the epidemiology of *Burkholderia*. Comparative genomic studies could be used to identify genetic regions involved in insect versus mammalian infection, with confirmation of mutation effects in the *M. sexta* model host. Alternatively, transposon mutant libraries in Bt or Bo strains could be tested for attenuation.

Bt is often used as a surrogate for investigating the pathogenicity of Bp, as it is so closely genetically related and is pathogenic in some mammals. To investigate *Burkholderia* infection in *M. sexta* further and to investigate the validity of the host as a model, the studies carried out in Chapter 4 aimed to characterise aspects of Bt infection over a 30 hour time-course and to reveal whether melioidosis-like mechanisms of pathogenesis are employed.

Chapter 4. *In vivo* time-course of *Burkholderia* insect infection and pathogenesis

4.1. Chapter summary

To investigate the *Manduca sexta* model of *Burkholderia* virulence further this chapter describes the use of haemolymph extraction and fluorescent confocal microscopy to characterise aspects of Bt infection over a 30 hour time-course. Bt bacterial cell numbers increased by four logs during the infection (whereas *E. coli* controls almost entirely cleared) and Bt cells appeared to survive within haemocytes. Signs of haemocyte (HC) cell death increased over time. Although formation of multi-nucleated giant cells (MNGCs) was not conclusively seen, another hallmark of *Burkholderia* infection in mammals – actin tails – were observed in a separate experiment at 24 and 36 hours post-injection. To the best of our knowledge this represents the first observation of *Burkholderia*-induced actin tails in invertebrate cells either *in vivo* or *in vitro*. The result correlates well with observations from mammalian studies and lends support to the validity of the *M. sexta* surrogate model of *Burkholderia* infection. Finally, preliminary results indicate that with further optimisation a flow cytometry-based assay could be a useful tool to rapidly quantify *M. sexta* haemocytes and their viability from haemolymph samples.

4.2. Introduction

In Chapter 3, dose response virulence assays allowed the median times to death (MTTDs) to be calculated for various *Burkholderia* strains in the *M. sexta* larva model of infection. This indicated which strains were more virulent in terms of how quickly they kill the host. However, externally visible signs such as melanisation, paralysis or death shed only limited light on the nature of the host-pathogen interaction. In other species, *Burkholderia* cellular pathogenesis hallmarks can include actin-remodelling, multi-nucleated giant cell (MNGC) formation, and apoptosis of host cells. As discussed in the main introduction, in a BALB/c mouse model of acute melioidosis Chin *et al* (2010) examined the status of bacterial load and host leukocytes at time-points during infection, and in a cockroach model Fisher *et al* (2012) reported that HCs harboured intracellular Bp bacteria and that some had formed MNGCs.

The aims of this chapter were to investigate the pathogenesis of a Bp-group species (Bt) in the *M. sexta* infection model, characterising the bacterial load and looking for cellular characteristics of *Burkholderia* infection that have been observed in mammalian hosts and, in the case of MNGCs, in the cockroach model. A secondary aim was to evaluate numbers of HCs, one aspect of the host response during the course of infection.

Aim: Investigating Bt pathogenesis in the *M. sexta* infection model

As described in Chapter 3 Bp, Bt and Bo are all virulent in *M. sexta* to varying degrees. Bt was the organism investigated in this chapter for several reasons: (i) although Bp is the causative agent of melioidosis its use would require CL3 facilities; (ii) Bt is often used as a surrogate for Bp due to extensive shared similarities; and (iii) Bt was actually more virulent in *M. sexta* than Bp. There were no reports of MNGCs observed in insects until very recently (Fisher *et al*. 2012), and it appears that actin tails have yet to be observed in insect hosts. If these same pathogenesis mechanisms occur in *M. sexta* infection then the *M. sexta* model could potentially be used to test mutants or anti-virulence therapeutics involved in those pathways.

Larvae were infected with GFP-labelled Bt E264 or an *E. coli* control, and haemolymph was collected at selected time-points post injection. Other studies have observed actin tails and MNGCs in cell cultures at 12 hours post-infection with Burkholderia. *M. sexta* virulence studies in Chapter 3 showed that a 10^6 CFU dose of Bt E264 kills by 48 hours post-injection. Initial microscopy was used to briefly assess the condition of HCs and bacteria at up to 48 hours post-injection so that an appropriate time-course could be planned. For confocal microscopy, to minimise the effects of variation between individual larvae batches of replicate larvae were bled and their haemolymph was pooled to produce slides. To minimise the effects of variation across the slide itself, ten images were captured per slide to generate averages. The time-course was performed in triplicate on different days.

Aim: Evaluating *M. sexta* haemocyte number and health over the course of infection

Finally, flow-cytometry and Guava ViaCount Reagent were used to measure *M. sexta* HC number and viability more quantitatively, towards an aim of establishing a reproducible semi-automated assay for future use. Replicate haemolymph samples were tested from Bt-infected and control larvae.

4.3. Results

4.3.1. Comparative virulence of Bt E264 wild-type and GFP strains

Assessing Bt infection using confocal microscopy would require the use of fluorescently-labelled bacteria, so it was necessary to confirm whether a GFP-expressing strain of Bt was similarly pathogenic to *M. sexta* compared to the wild-type Bt E264 strain.

Table 4.1 shows the survival of larvae after injection with different doses of wild-type or GFP-labelled Bt E264. Larvae injected with either *E. coli* Ec100 or Epi300 all survived the course of the assay and reached wanderer stage at day 6 (144 hours). Larvae injected with NaCl alone also reached wanderer stage at day 6 (138 hours).

Table 4.1. Numbers of larvae surviving infection with wild-type (WT) or GFP-labelled Bt E264 over seven days (n = 10). Experiment 1 tested doses 10^2-10^4 CFU (top) and experiment 2 repeated the 10^4 CFU dose (bottom). Hatched cells indicate no data available. Light grey = <100% alive. Dark grey = 0% alive. At the greatest dose tested (10^4 CFU, which was repeated) there was little difference in survival of larvae, with both strains killing all larvae by 90 hours post-injection.

Strain	Calculated dose (CFU per 100ul)	**Experiment 1**	No. alive (/10) at time-points																				
		Day:	1			2			3			4			5			6			7		
		Hour:	18	24	28	42	48	52	66	72	76	90	96	100	114	120	124	138	144	148	162	168	172
Bt E264 (WT)	$0.43x10^4$		10	10	10	10	10	10	9	5	3	0											
	$0.43x10^3$		10	10	10	10	10	10	10	9	8	2	1		0								
	$0.43x10^2$		10	10	10	10	10	10	10	10	10	10	10		6	6	4	0					
Bt E264 GFP	$0.33x10^4$		10	10	10	10	10	10	10	10	9	0											
	$0.33x10^3$		10	10	10	10	10	10	10	10	10	10	9		5	3	2	0					
	$0.33x10^2$		10	10	10	10	10	10	10	10	10	10	10		9	8	8	7	6		5	W	

Strain	Calculated dose (CFU per 100ul)	**Experiment 2**	No. alive (/10) at time-points																				
		Day:	1			2			3			4			5			6			7		
		Hour:	18	24	28	42	48	52	66	72	76	90	96	100	114	120	124	138	144	148	162	168	172
Bt E264 (WT)	$0.49x10^4$		10	10	10	10	10	10	3	2	1	0											
Bt E264 GFP	$0.37x10^4$		10	10	10	10	10	10	7	5	4	0											

Table 4.2 shows MTTD values and the significance of the survival curves for the different strains. Kaplan-Meier survival curves are shown in Figure 4.1. Both strains were virulent in *M. sexta*. The survival curves were significantly different for the wild-type and GFP strains. The GFP strain took longer than the wild-type to kill larvae in this experiment, although the difference between MTTD values did decrease as the dosage increased. The difference was 40 hours at a 10^2 CFU dose, and 6-8 hours at a 10^4 CFU dose. At the 10^4 CFU dose both strains killed all larvae by 72-90 hours post-injection.

Table 4.2. Median Time to Death (MTTD) values for larvae injected with either wild-type (WT) or GFP-labelled Bt E264. Error bars show SE of the median. Values for the 10^4 CFU dose were calculated from the combined data from experiment 1 and 2 (from experiment 1 the MTTDs were 72 hours for WT and 90 hours for GFP; from experiment 2 they were 66 hours for WT and 72 hours for GFP). The MTTD with the GFP strain is longer which suggests attenuation in virulene. However, the difference is less apparent as the dosage increases. At 10^4 CFU, the MTTDs are just 18 hours apart.

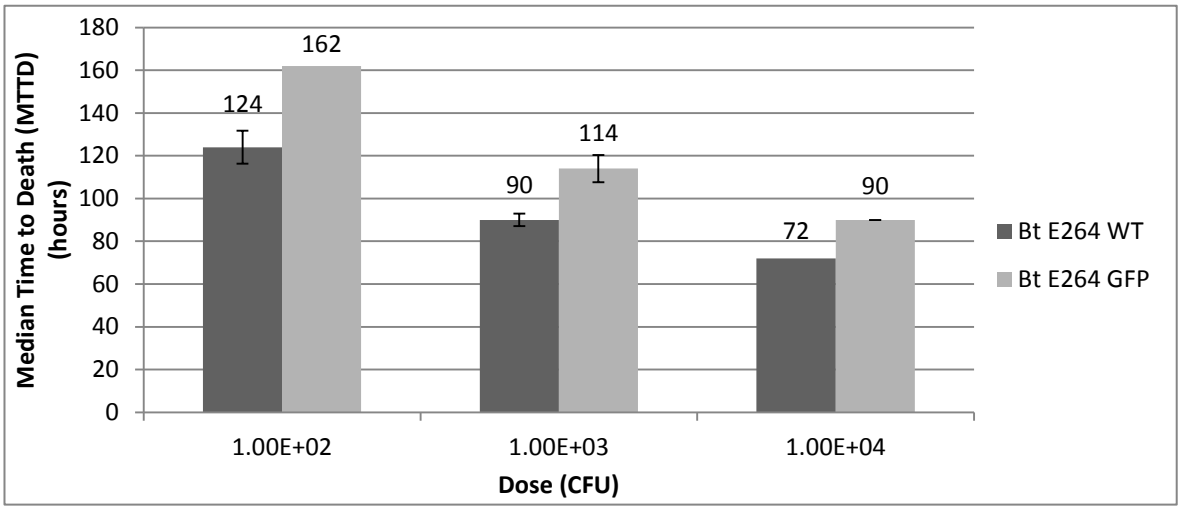

Figure 4.1. Kaplan-Meier survival curve for wild-type or GFP-labelled Bt E264. Data for the 10^4 CFU dose (denoted ^4) is combined from the two experiments. The curves start at 1.0 (all alive) and drop down the y-axis (cumulative survival) as the insects die. The point at which the curve ends indicates the number of surviving insects at the end of the assessment. In cases where insects survive, the curve line displays a small cross which is described in the key as a 'censored' case. Half of the larvae with 10^2 CFU GFP Bt survived to wanderer stage at 168 hours post-injection.

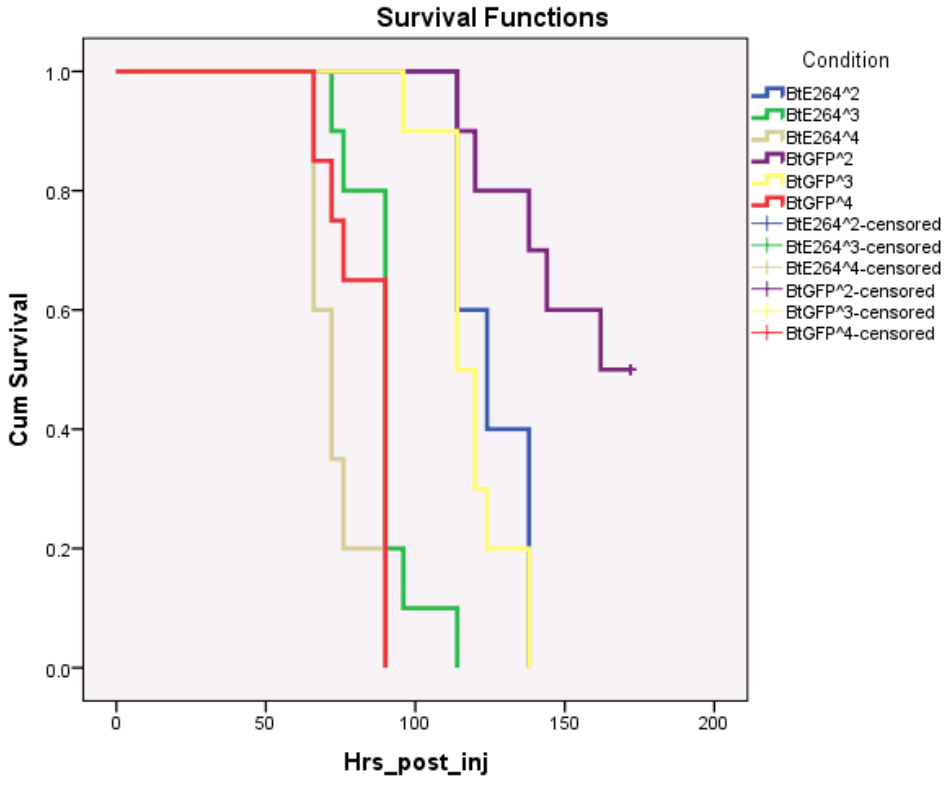

According to log rank (Mantel-Cox) pairwise significance calculations shown in Table 4.3, the difference between wild-type and GFP Bt E264 virulence was statistically significant as each dosage tested.

Table 4.3. Log-rank (Mantel-Cox) pairwise comparisons between *M. sexta* survival profiles when injected with wild-type or GFP Bt E264. NS = not significantly different, * $p \leq 0.05$, ** $p \leq 0.01$, *** $p \leq 0.001$. The survival was significantly different at each equivalent dose.

Bt E264 dose	**Comparative significance**
10^2	0.003 **
10^3	0.000 ***
10^4	0.004 **

Although the MTTDs were significantly different with the GFP-expressing strain of Bt E264 showing a longer time to kill *M. sexta* larvae, the GFP strain was still deemed useful for learning more about the dynamics of Bt infection. This was because: the strain was still lethal; as the dosage increased the difference was less noticeable, and the timecourse experiment could use a higher dose still; and the attenuation was thought to probably be a pleiotropic effect of GFP expression rather than due to loss of an important virulence mechanism.

4.3.2. Initial visualisation of infection

Before embarking upon the time-course itself, initial experiments were performed to confirm that slide preparation and actin staining were successful, and to gauge what time frame to sample within. Initial images were captured from samples collected at 5, 24, 30, 36 and 48 hours post-injection.

In the initial samples the TRITC-phalloidin staining of filamentous actin worked well. Haemocytes of various morphologies and sizes were apparent in all the samples and cellular projections had been well preserved (Figure 4.2). Beyond 5 hours post-injection there were clear differences in bacterial presence (Figure 4.3).

Figure 4.2. TRITC-phalloidin-stained (red) haemocytes from *M. sexta* larvae. Left: cells of different sizes and morphologies from un-infected larvae at 24 hours. Right: GFP-expressing (green) Bt E264 cells are visible on the surface of a haemocyte at 5 hours post-injection. The bottom-most bacterium appears to be partially inside the haemocyte.

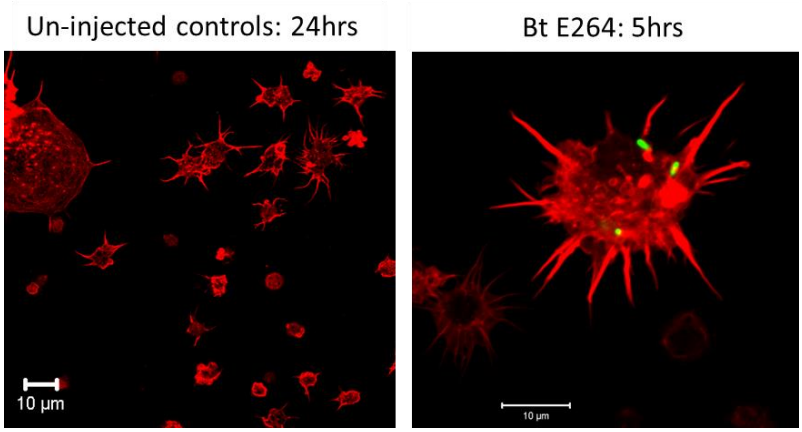

Figure 4.3. Cells from 48 hours post-injection. White light images (included in the left-hand panels) show healthy cells (Ec100, top left) and some dead cells and debris (Bt E264, bottom left). Top right: stained actin (red) reveals the extensive projections of healthy plasmatocytes. At 48 hours post-injection very few *E. coli* Ec100 cells remained (green; top panels), but many Bt bacteria remained (green; lower panels). Dozens of Bt E264 cells were clustered amongst disrupted host cells.

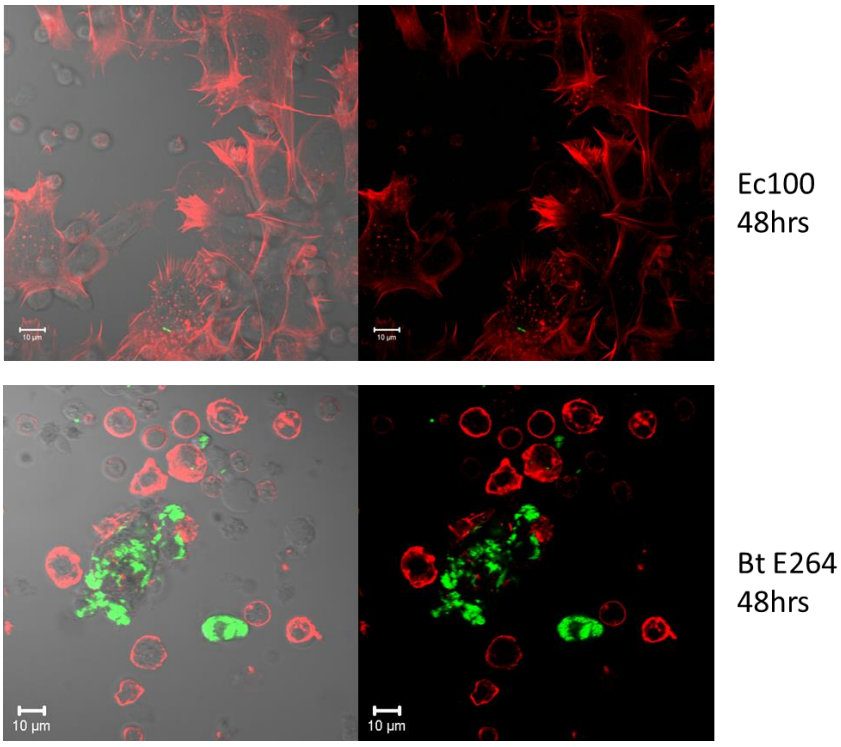

Figure 4.4 shows the presence of actin tails in the Bt-infected haemocytes at 24 and 36 hours post-injection.

Figure 4.4. Actin remodelling was evident in the 24hr and 36hr Bt E264 samples. Panel A: White arrows denote a host haemocyte cell with several actin tails (green GFP bacteria; red stained actin; composite image). Panel B: An orthogonal view shows that these particular actin tails are inside the haemocyte cell. Panels C-D: In each of these cases actin tails are visible protruding from a haemocyte.

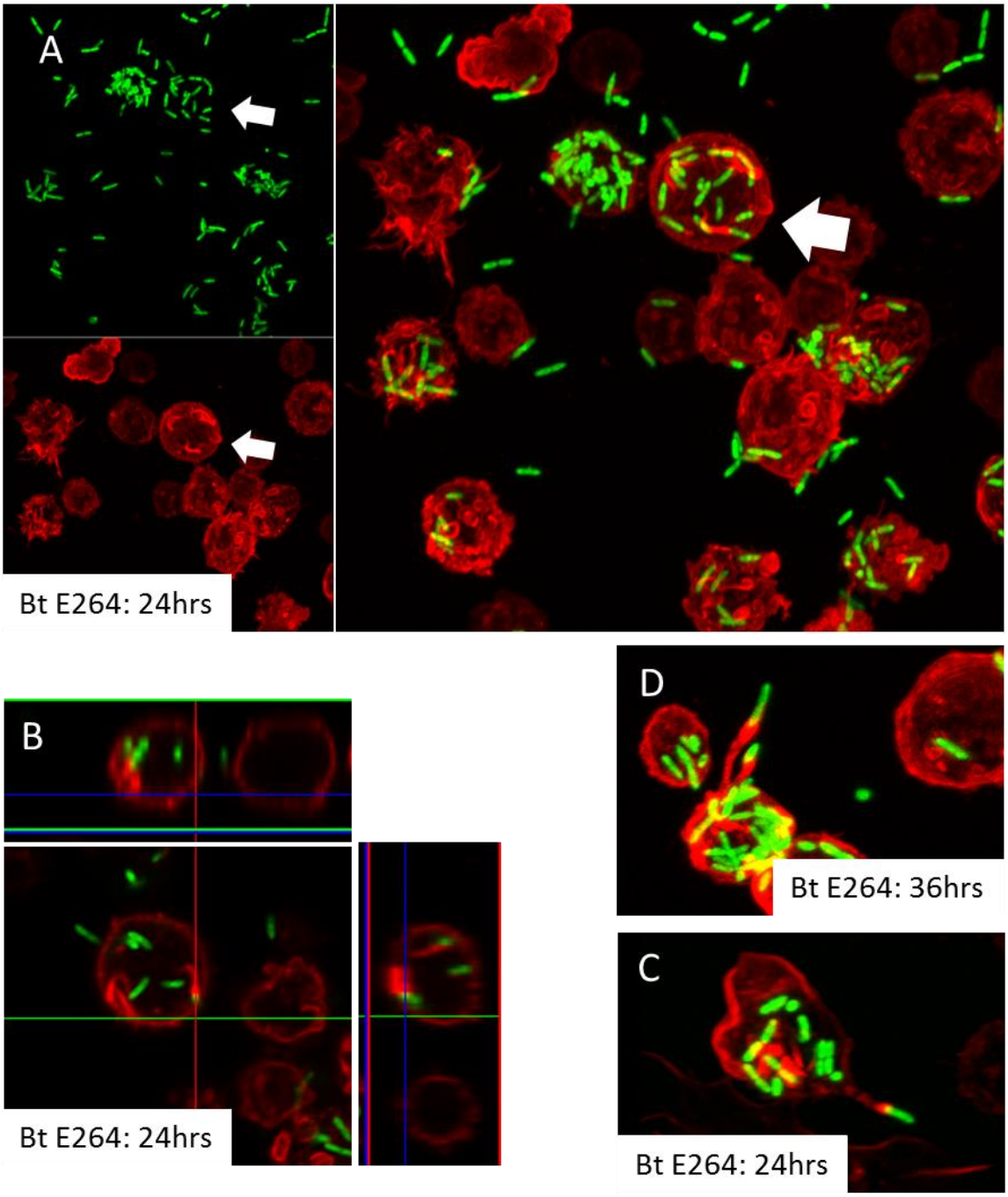

4.3.3. Time-course microscopy results

For the time-course itself, time-points were set up to collect data within the first 30 hours, especially within the first 24 hours; after 30 hours the majority of insect cells were lysed. DAPI dye was also used to stain nuclei, as this would enable easier counting of individual insect cells and assessment of cellular health (e.g. apoptotic cells or MNGC formation).

Control (no injection)

Haemocytes (HCs) were counted from the un-injected controls, with an average of 15.9 HCs per view (SE = 1.35). Cellular debris was observed in 10% of the images.

Bt E264 versus E. coli Ec100 over time-course

Figure 4.5 shows a representative sample of images from 0-30 hours post-injection with the GFP Bt or *E. coli* strains. The calculated means and standard errors (SE) of the replicates are shown for Bt E264 GFP (Table 4.4) and *E. coli* Ec100 GFP (Table 4.5), and those data are described in subsequent graphs and tables. Complete detailed results for each image are included in the supplementary DVD e-Appendix 4b.

Figure 4.5. Representative images from 3D-projections of Bt E264 GFP-infected (left) and *E. coli* Ec100 GFP-infected (right) haemolymph. GFP bacteria are green. In Ec100 images the few bacteria are indicated by white arrows. At 0 hours (within 45 minutes post-injection) very few bacteria of either species were present per view, and most were intracellular. By 18 hours there were still very few Ec100 and most were intracellular, but there were many Bt cells. Bt cells were both intracellular and extracellular, and were often associated with clusters of haemocytes or cell debris (red actin, blue nuclei). By 30 hours post-injection barely any Ec100 cells were observed but there were many extracellular Bt cells. Many haemocytes in the Bt samples were dead or dying and there was abundant cell debris.

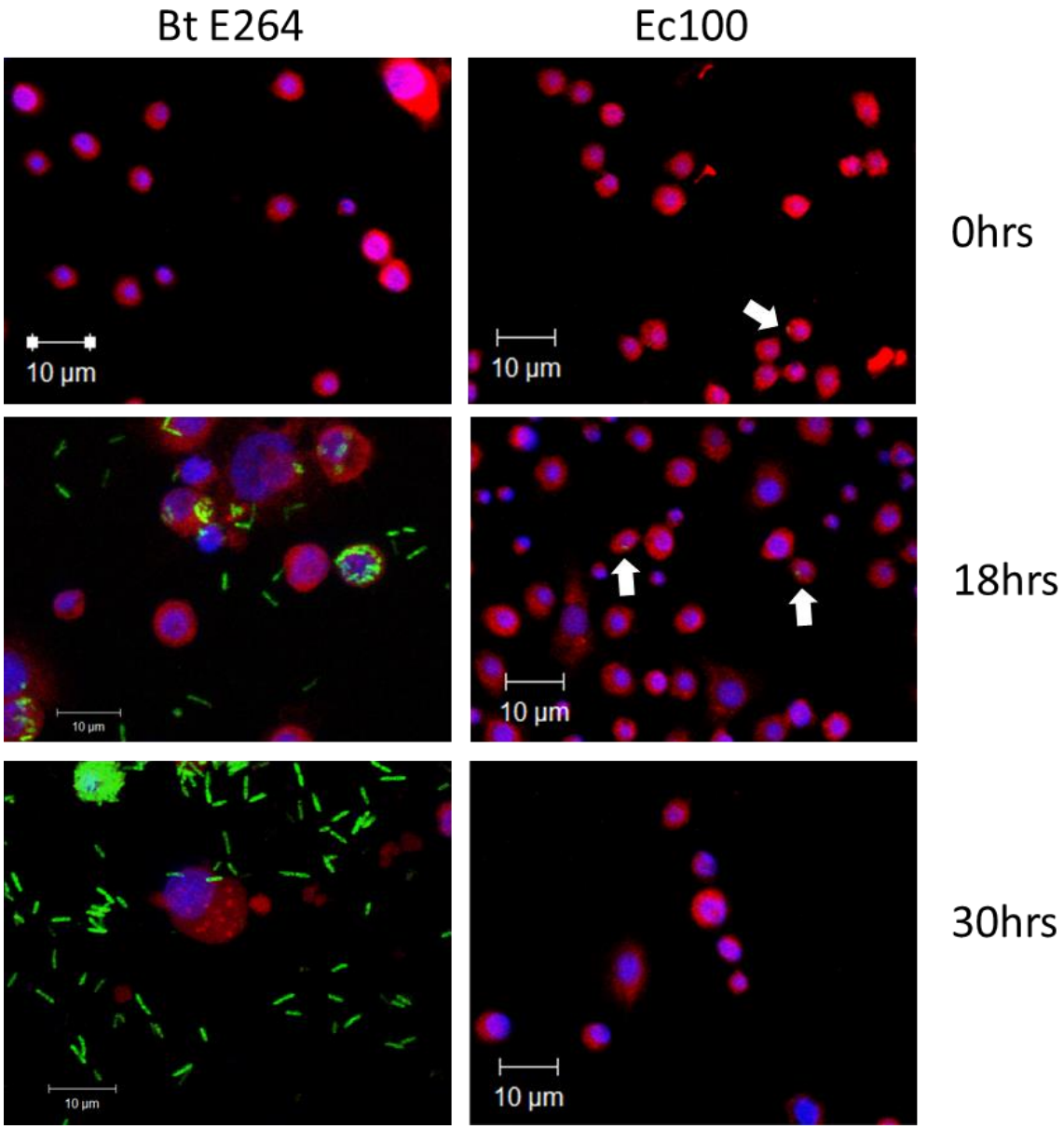

Table 4.4. Data from a time-course of Bt E264 GFP infection in *M. sexta.* Averages and standard errors (SE) from ten fields of view per slide, three slides per time-point. The data are described further in the chapter.

Bt E264 GFP			**HCs**		**Bacteria**			
Hr post-injection	**Replicate**		**Total HCs**	**Debris?**	**Total bacteria**	**Total extra-cellular**	**Total intra-cellular**	**Total attached**
0	**1**	**Average**	10.10	0.00	0.30	0.30	0.00	0.00
		SE	0.66		0.21	0.21	0.00	0.00
	2	**Average**	7.10	5.00	0.30	0.30	0.00	0.00
		SE	1.06		0.21	0.21	0.00	0.00
	3	**Average**	12.00	2.00	1.00	0.20	0.20	0.60
		SE	0.93		0.89	0.13	0.20	0.60
3	**1**	**Average**	6.00	6.00	1.00	0.80	0.10	0.10
		SE	0.79		0.39	0.42	0.10	0.10
	2	**Average**	12.50	6.00	0.60	0.60	0.00	0.00
		SE	1.45		0.27	0.27	0.00	0.00
	3	**Average**	12.10	1.00	3.60	1.50	1.70	0.40
		SE	1.41		1.40	0.48	1.10	0.27
6	**1**	**Average**	6.60	3.00	3.00	1.10	1.70	0.20
		SE	0.67		0.68	0.43	0.50	0.13
	2	**Average**	4.10	0.00	2.20	0.70	1.50	0.00
		SE	0.62		0.77	0.30	0.83	0.00
	3	**Average**	12.00	0.00	1.60	0.80	0.40	0.40
		SE	0.75		0.40	0.29	0.22	0.27
12	**1**	**Average**	30.70	6.00	12.50	2.00	9.30	1.20
		SE	0.63		1.40	0.58	1.41	0.44
	2	**Average**	40.60	7.00	14.90	2.80	11.30	0.80
		SE	3.92		2.17	0.80	1.89	0.33
	3	**Average**	26.20	2.00	16.40	1.00	12.90	2.50
		SE	1.55		3.06	0.33	2.81	1.05
18	**1**	**Average**	6.50	3.00	9.10	3.50	3.60	2.00
		SE	0.78		2.66	1.57	1.42	1.11
	2	**Average**	14.10	3.00	51.10	21.40	23.90	5.80
		SE	1.29		7.52	3.88	5.25	1.73
	3	**Average**	37.50	4.00	69.40	14.20	39.30	15.90
		SE	3.67		10.67	2.00	6.96	3.36
24	**1**	**Average**	1.30	2.00	97.10	82.60	7.70	6.80
		SE	0.26		8.94	5.79	4.26	2.31
	2	**Average**	4.30	2.00	35.40	17.60	12.90	4.90
		SE	0.73		6.39	3.04	4.02	1.63
	3	**Average**	2.60	3.00	24.40	14.80	7.90	1.70
		SE	1.03		4.63	2.69	3.53	0.83
30	**1**	**Average**	0.80	3.00	0.00	0.00	0.00	0.00
		SE	0.51		0.00	0.00	0.00	0.00
	2	**Average**	2.20	10.00	134.70	102.10	10.90	21.70
		SE	0.49		11.55	9.05	5.32	6.02
	3	**Average**	4.20	10.00	137.10	100.00	9.30	27.80
		SE	1.62		13.21	4.18	4.41	8.06

Table 4.5. Data from a time-course of *E. coli* Ec100 GFP infection in *M. sexta.* Averages and standard errors (SE) from ten fields of view per slide, three slides per time-point. The data are described further in the chapter.

Ec100 GFP			**HCs**		**Bacteria**			
Hr post-injection	**Replicate**		**Total HCs**	**Debris?**	**Total bacteria**	**Total extra-cellular**	**Total intra-cellular**	**Total attached**
0	**1**	**Average**	5.90	3.00	6.90	0.10	5.10	1.70
		SE	1.04		2.53	0.10	2.17	0.60
	2	**Average**	16.00	5.00	4.50	0.00	3.40	1.10
		SE	1.12		1.35	0.00	1.17	0.28
	3	**Average**	12.10	5.00	6.30	0.10	5.70	0.50
		SE	0.95		1.12	0.10	1.04	0.27
3	**1**	**Average**	7.00	10.00	3.10	0.00	3.10	0.00
		SE	0.77		1.08	0.00	1.08	0.00
	2	**Average**	22.80	6.00	14.70	0.40	14.20	0.10
		SE	0.84		1.67	0.22	1.67	0.10
	3	**Average**	11.60	3.00	6.00	0.10	5.30	0.60
		SE	0.69		1.00	0.10	0.93	0.27
6	**1**	**Average**	6.70	2.00	2.60	0.20	1.80	0.60
		SE	0.91		0.95	0.20	0.80	0.27
	2	**Average**	23.90	1.00	5.10	0.00	4.90	0.20
		SE	1.24		1.59	0.00	1.62	0.13
	3	**Average**	8.40	2.00	3.70	0.10	3.40	0.20
		SE	1.01		0.82	0.10	0.70	0.20
12	**1**	**Average**	42.70	2.00	3.60	0.00	3.60	0.00
		SE	1.54		1.19	0.00	1.19	0.00
	2	**Average**	55.90	3.00	5.90	0.00	5.60	0.30
		SE	1.62		1.77	0.00	1.62	0.30
	3	**Average**	9.50	8.00	1.40	0.00	1.40	0.00
		SE	1.05		0.48	0.00	0.48	0.00
18	**1**	**Average**	21.20	1.00	3.60	0.00	3.60	0.00
		SE	1.72		0.78	0.00	0.78	0.00
	2	**Average**	17.50	4.00	1.00	0.00	1.00	0.00
		SE	1.59		0.54	0.00	0.54	0.00
	3	**Average**	43.40	7.00	3.20	0.00	3.10	0.10
		SE	2.50		0.77	0.00	0.81	0.10
24	**1**	**Average**	9.50	4.00	1.30	0.00	1.30	0.00
		SE	1.45		0.62	0.00	0.62	0.00
	2	**Average**	10.80	0.00	0.50	0.00	0.50	0.00
		SE	1.09		0.31	0.00	0.31	0.00
	3	**Average**	14.50	1.00	0.90	0.00	0.90	0.00
		SE	1.25		0.50	0.00	0.50	0.00
30	**1**	**Average**	5.00	3.00	0.20	0.00	0.20	0.00
		SE	0.75		0.13	0.00	0.13	0.00
	2	**Average**	7.50	2.00	0.10	0.00	0.10	0.00
		SE	1.17		0.10	0.00	0.10	0.00
	3	**Average**	9.80	2.00	0.20	0.00	0.20	0.00
		SE	1.37		0.13	0.00	0.13	0.00

The number of intact HCs per view varies over the time-course (Figure 4.6). The numbers and the trend over time are similar between the two bacterial strains: 5-15 cells per view immediately following infection until 6 hours, then a peak of 30-40 cells at 12 hours, which tails off to below 10 cells at 30 hours. Figure 4.6 also shows the corresponding numbers of bacteria over time. The observed numbers of Bt E264 GFP and Ec100 GFP bacteria were similar from 0 hours until 6 hours post-injection – below 10 bacteria per field of view. After that, however, Ec100 numbers dropped to almost zero, and Bt E264 numbers steadily increased to around 80-100 bacteria per view at 30 hours.

Figure 4.6 Numbers of bacteria and intact *M. sexta* haemocytes per field of view at different time-points post-injection with GFP Bt E264 or *E. coli* Ec100 (mean and SE, *n* = 30 per time-point). HC numbers increase after injection in both cases, as a host response to infection. For Ec100 the numbers drop off again because the infection has been cleared. For Bt E264 they drop off again because the extracellular bacteria have been internalised and/or later because of host cell death. *E. coli* Ec100 numbers fell to almost zero per view. Conversely, Bt E264 numbersteadily increased over time.

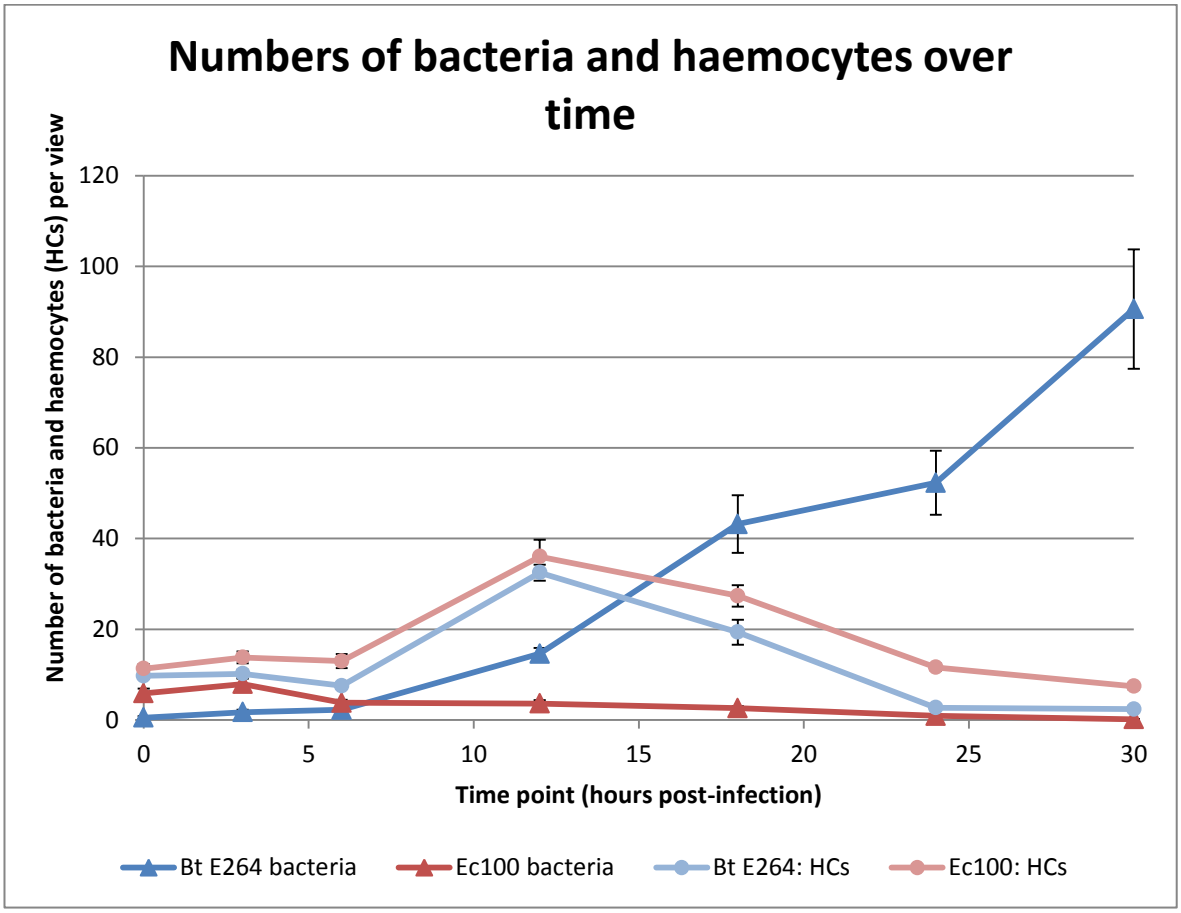

In addition to counting bacteria from the microscopy images, CFUs were enumerated from the samples bled from the insects and plated out onto agar. As shown in Table 4.6 and Figure 4.7, enumerated CFUs from the bacterial inoculum and from bled haemolymph samples reflect the results from Figure 4.6; Ec100 GFP numbers reduced over the time-course compared to the inoculum, and Bt E264 GFP numbers increased by four logs.

Table 4.6. Average bacterial CFU per ml in inoculum and in haemolymph extracted from larvae at time-points post infection. In cases where *n* = 1, no SE applies (labelled N/A = not applicable). Ave. = average. SE = standard error. ND = not determined. These data are visualised in Figure 4.8.

		Inoculum	Hours post-injection						
			0	3	6	12	18	24	30
Ec100 GFP	**Ave.**	**3.90 x10^5**	**6.00 x10^5**	**6.60 x10^5**	**7.20 x10^5**	ND	ND	**7.30 x10^4**	**9.90 x10^4**
	SE	N/A	N/A	N/A	N/A	N/A	N/A	2.33 x10^4	1.00 x10^3
Bt E264 GFP	**Ave.**	**8.00 x10^5**	**3.60 x10^5**	ND	**3.40 x10^6**	ND	ND	**2.91 x10^8**	**4.98 x10^9**
	SE	N/A	N/A	N/A	N/A	N/A	N/A	1.66 x10^8	1.44 x10^8
***n* =**		1	1	1	1			3	2

Figure 4.7. Bacterial CFU per ml in haemolymph extracted from larvae at time-points post infection (mean and SE); data and *n* values are shown in Table 4.6. Bt E264 numbers increase by several logs over the 30 hour time-course, while *E. coli* Ec100 numbers fell. These data indicate that *E. coli* cells were still present after 30 hours in the insect but, as seen from the microscopy images, these were relatively very rare.

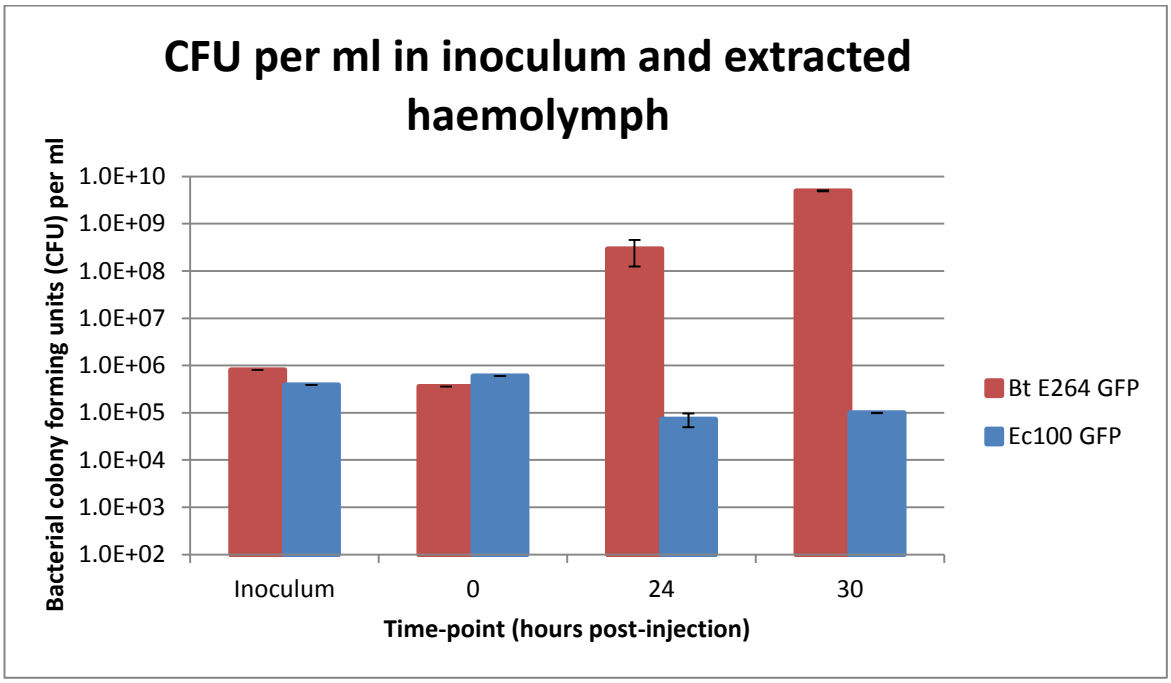

Figures 4.8 - 4.9 break down the total numbers of bacteria per field of view in terms of their location relative to haemocytes, for *E. coli* Ec100 GFP and for Bt E264 GFP. Note the different *y*-axis scales. For Ec100 the majority of cells were always intracellular and those numbers did not exceed 9 cells per field of view, with the greatest numbers seen at 3 hours post-injection. For Bt E264 most cells were intracellular up to 18 hours post-infection, after which time the number of extracellular bacteria rose dramatically. By 24

hours and particularly at 30 hours the majority of Bt E264 bacteria were extracellular and the number of intracellular bacteria had decreased.

Figure 4.8. Numbers of *E. coli* Ec100 GFP bacteria intracellular, attached to haemocyte surfaces, or extracellular per field of view at time-points post-injection (mean and SE, *n* = 30 per time-point)

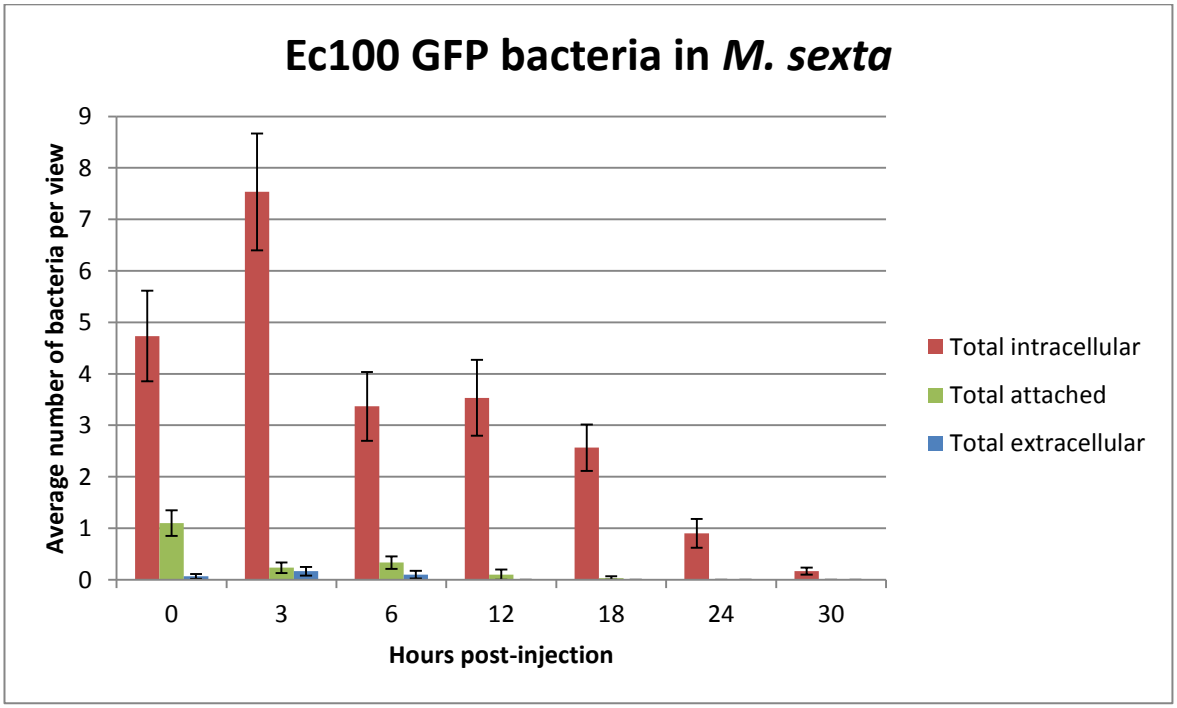

Figure 4.9. Numbers of Bt E264 GFP bacteria intracellular, attached to haemocyte surfaces, or extracellular per field of view at time-points post-injection (mean and SE, *n* = 30 per time-point)

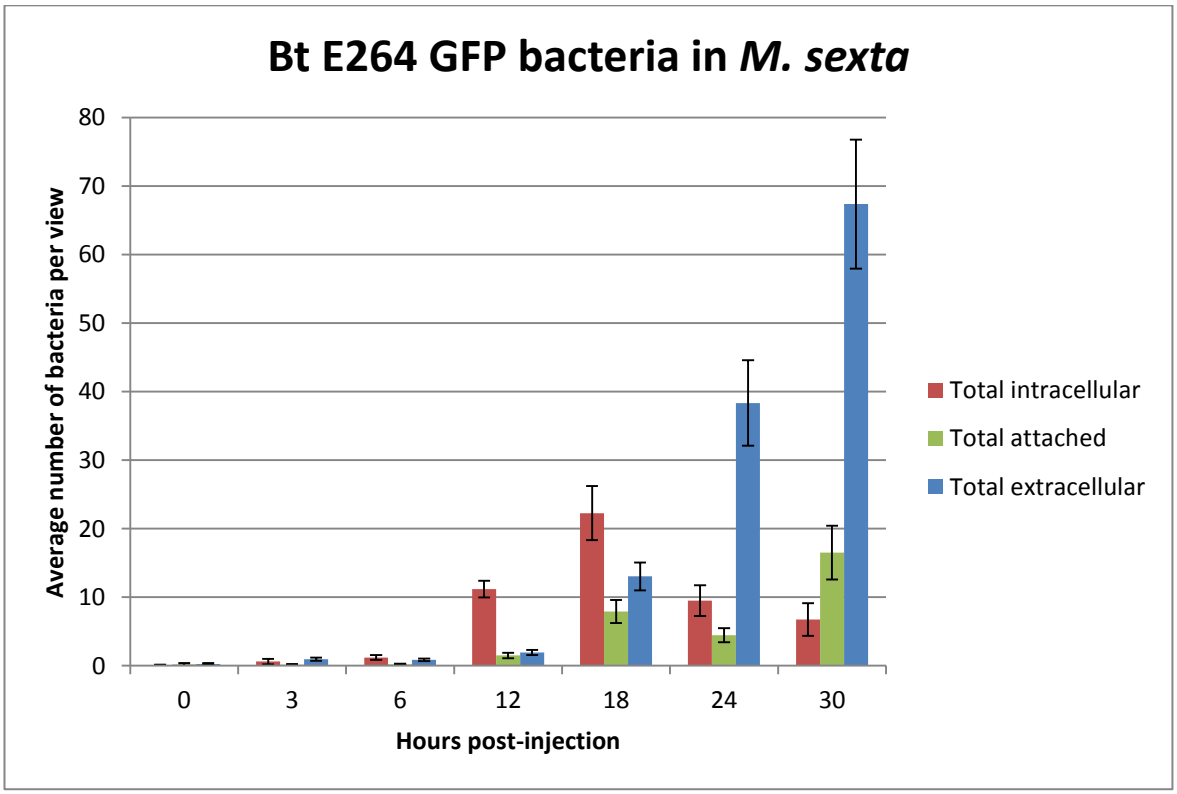

In Figure 4.10 the intra- or extracellular location of Bt E264 cells is also displayed as proportions of all the observed bacteria at each time-point. The proportion of intracellular Bt E264 increased from 0-12 hours as bacteria either entered HCs or reproduced inside them. It then reduced again as bacteria either escaped from HCs or were released as HCs were destroyed.

Figure 4.10. Proportions of Bt E264 GFP bacteria intracellular, attached to haemocyte surfaces, or extracellular per field of view at time-points post-injection (mean and SE, *n* = 30 per time-point). The intracellular proportion increases until 12 hours as bacteria either entered HCs or reproduced inside them. It then falls again as bacteria escaped or were released from HCs

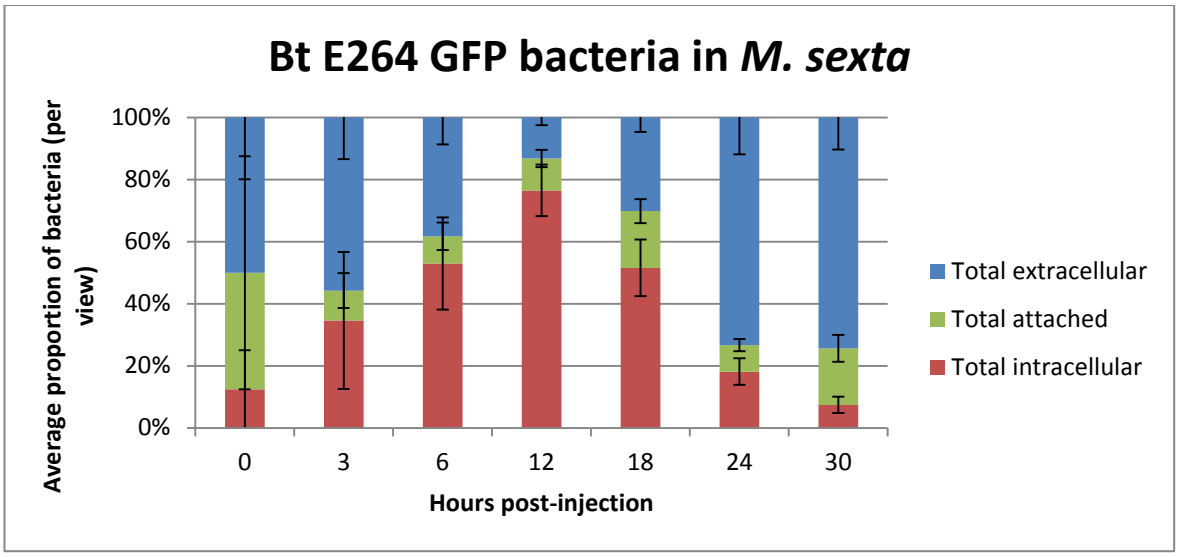

Data values from the Ec100 GFP-infected and Bt E264 GFP-infected samples were tested for significant differences using two-tailed T-tests for unequal variances (Table 4.7).

Table 4.7. Significance of differences in time-course data for *M. sexta* larvae injected with Ec100 GFP versus Bt E264 GFP. *p*-values were calculated by two-tailed T-test for unequal variances. * $p \leq 0.05$, ** = $p \leq 0.01$, *** = $p \leq 0.001$. Non-significant values are marked NS.

Time point (hrs)	Total haemocytes (HCs)	Bacteria		
		Total bacteria	Proportion intracellular	Proportion extracellular
0	0.170 NS	0.000 ***	0.000 ***	0.002 **
3	0.027 *	0.000 ***	0.000 ***	0.000 ***
6	0.003 **	0.053 NS	0.000 ***	0.000 ***
12	0.395 NS	0.000 ***	0.000 ***	0.000 ***
18	0.033 *	0.000 ***	0.000 ***	0.000 ***
24	0.000 ***	0.000 ***	0.000 ***	0.000 ***
30	0.000 ***	0.000 ***	0.000 ***	0.000 ***

In nearly all respects the data were significantly different. The exceptions were: the total number of HCs was not significantly different at 0 hours post-injection (as expected

because equivalent numbers were injected) or at 12 hours post-injection; the total numbers of bacteria per view were (marginally) not significantly different at 6 hours post-injection (when falling Ec100 numbers and rising Bt numbers were similar).

Other observations

Other observations were made non-quantitatively, regarding haemocyte health and possible hallmarks of *Burkholderia* pathogenesis.

Evidence of haemocyte cell death

Some evidence of damaged HCs was observed at all time-points and for both bacteria (Table 4.8). This included amorphous actin debris as well as nuclei stripped of actin, and condensed nuclei which were indicative of apoptosis. Examples of these 'stripped nuclei' are shown in Figure 4.11. In the *E. coli* Ec100 GFP time-course the most evidence of HC death was observed from 12 to 24 hours post-injection. This correlates with the observation that HC numbers peaked at 12 hours and then reduced. Levels of debris and stripped nuclei in the Bt time-course were increasingly high from 18 to 30 hours post-injection.

Table 4.8. Qualitative assessment of evidence of haemocyte cell death during Ec100 and Bt E264 infection time-courses from low (+) to high (++++). Based on observations from *n* =30 replicate images per time-point.

Hours post-injection	Bt E264	Ec100
0	+	+
3	+	+
6	++	+
12	+	++
18	++	++
24	+++	++
30	++++	+

Figure 4.11. Haemocyte cell death. Left panel: examples of haemocyte nuclei stripped of actin (white arrow). Right panel: condensed apoptotic nuclei (bright blue) amid cellular debris (actin components stained red) and extracellular Bt E264 GFP bacteria (green)

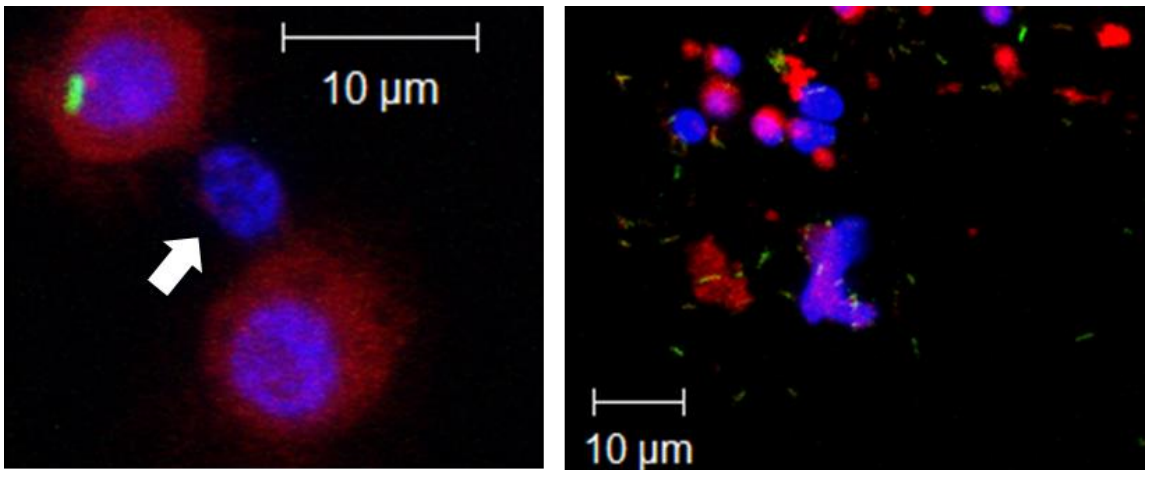

Evidence of actin remodelling and possible cell fusion

Ec100 and Bt E264 injected samples both showed clusters of HCs and a few unusual actin shapes at all time-points. However, these actin structures did not resemble characteristic shapes such as actin tails. Suspected actin-remodelled structures were examined closely using 3D projections and orthogonal views. No real actin tails were seen with Ec100 samples. The most convincing Bt tail-like structure was seen at 12 hours post-infection, as shown in Figure 4.12. It appears to form a 'bridge' between two HCs, each of which contains bacteria. 3D viewing revealed that the actin bridge is in contact with both cells. In this case propulsion by actin remodelling may have transferred a bacterium from one HC into another.

Figure 4.12. Possible actin re-modelling. An actin structure links two haemocytes, 12 hours post-injection with Bt E264 GFP. Each haemocyte contains bacteria. Panels show TRITC-phalloidin staining of actin (red), DAPI staining of nuclei (blue), GFP-labelled Bt E264 (green), and a composite image.

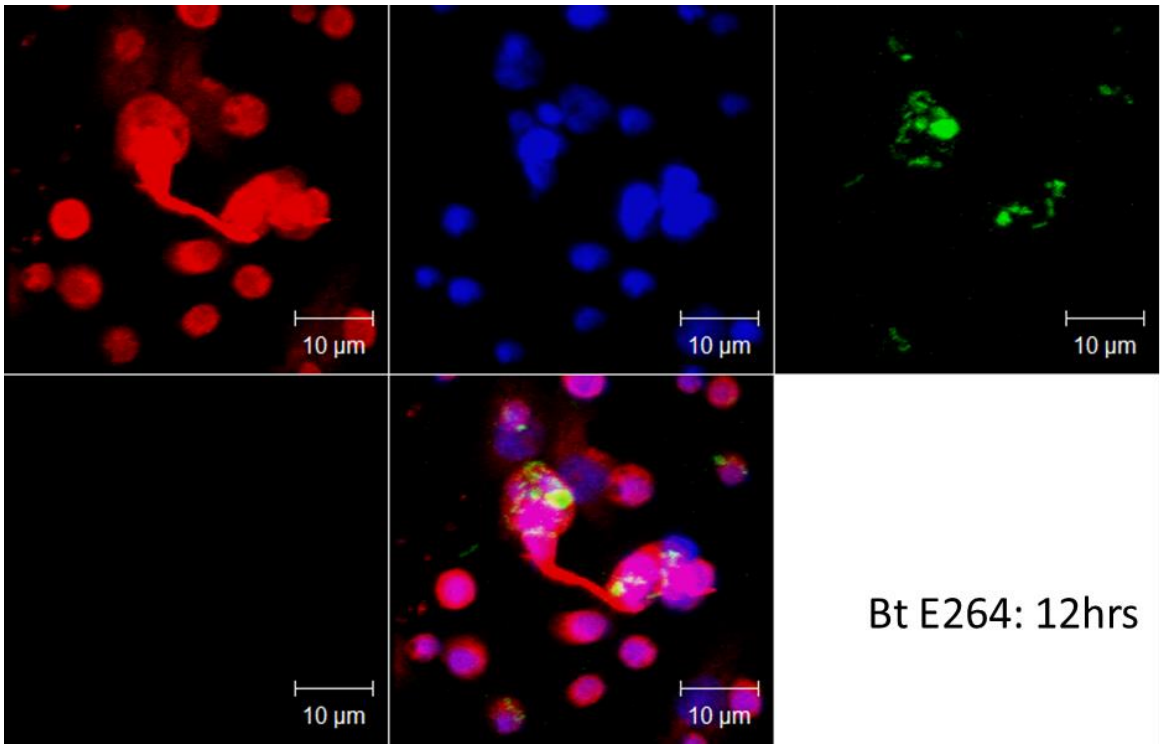

Figure 4.13 shows an example from six hours post-injection. The bacterium-containing HC appears to be making or breaking a link to the adjacent cell, but the join is not well stained and also looks less like a typical *Burkholderia* actin tail. This could be an example of cell-to-cell fusion, which leads to MNGC formation: when a peripheral projection containing bacteria makes contact and fuses with another cell.

Figure 4.13. Membrane protrusion. A physical link between haemocytes at 6 hours post-injection with Bt E264 GFP. A bacterium (green) -containing haemocyte (red with blue nucleus) is in contact with another cell, which itself is in close contact with a third. This image might depict cell-to-cell fusion, which leads to MNGC formation.

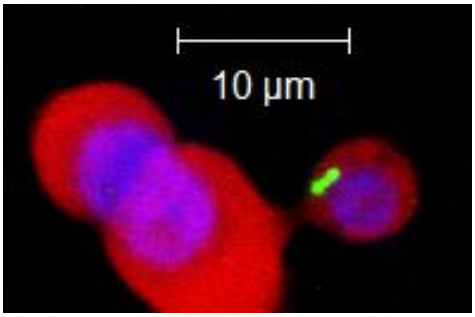

Evidence of MNGCs

The lower resolution of actin detail was also problematic for distinguishing true MNGCs from clusters of separate overlapping cells. 3D projections and orthogonal views confirmed that most suspected MNGCs were simply clusters of cells. Examples of clusters from Bt E264 samples and Ec100 samples are shown in Figure 4.14.

Figure 4.14. Examples of *M. sexta* haemocyte clusters. Panels A and B: examples of haemocyte clusters from Bt E264 GFP-infected larvae. Panels C and D: examples from *E. coli* Ec100 GFP-infected larvae. All samples pictured were from 24 hours post-injection. The fact these types of clusters were observed in the *E. coli* samples means that this is not a specifically *Burkholderia*-induced phenomenon

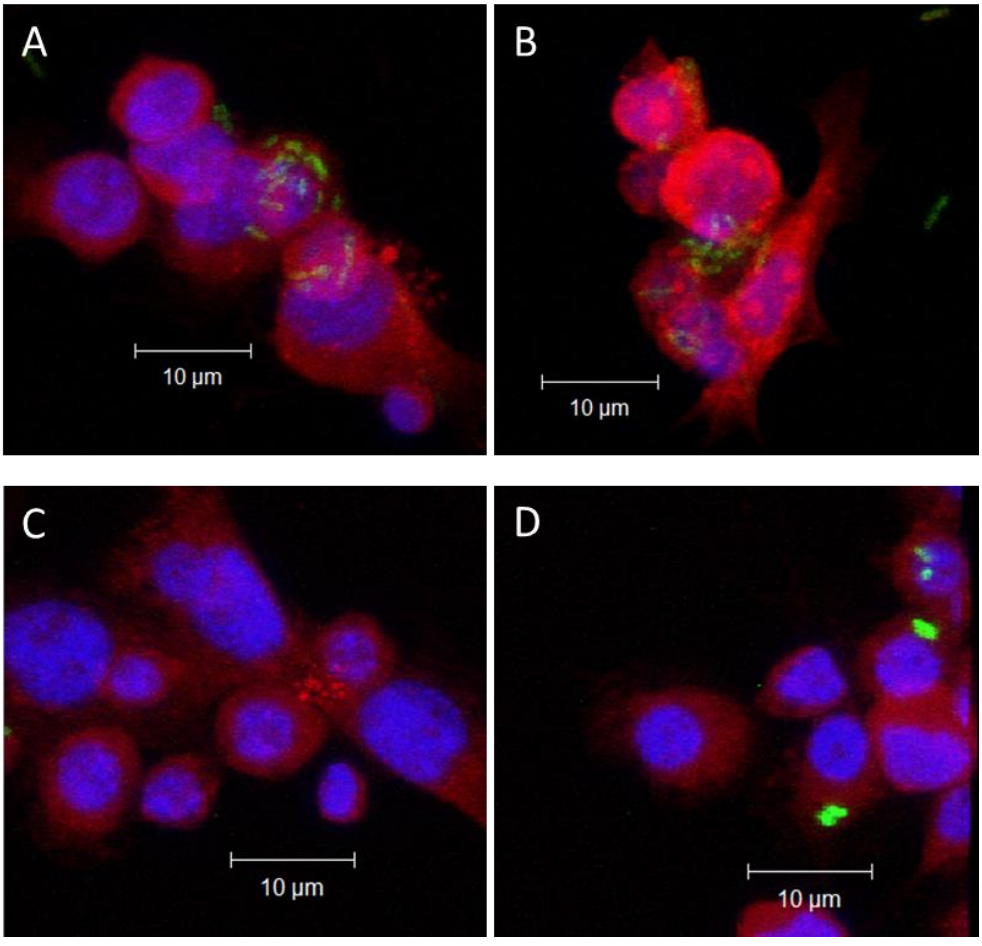

Some potential MNGCs were observed at 6, 12 and 18 hours post-injection with Bt E264 GFP, as shown in Figure 4.15.

Figure 4.15. Possible examples of mutli-nucleated giant cells (MNGCs) from Bt E264 GFP-infected larvae. Panel A: At 12 hours post-injection, with TRITC-phalloidin staining of actin (red), DAPI staining of nuclei (blue), GFP-labelled Bt E264 (green), white light, and a composite image. The white arrow indicates the position of a potential MNGC (with two nuclei). Panel B: The same image is presented in orthogonal view. Panel C: At 18 hours post-injection many bacteria are seen around a potential MNGC (white arrow).

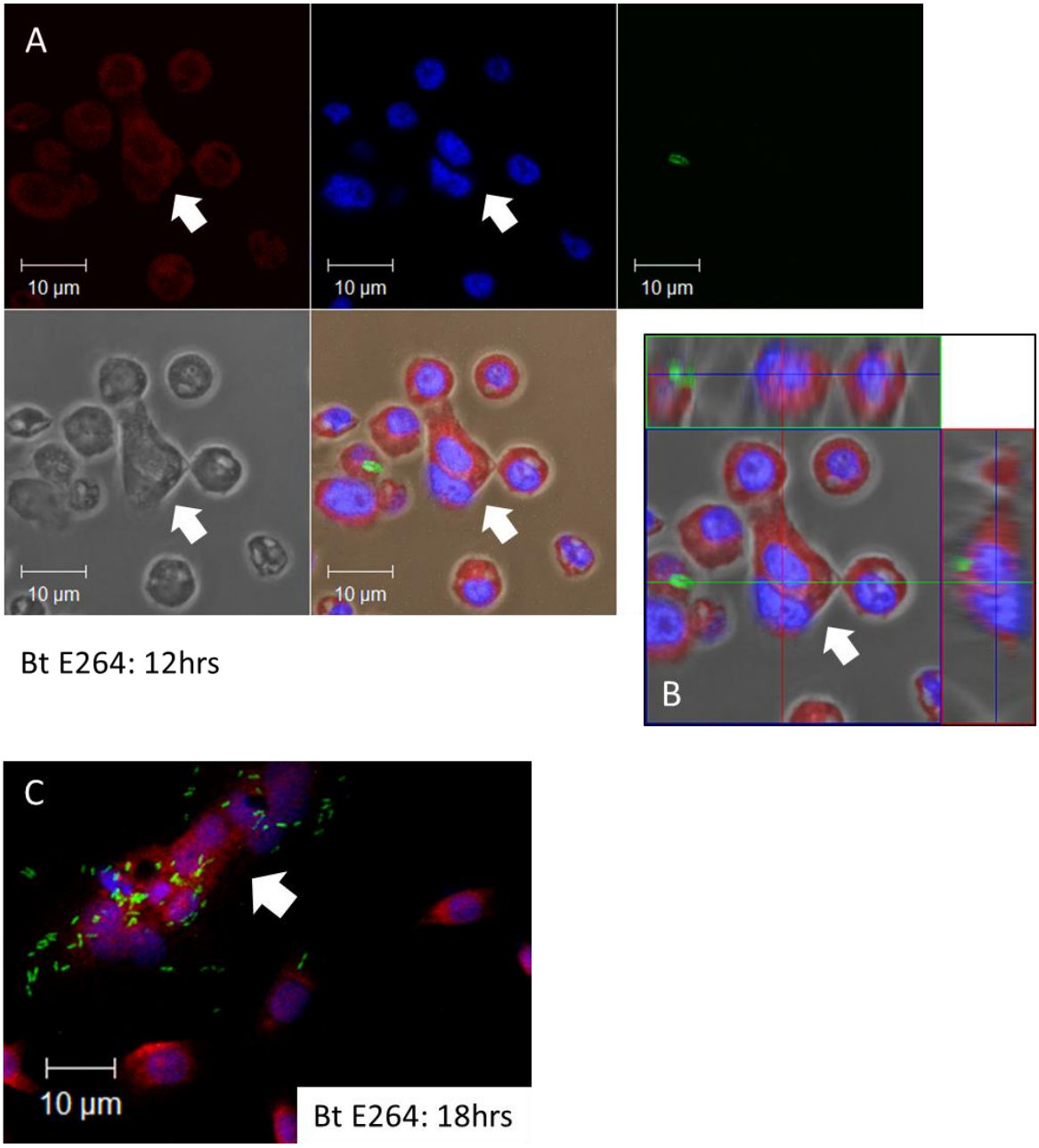

The image in Figure 4.15 panel C looks the most 'MNGC-like' but no 3D projection could be made of this image to verify its nature. Therefore it is not possible to say with certainty whether MNGCs or just clustered cells were observed in this time-course study.

4.3.4. ViaCount haemocyte quantification results

Cytometry was used to attempt to assess the number and viability of *M. sexta* haemocytes using Guava ViaCount Reagent and a Guava EasyCyte cytometer. Insect injections were set up in the same way as for the time-course experiment, with additional saline-injected or non-injected controls. All readings were made immediately following bleeding (and pooling and staining) at 24 hours post-injection.

In flow cytometry, a beam of light (a single wavelength) is directed onto a stream of liquid sample as it passes through the cytometer. A forward scatter (FSC) detector in line with the beam aims at the point where the light meets the passing sample. When suspended particles (0.2 – 150 µm in size) pass through the beam, the ray is scattered. Fluorescent entities within or on the particle may also be excited and detected by fluorescent detectors. The combination of scattered and fluorescent light is analysed in terms of fluctuations in brightness, revealing information about the particles. Each particle (or 'event') is plotted against the measurement parameters, producing a visualisation of the particle population. Subset regions on cytometry plots can be defined using 'gates'.

The ViaCount method measures FSC and two fluorescent wavelengths corresponding to (unspecified) dyes in the proprietary ViaCount reagent. FSC correlates with the cell volume (i.e. cell size); larger cells generate more scatter. The two fluorescent readings correspond to 'nucleated cells' (i.e. a nuclear dye which, in this case, stains insect cells) and 'viability' (i.e. a nucleic acid-binding dye which can only stain dead or dying cells). Figure 4.16 explains a representative ViaCount cytometry plot. Each sample shows two plots: the plot on the left shows 'Nucleated Cells' against 'Viability', while the right shows 'Viability' against 'FSC' (forward scatter). On the left-hand plot there are two almost-vertical 'gate' lines splitting the plot into three sections – the left-most section is the live cells, the middle section is the dying (mid-apoptotic) cells, and the right-most section is the dead cells. The plot is also bisected horizontally – this gate separates nucleated cells (top) from non-nucleated particles such as debris and bacteria (bottom). On the right-hand plot one gate bisects the plot vertically – this separates small debris (left) from larger cells (right), based on size (forward scatter).

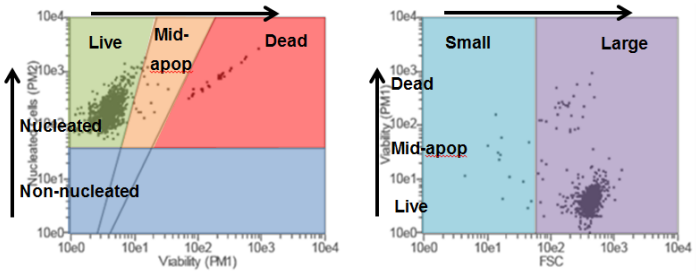

Figure 4.16. An explanation of the sections of a ViaCount cytometry plot. Mid-apop = mid-apoptotic.

Figure 4.17 shows representative ViaCount plots for each of the samples tested.

Figure 4.17. Representative cytometry plots of haemocytes in ViaCount assays. Six separate sets of plots were produced per condition. Left: nucleated cell reading vs. viability reading. Right: viability reading vs. forward scatter. In the controls, most insect cells were live and large. When-infected with bacteria, more insect cells became apoptotic. When infected with Bt E264 strains, more 'cells' were small – these may actually have been apoptotic stripped nuclei as seen in Figure 4.12.

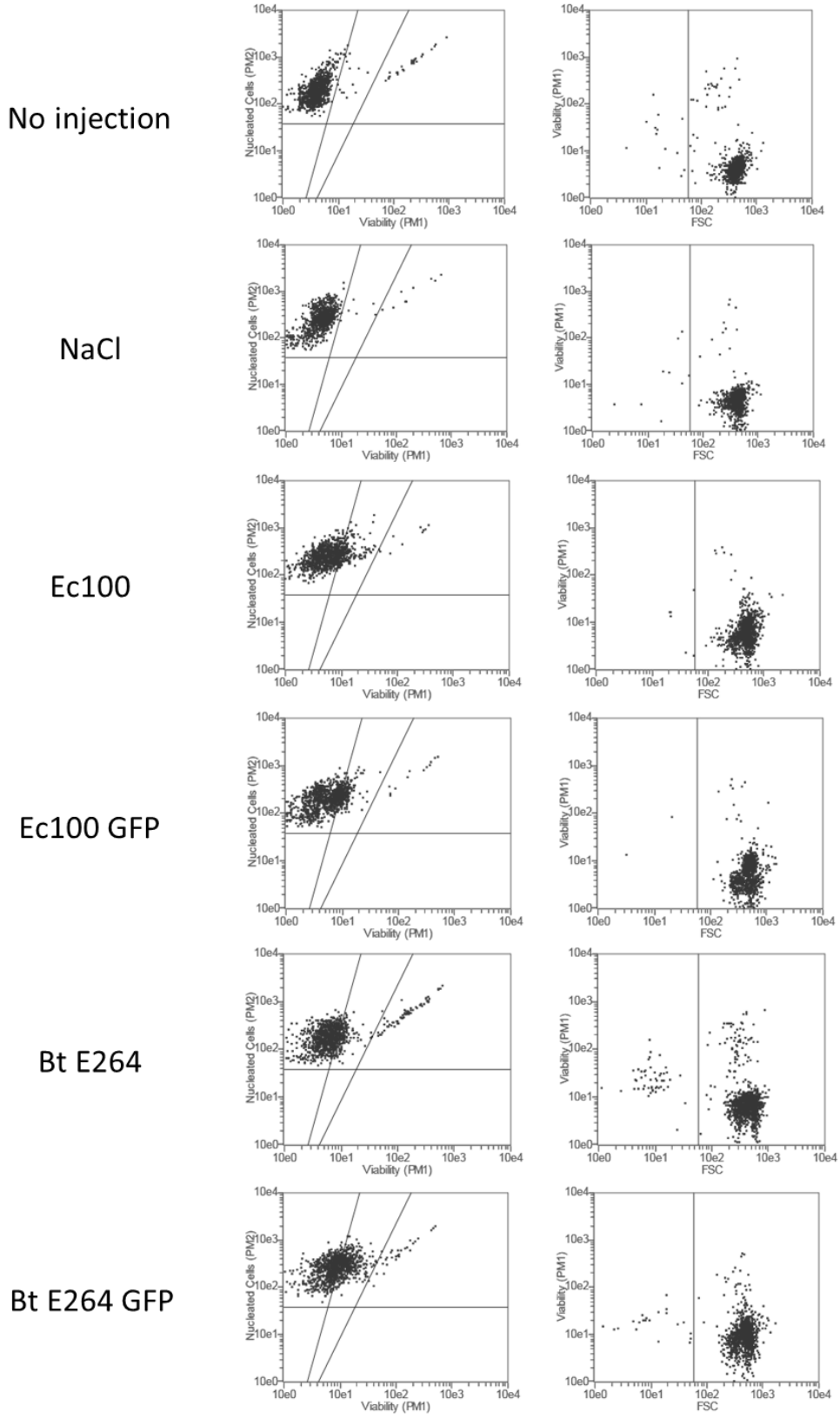

The complete ViaCount results are included in DVD e-Appendix 4c. Refering to Figure 4.17, in the 'no injection' sample haemolymph from healthy larvae contains mostly live cells, a few apoptotic cells and some dead cells. The majority of cells are large with a small subset of smaller cells. Injection of saline (NaCl) shows a very similar plot. Injection with any of the bacteria results in more insect cells falling within the mid-apoptotic gate. Injection with Bt E264 (either WT or GFP) results in more 'small' cells; these could be stripped nuclei as seen in Figure 4.11 (hence staining as nucleated and mid-apoptotic but generating little forward scatter).

Six sets of readings were taken per condition, except for NaCl which had three sets of readings. The average results are summarised in Table 4.9, and shown in Figures 4.18 – 4.19.

Table 4.9. Average ViaCount values for the concentration of insect cells per ml haemolymph, and the percentages of haemocytes which were viable, mid-apoptotic or dead

Condition	Cells per ml haemolymph	Viable (%)	Mid-apoptotic (%)	Dead (%)
No injection	3.76 x10^6	95.53	1.68	2.78
NaCl	4.69 x10^6	97.83	0.80	1.37
Ec100	4.11 x10^6	84.20	14.68	1.12
Bt E264	6.09 x10^6	78.62	17.48	3.90
Ec100 GFP	3.61 x10^6	82.48	16.22	1.30
Bt E264 GFP	7.54 x10^6	44.68	50.25	5.07

Haemocyte concentration

All HC concentrations were in the order of 10^6 cells per ml of haemolymph; the differences are visualised in Figure 4.18. The Bt E264-injected larvae had the highest number of HCs, with the GFP strain apparently being associated with more HCs than the wild-type strain in injected larvae.

Figure 4.18. Insect cell concentrations calculated by ViaCount assay (mean and SE). Using haemolymph samples bled at 24 hours post-injection with wild-type or GFP-labelled Ec100 or Bt E264 or controls

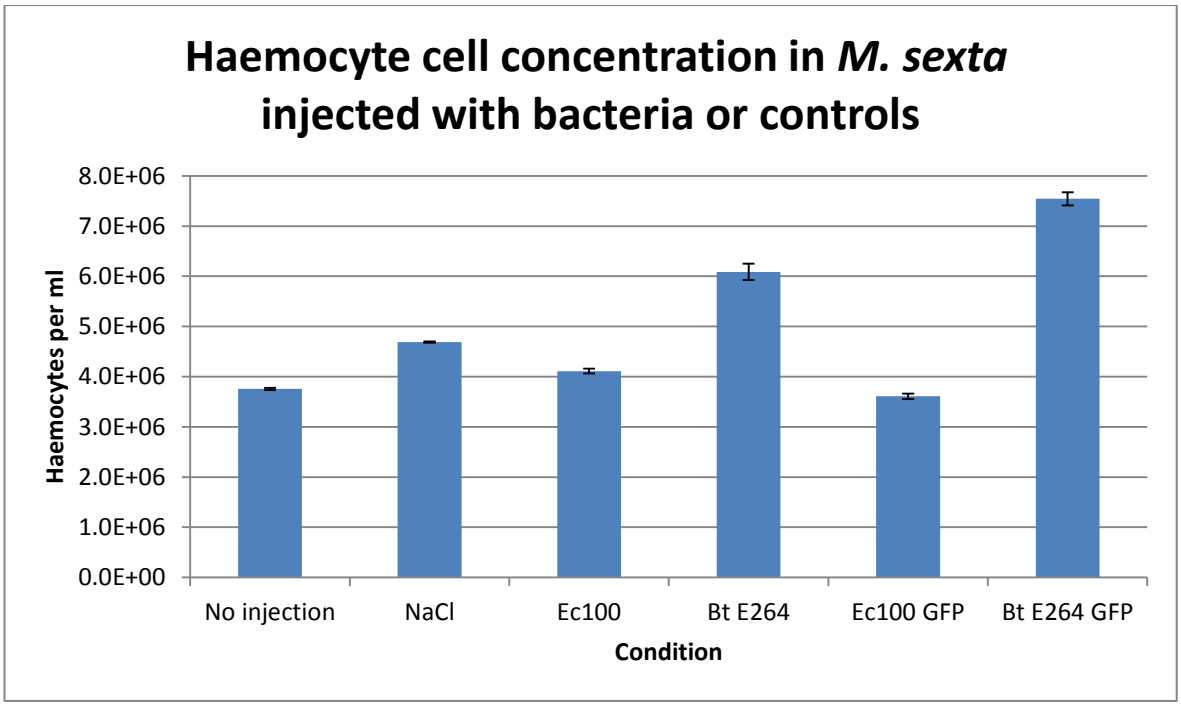

The significance of different HC concentrations between samples is shown in Table 4.10.

Table 4.10. Significance of differences in HC cell concentrations. Comparing ViaCount data from larvae 24 hours post-injection with controls or wild-type- or GFP-labelled *E. coli* Ec100 or Bt E264. *p*-values calculated by two-tailed T-test for unequal variances. NS = not significant, * $p \leq 0.05$, ** = $p \leq 0.01$, *** = $p \leq 0.001$.

T-test: Haemocyte concentration (cells/ml)						
	No injection	**NaCl**	**Ec100**	**Ec100 GFP**	**Bt E264**	**Bt E264 GFP**
No injection		0.002 **	**0.472 NS**	**0.551 NS**	0.003 **	0.000 ***
NaCl	0.002 **		**0.244 NS**	0.002 **	0.028 *	0.000 ***
Ec100	**0.472 NS**	**0.244 NS**		**0.325 NS**	0.011 *	0.000 ***
Ec100 GFP	**0.551 NS**	0.002 **	**0.325 NS**		0.002 **	0.000 ***
Bt E264	0.003 *	0.028 *	0.011 *	0.002 *		0.023 *
Bt E264 GFP	0.000 ***	0.000 ***	0.000 ***	0.000 ***	0.023 *	

HC concentration was not significantly different between un-injected controls, *E. coli* Ec100-injected, or *E. coli* Ec100-GFP injected larvae. NaCl-injected controls had a higher cell concentration compared to un-injected larvae ($p = 0.002$), which was not significantly different from the Ec100 value. The concentration for Bt E264 was significantly greater ($p < 0.05$) and the concentration for Bt E264 GFP was greater still ($p < 0.001$ compared to all others).

Haemocyte viability

HC viabilities were broadly similar between samples, except for the Bt GFP injected larvae. The data are visualised in Figure 4.19. Cells from NaCl-injected larvae had the greatest viability (97.8%), followed by non-injected larvae (95.5%).

Figure 4.19. Viability of insect cells calculated by ViaCount assay, displayed as the proportion of total cells which were live, apoptotic or dead (mean and SE). Haemolymph samples were bled at 24 hours post-injection with wild-type or GFP-labelled Ec100 or Bt E264, or controls

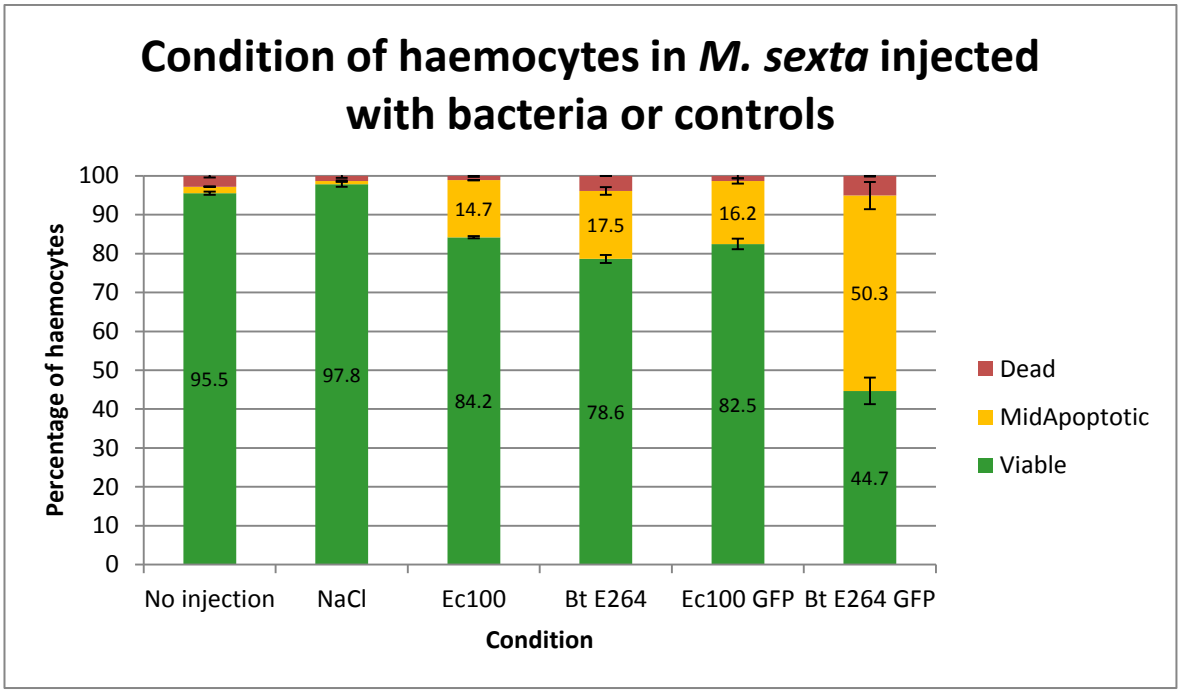

The significance of differences in HC viability between samples is shown in Table 4.11.

Table 4.11. Significance of differences in the percentage of viable insect cells. Comparing data from larvae 24 hours post-injection with controls or wild-type- or GFP-labelled *E. coli* Ec100 or Bt E264. *p*-values calculated by two-tailed T-test for unequal variances. NS = not significant, * $p \leq 0.05$, ** = $p \leq 0.01$, *** = $p \leq 0.001$.

T-test: Haemocyte viability (%)						
	No injection	**NaCl**	**Ec100**	**Ec100 GFP**	**Bt E264**	**Bt E264 GFP**
No injection		0.002 **	0.000 ***	0.000 ***	0.000 ***	0.000 ***
NaCl	0.002 *		0.000 ***	0.000 ***	0.000 ***	0.000 ***
Ec100	0.000 ***	0.000 ***		**0.275 NS**	0.037 *	0.000 ***
Ec100 GFP	0.000 ***	0.000 ***	**0.275 NS**		**0.106 NS**	0.000 ***
Bt E264	0.000 ***	0.000 ***	0.037 *	**0.106 NS**		0.000 ***
Bt E264 GFP	0.000 ***	0.000 ***	0.000 ***	0.000 ***	0.000 ***	

The saline- and non-injected control values were significantly different from each other ($p = 0.002$) and from all the other samples ($p < 0.001$). Cells from larvae injected with wild-type *versus* GFP-labelled Ec100 did not have significantly different viabilities (84.2% and 82.5%), indicating that the expression of GFP did not make Ec100 noticeably more or less pathogenic for *M. sexta* haemocytes.

Cells from larvae injected with wild-type Bt E264 were not significantly different in viability from those with Ec100 GFP (78.6%). Cells from larvae injected with Bt E264 GFP, however, had viability readings of just 44.7% ($p < 0.001$).

4.4. Discussion

4.4.1. Comparative virulence of Bt E264 wild-type and GFP strains

The virulence of GFP-labelled Bt E264 was compared to that of the wild-type strain for reference because GFP Bt E264 would be used in the microscopy experiments. The results showed that both strains were indeed virulent, with the GFP strain exhibiting a MTTD that was 38 hours longer at the 10^2 CFU dose. This implies reduced virulence. As the dosage increased the difference between the MTTDs decreased such that at a 10^4 CFU dose the difference was 6-8 hours. Injections for the microscopy analyses were of estimated 10^6 CFU doses, so it is likely that in those experiments the MTTD of the GFP strain would approximately match that of the wild-type. Overall the GFP strain was considered fit for purpose for imaging Bt infection in *M. sexta*.

4.4.2. Preliminary visualisation of infection

Preliminary injections and slide preparation were used to confirm that the method for TRITC-phalloidin staining of filamentous actin was successful and that bacterial GFP fluorescence was visible. Early infection (5 hours post-injection) and late infection (24, 36 and 48 hours post injection) time-points were sampled and imaged, as were un-injected controls. These images revealed that the staining and fluorescence were successful, with the actin staining showing a fine level of detail.

Actin-remodelling occurs during Bt infection of Manduca sexta

Crucially, actin tail formations were observed in the Bt-infected samples at 24 and 36 hours. These are believed to be the first recorded observations of *Burkholderia*-induced actin remodelling in an invertebrate host or even from an *in vivo* model as opposed to in cell cultures. Actin tails were observed both within HCs and projecting outwards from them, indicating that actin-remodelling in the *M. sexta* model enables intracellular movement and cellular escape, and the potential to spread directly from cell-to-cell.

4.4.3. Time-course microscopy results

So that nuclei could be visualised, DAPI staining was included in the triplicate time-course experiments. This would enable us to identify multi-nucleated giant cells (MNGCs). Unfortunately, in the time-course images although nuclei were stained well the actin staining did not show as much detail as in the initial experiments. This coincided with

using a new stock of TRITC-phalloidin dye. A range of concentrations and incubation times had been tested and this was the optimal condition. Regardless, the time-course did generate useful data.

Bt E264 GFP bacterial burden increases in Manduca sexta over thirty hours

Unlike the avirulent *E. coli* infection, Bt numbers increased steadily throughout the 30 hour infection in *M. sexta* from 10^5-10^6 CFU at 0 hours up to $>10^9$ CFU at 30 hours post-injection. These figures came from the enumeration of inoculum and haemolymph samples. The trend reflects the 'bacteria per field of view' figures obtained from counting cells in each microscopy image (under 10 Bt cells per view at zero hours up to approximately 90 cells per view at 30 hours).

Bt cells survive and multiply within Manduca sexta haemocytes

At 0hrs (within 45 mins of injection) barely any bacteria were visibly extracellular, having been internalised by HCs. It is not known whether this internalisation occurred by phagocytosis or by active entry by the bacteria. For example Inglis *et al* observed that Bp uses flagellum-mediated endocytosis to enter *Acanthamoeba* amoebae (Inglis *et al*. 2000; Inglis *et al*. 2003). It could be a combination of both.

Bt cells were seen surviving in high numbers inside HCs. For the first 12 hours most bacteria were intracellular. After that the balance shifted with increasing proportions of Bt cells being located extracellularly. At first the majority of HCs did not contain bacteria but those that did often contained numerous bacterial cells. Certain HC subtypes more commonly contained bacteria, primarily plasmatocytes and HP cells. Later, a greater proportion of HCs including granulocytes had intracellular or attached bacteria.

The total numbers of Bt bacteria increased throughout the time-course: approximately 30-fold from 0-12 hours and approximately a further six-fold from 12-30 hours. When also considering that the proportions of Bt cells that were intracellular increased to a peak at 12 hours post-injection, these results indicate that Bt cells multiplied within the *M. sexta* haemocytes.

In late infection many Bt cells were extracellular

From 12 hours post-injection Bt cells were visible in increasing numbers in the extracellular medium; by 24 hours and particularly at 30 hours there were large numbers, with more than 10^9 CFU per ml (average 90 bacteria per view) and less than 7% of those remaining intracellular at 30 hours post-injection. Bacteria probably ended up in the extracellular medium due to apoptosis or lysis of HCs they were inside (many HCs were

seen to be packed full of bacteria) and potentially due to actin-based propulsion out of HCs.

Haemocyte numbers peaked at twelve hours post-injection, followed by evidence of cell death

HC numbers were also assessed during the time-course, as an easily measurable aspect of the host response. Elevated haemocyte number is a response to – or a symptom of – bacterial infection (Auld *et al*. 2012). The number of free *M. sexta* HCs temporarily increases after injection of non-pathogenic *E. coli* (Au *et al*. 2004). Conversely, the insect pathogen *Photorhabdus luminescens* causes a dramatic decrease in HC number in infected larvae and the bacteria are able to avoid phagocytosis (Au *et al*. 2004).

Using the 'per field of view' measure, HC cell numbers increased from zero hours to a peak at 12 hours post-injection. This was true for both Bt E264 GFP and Ec100 GFP samples and fits well with published observations that a peak in HC number was seen at 8 hours after *M. sexta* infection with 10^5 *E. coli* (Au *et al*. 2004).

The increase in HC numbers is likely to be a response to the bacterial infection with a time lag of a few hours. The subsequent drop in HC numbers is possibly due to different reasons in the *E. coli* and Bt infections: *E. coli* Ec100 GFP cells were phagocytosed and killed by HCs such that very few remained in the haemolymph at 12 hours post-injection, so 'extra' recruited HCs may have been destroyed once no longer required. Conversely, Bt E264 GFP infection led to the death of many HCs, as evidenced by cellular debris and released bacteria.

Signs of apoptosis were observed. In Bt-infected samples condensed nuclei were seen from 6 hours post injection, more so at 18 hours, and were quiet extensive by 24 hours post injection. By 30 hours few HCs remained per field of view, and many of them were apoptotic. Condensed nuclei were also observed in the *E. coli* Ec100 GFP infection; these were mostly at the 24-30 hour time-points, but importantly there were also many healthy HCs in those instances. Therefore some apoptotic changes may be due to destruction of older HCs but Bt induced a noticeably greater incidence of HC death than was observed in the *E. coli* control.

Statistical significance of quantitative data

Calculating the significance of differences between Ec100 GFP and Bt E264 GFP showed that bacteria-related values (total number, proportion intracellular, proportion extracellular excluding attached) were significantly different at all time-points with the exception of total number at 6 hours post-injection. This was the point at which the decreasing *E. coli* Ec100

numbers matched the increasing Bt E264 numbers. Haemocyte numbers had larger *p*-values at most time-points indicating they were less divergent, although the differences were still significant in all but two cases: zero hours and 12 hours post-infection. It could be expected that there was no significant difference at zero hours as there has been insufficient time for a difference to emerge between the two infections. At 12 hours there was larger variation in replicate values which led to overlapping error bars. The reason why Bt E264 HC numbers were consistently lower than *E. coli* Ec100 HC numbers is not clear; it could be that both bacteria elicit an increase in HC numbers but Bt also kills a proportion of those, or that Bt stimulates less of an increase in HCs due to factors which aid immune evasion. As Bt is actually successful at surviving and apparently multiplying within HCs, the former explanation might be more plausible.

Further evidence of actin remodelling was limited

In the initial microscopy experiment actin tails were clearly apparent at 24 and 36 hours post-injection. In the time-course however, classic comet-tail structures were not seen. This could be due to: less detailed resolution of actin structures with the new TRITC-phalloidin stock; damage to delicate cellular structures during the slide preparation; or variation in the bacterial pathogenesis (i.e. the structures may not have been made in every Bt infection). The most convincing example resembled an actin bridge linking two bacteria-containing HCs at 12 hours post-infection with Bt E264 GFP.

Inconclusive evidence of MNGCs

Published images of *Burkholderia*-induced MNGCs in mammalian cells or cockroach HCs show distinct giant cells with rounded or branched shapes, one cell membrane and multiple nuclei (Suparak *et al*. 2005; Burtnick *et al*. 2011; Fisher *et al*. 2012; Galyov *et al*. 2010; Hasselbring *et al*. 2011). Upon 3D-imaging, formations that had looked like multi-nucleated cells were usually discovered to resemble multiple separate cells clustered together. Some cases could neither be dismissed as clusters nor conclusively accepted as true MNGCs, such as the images pictured in Figure 4.15 from 12 and 18 hours post-injection. In the 12 hours image the apparent ‘squashing’ of one nucleus may indicate that one HC is on top of another. The cell cluster pictured in Panel C of Figure 4.15 does look similar to MNGCs pictured in RAW 264.7 macrophages (Burtnick *et al*. 2011), showing multiple nuclei and bacteria around a large cellular mass. Unfortunately a Z-stack was not available for that image as it was taken in addition to the designated time-course images. Therefore it was not possible to study this structure in 3D detail and it cannot be confidently said that MNGCs were observed in this *M. sexta* time-course.

Bt E264 is reported to form fewer MNGCs than some other Bt strains (Wand *et al*. 2011). If MNGC numbers were low to begin with, the likelihood of capturing them in the time-course images is further reduced.

Other researchers have generally observed MNGCs in tissues of melioidosis patients and in monolayers in cell culture, i.e. where cells are relatively fixed in contact with or close to one another. Fisher *et al* reported seeing Bp MNGCs formed from cockroach haemocytes which implies that they can be formed from un-attached cells circulating in the haemolymph (Fisher *et al*. 2012). Further attention – perhaps with a different Bt strain – would be required to determine whether this process does also occur in *M. sexta*.

4.4.4. ViaCount quantification of haemocytes and their viability

The number of HCs counted from the confocal microscopy cannot be used to reliably calculate cell concentrations per volume of haemolymph because they show only the cells which adhered to the cover-slip (hence using 'per view' measures). Therefore, a cytometry method for assessing *M. sexta* HC number and viability was tested with a view to correlating our observations from microscopy with a semi-automated quantitative assay. Further work will be required to fully establish this assay but the initial results are promising.

Haemocyte concentration

The data were taken from duplicate experimental set-ups each with multiple readings. The fact that the standard error bars were tight supports the reliability of the cell concentration readings. At the time-point the readings were taken (24 hours post-injection) the Ec100 and Ec100 GFP samples show similar HC concentrations to the un-injected control. This reflects the Ec100 GFP data from the microscopy time-course where HC numbers at 24 hours had already returned (after a peak at 12 hours) to match the numbers at zero hours. This indicates that the *E. coli* infection has already been cleared and HC numbers have returned to normal. Injection with saline (NaCl) appears to have increased HC numbers; the reason for this is not clear.

Injection with Bt E264 and especially with Bt E264 GFP resulted in significantly higher HC concentrations. This is in contrast to the Bt E264 GFP data from the microscopy time-course, where HC numbers at 24 hours were lower than at zero hours.

This might be an erroneous reading effect explained by the clusters of cell debris which were observed by microscopy at that time-point. Debris is usually distinguished in the ViaCount assay by a lack of staining with the nuclear dye, and bacteria are too small to generate enough forward scatter. It is conceivable that clusters of debris may be large enough and may have enough attached (live-stained) bacteria to be recorded by the ViaCount program as HCs.

It is not clear why Bt E264 GFP – the strain used for the microscopy time-course – was associated with a greater HC concentration than the wild-type Bt E264 strain. The dose response experiments indicated that the GFP strain was slightly less virulent, so perhaps more HCs were still remaining intact or more debris clusters still had bacteria attached.

Haemocyte viability

Based on observations from the microscopy it was expected that HC viability at 24 hours post-injection would be lower with Bt than with *E. coli*, but cells from larvae injected with wild-type Bt E264 showed a statistically similar viability to those from Ec100 GFP-injected samples (78.6%). Another unexpected result was that cells from Bt E264 GFP-injected samples recorded a greatly reduced viability compared to wild-type Bt E264 (44.7%, $p < 0.001$). 50.3% of cells were designated as mid-apoptotic.

One reason for testing both GFP-labelled and wild-type strains of each bacterium was so that any effects attributable to GFP expression (including altered virulence or fluorescence artefacts) could be detected. No difference in HC viability readings was observed between Ec100 wild-type and GFP samples, as hoped. But, as the Ec100 bacteria were virtually all destroyed by 24 hours according to the microscopy and CFU counts, this does not help to reveal whether their GFP fluorescence affects the ViaCount readings.

According to correspondence with Millipore, bright GFP fluorescence (e.g. from bacteria within or upon a haemocyte) could potentially bleed into the wavelengths for the dead-cell dye, resulting in more apoptotic readings. This could account for the observed differences in viability readings between the Bt E264 strains. Alternatively, the result could be accurate – that over half of the HCs are indeed dead or dying – and the inaccuracy lies with the wild-type Bt E264 results. However, it was unexpected that the Bt E264-induced HC viability was not significantly lower than that for HCs which had encountered harmless Ec100 cells. Clearly more characterisation will be required for reliably informative data to be generated from this assay.

4.4.5. Potential directions for further work

The confocal microscopy visualisation of bacteria-haemocyte interactions allowed detailed monitoring of the progression of Bt infection in *M. sexta*. It was discovered that Bt survives and multiplies within *M. sexta* haemocytes, that extensive haemocyte death occurs at late infection, and *Burkholderia* actin tails were observed in invertebrate cells for the first time. These results fit well with observations from mammalian studies and lend support to the validity of the *M. sexta* surrogate model of *Burkholderia* infection.

Following our discovery in Chapter 3 that *B. oklahomensis* is unusually virulent in *M. sexta*, it would be fascinating to perform a similar time-course study with Bo strains. Equally, if it was practicable it would be interesting to use this technique towards understanding why Bp shows relatively low virulence in *M. sexta*.

If actin staining could be restored to the high level of detail seen in the initial images, it would be useful to repeat a Bt time-course and look once more for cellular pathologies including actin tails and MNGC formation. With electron microscopy it should also be possible to detect at what time-points bacteria were inside and escaping from phagocytic vacuoles.

With further characterisation and optimisation the ViaCount assay for infected *M. sexta* haemolymph could be a useful tool. If GFP-bacteria are to be used then GFP interference must be removed from the readings by running positive GFP controls and performing 'colour compensation'. Non-GFP bacteria should be fine to use, but in either case bacteria-only samples should be run to determine where they appear on the plot. More controls will be required to: (i) characterise the populations of healthy HCs (accounting for their heterogenous nature); (ii) characterise populations of HCs which are dead or dying as a result of abiotic means (controls); (iii) confirm that the gates for viability dye readings are set correctly; and (iv) ensure reproducibility. Once performing reliably, the assay could be used to generate quantitative data at more time-points during infections. As well as *Burkholderia*, this method could be applied to evaluate *M. sexta* health and immunity in response to other pathogens or toxic factors or treatments. Potentially, sub-regions of the cytometry plot could be defined to distinguish HC cell types, e.g. granulocytes from hyperphagocytes.

It was hoped that RT-PCR would also be used to analyse the transcription of specific virulence-related genes throughout the time-course study. Potential targets include *bimA* for actin-based motility or T3SS effector genes. RNA samples were obtained and processed for each time-point. However, the RT-PCR results showed problems of DNA contamination which could not be overcome within the limited time available. Therefore no

data are presented. Transcriptomic or proteomic analyses of bacteria during an *M. sexta* infection would tie in well with data regarding the numbers and health of bacteria and haemocytes. From the host response point of view, host gene expression has been probed in *C. elegans* and murine models of Bp infection (Ooi *et al*. 2012; Chin *et al*. 2010). With the *M. sexta* genome and transcriptomes now available, a similar approach could conceivably be used with *M. sexta*.

Chapter 5. Rapid Virulence Annotation of *Burkholderia pseudomallei*

5.1. Chapter summary

A genome-wide screen for Bp virulence-related genes was undertaken using multiple invertebrate infection hosts and a large expression library of *E. coli* fosmid clones with Bp genomic inserts. This chapter describes the outcomes of that approach. A statistical method was devised which enables quantitative analysis of Rapid Virulence Annotation (RVA) results and overcomes problems with reproducibility of biologically active clones. The calculated observed-to-expected hit ratio for genes allows the identification of a refined subset of the most convincing positive hits. The hits included many known and putative Bp virulence factors, and work was begun to create a deletion mutant in *kdpD*, a locus of particular interest. Ultimately, the lack of reproducibility from positive clones cast doubt on the appropriateness of the fosmid system for expressing Bp genes in *E. coli*. Preliminary RT-PCR analyses of the expression of candidate virulence factors are reported. Overall, the outcome highlights the importance of a thorough assessment of recombinant library expression capability when embarking on RVA-style screening. Nonetheless, the statistical method described here represents a useful tool for the analysis of past or future RVA data sets.

5.2. Introduction

As discussed in the main introductory chapter, Rapid Virulence Annotation (RVA) is a technique for the rapid identification of putative virulence factors of bacterial pathogens. The method employs an expression library – several thousand *E. coli* clones expressing fosmid-based inserts from the genomic DNA of the pathogen of interest. In this case, RVA was applied to Bp strain K96243.

While several factors have already been identified as playing a role in Bp virulence, much remains to be understood. Therefore the rapid generation, using an assumption-free approach, of a shortlist of putative factors for further investigation could be highly useful for the study of Bp, as it was for the study of *P. asymbiotica* (Waterfield *et al*, 2008). The

ability to investigate the genome of this CL3 pathogen under CL2 laboratory conditions is also a major benefit.

Bp K96423 was confirmed in Chapter 3 to be virulent to *M. sexta* larvae. Bp K96423 can also be predicted to evade predation by amoebae and nematodes based on high genetic similarity with Bt E264 which was shown in Chapter 3 to evade predation by *A. polyphaga* and *C. elegans*, and also based on the observations by Inglis *et al* (2000; 2003) of Bp interactions with Acanthamoebae. The *E. coli* fosmid expression strain Epi300 is not harmful to *M. sexta* larvae and is readily consumed by the bacteriovore species. Therefore any 'Gain of Toxicity' (GOT) of some clones would be attributed to the presence of the Bp DNA. GOT is indicated by signs of mortality or morbidity in the insect larvae, or by a lack of predation by the bacteriovores. In this chapter the Bp K96423 fosmid library was screened in each of the three invertebrate models.

This RVA of Bp differs from the original *P. asymbiotica* RVA in two respects. Firstly, only the three invertebrate assays were performed in parallel. An mGOT macrophage assay was performed in collaboration with another research group but the experimental work was not coordinated, and the macrophage assays used a combination of the fosmid library and an additional BAC library. The macrophage data was published (Dowling *et al*. 2010) and will be referred to in the results and discussion sections for comparison with the invertebrate RVA results. Secondly, the Bp RVA used a different expression system: fosmids as opposed to cosmids, and Epi300 *E. coli* as opposed to the EP1305 *E. coli* host (both from Epicentre). Fosmids are low-copy number cosmids based on the bacterial fertility plasmid (F-plasmid). They allow cloning of large DNA fragments and are considered to be more stable than high-copy number cosmids (Kim *et al*. 1992). The pCC1FOS fosmids used in this study are single-copy, but can be temporarily induced to a higher copy number by addition of CopyControl™ AutoInduction solution. However, this short-term up-regulation is optimal between 16-20 hours after addition to a starter culture, after which the suppliers report there may be problems with stability and toxicity of clones. Therefore the GOT assays were performed without addition of induction solution.

Aim: To use RVA to identify putative virulence-related genomic loci of Bp K96423

The primary aim was to use RVA – with the insect, amoeba and nematode host models – to identify 'hit' fosmid clones from the Bp K96423 fosmid library. If RVA led to a reproducible shortlist of fosmids with putative virulence-related activity the aim would then be to further pin-point the precise loci responsible, using transposon mutagenesis for example. It would also be possible to draw conclusions about the extent of overlap of Bp virulence factors relevant for the different invertebrate hosts.

Aim: To develop a new statistical approach for analysis of the RVA results and to assess quantitatively which regions, if any, were the most likely true RVA 'hits'

Unexpectedly, the shortlist fosmids with putative virulence-related effects seen in the first round of RVA screening was not reproducible, and there was little distinctive 'clustering' of multiple hit fosmids around genomic loci. Therefore, the secondary aim was to develop a more rigorous and quantitative method to statistically assess the hit results for clustering, and to look for evidence as to whether the 'hits' from the first round of screening did indeed include true hits or simply resembled a random sample.

5.3. Results

5.3.1. Analysis of the BPF library

First the genomic fosmid library itself was assessed for completeness of coverage and for evidence of Bp protein expression.

Coverage

The library end-sequences were batch-BLASTed and manually curated, which identified the coordinates of 2,396 fosmid inserts (67.45% of the library). The mean insert size was 35,323 bp. 3,552 clones x 35,323 bp = approximately 125.5 Mb of sequence. This equates to more than 17x coverage of the 7.2 Mb Bp K96423 genome. However, the end-sequences of many clones did not have good BLAST matches and therefore could not be located. Figure 5.1 shows the coverage of located clones.

Figure 5.1. Coverage of the Bp K96423 genome within the BPF fosmid library. The lengths of chromosome 1 (top) and 2 (bottom) are represented along the x-axes. Located inserts are spaced along the y-axes simply for ease of viewing.

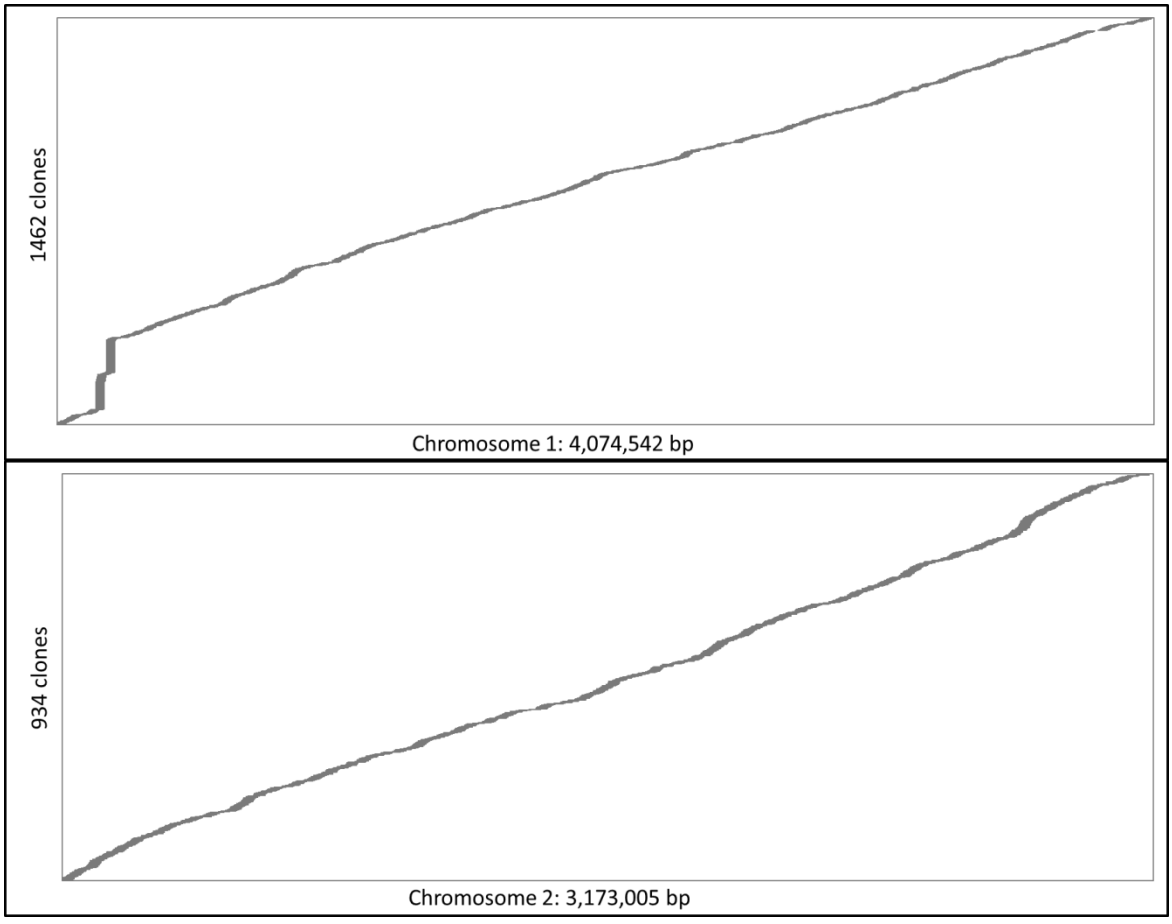

The library coverage was over 99.9% complete with one 8kb gap near the terminus of chromosome 1. Chromosome 1 also showed a heavily over-represented area around base pairs 17,900-20,000.

Protein expression from BPF clones

To look for evidence of protein expression, fosmids encoding the MprA metalloprotease were plated on mil agar plates. If successfully expressing, translating and exporting the protein this would result in proteolytic clearing of the milk agar. Table 5.1 shows the degree of proteolysis observed on 3% milk agar plates.

Table 5.1. Degree of proteolysis of milk agar exhibited by BPF fosmid clones and controls

Organism or BPF clones	Proteolysis	
	No extra regulation	With auto-induction solution
Bt E264	++++	NT
Epi300 *E. coli*	0	0
16b11 / 28f02 / 15b05 / 34f05 / 05b11 / 32b11 / 01a03	+	++

Plates were incubated at 37 °C and assessed after 72 hours. The degree of proteolysis is represented on a scale from 0 (no effect) to ++++ (extensive effect). NT = not tested

As shown in Figure 5.2 the Bt control plate showed extensive proteolysis of the milk agar. The mode of regulation of extracellular enzymes often differs between Bt and Bp (Vial *et al*., 2007), and additionally, the proteolytic effect may have resulted from the action of multiple enzymes as opposed to MprA alone. However, the effect serves as a clear indication of a positive proteolytic effect. On the other hand, the Epi300 *E. coli* background strain showed no clearing of the milk agar.

All of the BPF clones tested showed a slight proteolytic effect: a selection is shown in Figure 5.3 panel A. The effect took 48-72 hours to become apparent, unlike the Bt control which took less than 24 hours' incubation to show clearing. As shown in Figure 5.3 panel B, it was also evident that addition of the CopyControl™ solution increased the proteolytic ability of each clone but, importantly, some limited activity was still seen in areas of thick growth from clones grown without it.

Figure 5.2. Protease expression from Bt E264 and Epi300 *E. coli*. After 72hrs incubation at 37°C: (A) the milk agar was cleared by the Bt E264 positive control; (B) the Epi300 *E. coli* negative control plate remained opaque.

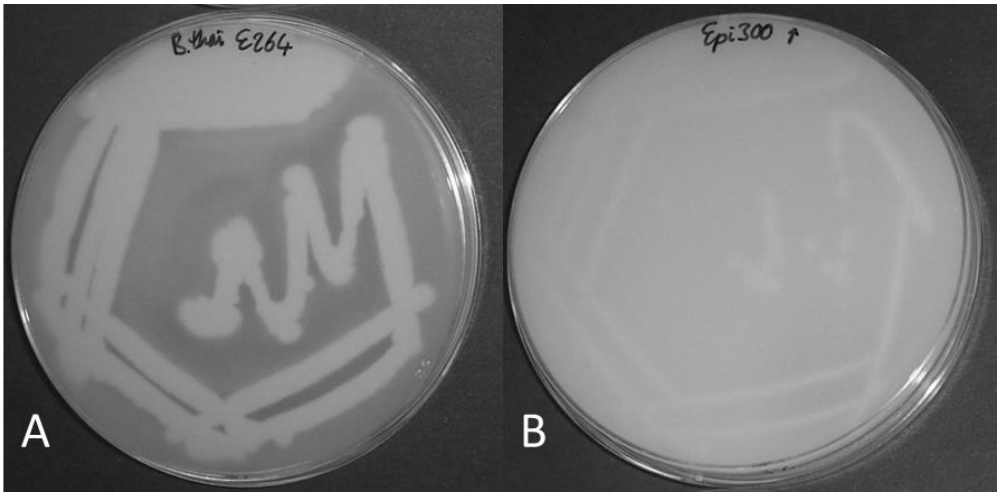

Figure 5.3. Metalloprotease expression from BPF clones. Following 72hrs' incubation at 37°C, BPF clones bearing a metalloprotease gene (BPSS1993) were able to lyse the milk in the areas of thickest bacterial growth. (A) Two representative MprA-bearing BPF clones. (B) Proteolysis was more pronounced when clones were grown with CopyControl™ Auto-Induction solution (left) than without (right), although limited clearing was still evident in the un-treated clones.

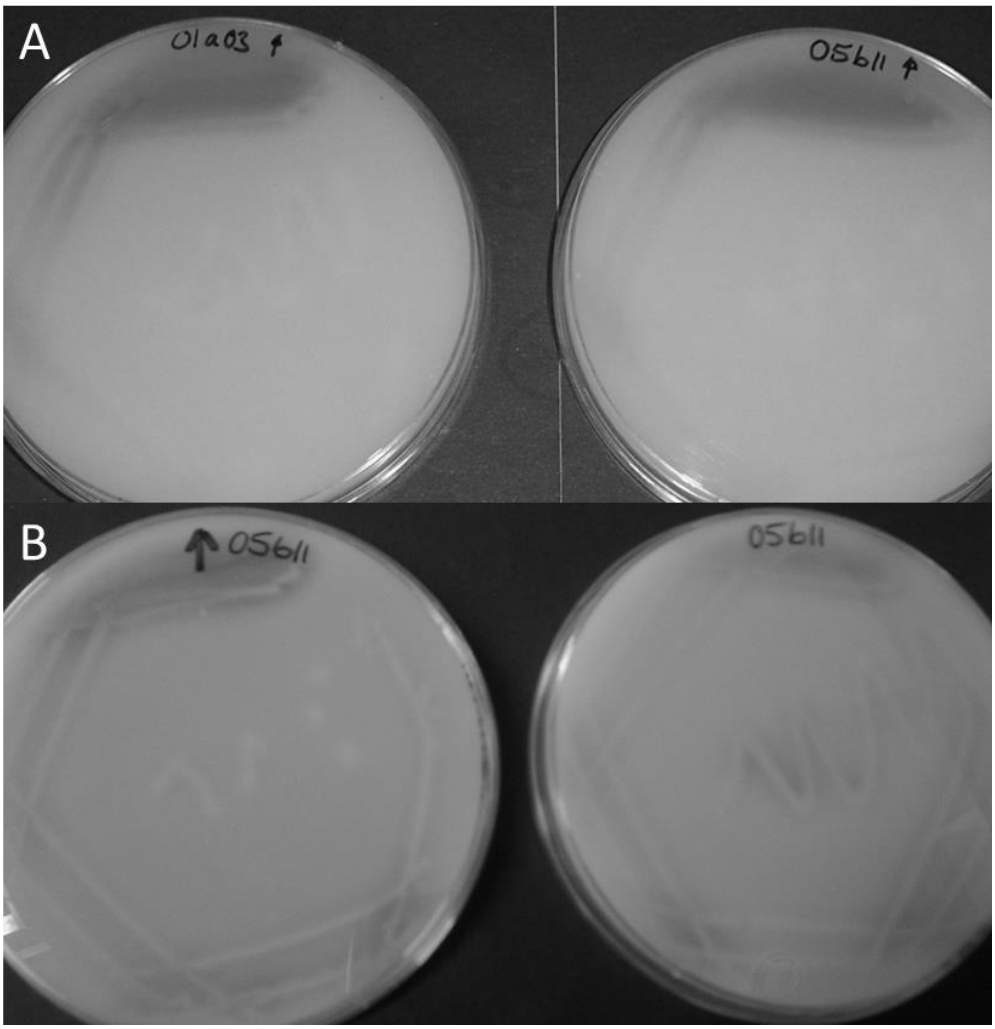

The evidence of proteolysis meant that Bp proteins could be successfully expressed and secreted in the recombinant system and therefore indicated that the system would be sufficient for RVA.

5.3.2. Initial RVA results and re-testing

Initially the RVA results were assessed by plotting their fosmid insert locations relative to the Bp K96423 genome and looking for evidence of clustered hits.

Numbers and different types of hits

The gain-of-toxicity (GOT) assays yielded semi-qualitative results. aGOT (amoeba-GOT) and nGOT (nematode-GOT) results were classed as either 'best' or 'possible' positives based on how clear-cut the result had been. Similarly, iGOT (insect-GOT) results were classed as 'best', 'possible higher', 'possible lower', or 'interesting phenotype' hits. Interesting phenotype hits were those which did not appear to have detrimental effects on larval development but the larvae showed a pink tinge which anecdotally may be immune system-related. 'Best' iGOT hits from the first round were those with which the injected larva had died (*n* = 33). Full details of the results are listed in DVD e-Appendix 5a. Numbers of each type of hit are summarised in Table 5.2.

Table 5.2. Qualitative classification of hits from GOT screens

	Best hits	Possible higher hits	Possible lower hits	Interesting phenotype hits	Total hits	Hits considered further:
aGOT	**202**	107	-	-	309	**202**
nGOT	**147**	53	-	-	200	**147**
iGOT	**33**	**20**	**73**	**32**	**158**	**158**

Mapping of positive fosmids to the Bp genome

The entire BPF library consisted of 3,552 clones. Of these, approximately 74% could be revived from -80 °C stocks and were tested in GOT screens (Table 5.3). RVA screening was conducted before Batch-BLAST results of end-sequences were available. Due to poor sequence data or poor BLAST results approximately 25-35% of positive clones could not be mapped. The rest were assigned to chromosome 1 or 2 as shown in Table 5.3. Positive GOT results were mapped to their corresponding locations along the Bp genome, as shown in Figure 5.4.

Table 5.3. Numbers and locations of positive hit results from BPF invertebrate GOT assays

	No. clones grown and tested (% of library)	Total positive hits (% of clones tested)	Locations of hit regions (% of total positive hits)		
			Un-mapped	Chromosome 1	Chromosome 2
aGOT	2632 (74.1%)	202 (7.7%)	58 (28.7%)	91 (45.0%)	53 (26.2%)
nGOT	2634 (74.2%)	147 (5.6%)	38 (25.8%)	70 (47.6%)	39 (26.5%)
iGOT	2630 (74.0%)	158 (6.0%)	56 (35.4%)	65 (41.1%)	37 (23.4%)
Average	74.1%	6.4%	30.0%	44.6%	25.4%

'% of library' values are based on 3552 BPF clones. Hits '% of clones tested' values are based on only those clones that grew and could be tested. The distribution of hits is shown - chromosome 1 or 2 or un-located due to poor sequence or BLAST data.

Figure 5.4. Positive fosmid distribution maps. Bp K96423 genome maps showing the locations of inserts from positive hit clones along chromosome 1 (top) and chromosome 2 (bottom). aGOT hits are shown in red, nGOT in blue, and iGOT in green.

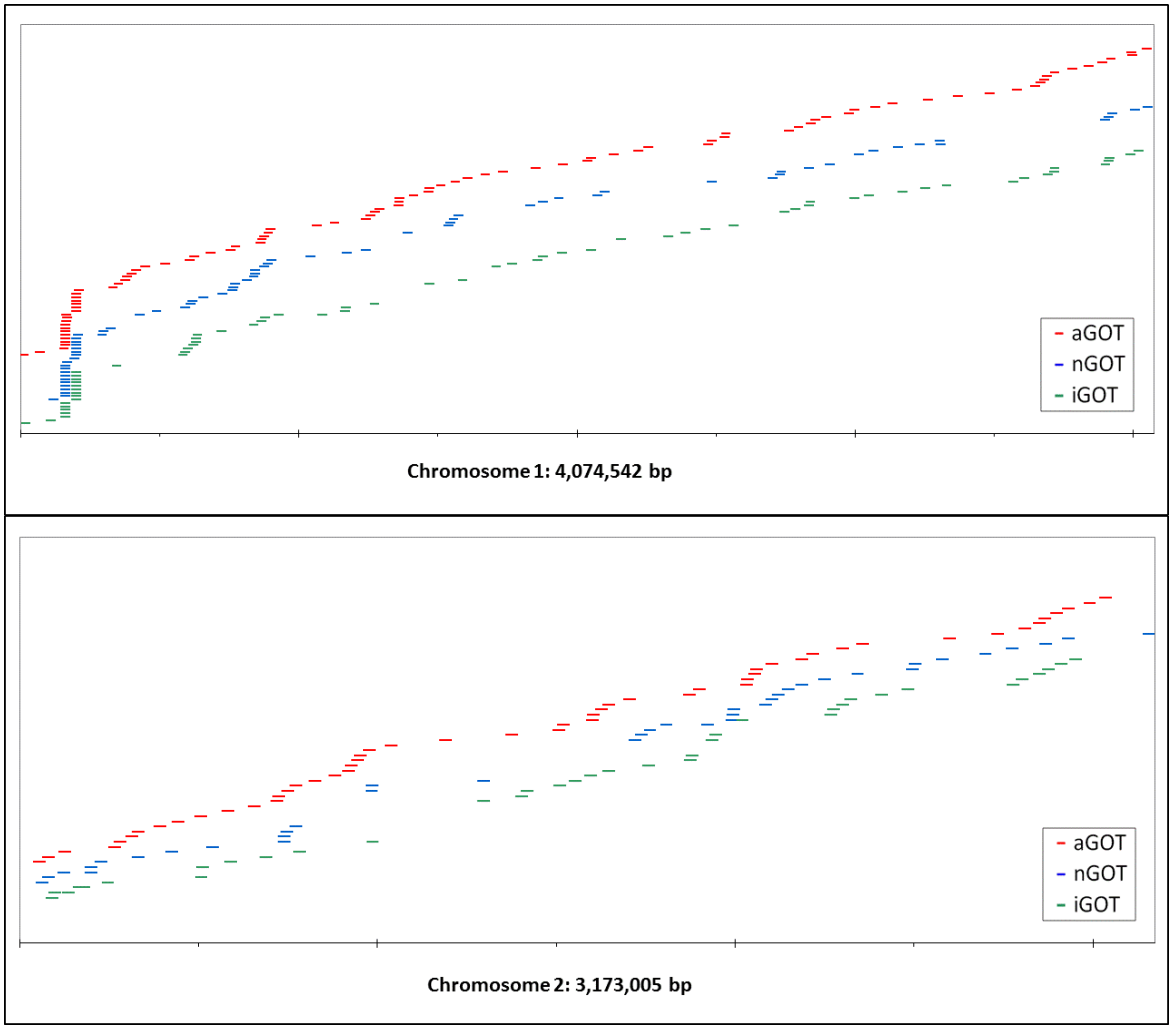

The positive hits were spread across the majority of the genome. Apart from a clustering of hits in the region which was heavily over-represented in the library itself (chromosome 1, base pairs 17,900-20,000), there were no particularly obvious clusters.

Retests of positive hits

When it came to re-testing the fosmids identified as hits in the first round of screening, it became apparent that there was little to no reproducibility. When the first 20 positive clones from aGOT and nGOT screens were re-tested using 10 replicate wells the results were not consistently reproducible (data not shown). Therefore it was decided that re-testing all the aGOT and nGOT positives would not be worthwhile.

Positive hits from iGOT were re-tested with 10 larvae each. Of the 33 clones which were lethal in the first round (i.e. scored 4 based on the original 0-4 scoring system), none reproduced the lethal effect. The average retest score was just 0.66 with a range of 0-0.70. These scores corresponded to only a very slight effect. Similarly, clones from the 'possible' or 'interesting phenotype' categories re-tested with an average score of 0.20 and a range of 0-0.70. A score of 1 was considered a small effect, so these re-test scores did not represent a great degree of morbidity. The re-tests suggested that either the original high scores may have been anomalous, or the virulence-related activity of the fosmids may have been lost or degraded over time.

5.3.3. Statistical analysis of RVA results

Which hits to consider in further analyses

As the re-testing was not appropriate for aGOT and nGOT and was not reproducible for iGOT it was not possible to refine a shortlist of fosmids for further study. Therefore it was decided which hits would be considered in the further (statistical) analyses. From the first screening round the aGOT and nGOT screens yielded a large number of positive hits, so only the 'best' hits were considered in all subsequent analyses (202 and 147 hits, respectively). iGOT had produced far fewer 'best' hits and fewer hits overall, so all iGOT hits (158 in total) were considered in analyses.

Descriptive statistics and correlations of coverage and hit distributions

BPF library Coverage values and Observed Hit values were determined as described in the methods section. Fosmids contained an average of 31.65 CDSs with standard deviation of 7.83 CDSs. 76,352 CDS representations were identified by the script output, with coverage across the Bp genome as shown in Figure 5.5.

Figure 5.5. BPF library coverage maps for chromosome 1 (top) and chromosome 2 (bottom). Chromosome 1 is also represented on a different scale (upper, inset) to illustrate the extent of coverage of the over-represented region.

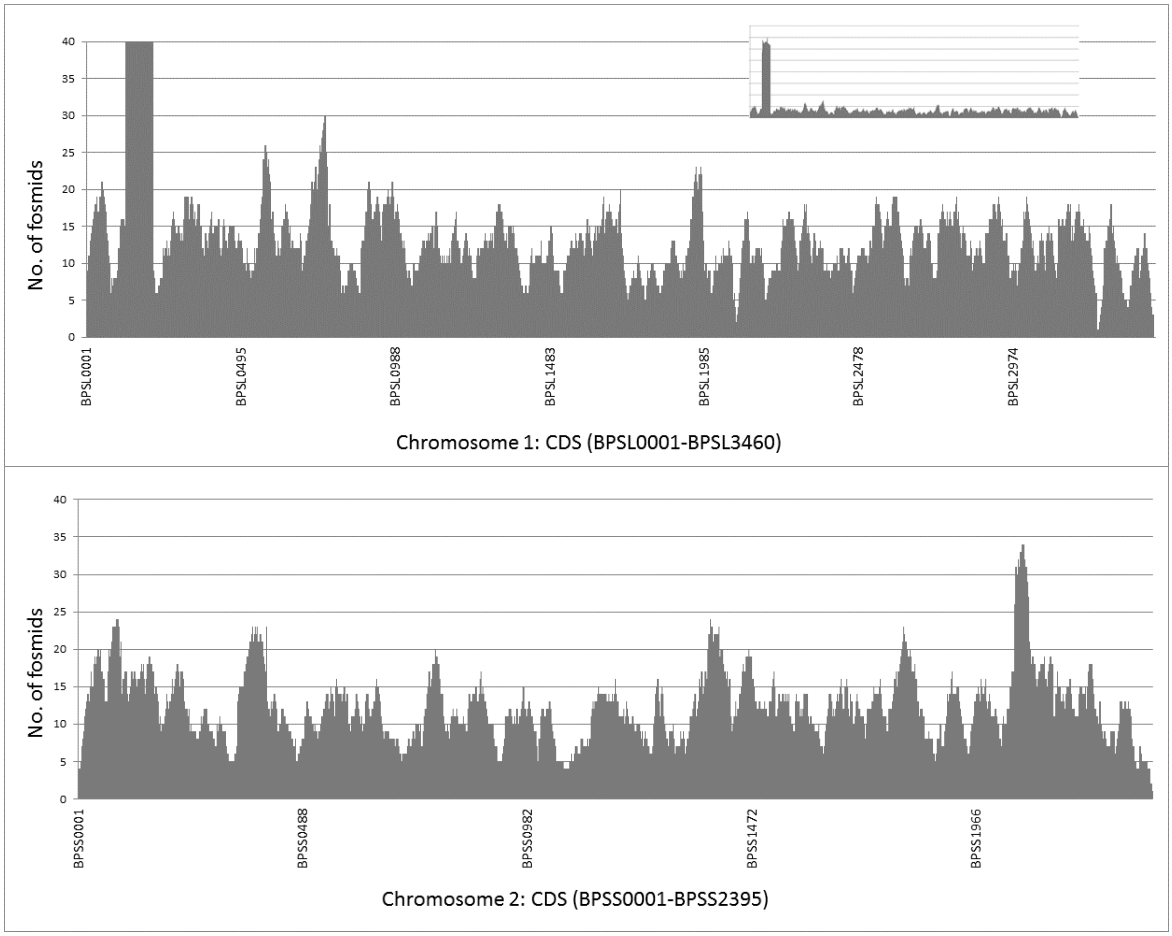

CDS by CDS, coverage varied considerably across each chromosome, with a few distinct peaks of higher coverage. If a random sample of fosmids was picked, it would be expected by chance to see more hits (i.e. clusters) at regions with higher coverage.

When excluding clones which did not grow and therefore could not be tested in the screens, the following coverage numbers were tested: aGOT = 57,228 CDS representations; nGOT = 57,228 CDS representations; iGOT = 57,170 CDS representations. This means that across the 5,855 CDSs present in the Bp genome the average coverage was between 9.77-9.78 fosmids per CDS. Further statistical calculations were based on that tested portion of the library only.

One-Sample Kolmogorov-Smirnov tests revealed that for all three GOT screens the Coverage and Observed Hit data did not fit the normal distribution ($p < 0.000$) and therefore further test statistics would need to be non-parametric. Full SPSS statistics reports are included in DVD e-Appendix 5b.

Scatterplots of each screen's Coverage and Observed Hits (Figure 5.6) show a positive correlation; CDSs which are represented more are generally hit more, as would be

expected. A portion of the data points in each case have very high coverage - these correspond to the heavily over-represented region of chromosome 1.

Figure 5.6. Scatterplot graphs for Observed Hits and Coverage data from aGOT, nGOT and all iGOT hits (top left, clockwise). If coverage alone was an accurate predictor of observed hits (Obs), the data points would fit a linear positive correlation, i.e. would align close to an imaginary diagonal line from the bottom left to top right corner. The presence of the data points on the far right gives the impression of that trend, but they represent the heavily over-represented region of chromosome 1. The majority of hits (in the range of up to 30x coverage) show only a weak linear correlation.

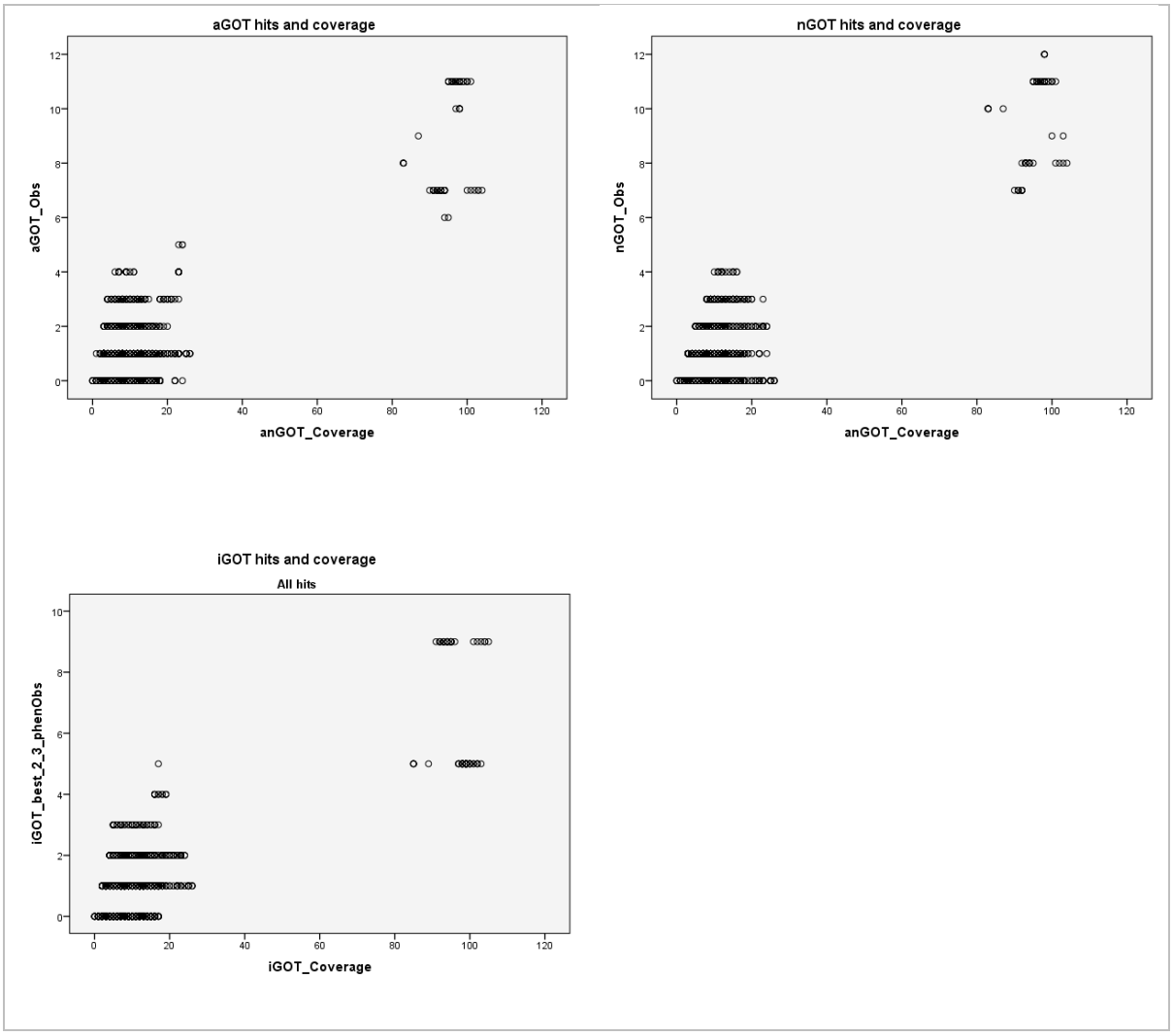

Correlation coefficients for CDS coverage and observed hits were calculated using the Spearman's rho statistic suitable for non-parametric data (Table 5.4).

Table 5.4. Spearman's Rho Correlation Coefficients for Coverage and Observed Hits

	aGOT Coverage	nGOT Coverage	iGOT Coverage
aGOT Observed Hits	**0.221****		
nGOT Observed Hits		**0.268****	
iGOT Observed Hits (all)			**0.304****

** Correlation is significant at the 0.01 level (2-tailed).

With a perfect positive correlation having a coefficient of 1.0, the calculated coefficients (0.221 – 0.304) showed a weak-to-moderate but significant correlation between CDS Coverage and Observed Hit data. This indicates that the degree to which a CDS is hit is not solely determined by its Coverage; other factors are at play, e.g. random effects or true-positive GOT effects.

Correlation between observed and expected hit values

Table 5.5 shows the Spearman's rho correlation coefficients for Observed hits and Expected hits. As the Expected hits are calculated based on CDS coverage, it would be expected that this would produce a similarly weak-to-moderate correlation.

Table 5.5. Spearman's Rho Correlation Coefficients for Expected and Observed Hits

	aGOT Expected Hits	nGOT Expected Hits	iGOT Expected Hits
aGOT Observed Hits	**0.204****		
nGOT Observed Hits		**0.331****	
iGOT Observed Hits (all)			**0.331****

** Correlation is significant at the 0.01 level (2-tailed).

A weak-to-moderate but significant correlation was indeed seen between Expected Hits and Observed Hits (0.204 – 0.331). If the hits had been distributed exactly as expected according to the Coverage alone this would have yielded a perfect correlation of 1.0.

Descriptive statistics for Obs/Exp ratio data

Ratios of Observed/Expected hits were calculated for each hit CDS, as described in the methods section. Descriptive statistics for the Ratios use median rather than mean values because the data was non-normal.

When considering the aGOT hits, nGOT hits and all iGOT hit types, the median Ratio was 2.0. This means the median trend for hit CDSs was to be hit twice as often as expected. Excluding the iGOT 'phenotype' hits did not affect this result. Excluding the 'lower possible' hits, and subsequently the 'higher possible' hits too, did affect the result; the median trend was for CDSs to be hit six- and ten-times as often as expected. This indicates that hit clones that were qualitatively categorised as 'best' or 'higher possible' actually did cluster around particular CDSs more, supporting the theory that, despite a lack of reproducibility, true GOT effects did occur during screening.

Confidence intervals (CIs) for the medians were constructed without any distribution assumptions and values for the upper limit were noted (Table 5.6). These values enable average or below-average Ratios to be disregarded, leaving a sub-set of hits with high ratios. Ratio values above those upper limits are at least as great as the true median value, with at least 95% or 99.9% confidence.

Table 5.6. Descriptive statistics for the GOT screens' Obs/Exp Ratio data. *n* = number of hit CDSs. Median = median average observed/expected (Obs/Exp) ratio. Upper bounds of Confidence Interval for the medians (CI) are shown (95% and 99.9% confidence that the median is less than or equal to the figure shown).

Obs/Exp Ratio	***n***	**Upper confidence interval of the median**	
		95%	**99.9%**
aGOT	3021	2.0	2.0
nGOT	2064	2.0	2.0
iGOT (all hits)	2181	2.0	2.0
iGOT (excl. phenotype hits)	1206	3.0	3.0
iGOT (best & higher possible hits)	778	6.0	6.0
iGOT (only best hits)	442	10.0	12.0

In most cases the 99.9% upper confidence interval level is the same as for the 95% upper confidence level, with the exception of for the iGOT best hits. This simply indicates that the iGOT best hits had greater variability among high Obs/Exp Ratio values.

Refining the GOT hits

The upper median CI values were used to eliminate CDSs which were not hit more than the average, leaving the numbers of CDSs shown in Table 5.7. DVD e-Appendix 5c lists all the CDSs in the refined subset with their Obs/Exp Ratios, genome coordinates, gene ontology (GO) information and other published annotations.

Table 5.7. Refined numbers of hit CDSs based on Obs/Exp ratios

	Original number of hit CDSs	Number of refined hit CDSs	Percentage of original number
aGOT	3021	1190	39.4 %
nGOT	2064	1209	58.6 %
iGOT (all hits)	2181	1174	53.8 %

All the refined hit CDS Obs/Exp Ratios were plotted on genome maps (Figures 5.7-5.9). This allows the visualisation of regions with Obs/Exp Ratios higher than the upper CIs for the medians, i.e. those which were hit particularly more than expected by chance.

Figure 5.7. Graphs showing Obs/Exp Ratios for aGOT hit CDSs. Hit CDSs are aligned to the genome (chromosome 1, top; chromosome 2, bottom). The average (median) Ratio is 2.0 or below. Ratios greater than 2.0 are highlighted in bright red. Some CDSs were hit up to 13 times more than expected.

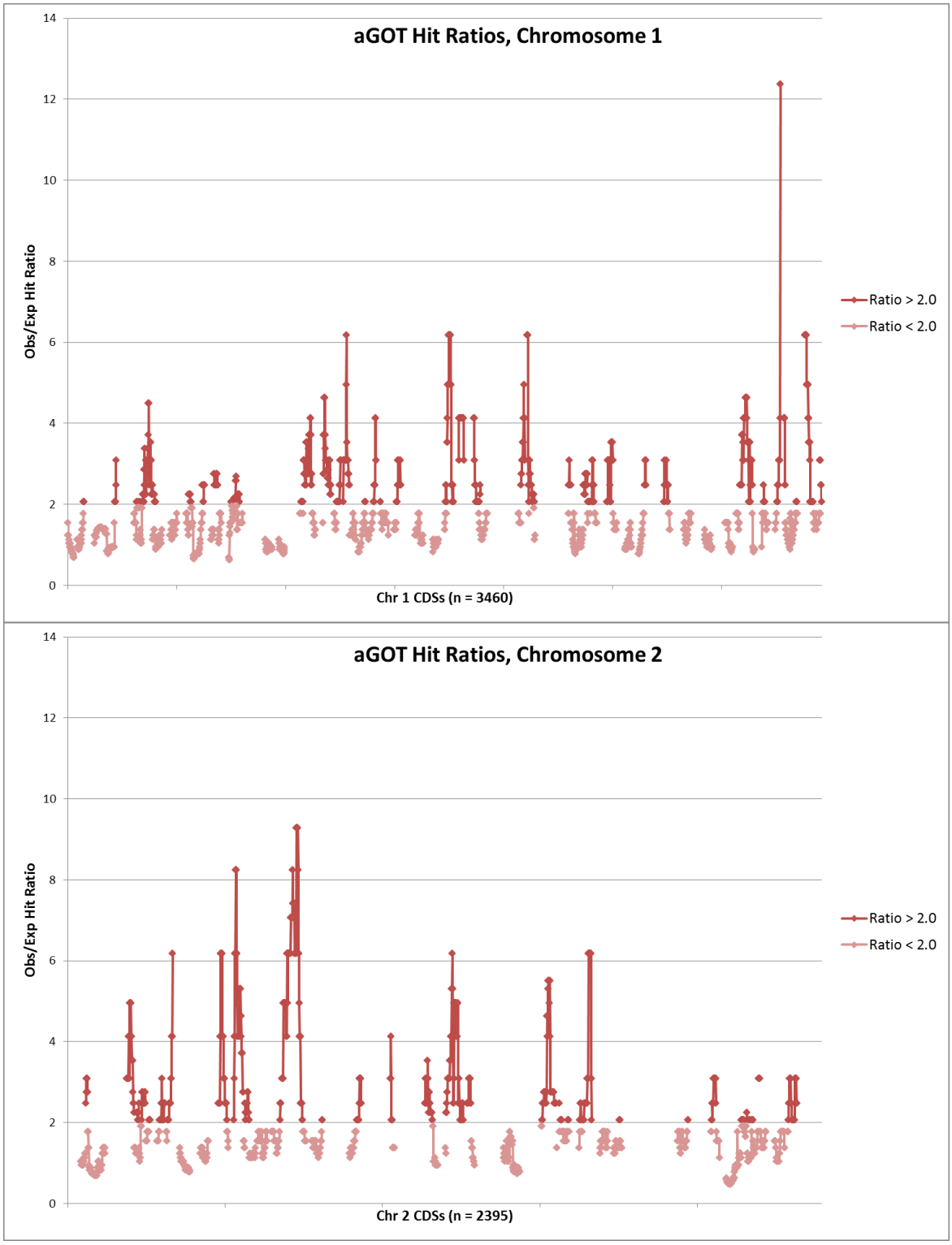

Figure 5.8. Graphs showing Obs/Exp Ratios for nGOT hit CDSs. Hit CDSs are aligned to the genome (chromosome 1, top; chromosome 2, bottom). The average (median) Ratio is 2.0 or below. Ratios greater than 2.0 are highlighted in bright blue. Some CDSs were hit up to 6.5 times more than expected

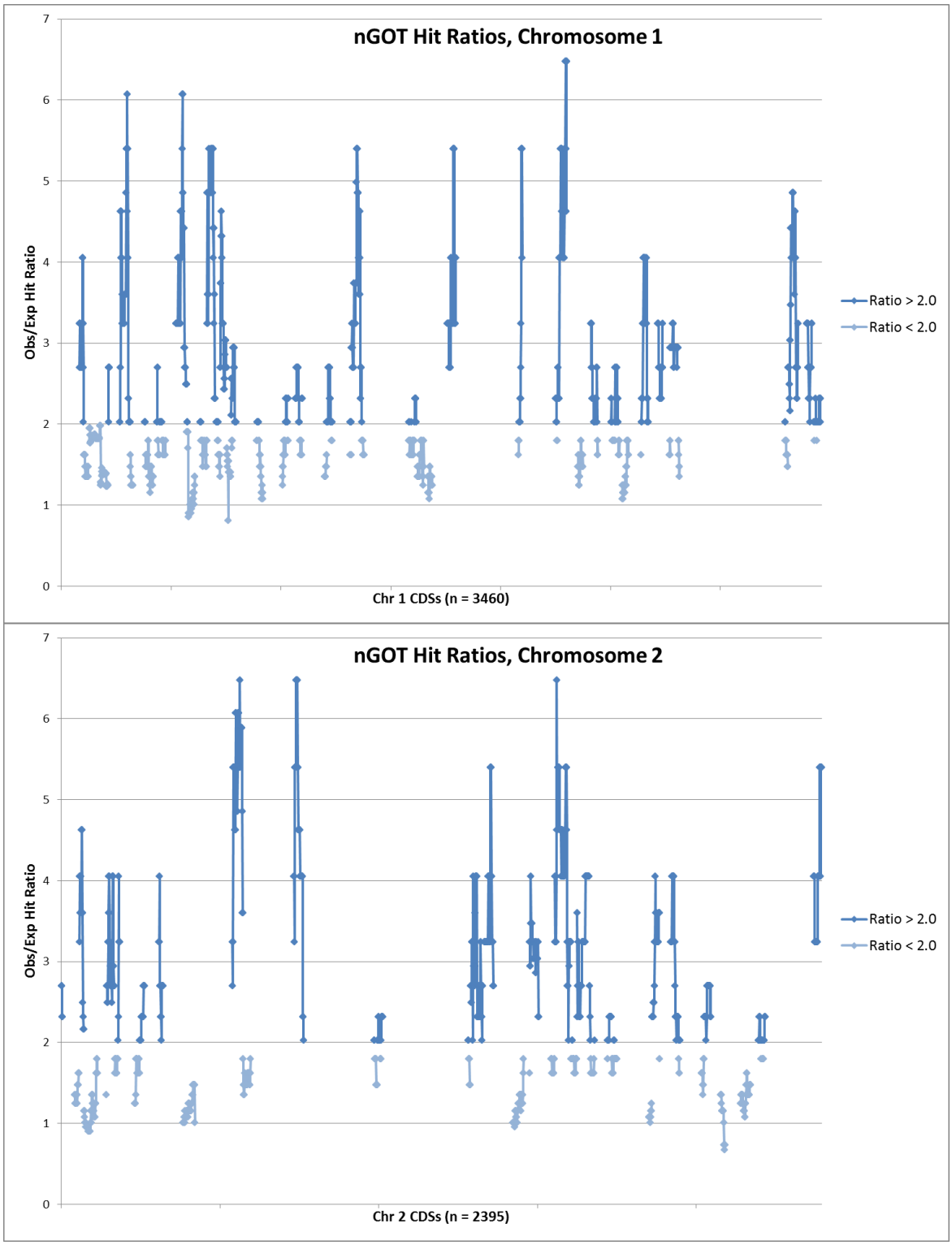

Figure 5.9. Graphs showing Obs/Exp Ratios for all iGOT hit CDSs. Hit CDSs are aligned to the genome (chromosome 1, top; chromosome 2, bottom). The average (median) Ratio for all hits is 2.0 or below. Ratios greater than 2.0 are highlighted in bright green. Some CDSs were hit up to 11 times more than expected.

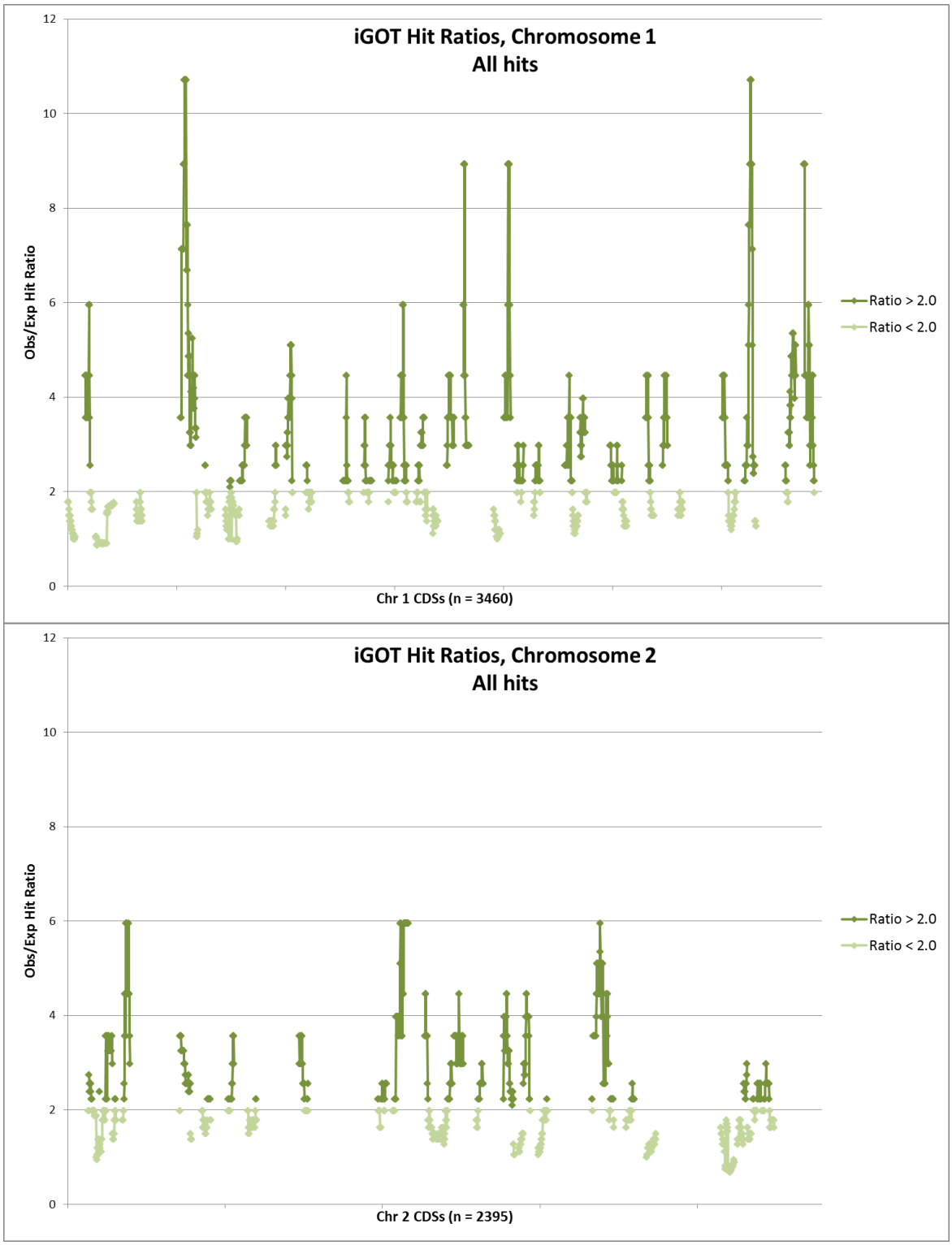

Having taken into account variations in the coverage of the tested fosmid library to generate Obs/Exp Ratios, it was apparent that some regions were 'hit' considerably more than average. These represent the loci most likely to have shown true GOT effects in the first round of scrrening, despite the lack of reproducibility in re-testing.

Comparing hits between invertebrate GOT screens

The refined hits (those with Ratios greater than or equal to the upper CI for the median) were analysed to see how much overlap there was between hits from the three different invertebrate screens. CDSs from the refined hits were hit in one or more screens as shown in Figure 5.10.

Figure 5.10. Number of CDSs unique to or shared by different GOT screens (total 2,756 CDSs)

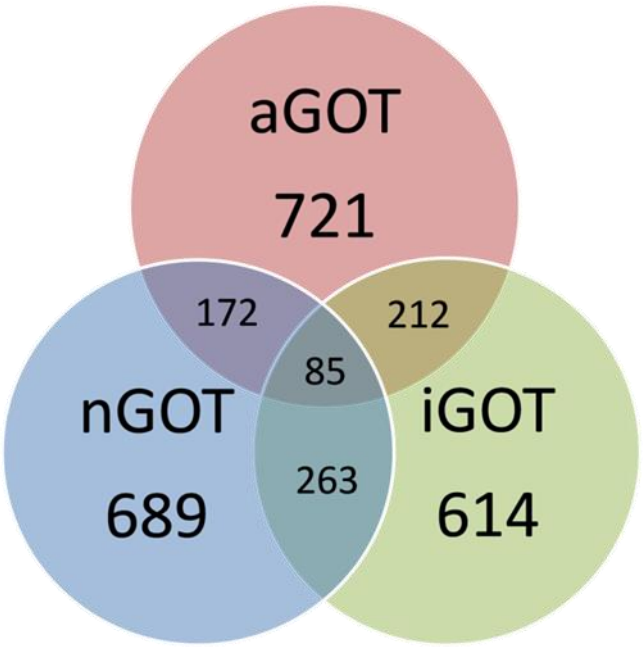

CDSs hit in one model only =	73.4 %
CDSs hit in two models =	23.5 %
CDSs hit in all three models =	3.1 %

Mapping refined hit 'regions' from all screens

Refined hit regions were defined as those containing one or more CDSs with Obs/Exp hit ratios at least equal to the median ratio, as described in the methods section. DVD e-Appendices 5d and 5e contain complete details about the GOT Regions in terms of genomic coordinates and the average and maximum Obs/Exp Ratio of the CDSs within each region.

Table 5.8 shows the numbers of hit regions from aGOT, nGOT and iGOT ('all hits' and 'best hits').

Table 5.8. Numbers of GOT Regions, by GOT assay type and by chromosome. CI = confidence interval

	Number of GOT Regions		
	Chromosome 1	**Chromosome 2**	**Total**
aGOT	37	29	66
nGOT	34	27	61
iGOT (all hits)	30	27	57
iGOT (only best hits, 95% CI)	6	5	11

The refined hit regions were used in order to plot the new results from all three screens onto the same map; in Figure 5.11 the different GOT screens (plus an iGOT subset) are arranged and labelled on horizontal tracks.

Figure 5.11. Refined hit regions of the Bp K96423 genome according to iGOT, nGOT and aGOT. These regions all show observed-to-expected hit ratios equal to or higher than the median ratio for hit CDSs. For most data the 95% and 99.9% confidence intervals (CI) are the same. iGOT best hits are shown using the 95% CI. Horizontal tracks for each data subset are labelled at the right. There is a mixture of overlapping refined hit loci and loci which were refined hits in only one screen.

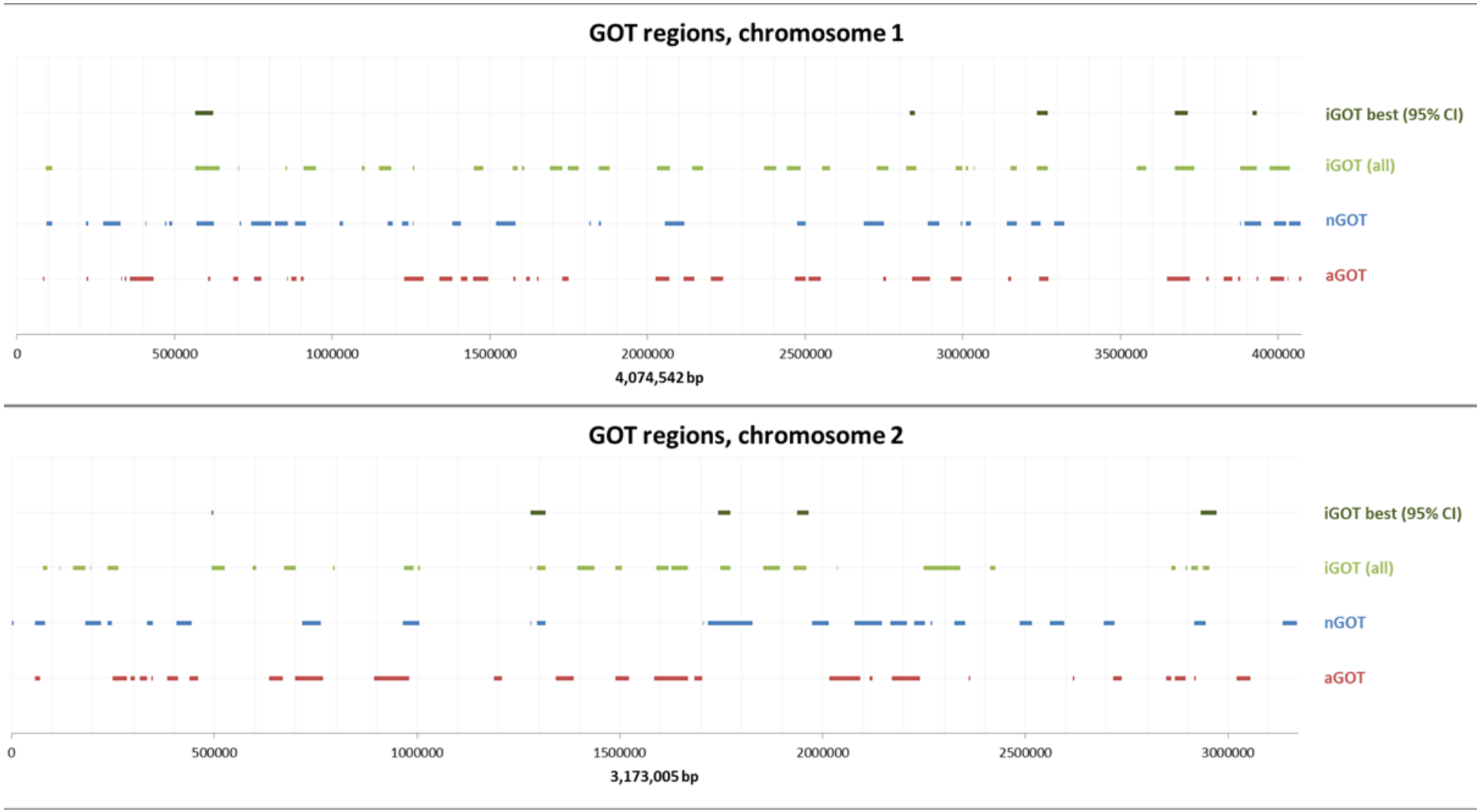

Out of interest to see whether the different subjective scores of different iGOT hit types corresponds to any interesting variation in refined hit regions, Table 5.9 and Figure 5.12 show the refined regions based on the different subsets of iGOT hits.

Table 5.9. Numbers of GOT Regions, by iGOT hit type and by chromosome. CI = confidence interval

	Number of GOT Regions		
	Chromosome 1	**Chromosome 2**	**Total**
iGOT (all hits)	30	27	57
iGOT (excl. phenotype hits)	7	13	20
iGOT (best & higher possible hits)	24	15	39
iGOT (only best hits, 95% CI)	6	5	11
iGOT (only best hits, 99.9% CI)	4	6	10

In Figure 5.12 the lowest track shows the refined regions from the analysis of all iGOT hits (ratios at least equal to 2). The highest track shows results from only the best hits with the most stringent upper CI cut-off (ratios at least equal to 12). It seems that there is little difference in the overall pattern between 'all hits' and 'best & higher possible' hits (which excluded both 'lower possible' and 'phenotype' hits). This implies that the 'best & higher possible hits' results strongly contribute to the regions defined for 'all hits'. Similarly, most regions that are identified from 'best hits' are present in all the sub-sets, suggesting that they truly were the most reliable hits; not only were their original GOT scores higher but they were also hit more times.

For most subsets of data the 95% and 99.9% CIs of the median gave the same value but for the iGOT best hits two different values were given. In this figure both were used as cut-off values for the ratios. The 95% and 99.9% confidence intervals gave very similar results in terms of the locations of hits because most best hit ratios were equal to at least 12.

As there were not major differences between most subsets of iGOT data (or between the two confidence intervals for the best hits), all further analyses of iGOT will continue to concentrate only on the results from 'all hits' and 'best hits' (95% CI).

Figure 5.12. Refined hit regions of the Bp K96423 genome according to iGOT with different analyses of the data. These regions all show observed-to-expected hit ratios equal to or higher than the median ratio for hit CDSs. For most data the 95% and 99.9% confidence intervals (CI) are the same. Two tracks are shown for iGOT best hits to reflect the different CI values. Horizontal tracks for each data subset are labelled at the right.

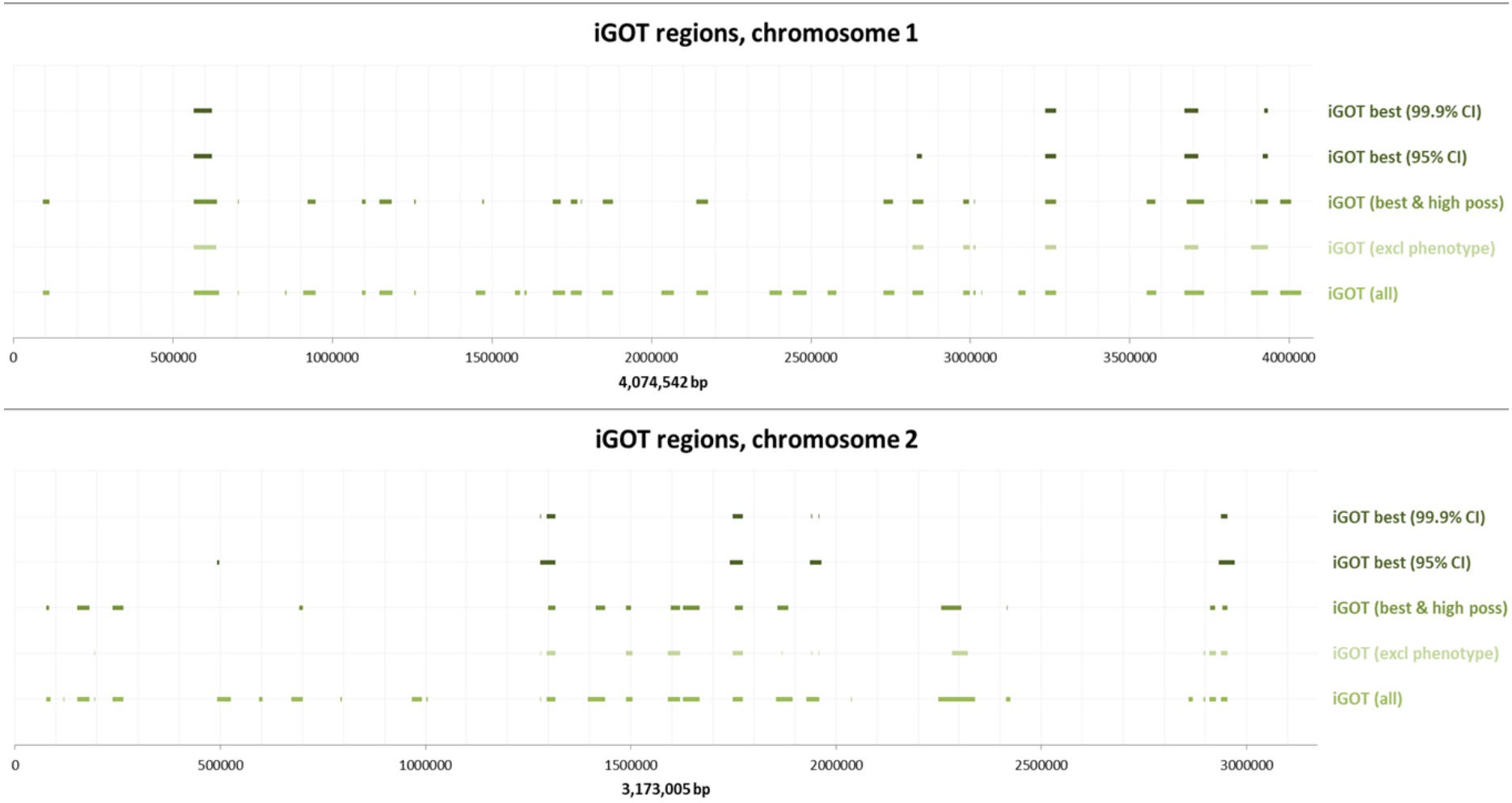

Functional annotations of hits

Thanks to the availability of annotations for the Bp K96423 genome it was possible to look for patterns in the annotated functions of hi CDSs. The JCVI database was used to find gene ontology (GO) data (http://pathema.jcvi.org).

Pie charts in Figures 5.13 – 5.15 show the frequencies of different GO annotations which occurred two or more times.

Table 5.10 summarises the same GO annotations for all three GOT screens. The vast majority of CDSs stated “no GO annotation on JCVI”. For those that did have GO accession numbers, many corresponded to “biological process unknown”.

Figure 5.13. Pie chart showing frequency of GO annotations among refined hit aGOT CDSs. Annotations which occurred only once were combined into the 'individual GO terms' category. The 'Other' portion of the pie chart is expanded for ease of viewing.

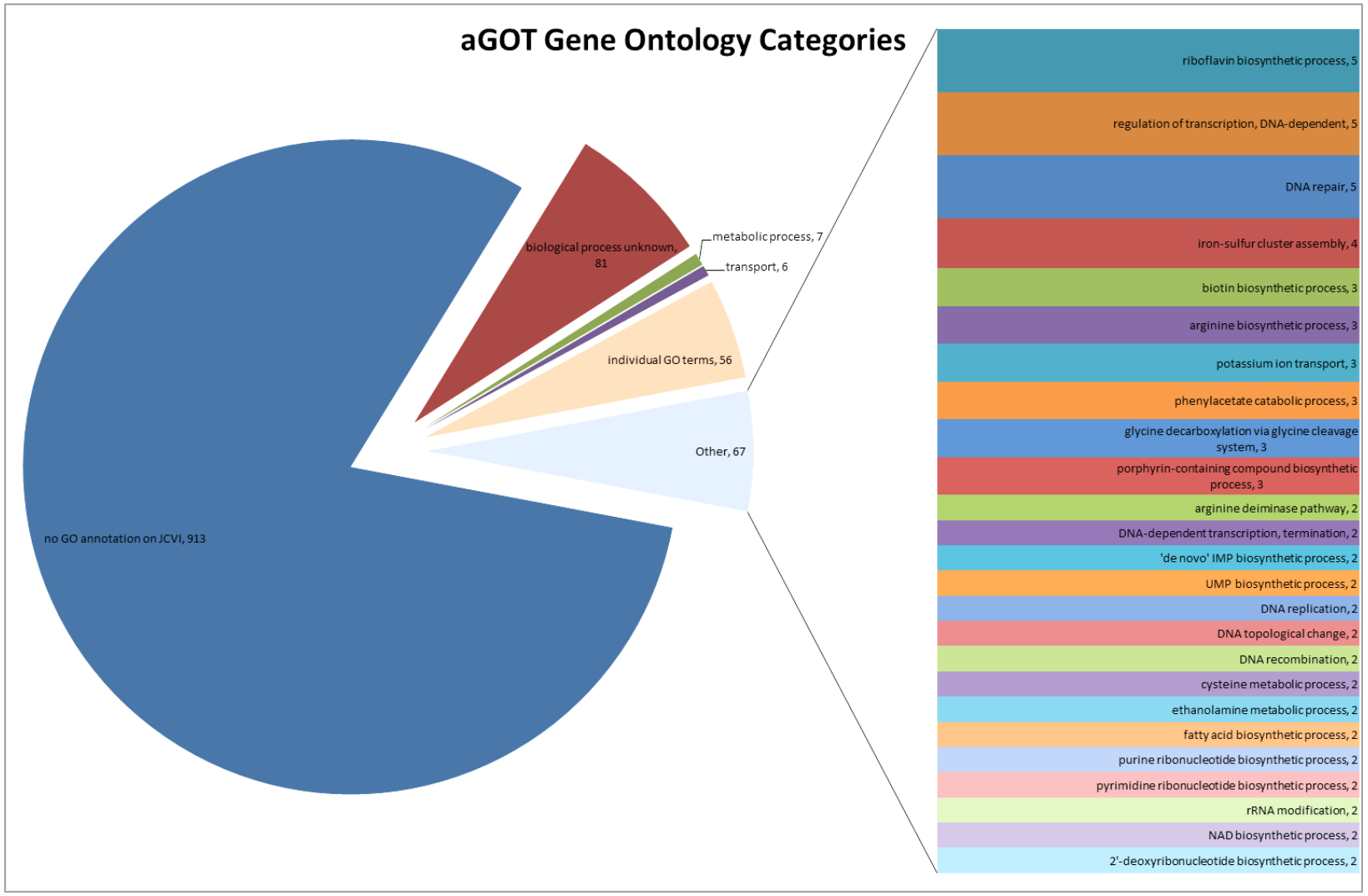

Figure 5.14. Pie chart showing frequency of GO annotations among refined hit nGOT CDSs. Annotations which occurred only once were combined into the 'individual GO terms' category. The 'Other' portion of the pie chart is expanded for ease of viewing.

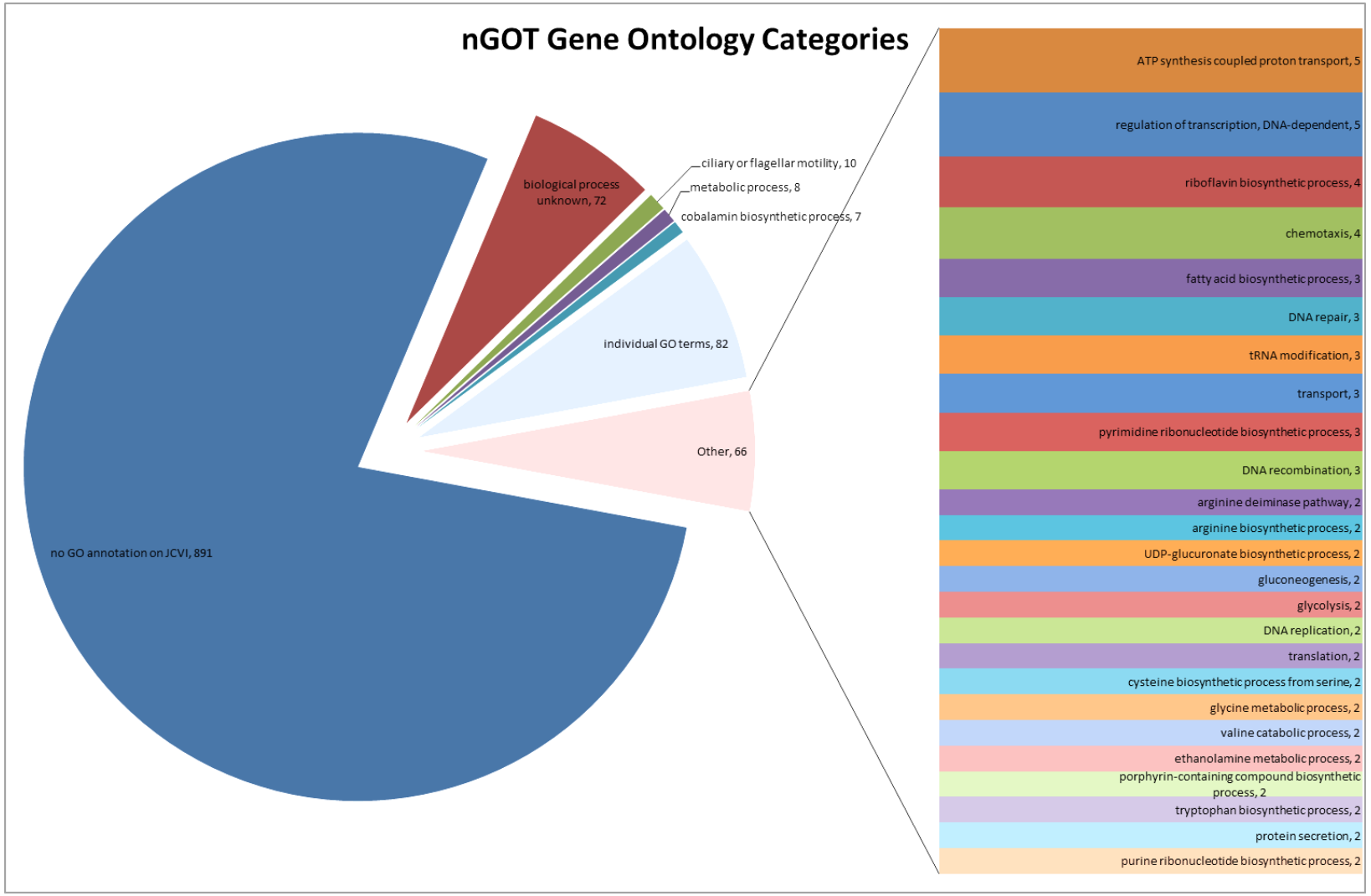

Figure 5.15. Pie chart showing frequency of GO annotations among all refined hit iGOT CDSs. Annotations which occurred only once were combined into the 'individual GO terms' category. The 'Other' portion of the pie chart is expanded for ease of viewing.

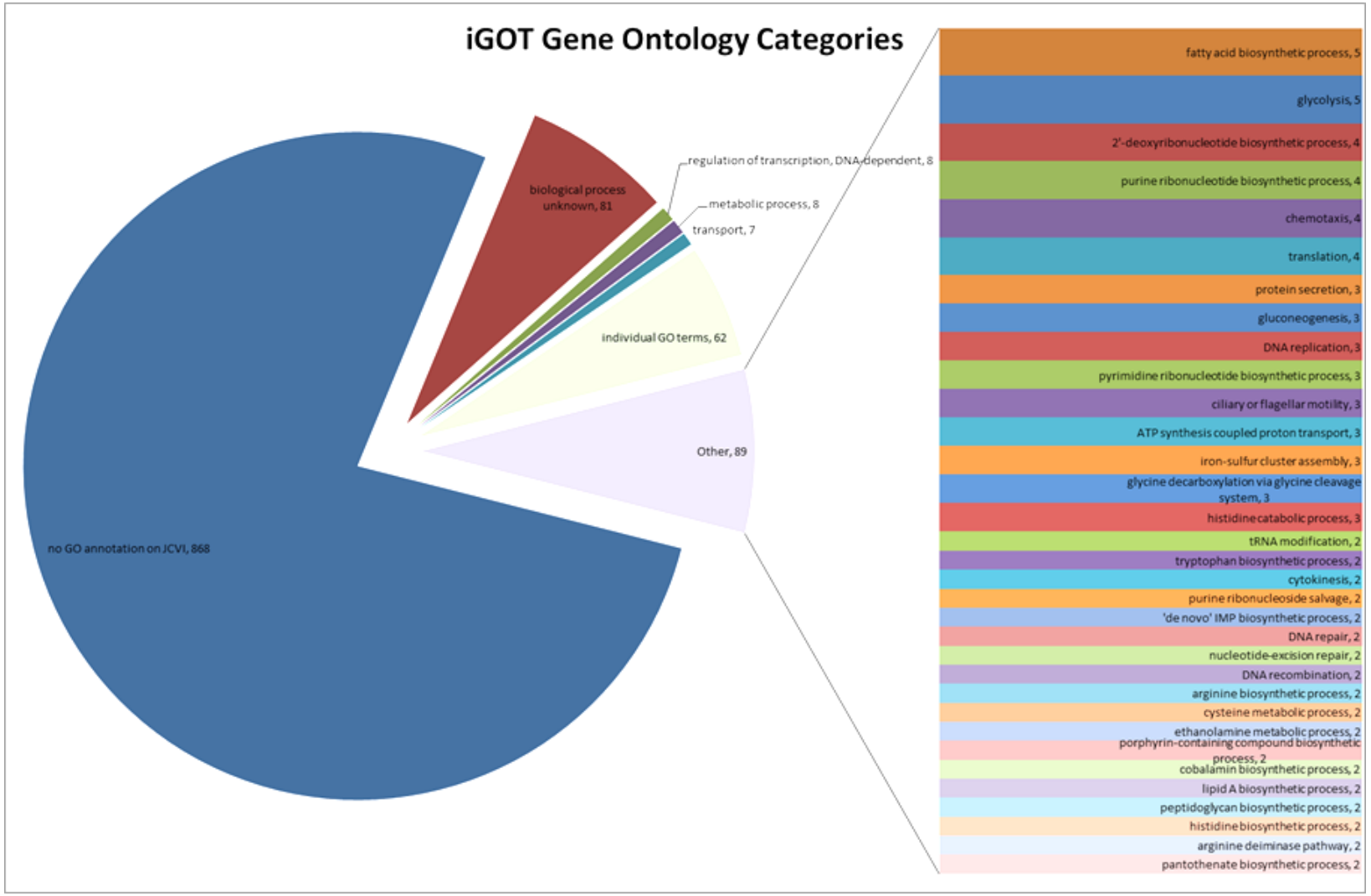

Table 5.10. Summary of common GO annotations from refined hits of the three GOT screens

GO Annotations	aGOT	nGOT	iGOT
>3 mentions	Undefined metabolic processes	Ciliary or flagellar motility	DNA-dependent transcriptional regulation
	Transport functions	Undefined metabolic processes	Undefined metabolic processes
	Riboflavin biosynthesis	Cobalamin biosynthesis	Transport functions
	DNA-dependent transcriptional regulation	ATP-coupled proton transport	Fatty acid biosynthesis
	DNA repair	DNA-dependent transcriptional regulation	Glycolysis
	Iron-sulfur cluster assembly	Riboflavin biosynthesis	Deoxyribonucleotide biosynthesis
		Chemotaxis	(Purine) Ribonucleotide biosynthesis
			Chemotaxis
			Translation
3 mentions	Biotin biosynthesis	Fatty acid biosynthesis	Protein secretion
	Arginine biosynthesis	DNA repair	Gluconeogenesis
	Potassium ion transport	tRNA modification	DNA replication
	Phenylacetate-catabolic process	Transport functions	(Pyrimidine) Ribonucleotide biosynthesis
	Glycine decarboxylation	(Pyrimidine) Ribonucleotide biosynthesis	Ciliary or flagellar motility
	Porphyrin compound biosynthesis	DNA recombination	ATP-coupled proton transport
			Iron-sulfur cluster assembly
			Glycine decarboxylation
			Histidine-catabolic process
2 mentions	Arginine deiminase	Arginine deiminase	tRNA modification
	Transcriptional regulation	Gluconeogenesis, glycolysis	Cytokinesis
	DNA replication, topology, recombination	DNA replication	(Purine) Ribonucleoside salvage
	rRNA modification	Translation	DNA repair, recombination
		Protein secretion	Arginine deiminase pathway
	Biosynthesis of: IMP, UMP, fatty acids, ribonucleosides, deoxyribonucleotides, NAD	Biosynthesis of: arginine, UDP-glucoronate, cysteine, porphyrin compounds, tryptophan, (purine) ribonucleotides	Biosynthesis of: IMP, tryptophan, arginine, cobalamin, porphyrin compounds, lipid A, peptidoglycan, histidine, pantothenate
	Metabolism of: cysteine, ethanolamine	Metabolism of: glycine, valine, ethanolamine	Metabolism of: cysteine, ethanolamine

Tables 5.11 – 5.13 summarise other annotations collated from the ‘Artemis’ information; Table 5.11 shows annotations common to all three GOT screens, Table 5.12 shows those common to two of the screens, and Table 5.13 shows those which were only see in individual screens.

Table 5.11. 'Artemis' annotations: CDSs hit by all three GOT screens. *Asterisks denote cases where the iGOT hits were from the 'best' hits

CDSs hit by all three GOT screens		
Artemis annotations of hits from all three GOT screens	Lipoproteins	*
	Chemotaxis	*
	Regulatory proteins, transcription repressors, sigma factors, H-NS-like	*
	K+ transport proteins, glutathione-regulated K+ efflux KefB or TrkB, Kup or TrkD, homologue of human K+ channel	*
	ABC transporters (e.g. for polyamines, glutamate, proline, betaine, phosphate, D-methionine, choline, arginine, ornithine, sulphate, sugars, branched amino acids, iron, histidine, taurine, oligopeptides)	*
	Histidine binding/transport	*
	Multi-drug efflux transporters, antibiotic/polymixin/arsenite resistance or synthesis	*
	Iron scavenging, heme/porphyrin/bacterioferritin functions, ferredoxin proteins	*
	Cytochrome C precursors/signal peptides/subunits	*
	Fimbrial proteins/chaperones, TadB/TadC, type IV pilus	*
	Electron transfer flavoproteins	*
	Starvation response proteins	*
	Hypothetical proteins	*
	Prophage integrase proteins, transposases, insertion elements, recombinases	
	Arginine biosynthesis/ binding, ornithine metabolism	
	Copper transport/homeostasis, heavy metal binding	
	Biotin biosynthesis	
	Redox functions, glutaredoxin, TrxA/ TrxB, glutathione transferase	
	Mg^{2+} and cobalt efflux	
	Major Facilitator Superfamily (MFS) transporters	
	TCS signal transduction systems	
	Proline and betaine transport/ binding	
	Conjugal transfer proteins	
	Ethanolamine operon regulatory protein EutR	
	Cadmium/lead/zinc cation efflux and response	
	Polyketide synthases (PKSs), non-ribosomal peptide synthetases (NRPSs)	
	Osmotic response lipoprotein OsmE	
	Arabinose/proton symporter	
	Polyamine transport/acetyltransferase	

Table 5.12. Additional Artemis annotations: CDSs hit by two out of three GOT screens. *Asterisks denote cases where the iGOT hits were from the 'best' hits

CDSs hit by two out of three GOT screens		
Artemis annotations of hits from n & iGOT	Porin protein precursors	
	Stress response proteins	
	Outer membrane proteins/lipoproteins/precursors/receptors	*
	DNA repair	*
	RNA polymerase sigma-54	*
	Homoserine lactone (HSL) efflux protein	*
	Ribonucleotide biosynthesis	*
	Putative exported proteins	
	DNA competence	
	Dehydratase/racemase enzymes	
	Similar to *Bordetella pertussis* Vgr-6	
	Alginate biosynthesis	
	Capsule synthesis genes	
Artemis annotations of hits from a & iGOT	Similar to QseB/C TCS	
	Activator of quorum sensing auto-inducer (AI) transcription	*
	Xanthine dehydrogenase	*
	Sodium ion/ proton exchange	
	Nutrient depletion / cold-shock response proteins	*
	Secretion proteins / toxin transporter	*
	Clp-protease associated stress response	*
	Type VI secretion-related genes SciB, SciC	*
Artemis annotations of hits from a & nGOT	Chromate transport	
	Syr-P-like (syringomycin) genes	
	Rhamnolipids (rhlA, rhlB)	
	Spa/Bop/Inv/mxi type 3 secretion system (T3SS)	
	Hpa/Sct T3SS	

Table 5.13. Additional Artemis annotations: CDSs hit in only one GOT screen. *Asterisks denote cases where the iGOT hits were from the 'best' hits

CDSs hit in only one GOT screen

Artemis annotations of hits from aGOT only	Carboxypeptidase	
	KdpFABCDE system	
	NAD/NADH dehydrogenase	
	Osmolarity sensing proteins EnvZ/OmpB-like	
	Hydrogen peroxide-induced gene	
Artemis annotations of hits from nGOT only	Flagella synthesis operons	
	Manganese ion transport	
	Mannose/ cell wall synthesis	
	SurA survival protein	
	Heat shock proteins	
	Malonate transporter and decarboxylase	
	Pyoverdine synthesis, ornithine/ cobalamin	
	Similar to *E. coli* shiga toxin subunit	
	Salmonella invasion protein IagB	
Artemis annotations of hits from iGOT only	Nitrate/nitrous oxide reductase	*
	Amino acid metabolism and biosythesis	*
	Cell division proteins	*
	ABC transport of arginine/ glycine/ betaine/ L-proline	*
	Haemagglutinin / cell wall anchor protein	*
	GTPase	
	O-antigen transporter	

5.3.4. Relation to known and putative Bp virulence factors

As described in the methods section, details of known or putative Bp virulence factors were collated. Tables 5.14 – 5.16 list the known or putative virulence factors that were identified as refined hits in aGOT, nGOT and iGOT respectively.

Table 5.14. aGOT refined hit CDSs with known or putative roles in *Burkholderia* virulence

CDS number	Gene Name	Function	Role In Virulence, Other Details	References
TYPE VI SECRETION				
BPSL3096 - 111		T6SS-6	Type VI Secretion	Burtnick *et al* 2011; Schell *et al* 2007; Shalom *et al* 2007
BPSS0515 - 33		T6SS-2	Type VI Secretion	Burtnick *et al* 2011; Schell *et al* 2007; Shalom *et al* 2007
BPSS1493 - 511	*including virG, virA, hcp1/tssD, tssE, clpV1, vgrG1, tagB, tssJ, icmF1*	T6SS-1	Type VI Secretion: Actin Modelling And MNGC Formation. T6SS-1 Is Flanked By BimA and Bsa T3SS. Mutants Caused Some Actin Modelling Defects And MNGC Defects	Burtnick *et al* 2011; Schell *et al* 2007; Shalom *et al* 2007; Sun *et al* 2010; Chieng *et al* 2012
BPSS1512	*TssM*		Host Ubiquitination Interference, Immune Evasion	Tan *et al* 2010
BPSS1514 - 5	*including folE*		Up-Regulated By VirAG (TCS Within T6SS-1 Locus)	Burtnick *et al* 2011
BPSS2103 - 09		T6SS-3	Type VI Secretion	Burtnick *et al* 2011; Schell *et al* 2007; Shalom *et al* 2007
TYPE III SECRETION				
BPSL1105	*bspR*	Extended Regulation Of T3SS-3		Sun *et al* 2011
BPSS1516 - 7	*including BopC*	T3SS-3-Related	BopC Effector And Chaperone Of BopC	Muangman *et al* 2011
BPSS1520-2	*including bprC*	T3SS-3-Related	Extended T3SS-3 Regulon/Cluster	Sun *et al* 2011
BPSS1535 - 9	*including bsaU*	T3SS-3	Type III Secretion (Bsa System); BsaU Involved In Phagosomal Escape	Pilatz *et al* 2006
BPSS1607 - 30		T3SS-2	Type III Secretion Hrp-Like	
SECONDARY METABOLISM				
BPSL1779		Secondary Metabolism, Hydroxamate Siderophore Biosynthesis	Fourteen Clusters Encoding Possible Antibiotic, Surfactant, And Siderophore Biosynthesis Pathways	Holden *et al* 2004
BPSS1199		Unknown Molecule, NRPS	NRPS/PKSs	Biggins *et al* 2012

CDS number	Gene Name	Function	Role In Virulence, Other Details	References
EXOPROTEINS				
BPSL0338		Phospholipase C	Exoproteins	Holden *et al* 2004
BPSS0666		Putative Collagenase	Exoproteins	Holden *et al* 2004
QUORUM SENSING				
BPSL2347	*luxR*	Quorum Sensing		Ulrich *et al* 2004
BPSS0481 - 7	*hmqABDEFG*	Quorum Sensing - Hmaq Signalling		Diggle *et al* 2006; Vial *et al* 2008
BPSS1180	*luxI*	Quorum Sensing		Ulrich *et al* 2004
ADHESINS				
BPSL2063		Adhesin; Autotransporter	Autosecreted, Attachment	Holden *et al* 2004; Adler *et al* 2011
BPSS0908		Adhesin; Autotransporter	Autosecreted, Attachment	Holden *et al* 2004; Adler *et al* 2011
BPSL1075	*boaB*	Adhesin; Autotransporter	Autosecreted, Attachment	Balder *et al* 2010
OTHER				
BPSS1492	*BimA*	Autotransporter	Autosecreted Protein Required For Actin-Based Motility	Adler *et al* 2011; Stevens *et al* 2005b
BPSL0776	*recA*		Homologous Recombination, SOS Response	Cuccui *et al* 2007
BPSL1060		Putative Hypothetical Bacteriophage Protein		Cuccui *et al* 2007
BPSL1103	*nth*	Putative Endonuclease III	DNA Replication, Recombination, And Repair	Cuccui *et al* 2007
BPSL3168	*aroB*	Dehydroquinate Synthase	Chorismate Biosynthesis	Cuccui *et al* 2007
BPSL1505	*rpoS*	Sigma Factor	MNGC Formation, Transcriptional Regulation	
BPSL0395		Cytidylyltransferase		Pilatz *et al* 2006
BPSL1174 - 5	*kdpD, kdpE*	KdpD/KdpE TCS	Roles In Homeostasis And Virulence; Intracellular Persistence, Stress Resistance	Xue at al 2011; Alegado *et al* 2011; Hughes *et al* 2010
BPSL0349		Hypothetical Protein	Differential Regulation in Primary versus Relapsing Melioidosis	Velapatino *et al* 2012
BPSL1743 - 5	*arcA, arcB, arcC*	Arginine Deiminase, Ornithine Carbamoyltransferase, Carbamate Kinase; Anaerobic Growth, Acid-Resistance	Differential Regulation in Primary versus Relapsing Melioidosis	Velapatino *et al* 2012

CDS number	Gene Name	Function	Role In Virulence, Other Details	References
BPSS1562		Kumamolysin; Post-Translational Modification, Chaperones	Differential Regulation in Primary versus Relapsing Melioidosis	Velapatino *et al* 2012
BPSL1067			Up-Regulated In Macrophages	Chieng *et al* 2012
BPSL3354		Putative Cytochrome	Up-Regulated In Macrophages	Chieng *et al* 2012
BPSL3428		Set Domain Protein	Mutation of Homologue Attenuated Bt Virulence To Dictyostelium	Hasselbring *et al* 2011
BPSS1722		Malate Dehydrogenase	Mutation of Homologue Attenuated Bt Virulence To Dictyostelium	Hasselbring *et al* 2011
BPSL0558 -9		Toxin-Antitoxin Module	Toxin-Antitoxin Module, On GI	Butt *et al* 2012
BPSL3260 - 1		Toxin-Antitoxin Module	Toxin-Antitoxin Module, On GI	Butt *et al* 2012

Table 5.15. nGOT refined hit CDSs with known or putative roles in *Burkholderia* virulence

CDS number	Gene name	Function	Role In Virulence, Other Details	References
TYPE VI SECRETION				
BPSS0525 - 0533		T6SS-2	Type VI Secretion; BPSS0529 Up-Regulated In Macrophages	Burtnick *et al* 2011; Schell *et al* 2007; Shalom *et al* 2007; Chieng *et al* 2012
BPSS0166, BPSS0177 - 82		T6SS-4	Type VI Secretion	Burtnick *et al* 2011; Schell *et al* 2007; Shalom *et al* 2007
TYPE III SECRETION				
BPSS1525	*bopE*	T3SS-3-Related	Effector Protein. Guanine-Nucleotide Exchange For Rho-GTPases That Regulate Actin Network; Invasion Role Evident In Cell Model But Not Mammalian Infection Models	
BPSS1529	*bipD*	T3SS-3-Related	Translocator Protein; Needle Tip, Expressed *In Vivo*. Invasion of Non-Phagocytic Cells, Phagosomal Escape	
BPSS1532	*bipB*	T3SS-3-Related	MNGC Formation	
BPSS1534	*BsaZ*	T3SS-3	Structural Protein; Mutants Delayed In Phagosomal Escape	Pilatz *et al* 2006
BPSS1535 - 54	*including bsaU, bsaQ, bprP, bprQ*	T3SS-3	Type III Secretion; BsaU Involved In Phagosomal Escape. BsaQ Required For Secretion Of BopE And BipD Effectors	Pilatz *et al* 2006; Sun *et al* 2011
BPSS1603, BPSS1607, BPSS1612 - 30		T3SS-2	Type III Secretion, Hrp-Like	
SECONDARY METABOLISM				
BPSL1774 - 9		Secondary Metabolism, Malleobactin NRPS	Hydroxamate Siderophore Biosynthesis. Fourteen Clusters Encoding Possible Antibiotic, Surfactant, And Siderophore Biosynthesis Pathways	Holden *et al* 2004; Biggins *et al* 2012
BPSL2233		Unknown Molecule, NRPS	NRPS/PKSs	Biggins *et al* 2012
BPSS0160		Secondary Metabolism: Isonitrile	NRPS/PKSs	Biggins *et al* 2012
BPSS0311		Secondary Metabolism: Malleilactone, PKS	NRPS/PKSs	Biggins *et al* 2012
BPSS2329		Unknown Molecule, PKS	NRPS/PKSs	Biggins *et al* 2012
EXOPROTEINS				

CDS number	Gene name	Function	Role In Virulence, Other Details	References
BPSL2403		Phospholipase C	Exoproteins	Holden *et al* 2004
BPSS0067	*plc-3*	Phospholipase C	Exoproteins	Korbsrisate *et al* 2007; Holden *et al* 2004
BPSS1993	*mprA*	Serine Peptidase, Metalloprotease A	Exoproteins; KO Attenuates Virulence to *Dictostelium*	Hasselbring *et al* 2011; Holden *et al* 2004
QUORUM SENSING				
BPSS1569 - 70	*luxR, luxI*	Quorum Sensing		Ulrich *et al* 2004
ADHESINS				
BPSL0782	*pilA*	Type IV Pilin Subunit	Attachment	
FLAGELLIN				
BPSL3319	*fliC*	Flagellin; Flagellar Component	Invasion Of *Acanthamoebae*, Immune Stimulation	Inglis *et al* 2003; Chua *et al* 2003; DeShazer *et al* 1997
CAPSULAR POLYSACCHARIDE				
BPSL2769 - 82		CPS Cluster IV	Capsular Polysaccharide	Reckseidler-Zenteno *et al* 2005
BPSS1828 - 35	*including hepB, wabG, cheA, cap1E, BceG, Wzc, wza, wzb, rkpK, wcaJ, manC*	CPS Cluster III	Capsular Polysaccharide	Lazar-Adler *et al* 2009; Sarkar-Tyson *et al* 2007; Reckseidler-Zenteno *et al* 2005
OTHER				
BPSL0776	*recA*		Homologous Recombination, SOS Response	Cuccui *et al* 2007
BPSL1060		Putative Hypothetical Bacteriophage Protein		Cuccui *et al* 2007
BPSS0993		Superoxide Catalase	Intracellular Stress	Holden *et al* 2004
BPSS1997		Oxacillinase	Beta-Lactamase Drug Resistance	Holden *et al* 2004
BPSS1701		tRNA Pseudouridine Synthase A	Mutation of Homologue Attenuated Bt Virulence To Dictyostelium	Hasselbring *et al* 2011
BPSL0659	*surA*	FKBPs And Parvulins	FKBPs And Parvulins	Norville 2011 thesis
BPSL2254		FKBPs And Parvulins	FKBPs And Parvulins	Norville 2011 thesis
BPSL0886		Hypothetical Protein	Up-Regulated In Macrophages	Chieng *et al* 2012
BPSL1067		Hypothetical Protein	Up-Regulated In Macrophages	Chieng *et al* 2012

CDS number	Gene name	Function	Role In Virulence, Other Details	References
BPSL1771	*cbiG*	Cobalamin Biosynthesis Protein	Up-Regulated In Macrophages	Chieng *et al* 2012
BPSL2759		Putative Short-Chain Dehydrogenase	Up-Regulated In Macrophages	Chieng *et al* 2012
BPSS0142		Sugar ABC Transport System, ATP-Binding Protein	Up-Regulated In Macrophages	Chieng *et al* 2012
BPSS0143		ROK Family Transcriptional Regulator	Up-Regulated In Macrophages	Chieng *et al* 2012
BPSS1279		Threonine Dehydratase	Up-Regulated In Macrophages	Chieng *et al* 2012
BPSS1892 - 3	*catA, catC*	Catechol 1,2-Dioxygenase	Up-Regulated In Macrophages	Chieng *et al* 2012
BPSL1743 - 5	*arcA, arcB, arcC*	Arginine Deiminase, Ornithine Carbamoyltransferase, Carbamate Kinase; Anaerobic Growth, Acid-Resistance	Differential Regulation in Primary versus Relapsing Melioidosis	Velapatino *et al* 2012
BPSS1562		Kumamolysin; Post-Translational Modification, Chaperones	Differential Regulation in Primary versus Relapsing Melioidosis	Velapatino *et al* 2012
BPSS1888		Aromatic Oxygenase; Inorganic Ion Transport, Metabolism	Differential Regulation in Primary versus Relapsing Melioidosis	Velapatino *et al* 2012
BPSL0558 - 9		Toxin-Antitoxin Module	Toxin-Antitoxin Module, On GI	Butt *et al* 2012

Table 5.16. iGOT refined hit CDSs with known or putative roles in *Burkholderia* virulence

CDS number	Gene name	Function	Role In Virulence, Other Details	References
TYPE VI SECRETION				
BPSL3096 - 111		T6SS-6	Type VI Secretion	Burtnick *et al* 2011; Schell *et al* 2007; Shalom *et al* 2007
BPSS0098		T6SS-5	Single Gene Of Type VI Secretion Cluster	Burtnick *et al* 2011; Schell *et al* 2007; Shalom *et al* 2007
BPSS0177 - 85		T6SS-4	Type VI Secretion	Burtnick *et al* 2011; Schell *et al* 2007; Shalom *et al* 2007
BPSS1493		T6SS-1	Single Gene Of Type VI Secretion: T6SS-1 Is Flanked By BimA And Bsa T3SS. Mutants Caused Some Actin Modelling Defects And MNGC Defects	Burtnick *et al* 2011; Schell *et al* 2007; Shalom *et al* 2007
TYPE III SECRETION				
BPSS1385		CHBP Cyclomodulin	T3SS Effector: Similar To Cycle Inhibiting Factor (Cif) Of EPEC/EHEC. Cytopathic And Actin Reorganisation Effects. Inhibits Eukaryotic Ubiquitination Pathway	Jubelin *et al*, 2009; Yao *et al* 2009; Cui *et al* 2010; Felgner *et al* 2009
SECONDARY METABOLISM				
BPSS0130 - 2		Secondary Metabolism: Terphenyl, NRPS	NRPS/PKSs	Biggins *et al* 2012; Biggins *et al* 2011
BPSS0584 - 5		Secondary Metabolism: Pyochelin Siderophore Biosynthesis	Fourteen Clusters Encoding Possible Antibiotic, Surfactant, And Siderophore Biosynthesis Pathways	Holden *et al* 2004
EXOPROTEINS				
BPSL0808		MucD Ser Protease Homologue	Exoproteins	Holden *et al* 2004
BPSS0067	*plc-3*	Phospholipase C	Exoproteins	Korbsrisate *et al* 2007; Holden *et al* 2004
QUORUM SENSING				
BPSL2347	*luxR*	Quorum Sensing		Ulrich *et al* 2004
ADHESINS				
BPSL0782	*pilA*	Type IV Pilin Subunit	Attachment	
BPSS1434	*BpaA*	Adhesin; Autotransporter	Autosecreted, Attachment	Adler *et al* 2011; Holden *et al* 2004

CDS number	Gene name	Function	Role In Virulence, Other Details	References
OTHER				
BPSL2140	*ppsA*	Putative Phosphoenol Pyruvate Synthase	Carbohydrate Transport And Metabolism	Cuccui *et al* 2007
BPSL2519	*serC*	Phosphoserine Aminotransferase	Serine Biosynthesis	Cuccui *et al* 2007
BPSS0993		Superoxide Catalase	Intracellular Stress	Holden *et al* 2004
BPSS1383		FKBPs And Parvulins	FKBPs And Parvulins	Norville 2011 thesis
BPSL1528		Putative Exported Protein	Unknown Mechanisms But Important For Intracellular Replication And Survival	Pilatz *et al* 2006
BPSL1001	*sodC*	Superoxide Dismutase	Intracellular Stress	Vanaporn *et al* 2011; Holden *et al* 2004
BPSS1039 - 40	*irlS, irlR*	Invasion Related Locus TCS	Invasion Of Cells But Not Mammalian Virulence	
BPSL1817		Putative Lipoprotein		Chieng *et al* 2012
BPSL3354		Putative Cytochrome		Chieng *et al* 2012
BPSS0140		Sugar ABC Transport System, Lipoprotein	Up-Regulated In Macrophages	Chieng *et al* 2012
BPSS0433		Hypothetical Protein	Up-Regulated In Macrophages	Chieng *et al* 2012
BPSS1279		Threonine Dehydratase	Up-Regulated In Macrophages	Chieng *et al* 2012
BPSS1701		tRNA Pseudouridine Synthase A	Mutation of Homologue Attenuated Bt Virulence To Dictyostelium	Hasselbring *et al* 2011
BPSL1743 - 5	*arcA, arcB, arcC*	Arginine Deiminase, Ornithine Carbamoyltransferase, Carbamate Kinase; Anaerobic Growth, Acid-Resistance	Differential Regulation in Primary versus Relapsing Melioidosis	Velapatino *et al* 2012
BPSL0558 - 9		Toxin-Antitoxin Module	Toxin-Antitoxin Module, On GI	Butt *et al* 2012
BPSL2333 - 4		Toxin-Antitoxin Module	Toxin-Antitoxin Module	Butt *et al* 2012

Table 5.17 summarises the two genomic regions which are known or putative virulence loci and were common to all three invertebrate GOT screens.

Table 5.17. CDSs hit in all three GOT screens with known or putative roles in Bp virulence

CDS number	Gene name	Function	Role in virulence, other details	References
BPSL0558 - 9		Toxin-Antitoxin Module	Toxin-Antitoxin Module, on GI	Butt *et al* 2012
BPSL1743 - 5	*arcA, arcB, arcC*	Arginine Deiminase, Ornithine Carbamoyltransferase, Carbamate Kinase; Anaerobic Growth, Acid-Resistance	Differential Regulation in Primary versus Relapsing Melioidosis	Velapatino *et al* 2012

These are discussed further in the following discussion section.

Table 5.18 briefly summarises the occurrence of several key virulence determinant categories among the hits from the three screens, based on GO annotations, Artemis annotations and known or putative virulence factors.

Table 5.18. Occurrence of hits in a selection of virulence-related functional categories, by GOT type. X denotes occurrence.

	aGOT	nGOT	iGOT (all hits)
TYPE VI SECRETION	X	X	X
TYPE III SECRETION	X	X	X
SECONDARY METABOLISM	X	X	X
EXOPROTEINS	X	X	X
QUORUM SENSING	X	X	X
ADHESINS	X	X	X
FLAGELLIN		X	
CAPSULAR POLYSACCHARIDE		X	
OTHER:			
Toxin-Antitoxin Module	X	X	X
arcABC Arginine / Ornithine Metabolism Genes	X	X	X

Hits in 'mGOT'-style macrophage assay

As discussed in the introduction, Dowling *et al* (2010) screened the Bp K96423 fosmid library and a BAC library against a macrophage cell line. Results from that study were compared to the results from the three invertebrate GOT screens. Full lists of invertebrate GOT hits in common with the macrophage results from Dowling *et al*. (2010) can be found in DVD e-Appendix 5f. They are summarised in Table 5.19.

Table 5.19. Numbers and functions of CDSs which were hits in invertebrate GOT screens and a macrophage assay performed by Dowling *et al*. (2011)

Assay/s:	No. of CDS hits in common with macrophage assay (% of refined hits)	Including:
aGOT	286 (24.0%)	Type VI secretion: T6SS-6, T6SS-2 BimA (actin motility) Malate dehydrogenase (Bt homologue hit in *Dictyostelium* assay; Hasselbring *et al*. 2011) Hypothetical proteins up-regulated in macrophages Hypothetical bacteriophage protein
nGOT	267 (22.1%)	Type VI secretion: T6SS-4 Two NRPS/PKSs Phospholipase C MprA metalloprotease Sugar ABC transporter Transcriptional regulator tRNA pseudouridine synthase A Hypothetical proteins up-regulated in macrophages Hypothetical bacteriophage protein
iGOT (all hits)	224 (19.1%)	Type VI secretion: T6SS-6, T6SS-5, T6SS-4 Toxin-Antitoxin module Phospholipase C tRNA pseudouridine synthase A FKBP/parvulin
All 3 invertebrate GOT screens	20 (23.5%)	2 genomic regions: BPSL2629-30 (probable aminotransferase), BPSL3362-80 (glycine decarboxylation / gluconeogenesis / ethanolamine metabolism)

Using the refined hit data to test whether the 'hits' resemble a random sample from the Bp K96423 genome

Assuming RVA-style screening is effective, certain regions of a pathogen's genome would be considered more likely to be identified as hits, including known or putative virulence-related factors and perhaps genomic islands (GIs; which are known to often include virulence-related factors). If the Bp RVA was successful in identifying virulence-related regions it would be expected that the proportions of known virulence determinants or GIs would be enriched in the portion of RVA hits compared to in the genome overall.

Proportions of virulence determinants

Table 5.20 summarises the proportion of GOT hits that were annotated virulence-related CDSs, compared to the overall genomic proportion.

Table 5.20. Proportions of CDSs in the Bp genome or in GOT hits with known or putative roles in virulence

	Proportion of virulence-annotated CDSs in genome	Proportion of virulence-annotated CDSs in GOT hits	Significant? (Using Z-test for proportions, p = 0.05)
aGOT	418 / 5855 = 7.1%	128 / 1190 = 10.8%	No
nGOT		118 / 1209 = 9.8%	No
iGOT (all hits)		59 / 1174 = 5.0%	No

The proportion was slightly higher among the aGOT and nGOT hits compared to the genome overall and slightly lower in the iGOT hits. However, the differences were not significant.

Proportions of genomic islands

Bp K96423 has 16 GIs containing 450 CDSs (7.7% of the genome). The numbers and percentages of GOT hit CDSs which are located within GIs are shown in Table 5.21.

Table 5.21. Numbers and proportions of CDSs hit in GOT screens which are located in genomic islands (GIs)

	GI numbers:	Number of CDS hits in GIs (% of hits)
aGOT	3, 4, 7, 10, 11, 12, 14	48 / 1190 = (4.0%)
nGOT	1, 3, 4, 11, 16b	48 / 1209 = (4.0%)
iGOT (all hits)	1, 3, 4, 5, 10, 11, 12, 13, 15, 16b	97 / 1174 = (8.3%)
All 3 GOT screens	3	10 / 85 = (11.8%)

The proportion of GI-located CDSs was slightly higher among the iGOT hits and among hits common to all three screens compared to the overall genomic proportion. The proportion was slightly lower for the aGOT and nGOT hits. However, once again the differences were not significant; GIs were not represented in the GOT hits significantly higher than in the genome as a whole (Z-test for proportions, independent groups, p = 0.05).

Comparing virulence determinant and GI representation among the GOT hits versus the overall genome did not reveal significant enrichment in either. This may suggest that the GOT screens did not successfully identify virulence-relatd regions. However, it should be remembered that most annotated virulence determinants are identified relating to activity in mammalian systems; it could be the case that invertebrate-relevant factors share little overlap with those relevant to mammals.

5.3.5. Follow-up 1: Final re-resting of key positive hits

After analysing the GOT results for the presence of known or putative virulence factors, a small selection was re-tested in *M. sexta* larvae (as it was considered the easiest model to assess). The results are shown in Table 5.22.

Table 5.22. Survival of larvae injected with BPF fosmids of interest

Fosmid	**Encoding region:**	**Plus/minus auto-induction solution**	**Number surviving at 96 hours post-injection (out of 10)**	
			M. sexta	***G. mellonella***
29d10	*kdpDE* & *kdpFABC*	-	10	10
		+	10	10
32e10	*kdpDE*, no *kdpFA*	-	10	10
		+	10	9
19e10	CHBP cyclomodulin *bpss1385*	-	10	10
		+	10	10
02e09	T6SS-6	-	10	10
		+	10	10
33e06	Sugar ABC transporter	-	10	10
		+	10	10

By 96 hours post-injection one *G. mellonella* larva had died but the rest remained healthy. From the *M. sexta* larvae no insects died, with just one remaining slightly smaller.

None of the injected fosmids appeared to reproduce any virulent or immunogenic effects on the larvae, as was the case in the original re-testing of iGOT hits.

5.3.6. Follow-up 2: Preliminary fosmid RT-PCR results

It was considered that despite seeing evidence of metalloprotease expression, the fosmid library may be poor at expressing Bp proteins. RT-PCR would provide a means to test for RNA transcripts of selected genes. Figure 5.16 and Table 5.23 show the results of attempts to assess expression of virulence-related genes using RT-PCR.

Figure 5.16. RT-PCR results from BPF fosmid clones. Panel A: complete RT-PCR reactions. Panel B: equivalent reactions lacking reverse transcriptase, as a control for DNA contamination. 100bp # denotes 100 bp DNA ladder; the position of the 200 bp band is indicated. Expected product sizes were 150-247bp (see Table 89). Upwards arrow (↑ relative to text) denotes the addition of Auto-Induction solution during overnight growth.

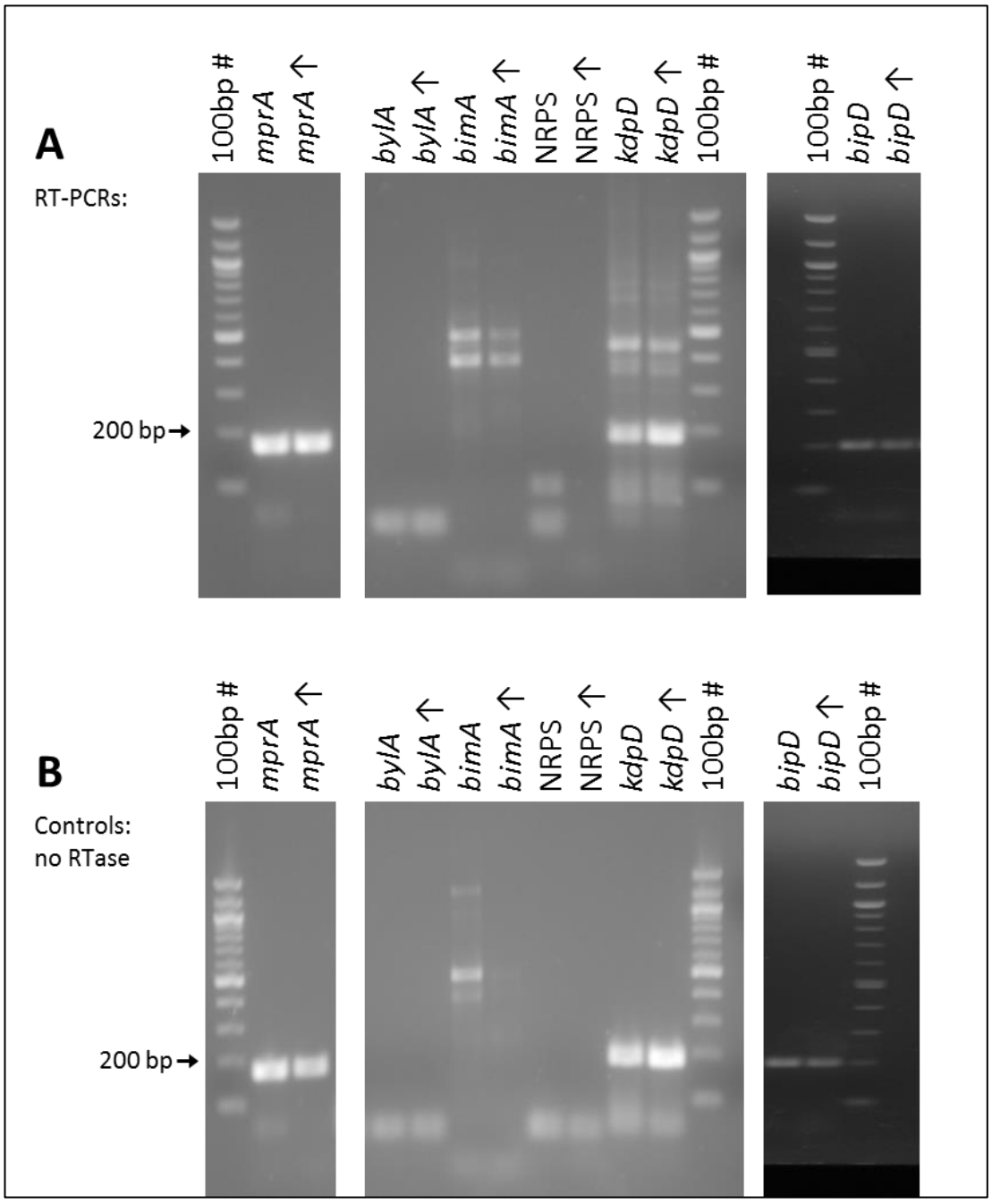

Table 5.23. Initial RT-PCR results from six BPF fosmid clones

Target	Bp CDS	Expected PCR product size (bp)	Result	Effect of Auto-Induction
mprA	*bpss1993*	173	Correct band but DNA contamination	Results identical
bylA	*bpss1269*	150	Band < 100bp due to non-specific priming or primer dimerisation	Results identical
bimA	*bpss1492*	234	Non-specific priming: unexpected bands at 400 and 500 bp	Bands slightly fainter in auto-induced sample. No DNA contamination in auto-induced sample.
NRPS	*bpsl1777*	247	Band < 100bp due to non-specific priming or primer dimerisation	Bands absent from auto-induced sample. Identical result in RTase-free control
kdpD	*bpsl1174*	188	Correct band is present but non-specific priming too. DNA contamination	Results identical
bipD	*bpss1529*	201	Correct band but DNA contamination	Results identical

It was apparent that despite having performed an on-column DNase digestion many of the RNA samples were still contaminated with DNA. The prepared RNA samples were re-digested with DNase (off-column) and re-purified as described in the methods section.

Addition of AutoInduction solution did not appear to affect band presence or increase intensity of the bands compared to non-induced samples.

A further round of reactions was performed for more RT-PCR targets, with templates which had been treated with DNase both on- and off-column. As the Autoinduction solution did not appear to affect banding patterns in Figure 5.16, the new RT-PCRs used non-induced templates only. The results are shown in Figure 5.17 and Table 5.24.

Figure 5.17. Repeat RT-PCR results from BPF fosmid clones. 100bp # denotes 100 bp DNA ladder; the position of the 200 bp band is indicated. Expected product sizes were 150-247bp (see Table 90). No cultures were treated with AutoInduction solution. Complete reactions and equivalent reactions lacking reverse transcriptase (control) are paired together.

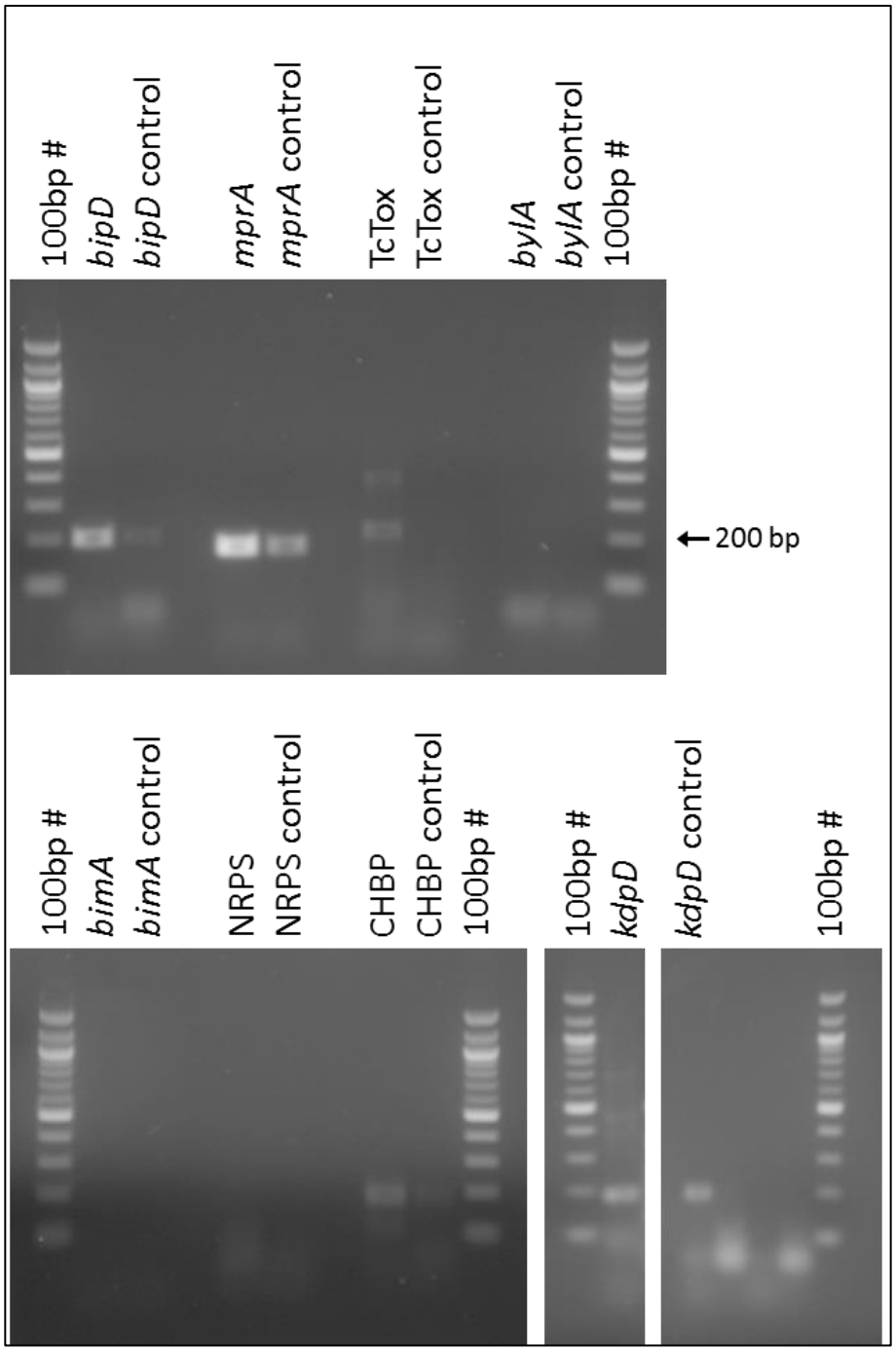

Table 5.24. RT-PCR results from eight BPF fosmid clones

Target	Bp CDS	Expected PCR product size (bp)	Result
bipD	*bpss1529*	201	Correct band present, slight DNA contamination remaining
mprA	*bpss1993*	173	Correct band present, DNA contamination remaining
TC toxin	*bpsl0590*	240	**Correct band plus one non-specific product. No DNA contamination**
bylA	*bpss1269*	150	No band present
bimA	*bpss1492*	234	No band present
NRPS	*bpsl1777*	247	No band present
CHBP	*bpss1385*	183	Correct band present, slight DNA contamination remaining
kdpD	*bpsl1174*	188	Correct band present, plus faint non-specific bands. DNA contamination

DNA contamination or lack of RT-PCR product was again a problem. For one target (the TC toxin gene) the expected band was seen and there was no evidence of DNA contamination, which suggests that the Bp K96423 gene *bpsl0590* was at least transcribed in the recombinant *E. coli* system. Howeer, further evidence would be needed to conclusively assess the success and extent of Bp gene expression in this recombinant system.

5.3.7. Follow-up 3: Investigating Bp *kdpD*

As discussed in the introduction, the *kdpD/kdpE* two-component system (TCS) was a GOT hit of particular interest and one major aim was to generate a knock-out (KO) mutant in the Bp-related CL2 organism Bt.

Included in Appendix A is the transcript of a paper published in PLoS Pathogens (Freeman *et al.* 2013) which reviews a significant body of evidence regarding a role for *kdpDE* in bacterial virulence and survival.

Attempts to delete or over-express Bt kdpD

Unfortunately, attempts to construct a KO vector all failed despite multiple attempts and modifications to the methods and primers used. Approach #1 resulted in a non-specific product in greater quantity than the desired product, and gradient PCR did not help the specificity. The strategy switched to approach #2 which was a simplified method, and a more efficient polymerase was used. The new approach used a different cloning vector, so primers needed to be re-designed. Initially PCR of the left flank was successful but later failed. DMSO concentration was optimised for the reaction but satisfactory PCR

products were not produced for the right flank. New primers (approach #2.1) for the right flank attempted to lower the annealing temperature, which was very high (the same as the extension temperature). Eventually both flanks were successfully amplified and gel-extracted and were used as template for the cross-over PCR: the desired product was very faint and an unwanted band was very strong. Pooling the reactions and gel-extracting the correct band did not yield sufficient DNA. Approach #2.2 used primers picked from a less constrained region around *kdpD,* following advice that considerably longer flanks would be needed for chromosomal deletion of *kdpD* (based on previous *kdpD* KO attempts in other species; I. Vlisidou, unpublished). This also meant that primers could be designed with lower annealing temperatures. In that attempt the right flank PCR was successful but the left flank PCR produced multiple extra products, one of which was too close in size to the expected product to allow gel extraction.

The attempt to clone *kdpDE* into an over-expression vector was promising; a correctly sized PCR product was generated and both the insert and plasmid were digested giving the correct plasmid fragments. But each time ligation and transformation was attempted the vector-only control produced a lawn of colonies, indicating that there was uncut vector still present. The colonies on the ligation mix transformation plate were therefore not reliable. The process was repeated from restriction digestions to transformation, but the same result was seen and time limitations halted further attempts.

kdpD transgenic transcription in response to host

The *kdpD* gene was also investigated in terms of its expression by Bp fosmid library clones. Figure 5.18 and Table 5.25 show the results of attempts to assess expression of *kdpD* using RT-PCR, from fosmids before injection into *M. sexta* and from *M. sexta* haemolymph 30 minutes post-injection. One fosmid encoded complete Kdp structural genes as well as KdpDE, and another fosmid lacked two structural genes.

Figure 5.18. RT-PCR results from fosmids bearing the *kdpD* gene, before and after injection into *Manduca* host. Panel A: complete RT-PCR reactions. Panel B: equivalent reactions lacking reverse transcriptase, as a control for DNA contamination. 100bp # denotes 100 bp DNA ladder; the position of the 200 bp band is indicated. Fosmid 29d10 contains the complete kdp operons (both *kdpD/kdpE* TCS and *kdpFABC* structural genes). Fosmid 32e10 lacks *kdpF* and *kdpA* but the KdpD/KdpE TCS is intact. Lanes are labelled as either 'in.' or '30'', denoting whether the template RNA was derived from inoculum or from haemolymph extracted from the larva 30 minutes post-injection.

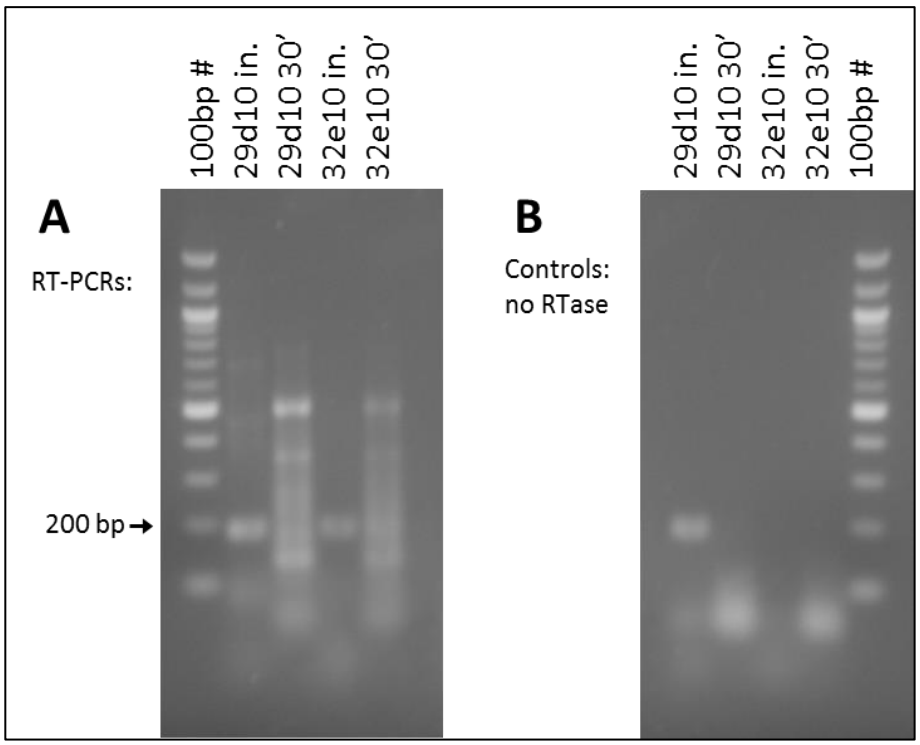

Table 5.25. RT-PCR results from Bp *kdpD*-containing BPF fosmid clones

Target	Expected PCR product size (bp)	Fosmid	Template derived from:	Result
kdpD, bpsl1174	188	29d10	Inoculum	Correct band is present, as well as faint non-specific bands. DNA contamination
			Haemolymph extract	Smear likely due to (poor purification of template?). Non-specific bands. 188 bp product not apparent. No DNA contamination?
		32e10	Inoculum	Correct band is present. No DNA contamination
			Haemolymph extract	Smear likely due to (poor purification of template?). Non-specific bands. 188 bp product is faint. No DNA contamination?

kdpD was detected in both sets of inoculum, although there was DNA contamination in the fosmid 29d10 sample. When RNA purified from haemolymph extracts was used as a template, the reactions produced a smeared assortment of non-specific bands. A band corresponding to 188 bp was faintly visible in 32e10, but overall these preliminary results were inconclusive.

5.4. Discussion

5.4.1. Initial assessments of the BPF library

The BPF library was found to have good coverage of the Bp K96423 genome. There was only a single 8 kb gap and based on the average fosmid insert size the estimated coverage was over 17-fold. However, nearly one-third of the fosmid inserts either lacked end-sequence data or the data was insufficient to find a reliable BLAST match. Based on the available end-sequences, a coverage map was plotted which revealed a highly-over-represented region towards the start of chromosome 1 (*bpsl0126 – 0209*). This was most likely an artefact caused either during library construction (e.g. that region contains an element which predisposes it to be cloned) or from incorrect BLAST assignment.

When checking for protein expression from the library the MprA metalloprotease was chosen on the basis that an obvious phenotype would be visible on skimmed milk plates. The plates did indeed clear – not to the extent of the Bt control plate, but the Bt example is a complete organism and the other shows the effects of a cloned 35kb region only. Nonetheless the metalloprotease gene must have been successfully transcribed and translated in the *E. coli* system, because the protein was secreted and effective.

The proteolysis effect was evident without the addition of auto-induction solution, but was clearly greater when the fosmid copy number had been increased. Due to an oversight, RVA testing of the BPF library had already begun in all three invertebrate screens before the effect of auto-induction solution was observed. The effect of auto-induction solution peaks at around 20 hours after addition to the culture, after which the manufacturers warn there are issues with clone stability and toxicity in the *E. coli* culture. This information, together with the fact that MprA-mediated proteolysis did occur in the single-copy fosmids and a number of positive results had already been obtained from the GOT assays, led to the decision to continue RVA without up-regulating copy number.

5.4.2. RVA screening results

A reasonable number of hit fosmids were identified in the first round of screening in each of the GOT assays. With the exception of the region which was over-represented in the library itself, plotting the hit inserts to their corresponding genomic locations did not reveal particularly obvious clusters of hits, unlike in previous RVA studies (Waterfield *et al*. 2008; F. Dorati, personal communication).

In 33 cases *M. sexta* larvae had died but unfortunately the re-testing of positive clones revealed that the lethal effect was not reproducible for any of those clones. Whereas

previous RVA studies had shown clear GOT positives, the BPF positives were not consistently reproducible during re-testing; iGOT results were consistent within a batch of replicates but had lower average scores than the original test, and aGOT or nGOT results were inconsistent within a batch of replicates (data not shown). Re-testing was completed for all the iGOT positive clones. For the aGOT and nGOT positives re-testing was not completed due to the inconsistency seen in the replicates.

According to previous experience in our laboratory, some *Photorhabdus* cosmid clones have been known to be very unstable and sequencing has revealed that internal portions have deleted out. For example, some NRPS secondary metabolite cosmids (which contain many repeat sequences) have ceased to have their originally-observed effects, perhaps due to internal deletions. It is possible that the BPF fosmids were subject to similar degradation, although fosmids are reportedly more stable than cosmids (Kim *et al*. 1992).

The uneven coverage of the library meant that many positives were located at the over-represented region. This inspired a new approach to analysing the positive hits: to assess whether there was any clustering of hits relative to the actual library coverage. The fact that the BPF hits did not have strong reproducible phenotypes cast doubt on their validity and it was hoped that this new analysis approach would identify the most likely true-positive hits. If the positives were all false and were simply a random selection from the library then the number of times a CDS was hit would correlate strongly with the number of times it was represented in the library.

5.4.3. Insights from statistical analyses of RVA hits

By transforming the fosmid coordinates to correspond to CDSs, a much more detailed assessment could be made of the library coverage (Figure 5.5). For example, the average coverage for a CDS was found to be just below ten-fold, as opposed to the 17-fold figure which was based on average insert size. Fosmid clones which did not grow and therefore were not tested were also excluded from this new coverage analysis. For each GOT screen the CDSs' coverage and observed hits did show a significant positive correlation but the coefficient values were only 0.221-0.304, indicating that coverage-level alone was not a particularly strong predictor of observed hits. Other factors at play could be random effects or could be true gain-of-toxicity effects. 'Expected' hits values were calculated by re-distributing the total number of CDS hits throughout the genome as would be expected according to the actual coverage levels. Comparing the expected and observed hits for CDSs showed another significant moderate positive correlation (maximum 0.331). If the hits had been distributed exactly as expected according to the coverage alone this would

yield a perfect correlation of 1.0; as before, other factors are influencing the correlation. The median observed-to-expected ratio values were calculated for the screens and confidence limits were calculated for the spread of data points around the median; the cut-off value was usually the median value itself. Hits with ratios below that value (up to 60.6% of cases) were eliminated as background noise and hits with ratios above the upper confidence limit were plotted on new maps. Using these observed-to-expected ratios allowed the relative 'strength' of hits to be visualised. Refined hit regions from the different GOT screens were also plotted on the same axes for comparison; as illustrated in a pie chart of hit-CDS overlap between the screens, nearly three-quarters of CDS hits were only hit in one model and just 3% of CDS hits were common to all three models.

The new maps showed that refined hit regions were still quite dispersed throughout the genome, so functional annotations were used to help investigate the results further.

Before discussing the functional roles of the GOT hits it should be noted that there is evidence both for and against their validity. Supporting evidence includes the fact that Bp gene expression was seen from the *mprA*-bearing fosmids, that some CDSs had very high observed-to-expected hit ratios, and that many known or putative virulence-related genes were among the GOT hits. Comparing the refined hit CDSs to a comprehensive list of known and putative Bp virulence factors revealed a lot of overlap. However, a considerable proportion of Bp genes (7.1%) are annotated as having some link to virulence, so to discover whether virulence-annotated CDSs were particularly highly represented in the GOT results, the proportions were compared. The proportion was actually slightly lower in iGOT hits than in the whole genome, and slightly higher in aGOT and nGOT hits, but none of the values were significantly different from the genomic proportion. According to this result the 'positive' hits could just resemble a random sample of the genome, i.e. they could be false-positives. On the other hand, the majority of virulence-related information for Bp genes so far comes from mammalian models, and only a minority of the CDSs are linked specifically to invertebrate infection. So it could be the case that the refined hits are true-positives and that the only *known* virulence factors identified were those which are relevant to multiple host taxa or where annotated evidence comes from invertebrate models: there could also be totally novel virulence factors among the other hits. A similar analysis looked at whether GI-encoded genes were enriched in the hits, as GIs often encode virulence-related factors. Bp K96243 contains 16 GIs across its two chromosomes. Due to Bp's usual environmental lifestyle it can be reasoned that its horizontally acquired GIs are likely to contain some genes involved in virulence against insects and bacteriovores. Yet statistically, proportions of CDSs located on GIs were again the same in the GOT hits as in the genome overall, indicating again that the GOT hits resemble a random sample.

Annotations

The number and diversity of functional annotations among the hit genes is considerable, so some interesting highlights and recurring themes will be discussed. The initial approach was to use GO annotations of biological processes but the vast majority of CDSs had no GO annotations, and many were simply annotated as 'biological process unknown'. The next most highly occurring annotations included: undefined metabolic processes, DNA transcription regulation, transport, riboflavin biosynthesis and ribonucleotide or deoxyribonucleotide biosynthesis. It is possible that fosmid expression of transcriptional regulators (including activators, repressors and sigma factors) could have detrimental effects on the invertebrate host if, for example, products of the regulatory targets are virulence factors or increase the rate of bacterial growth. This could occur either through regulating other Bp genes within the same fosmid or through aberrant regulatory effects on *E. coli* genes. Similarly, transport functions could facilitate the import of nutrients and cofactors away from the host or the export of virulence factors or immunogenic factors from the bacterium. Riboflavin biosynthesis is required for a wide variety of cellular processes, redox reactions and energy metabolism. There are no obvious direct links to virulence. Initially the same might be said of ribonucleotide or deoxyribonucleotide biosynthesis but pathways for purine synthesis have been explicitly linked to virulence of many pathogens including Bp (Schwager *et al*. 2012). Genes for these pathways have been demonstrated to be up-regulated during host infection by *Vibrio vulnificus* and *Listeria monocytogenes* (Kim *et al*. 2003; Klarsfeld *et al*. 1994). The *de novo* purine biosynthesis pathway is required for the Bp intracellular lifecycle such that mutants are harmless and rapidly cleared from immunocompetent mice and are still avirulent even in immunodeficient mice (Pilatz *et al*. 2006; Propst *et al*. 2010). A transposon mutant screen of Bcc against invertebrates showed that mutations in the purine and pyrimidine biosynthesis pathways are attenuating in *C. elegans*, *Drosophila melanogaster* and *G. mellonella* models (Schwager *et al*. 2012). This was not simply due to a complete inability to survive without those pathways (auxotrophy) as the bacteria could persist in low numbers inside the *G. mellonella* host. Schwager *et al* (2012) hypothesised that the host environment supplies enough nutrients for survival of the mutant but not enough for energetically expensive proliferation or virulence factor production. By extension, the *over-expression* of genes in those pathways could have given greater potential for growth (and/or virulence) of BPF clones.

To supplement the GO data, information was also taken from the annotations which accompany the published Bp K96423 genome sequence (referred to as 'Artemis' annotations, after the genome browser). Much of this information is based on similarity to orthologous genes. K^+ transport genes were hits in all screens, as were many ABC

transporters, genes for iron scavenging and the EutR regulatory protein for ethanolamine utilisation. The Kdp K^+ transport-related genes will be expanded upon later in the discussion. ABC (ATP-Binding Cassette) systems transport a diverse range of substances. In prokaryotes, ABC systems function for both import (e.g. of iron-siderophore complexes or oligopeptides) and for export (e.g. of haemolysin, polysaccharides or antibiotics) (Harland *et al*. 2007). The targets of the ABC systems hit in the GOT screens include polyamines (putrescine and spermidine), amino acids (namely L-proline, D-methionine, choline, arginine, taurine, histidine, ornithine and branched amino acids), oligopeptides, sugars, glutamate, betaine, phosphate, sulphate and iron.

Iron scavenging both aids the bacterium's survival and is detrimental to the host, as both organisms compete for a limited supply of iron. Iron is vital for many cellular enzymes and processes including DNA synthesis and electron transport (Lieu *et al*. 2001). Siderophore production genes are negatively regulated by the *fur* (ferric uptake regulator) repressor, and become de-repressed when iron is limited. Siderophores scavenge ferric iron from the proteins it is bound to, such as haemoglobin and ferritin. Genes for porphyrin compound biosynthesis and iron-sulphur cluster assembly were also hits. Iron-sulphur clusters are required for critical biochemical pathways, including respiration, photosynthesis, and nitrogen fixation (Ayala-Castro *et al*. 2008).

Regarding the EutR regulator, a study of *P. luminescens* using a promoter-trap library and a *G. mellonella* host model revealed that the ethanolamine utilisation genes were up-regulated during insect infection, which likely reflects a metabolic shift to use nutrients that are enriched in the host; ethanolamine can be derived from cell membranes (Münch *et al*. 2008; Garsin 2010). More recently it was reported that ethanolamine utilisation is involved in the proliferation of *Salmonella typhimurium* in a *C. elegans* host (Srikumar & Fuchs 2011). Utilisation of ethanolamine requires cobalamin, and indeed cobalamin synthesis genes were also hits in the nGOT and iGOT screens.

Interestingly, many annotations referred to biosynthesis, transport or metabolism of arginine and polyamines including ornithine, spermidine and spermine. For bacteria, polyamines help to maintain cell growth and viability by influencing gene expression and protecting cells from oxidative damage (Chan & Chua 2010). In Bp, spermidine regulates expression of multi-drug efflux pumps which export antibiotic compounds and quorum sensing molecules. In mammalian hosts, polyamines are used to regulate the cytokine pro- inflammatory response (Das *et al*. 2010). Therefore an interesting bacteria-host competition exists for these substances. Transporting or metabolising the polyamines could help Bp; (a) because spermidine affects quorum sensing, swimming motility and biofilm formation in strain KHW (Chan & Chua 2010), and (b) by hijacking the host

response, as spermine is used by *H. pylori* to inhibit the host pro-inflammatory cytokine response (Bussière *et al*. 2005). In terms of the fosmid expression system, polyamines normally affect translation of several *E. coli* transcription factors, so changes to polyamine levels in BPF clones (due to encoded transport or metabolic genes) could result in aberrant changes to *E. coli* gene expression (Chan & Chua 2010). Alternatively, increased polyamines may help the clones to resist oxidative stress in the hosts.

Known or putative virulence factors

There was evidence to support the proof of principle - that the RVA had successfully identified putative virulence factors of Bp K96423. As summarised in Tables 5.14 – 5.16, hits from all three screens corresponded to many known or putative virulence factors. These included secreted exoproteins (particularly phospholipase C) and genes for quorum sensing including the *luxI* and *luxR* genes and a cluster for HMAQ (4-hydroxy-3-methyl-2-alkylquinoline) signalling. Interestingly, the immunogenic factors flagellin and capsular polysaccharide (CPS) were only hit in the nematode screen. The SurA survival protein (a Bt mutant of which was tested in *M. sexta* in Chapter 3) was a hit in nGOT. SurA is a periplasmic chaperone and peptidyl-prolyl isomerase (PPIase) involved in maintaining the cell envelope. As discussed in the introduction for chapter 3 SurA is implicated in the virulence of several pathogens (Behrens-Kneip 2010), and the Bt E264 mutant is attenuated (probably due to pleiotropic effects) in cell-based assays and in *G. mellonella* (Norville 2011), as well as in *M. sexta*. Four virulence determinant types that featured heavily in hits from all the screens were T6SSs, T3SS components, adhesins and secondary metabolites.

T6SSs

T6SSs are widespread in Gram-negative bacteria and appear to have quite diverse functions which can aid environmental survival as well as virulence inside hosts (Bingle *et al*. 2008). Bp has six T6SSs and there is a large body of evidence for the role of T6SS-1 in Bp virulence. T6SS-1 is important for virulence in hamster models, intracellular growth in macrophages, and for actin motility and MNGC formation (Schell *et al*. 2007; Burtnick *et al*. 2011; Shalom *et al*. 2007). Recently the system was found to be regulated by distinct mechanisms when in macrophages as opposed to on medium; intracellular expression is depended on the VirAG two-component system (TCS) and growth on medium was dependent on the regulator BprC (Chen *et al*. 2011). The two regulators initiate transcription at different start sites within the T6SS, and both are critical for T6SS-1 function in macrophages and for full virulence in mouse models. Bp T6SS-1 has been suggested to target the innate immune system, based on the observation that its mutation is attenuating in insects (specifically cockroaches) as well as rodents (Fisher *et al*. 2012).

The full T6SS-1 system was hit in the amoeba GOT screen, and one CDS was hit in the insect screen (surrounding genes were also hit but did had below-average ratios). Each of the other five T6SSs was also hit in at least one screen, with full clusters hit for T6SS-2 (aGOT and nGOT), T6SS-4 (iGOT) and T6SS-6 (aGOT and iGOT). Chieng *et al* found that one gene of the T6SS-2 was differentially regulated inside macrophages, but so far there is little published data regarding the activity of the other Bp T6SS systems.

T3SSs

Bp has three T3SSs, and T3SS-3 in particular has been well studied. Also known as the Bsa (*Burkholderia* secretion apparatus) system, T3SS-3 is integral to the ability of Bp to invade cells and escape vacuoles, and multiple effectors have been identified (Stevens *et al*. 2002; Stevens *et al*. 2003; Muangman *et al*. 2011; Pilatz *et al*. 2006). Parts of the T3SS-3 cluster were hit in aGOT and nGOT, as was the T3SS-2 cluster. In iGOT only a single T3SS-related gene was hit: CHBP ('Cif Homologue from *B. pseudomallei*'), a cyclomodulin which is suspected to be an effector of T3SS-3 (Galyov *et al*. 2010). Cyclomodulins allow bacteria to manipulate eukaryotic host cellular processes (such as actin remodelling and ubiquitination), and transcription of this particular Bp gene was identified as up-regulated in a macrophage model (Chieng *et al*. 2012; Yao *et al*. 2009; Cui *et al*. 2010).CHBP is actually encoded some distance from the T3SS-3 cluster which explains why this gene was hit in iGOT and other T3SS-3 genes were not. Perhaps fosmid expression of CHBP interfered with the normal cell-cycle of insect host cells. Although whole T3SS operons were not recovered in the GOT screens, evidence from previous RVA work does suggest that the presence of certain effector genes alone can have a negative effect on the host, independent of the normal delivery mechanism (Waterfield lab; unpublished data)

Adhesins

Adhesins were also hits in all three screens. The *pilA* gene encodes a structural type IVA pilin subunit. It has been demonstrated to be involved in adherence to eukaryotic cells and a Bp *pilA* mutant has been shown to have reduced virulence in nematode and mouse infection models (Essex-Lopresti *et al*. 2005). Interestingly in the insect pathogen *Xenorhabdus*, a fimbrial structural subunit has also been shown to act as a pore forming toxin (Banerjee *et al*. 2006). The other four adhesins are autotransporters. Lazar Adler *et al* (2011) reviewed the current state of knowledge about the role of autotransporters in Bp and Bm virulence, as autotransporters play key virulence roles in other bacterial pathogens. So far, the information is limited but the adhesins hit in the GOT screens have been described as immunogenic or serodiagnostic, and one (BoaB) has been implicated in adhesion to epithelial cells (Lazar Adler *et al*. 2011; Balder *et al*. 2010).

NRPS/PKS secondary metabolites

Polyketide synthases (PKSs) and non-ribosomal polypeptide synthetases (NRPSs) produce a diverse range of low molecular weight organic compounds, which sometimes have roles in virulence. The *P. asymbiotica* RVA analysis identified many PKS/NRPS loci as virulence factors and similarly, seven distinct PKS/NRPS loci were highlighted in the Bp screens. Biggins *et al* (2011) recently identified several novel compounds produced by Bp NRPS/PKSs (Biggins *et al*. 2011) and found that the PKS malleilactone is a cytotoxic siderophore; the Bt homologue is involved in full virulence against *C. elegans* (Biggins *et al*. 2012). The malleilactone PKS was indeed hit in the nGOT screen, along with malleobactin NRPS and two NRPS/PKSs with unknown products. Interestingly the nematode GOT screen identified a CDS which had some homology to pyoverdine, a fluoresecent iron-binding NRPS from *Pseudomonas* spp., but this CDS was not classified as a PKS/NRPS locus in the study by Biggins *et al* (2011) and was therefore absent from the list of known and putative virulence factors. Another PKS/NRPS absent from the list of virulence factors is homologous to the *syrP* product syringomycin of *Pseudomonas syringae* (Zhang *et al*. 1997), and this operon was hit in the aGOT and nGOT screens. The remaining aGOT hits were another uncharacterised NRPS and a siderophore gene of the malleobactin cluster. In iGOT different loci again were hit: one unknown NRPS and the pyochelin siderophore. Generally, different secondary metabolites were hit in the various GOT screens, which could reflect partitioning of functions which are relevant to different host or predator encounters.

Other virulence factors which were hit in all screens were toxin-antitoxin (TA) modules (one particular module was hit in all screens) and *arcABC*, a cluster of genes for the arginine deiminase pathway. TA modules are typically a pair of genes in the same operon, coding for a toxin which induces a bacteriostatic or bactericidal effect on the bacterium itself, and a cognate antitoxin which blocks that activity. In *E. coli* TA modules have been shown to contribute to the formation of persister cells, so it has been suggested that they may contribute to the ability of Bp to persist as a chronic dormant infection. In a recent study, transgenic over-expression of Bp K96423's eight TA toxins in *E. coli* did decrease bacterial growth rate in three cases, and also in one more case when an *E. coli* homologue of the antitoxin was deleted (Butt *et al*. 2012). The two TA modules which were hit in the GOT screens (BPSL0558-9 in all screens, BPSL2333-4 in iGOT) were among those which caused no effect in the study by Butt *et al*., but they were unable to identify antitoxin homologues to delete in their *E. coli* host strain MG1655. For TA modules to be hit in the GOT screens either the toxin must be expressed more greatly than any corresponding antitoxins (allowing the clone to persist through host responses) or, perhaps more fittingly for the timescale of these screens, the antitoxin was expressed

highly enough to block the toxin (thereby removing fine control of bacterial growth and giving rapid proliferation).

The arginine deiminase pathway allows anaerobic growth using arginine as a substrate (Maghnouj *et al*. 1998). In species including the Streptococci this pathway is important for survival in acidic environments, as ammonia produced from the arginine neutralises acid (Gruening *et al*. 2006; Casiano-Colón & Marquis 1988). This could lend a survival advantage to fosmid clones encountering acid killing mechanisms in the model hosts. Additionally the arginine deiminase system can also be a major provider of ATP which enables greater bacterial growth, and in some organisms the carbamate kinase can work in the reverse reaction direction to contribute to pyrimidine synthesis (Casiano-Colón & Marquis 1988), which is relevant to Bp virulence as already discussed. An analysis of proteins from patients with primary versus relapsing melioidosis revealed that the *arcABC* genes were highly expressed in the relapse isolate, presumably enabling anaerobic growth and/or acid resistance (Velapatiño *et al*. 2012).

mGOT

As described earlier, a recent publication reported the results of a macrophage assay using this same Bp fosmid library in combination with a Bp BAC library (Dowling 2011). The results of the mGOT screen were therefore compared with our invertebrate assays. The proportion of hits in common was (slightly) greatest for aGOT (fitting the observation that amoebae and macrophages have many mechanistic similarities), and lowest for iGOT. Just 85 CDSs were hit in all three invertebrate screens and, of those, 20 were also hit in the macrophage results. They correspond to two genomic regions: two genes including a probable aminotransferase, and a cluster of eighteen CDSs including genes for glycine decarboxylation, gluconeogenesis and ethanolamine metabolism. Ethanolamine metabolism has already been discussed in terms of its links to virulence. Glycine is a precursor for ethanolamine, and glycine decarboxylation is also linked to the biosynthesis of purines and pyrimidines (Bauwe & Kolukisaoglu 2003). Aminotransferases are important for the production of amino acids, but have not been directly linked to virulence.

5.4.4. Problems with the BPF expression system

The Bp hits were spread throughout the genome rather than clustered (even when only the refined subset was plotted) and unlike previous RVAs they had only weak or non-reproducible effects in the GOT screens. The same was true for all three screens, regardless of host. Known virulence factors and GIs were not enriched in the hits compared to the genome as a whole. Although the *mprA* gene product was being

expressed, it seemed likely that there was some problem with the expression of Bp fosmid inserts.

Dowling *et al* (2010) reported anti-macrophage activity of some genomic loci but it is unclear whether these results came from the fosmids or the BAC clones they supplemented the library with. The list of positive hit CDSs reported from their assays accounts for 1474 CDSs (25.2%) of the genome, a similar number to the invertebrate GOT screens (1190, 1209, and 1174 CDSs in aGOT, nGOT and iGOT). Notably they also used crude lysates of the bacterial cells which would circumvent any problems with transportation of gene products, assuming translation and folding were successful.

Correspondence with a research group based at the Genome Institute of Singapore (GIS) revealed that they had also constructed a similar Bp fosmid library using genomic DNA collected from 39 clinical strains of Bp. They used their own custom microarrays to analyse the coverage of Bp genes within their library (based on transcripts), and discovered that unlike normal Bp transcription patterns there was extensive anti-sense transcription in the fosmid library (J. Kreisberg, unpublished data). Transcription start sites were preserved but there appeared to be 'run-on' transcription past the usual termination sites. Efficient expression in a recombinant system (or following horizontal gene transfer) requires compatibility with the host strain's machinery for transcription termination as well as initiation. Antisense RNA can cause gene silencing (Kleinjan & Van Heyningen 2003) and it is possible that this is a previously unappreciated obstacle towards the expression of foreign genetic material in constructed systems like the fosmid library. Coincidentally, the CDS which was the single most highly transcribed gene in the GIS's library was the *mprA* gene. If a similar phenomenon was occurring in our own library, it is possible that one of relatively few properly-transcribed genes was inadvertently selected when fosmid expression was assessed early on.

A small selection of fosmids was re-tested once more in *M. sexta,* and also in *G. mellonella* (as it is generally a more susceptible model). Two of the fosmids encoded the *kdpDE* genes, which were hit in aGOT and are discussed in more detail in the following section. The remaining three were iGOT hits which encoded some of the known or putative Bp virulence factors: one for immune evasion which also encoded a phospholipase; one for a complete T6SS operon; and one with a virulence-related TCS and an ABC sugar transport operon up-regulated in macrophages. The fosmids were tested with and without auto-induction solution to enhance copy number, but none of the clones showed toxic effects in either model.

Preliminary attempts were made to use RT-PCR to determine if transcription was occurring in the BPF fosmids. The targets were *mprA*, *bimA*, *bipD*, an NRPS gene, the

CHBP cyclomodulin, *bylA* and a TC toxin. *mprA* was selected because the fosmids were known to be capable of its expression. BimA and BipD are well-known Bp virulence determinants and were hits in aGOT and nGOT respectively. The NRPS gene was an nGOT hit. The CHBP cyclomodulin was an iGOT hit. BylA and the TC toxin were hits in the macrophage/crude lysate assay by Dowling *et al*. (2010); it was of interest to see if loci which were hits in that screen were expressed in our fosmid clones. Toxin Complex (TC) toxins are potent against invertebrates (Hares *et al*. 2008; Yang *et al*. 2012). *bylA* is an orthologue of the *Ps. syringae* NRPS/PKS *sylA*. Its product (syringolin A) inactivates the eukaryotic proteasome (Ramel *et al*. 2012). Due to time limitations only preliminary experiments could be performed; without optimisation most of the samples showed either DNA contamination (whereby the presence of a band does not necessarily indicate RNA transcripts) or no PCR products. Where no products were seen no conclusions can be drawn, as there were no true-positive controls in this set-up. However, in one case a band was present at the expected size and no DNA contamination was evident: the TC toxin gene *bpsl0590* does appear to be transcribed in the fosmid system. Beyond that these preliminary RT-PCR results remain inconclusive.

5.4.5. Attempts to investigate *kdpDE* in *Burkholderia*

The fact that the *kdpD* and *kdpE* genes (*bpsl1174* and *bpsl1175*) were hit in the aGOT screen was of particular interest because the *P. asymbiotica* RVA had identified that particular TCS, which regulates Kdp, a potassium ion transport ATPase (Waterfield *et al*. 2008). When the *P. asymbiotica kdp* genes were expressed in *E. coli* they were found to confer the ability to persist within *M. sexta* haemocytes (Vlisidou *et al*. 2010). In fact, although the regulation of the Kdp K^+ pump serves an important homeostasis role in low-K^+ environments, the *kdpDE* TCS is increasingly being identified as a pleiotropic virulence factor (as reviewed in Appendix A). In diverse bacterial species KdpDE uses mechanisms distinct from K^+ regulation to play a direct or indirect role in virulence. In several cases the TCS is linked to oxidative, osmotic and antimicrobial stress responses, which aid the persistence of pathogens within the host and in the intracellular environment (Alegado *et al*. 2011; Moule *et al*. 2010; O'Loughlin *et al*. 2010). In *Salmonella typhimurium* the KdpDE TCS was essential for colonisation of *C. elegans* (Alegado *et al*. 2011). In *Staphylococcus aureus kdpDE* transcription is up-regulated in response to macrophages and even responds to quorum signalling, and KdpE is able to directly bind to the promoter sequences of multiple virulence genes and up- or down-regulate their transcription (Xue *et al*. 2011; Zhao *et al*. 2010). Genes up-regulated by KdpE include colonisation factors *spa* (Staphylococcal protein A) and *cap* (for capsule synthesis). A negative regulatory effect is elicited upon local invasion enzymes and toxin genes (Xue *et al*. 2011). In

Enterohaemorrhagic *E. coli* (EHEC) H7:O157 KdpE can act as a non-cognate response regulator for the histidine kinase QseC, which responds to mammalian host adrenergic signals (Hughes *et al*. 2009). This allows EHEC to efficiently regulate gene expression in response to the host. Via KdpE, QseC can regulate not only the Kdp ATPase but also over 80 genes including the regulator *ler*. *ler* is the master regulator of the Locus of Enterocyte Effacement (LEE) genes, which are required for creating the intestinal lesions characteristic of EHEC pathogenesis.

For these reasons it was of great interest to investigate the KdpDE TCS further in *Burkholderia*. Rather than use the Bp fosmid system, attempts were made to knock-out (KO) or over-express the genes directly in Bt. It was envisaged that a KO strain and complemented KO strain would be tested for attenuation in invertebrate and cellular virulence assays. Failing a KO mutant, over-expression of the genes might be technically easier to accomplish and – although the effects would not be as clear-cut as the effects of a non-polar KO – could still offer insights into the role of KdpDE in Bt. Unfortunately despite several attempts, the KO or over-expression constructs were not successfully completed within time limitations. Difficulties in creating Kdp KOs have been experienced for other bacterial species (I. Vlisidou, personal correspondence).

RT-PCR was also used to investigate transcription of *kdpD* in response to injection into the *M. sexta* larva. The KdpD sensor kinase is thought to respond to stimuli associated with virulence (e.g. phagocytosis) and stress (e.g. oxidative and antimicrobial stress) (Voyich *et al*. 2005; Hou *et al*. 2002; Alegado *et al*. 2011; Moule *et al*. 2010; O'Loughlin *et al*. 2010). Based on the observation that *kdpD* is up-regulated in macrophages (Zhao *et al*. 2010; Hou *et al*. 2002) it would be interesting to see if the same result occurs in the insect host, when the bacteria are exposed to haemocytes. Two fosmids were used, one which bore all the genes for the ATPase structure as well as the KdpDE TCS and another which lacked some structural genes (*kdpA* which is integral and *kdpF* which is expendable). Again only preliminary results were obtained. The method had not been optimised and RT-PCR from the haemolymph extracts produced unclear smeared patterns on electrophoresis gels. One fosmid sample was DNA contaminated, but the other was not and indicated that *kdpD* was transcribed in the inoculum prior to injection. Overall the results were inconclusive and the method requires further optimisation.

5.4.6. Lessons from Bp RVA and the new statistical analysis approach

RVA is intended to be used as a rapid and preliminary way to highlight genomic regions with a putative role in virulence, so that a shortlist of interesting regions can then be more

thoroughly investigated to confirm the effects and pinpoint the exact loci responsible. This RVA of Bp encountered problems which are suspected to be due to the Bp-fosmid expression system. Bp K96423 has a GC content of 68.0% compared to 50.8% in *E. coli* K12. Expression libraries of organisms with difficult codon biases are often made in 'universal translation' strains of *E. coli* such as Rosetta but the original purpose of the BPF library was for sequencing rather than expression. A clear lesson learned from this study is the need for a more comprehensive assessment of whether a genomic library is fit for purpose before embarking on GOT screening. RT-PCR or microarray should be used to assess transcription and more importantly protein translation should be confirmed, e.g. by western blot with specific antibodies to a range of targets. Analysing different cellular fractions or supernatants would also help to reveal whether proteins were being expressed in the appropriate locations.

It is still not clear what proportion of the Bp GOT hits were true-positives. Did some have true GOT effects in the first round of screening but later failed to work due to deletions and recombination, as was observed in some *P. asymbiotica* cosmids? Did some have true effects that were subtle or inconsistent and therefore were not reproduced in the re-tests? Or were there never any toxicity effects, and variation in scores was simply due to the nature of the GOT scoring system (i.e. qualitative, somewhat subjective despite efforts to maintain consistency, and $n = 1$ in the first round)? The use of positive and negative controls, and the fact that the invertebrate models themselves have been successfully used previously, should suggest that this was not the case.

The development of a quantitative analysis for this RVA has resulted in a useful approach which can also be applied to previous or future results. The approach entails the use of a bioinformatics script to automatically calculate the coverage level of each CDS, a database to store relevant information about CDSs or GOT results, and statistics to eliminate CDSs with observed-to-expected hit ratios below a threshold. Providing the positive results are reliable, this new analysis approach allows statistically meaningful summaries to be made with relative ease. It also enables quantitative values to be used instead of qualitative results, and takes into account any discrepancies in library coverage.

When applying this analysis some caution and common sense are necessary to avoid finding significance where it may not actually exist; if the library is known to express the transgenic proteins and positive results are reproducible then there is a sound basis for accepting the findings of the analyses. Unfortunately in the case of this Bp RVA, it is not appropriate to draw firm conclusions with the evidence available so far.

5.4.7. Recently published invertebrate models for Bp virulence factor discovery

Since the Bp RVA screening was conducted, several more publications have described the use of invertebrate models to investigate *Burkholderia* virulence. Some studies served to validate the infection models, i.e. the *G. mellonella* model for Bp, Bt and Bo isolates (Wand *et al*. 2011) and the cockroach insect model for Bp which also confirmed that T6SS-1 (but not T6SS-2 – T6SS-6) was important for full virulence in both cockroach and mouse models (Fisher *et al*. 2012). The Bp / *C. elegans* host-pathogen interaction has recently been studied in some detail, as discussed in earlier chapters. Particular host genes were seen to be repressed and induced during Bp infection which gave a survival advantage to the bacterium, and it has been postulated that Bp may use a chemorepellent to ward off nematode predators, but the identity of the Bp factors responsible for these effects is not yet known (Ooi *et al*. 2012).

At the same time of the RVA screening one study reported the use of multiple infection hosts to study bacteria of the Bcc species – the *Burkholderia* cepacia complex mentioned in the main introductory chapter. Mutants of published virulence genes were screened in parallel in hosts from several different taxa to uncover the overlap between virulence mechanisms: *C. elegans* nematodes, *G. mellonella* insect larvae, the alfalfa plant, and mice or rats (Uehlinger *et al*. 2009). A few conserved mechanisms of pathogenicity were uncovered: N-Acyl homoserine lactone (AHL)-dependent QS was highly conserved as a regulatory mechanism for virulence gene expression. Siderophores and LPS were important for virulence in all the animal models. However, most mechanisms were host-specific with little correlation even between the invertebrate models, which serves as a warning that caution ought to be used when extrapolating findings from non-mammalian infection models to mammalian pathogenesis and *vice versa*, at least for Bcc species. This investigation only tested targeted mutants and did not aim to identify novel virulence factors.

A particularly relevant study used a high-throughput assay to test 1,500 Bt transposon mutants against the amoeba *Dictyostelium discoideum* (Hasselbring *et al*. 2011). First, the assay was validated by confirming that mutation of a known virulence factor (T3SS-3) decreased Bt resistance to predation by *D. discoideum*, and that published levels of virulence of Bp strains correlated with the observed plaque assay results. 13 transposon library mutants were more susceptible to predation. Two of those mutants did not show a reproducible effect, and one was an auxotroph. The remaining ten were identified by sequencing. Six mutants were studied further in quantitative assays and their survival in macrophages correlated with their resistance to amoeba predation. Those mutants bore

mutations in three hypothetical proteins, a sensor kinase, a SET domain protein and a serine peptidase. Orthologues of four of those mutated genes were disrupted in Bp strain DD503; quantitative assays confirmed that the Bp mutants were also more susceptible to predation by the amoebae. In macrophages one Bp mutant (the sensor kinase *bpsl0127*) showed reduced replication during early stages of infection. That mutant was confirmed as attenuated in a mouse model. Some of the other Bp mutants had altered abilities to lyse macrophage cells and form MNGCs. Four of the ten sequenced mutants from that study were hits in the GOT assays but two of those were not tested further by Hasselbring *et al* (2011) because they were in metabolic genes (malate dehydrogenase and a tRNA pseudouridine synthase A). The SET domain protein was hit in nGOT. SET domain proteins are eukaryotic-like and are proposed to function in host-pathogen interactions (Alvarez-Venegas *et al*. 2007). The serine peptidase mutant was actually in the *mprA* metalloprotease gene; clearing of milk agar plates showed that this gene was expressed in BPF fosmids and it was actually a hit in aGOT.

Another transposon library for *Burkholderia* virulence factor discovery was in a species of the *B. cepacia* complex (Bcc), *B. cenocepacia* H111 (Schwager *et al*. 2012). Around 5,500 transposon mutants were tested in *C. elegans* and 23 showed attenuated virulence. Those mutants were then tested in a *Drosophila melanogaster* model (six were attenuated), and positive results from that model were also tested in *G. mellonella* (five were attenuated). The five mutations that were attenuating in all the invertebrate screens were in three purine biosynthesis genes, one pyrimidine biosynthesis gene and one aromatic amino acid (shikimate) biosynthesis gene (Schwager *et al*. 2012). As already discussed the purine and pyrimidine biosynthesis pathways were refined hits in all of the GOT screens. The Bcc species are less closely related to Bp than Bt, Bm and Bo are. But like Bp they live environmental saprophytic lifestyles and are opportunistic pathogens (of the lungs of immunocompromised humans) so results from this similar invertebrate screen for virulence factors may be very informative.

5.4.8. Future directions

If work was to continue it would be a priority to confirm the expression status of the BPF library, and therefore the validity of the RVA results. Use of a Bp genome-wide microarray like that used by the GIS research group would give a comprehensive understanding of the transcription patterns in the fosmids, and might reveal similar examples of terminator read-through and anti-sense transcription. As that resource was not available, some preliminary RT-PCR analysis was used. The RT-PCR technique requires optimisation in terms of product specificity and DNA elimination from the RNA samples. Identification of a target which is reliably expressed and detected by RT-PCR would be useful as a positive

control, which is currently lacking. Proving that proteins are expressed is preferable to confirming transcription alone. It would be highly unlikely that all Bp proteins would be expressed in this type of transgenic system (for example, where successful expression is dependent on additional factors that are not included in the same fosmid insert) so a considerable range of targets might need to be assessed. Protein gels could be analysed in terms of banding patterns relative to controls, or Western blotting could be used to probe targets for which specific antibodies are available. Cellular fractions and supernatants could be probed to confirm the location of the proteins and to discover if proteins which are normally secreted in Bp were successfully secreted in the transgenic system. If not, it might be appropriate to use a combination of cellular lysates and whole cells in GOT assays.

It would be interesting to apply the statistical analysis approach to previous RVA studies to see how well the refined observed-to-expected ratios correspond to the known and newly-identified virulence factors. Regions which did not appear to have hit-clusters could still have had high hit rates relative to their coverage, and may yet be harbouring unidentified virulence determinants.

Chapter 6. General Discussion

The work described in this thesis was conducted with two main aims: (i) to evaluate and begin to characterise the *Manduca sexta* larva as a model host for Bp-group infections (Chapters 3 and 4); and (ii) to use *M. sexta* and other invertebrate hosts in parallel to screen a recombinant Bp library for the identification of putative virulence-related loci (Rapid Virulence Annotation; Chapter 5).

6.1. *Manduca sexta* as a model host for Bp-group infections

Summary

Based on a combination of infection assays by direct injection, oral toxicity / infectivity assays, and analyses of haemolymph and HCs post-injection, the *M. sexta* larva appears to be an interesting and potentially useful host for the study of Bp-group pathogens.

M. sexta does not reflect the relative virulence of different Bp-group species in humans as well as the *G. mellonella* larva does (Wand *et al*. 2011; Schell *et al*. 2008). However, there are certainly some conserved hallmarks of virulence which may be due to the same molecular mechanisms: intra-phagocyte survival and multiplication, actin remodelling, host-cell death and acute sepsis were all observed. Therefore although *M. sexta* would not be an ideal model to test the relative human-virulence of novel Bp-group strains, these aspects of the infection process could potentially be studied in this larva, e.g. by testing mutants or inhibitors of those pathways. Insect hosts remain attractive complementary models to supply data while reducing the overall amount of mammalian experimentation required. Additionally, whether mutants are similarly attenuated in both *M. sexta* and other models (e.g. mice) may tell the researcher whether the factor in question targets the innate branch of the immune system.

The fact that haemolymph and HCs can be obtained easily and in relatively large quantities from this host mean that the infection can be allowed to occur *in vivo* in the whole organism, before samples are quite rapidly extracted and analysed. The process from extraction to fixing for microscopy takes less than one hour and from extraction to ViaCount reading takes ten minutes. *G. mellonella* larvae produce considerably less haemolymph and HCs per larva, and researchers have reportedly experienced difficulty imaging their HCs due to problematic auto-fluorescence (M. Bokori-Brown; personal

correspondence); no detailed analyses of pathogenesis within the *G. mellonella* host have been published.

On another level, the virulence of the Bp-group in *M. sexta* opens up interesting questions about the natural ecology of Bp-group *Burkholderia* and invertebrates. The discovery that Bo is highly virulent to *M. sexta* is exciting. Only four Bo isolates (comprising the two strain sequence-types tested in this study) have been obtained so far. Due to their virtual lack of virulence in humans or other tested mammals they have not been a priority for melioidosis-centric research. In this study it was discovered that most of the tested Bt strains are also highly virulent in *M. sexta*. The majority of *Burkholderia* publications describe Bt as 'avirulent' or 'non-pathogenic'; some qualify these classifications as 'to mammals' (despite the fact that a high dose of Bt is lethal to hamsters), but others do not. It seems clear that the overall virulence of Bo and Bt has been unknown or understated, probably due to the focus on human melioidosis. From an entomological (or broader invertebrate zoology) point of view these are interesting and virulent pathogens. Bt is highly pathogenic for insects and nematodes, as shown by an increasing number of studies (Schell *et al*. 2008; Wand *et al*. 2011; Fisher *et al*. 2012; Pilátová & Dionne 2012; Ooi *et al*. 2012; O'Quinn *et al*. 2001; Day & Sifri 2012) and it now also appears that Bo is highly pathogenic for *M. sexta.* It will be interesting to learn what other species Bo is virulent to – likely to other invertebrates and perhaps more taxa. Pilátová & Dionne (2012) suggested that the high virulence of Bt in the fly suggests that Bt may be a natural pathogen of invertebrates. On that same basis the conclusion could be extended to Bo; the rapidity of *M. sexta* death with injected Bo and the toxicity of Bo supernatant to neonates suggest that the organism is well-equipped as a pathogen of insects, or at least to avoid predation by them via the use of paralytic agents.

The fact that Bo and Bt were toxic or infectious to *M. sexta* neonates via the oral route is important as this represents the most likely route of natural infection. In one experiment Bt killed most larvae before day 8, and the survivors were of weights comparable to controls. In subsequent experiments only a minority of larvae died, but the majority of survivors were significantly underweight. It is likely that they were not feeding, either by choice to avoid the Bt or Bo (implying they can sense it), or due to an inability (e.g. caused by a paralytic agent). Bo cell-free supernatant was as harmful to the larvae (in terms of weight gain) as complete culture, which adds to the evidence from *C. elegans* and *D. melanogaster* studies that Bp-group pathogens release a soluble toxic factor which is active against invertebrates (O'Quinn *et al*. 2001; Ooi *et al*. 2012; Lee *et al*. 2011; Day & Sifri 2012). Bt cell-free supernatant was not shown to have the same effect, although interestingly, 'cell-reduced' un-filtered supernatant was more harmful (in terms of weight gain) than complete Bt culture. These experiments will need to be repeated in a

systematic manner to reliably confirm the observations made so far. It will be important to discern whether infection or intoxication (or a combination) is the primary means of the harmful effect caused by Bo and Bt to *M. sexta* neonates. Paralysis is also observed in mammalian models of melioidosis (Brett *et al.* 2007); it would be interesting to know to what extent the paralytic effect in vertebrate and invertebrate hosts is mediated by the same factors.

Bt and Bo virulence

Although Bt and Bo are considered avirulent to humans both have been isolated more than once from human clinical infections. These were associated with traumatic injuries which allowed extensive contact between bacteria and host without the usual first-line defence barriers (e.g. intact skin for cutaneous infection or digestive enzymes for ingestion). Once inside the host, Bt and Bo infections managed to persist for several weeks in some cases (Glass, Gee, *et al*. 2006; Glass, Steigerwalt, *et al*. 2006; Nussbaum *et al*. 1980). The adaptability of *B. cepacia* complex (Bcc) species – which include saprophytes, plant symbionts, plant pathogens and opportunistic human pathogens – is such that no Bcc species are permitted for use in biotechnological applications (Vial *et al*. 2011). Bp-group species have a similar propensity to reorganise their DNA (Holden *et al*. 2004; Sim *et al*. 2010). Considering the close genetic relatedness of Bt and Bo to human-pathogenic Bp and Bm it is not surprising that occasional human infections with Bt and Bo have been reported. The Bo strains were isolated in the 1970s and no incidences of Bo clinical infection have been reported since then (McCormick *et al*. 1977; Nussbaum *et al*. 1980), although it is possible that asymptomatic or undiagnosed human infections have occurred. It would be interesting to learn if more natural and/or clinical Bo isolates can be identified, and to assess their prevalence, diversity and virulence.

The *M. sexta* findings agreed with results from mammalian models in one respect which those from *G. mellonella* did not: Bt CDC 272 exhibited low virulence in *M. sexta*. This strain has low or no virulence in mammals, but Wand *et al* reported that it was virulent to *G. mellonella* (Wand *et al*. 2011). Taken together with the fact that Bo is highly pathogenic to *M. sexta* but dramatically less so in *G. mellonella* (and that the reverse is true for Bp), this discrepancy between the two lepidopteran insects is intriguing and warrants in-depth investigation. There may be a fundamental difference in the immune response of the two hosts, or perhaps the hosts carry different cues (e.g. hormones or cellular markers) to which the bacteria respond. Elucidating the causes of this difference would be informative for the understanding of *Burkholderia* pathogenicity and for the wider field of bacteria-insect interactions in general.

***Burkholderia* variability within experiments**

One general observation from the experiments described in Chapters 3 and 4 was that the outcome of infections was variable, even when using the same strain in the same conditions, or even within the same experiment. For example, *M. sexta* injected with Bp K96423 did not all die, and those that survived appeared to be in good general health. The presence of melanocytic spots on some larvae showed that they had exhibited an immune response. Therefore the Bp infection was either lethal or was apparently cleared, presumably determined by the particular host-pathogen relationship in each case. In one set of experiments Bt CDC 272 did not kill any larvae, yet in a repeat experiment it did kill all larvae, albeit at a slow rate. In the first feeding experiment Bt E264 killed 70% of neonates and the survivors were a normal weight, whereas in subsequent experiments it killed less than 22% of larvae yet the survivors were significantly reduced in weight. *Burkholderia* exhibit a high degree of variability, as discussed in the main introduction, including within-strain variability. Bm and Bp have been reported to change genetically within the course of a single infection (Price *et al*. 2010; Hayden *et al*. 2012). There is evidence to suggest that phase variation is one mechanism contributing to within-species differences (Vial *et al*. 2010; Song *et al*. 2009; Arnold *et al*. 2007), and toxin-antitoxin (TA) systems appear to allow the formation of dormant 'persister' phenotypes (Butt *et al.* 2012). It is plausible that differing proportions of variant sub-populations could lead to the variable outcomes of infection observed in this study. Further work could repeat infections and feeding assays a sufficient number of times in order to characterise the range of 'typical' results with each strain. Numerous other Bp and Bt strains exist which could also be investigated.

Further directions

One key experiment would be to systematically repeat the *M. sexta* Bt and Bo feeding assay using whole culture, washed cells, cell-free supernatant and the heat-treated equivalent of each of those. In addition to feeding, each component should also be injected into fifth-instar larvae; aside from the Bp K96423 infection, no injection assays used heat-killed cells as a control and it would be interesting to discover more about the immunogenicity (or heat-labile toxicity) versus the infectivity of the strains. To obtain supernatant in this study the cultures were centrifuged. It is possible that the toxic factor in the Bo supernatant may have originally been cell-attached rather than secreted into the medium, and that centrifugation was at a great enough speed to shear the factor from the cells. To investigate this it would be useful to test and optimise the centrifugation speed.

Another key priority would be to determine to what extent temperature affects the outcome of invertebrate-*Burkholderia* interactions, particularly with reference to the differences in

relative virulence of Bp-group strains in *M. sexta* (maintained at 25 °C) and *G. mellonella* (maintained at 37 °C). For comparison with the results of the *D. melanogaster* Bt infections, 18 °C could also be tested. *M. sexta* larvae could be injected and maintained at 18 °C and 25 °C, and also at 37 °C if a suitably large cohort of un-injected and saline-injected controls was included to account for the reduced overall health of *M. sexta* at that temperature. *G. mellonella* larvae could also be injected and maintained at all three temperatures. Median times to death could be calculated as before; it would also be interesting to calculate bacterial load or 50% lethal doses at a particular end-point.

6.2. Rapid Virulence Annotation of Bp K96423

Summary

As discussed in Chapter 5, Rapid Virulence Annotation (RVA) – a genome-wide screen for virulence-related genes using three invertebrate hosts – produced less clear-cut results for Bp than it had done for *Photorhabdus* species (Waterfield *et al*. 2008). There was less obvious 'clustering' of hit fosmids around genomic loci. This could be related to the Bp pathogen itself, as its large and flexible genome encodes numerous and variable virulence factors, most likely with considerable redundancy (Wiersinga *et al*. 2012; Holden *et al*. 2004). However, there was also a problem with a lack of reproducibility from hit fosmids. Both the lack of 'clustering' and the perceived loss of biological activity could relate to the fosmid-based expression system. A multiple-strain Bp library constructed by another research group, using the same fosmid expression system, was discovered by them to yield low transcription with erratic read-through beyond stop codons, producing extensive anti-sense transcripts (J. Kreisberg, personal communication). From the Bp K96423 fosmid library used in this study, metalloprotease activity from fosmid clones was an early indication of successful expression from the system. Unfortunately no further characterisation of fosmid expression was undertaken prior to completion of RVA screening, and later attempts to analyse gene transcription by RT-PCR were halted by time limitations.

It remains unclear to what extent Bp genes were expressed in the fosmid system, and what proportion of hits were due to real effects in the RVA screens. The metalloprotease gene was indeed hit in the amoeba bioassay. The most compelling support for the validity of the original hits is that iGOT hits that were classed as 'best' or 'higher' (based on qualitative assessment of larva health) actually did also have higher observed-to-expected ratios than 'lower' hits. The median ratio for all iGOT hits was 2 (i.e. they were hit two-times the calculated expected rate) but the median ratio for best hits was 10. This means that the genomic regions which were associated with the strongest iGOT effects in the first

round of screening really were hit considerably more often than expected. It should be noted that the scoring of any fosmid as a hit was independent of other fosmids' scores – the contents of each fosmid was not known at the time of screening and fosmids were arrayed randomly in 96-well plates, not in any meaningful order. In re-testing however, the effects were not reproduced. It is unknown whether this loss of biological activity was due to fosmid instability, recombination within the Bp insert DNA, variation in levels of normal or antisense transcription, or another factor.

The newly devised statistical approach allowed the identification of the most likely true-positive RVA hits. Hits with an observed-to-expected hit ratio below the median ratio value (for hits) were removed from the dataset. For future work this threshold could easily be adjusted, to find the top 5% of ratios for example. Whether any of the hit genes are true virulence determinants would need verification, as would be the case with any RVA results regardless of problems with expression and reproducibility. The refined subset of hits from the RVA bioassays included known Bp virulence factors such as T3SS, T6SS, iron scavenging molecules, and secondary metabolites. It also included unexpected factors such as genes annotated for potassium ion (K^+) transport.

The fact that the Kdp operons were identified in aGOT screening was of particular interest because KdpD/KdpE was previously a bioassay hit for *Photorhabdus asymbiotica*, for which it has been shown to play an important role in intracellular survival (Vlisidou *et al*. 2010). The Kdp operons encode a K^+-ATPase (KdpFABC) and a two-component regulatory system (KdpD/KdpE) respectively. Although it has widely been known for its role in K^+ homeostasis, the KdpD/KdpE two-component system (TCS) has increasingly been linked to the virulence and survival of bacterial pathogens. This topic is extensively reviewed in Appendix A: 'The KdpD/KdpE Two-Component System: Integrating K+ Homeostasis and Virulence'. Considerable efforts were made to construct a Bt KdpD/KdpE mutant, or to over-express the TCS, in order to investigate its role in Bp-group virulence. Unfortunately no cloning constructs were completed within the available time. This remains an area of great interest which warrants further investigation.

Further directions

A recombinant expression system was useful for the study of Bp genes because of the containment requirements for Bp. Having discovered that Bt and Bo are highly virulent in *M. sexta* it would be interesting and feasible to perform a genome-wide screen with one or both of those species. The fact that they can be handled at CL2 means that a random transposon mutant library or transposon directed insertion-site sequencing (TraDIS) could be used instead of a fosmid expression system (Langridge *et al*. 2009). The analysis would then look for loss-of-function (longer larval survival compared to the wild-type

strain) as opposed to gain-of-function. Redundant factors could therefore be missed, but potential problems with transgenic expression would be avoided. Similarly, sequence-tagged mutagenesis (STM) could be used to identify genes required for survival inside the *M. sexta* host by bleeding the haemolymph and assessing which tags are absent (and therefore which genes are essential) (Saenz & Dehio 2005). Mutants of interest could be GFP-labelled and analysed by fluorescent confocal microscopy to compare their infection progression in *M. sexta* compared to non-mutant strains.

An important lesson from this RVA study was the need to thoroughly test that expression libraries are fit for purpose before embarking on similar approaches. One positive outcome is that the statistical method devised to analyse these results could easily be applied to past or future RVA data. By quantifying the true best hits accounting for variations in actual genome coverage, some different results may become apparent.

Appendix A

The KdpD/KdpE Two-Component System: Integrating K^+ Homeostasis and Virulence

Zoë N. Freeman[1], Steve Dorus[2], and Nicholas R. Waterfield[1]*

*Corresponding author. Tel.: +44(0)1225 384292. Email: N.R.Waterfield@bath.ac.uk

[1] *Department of Biology and Biochemistry, University of Bath, Claverton Down, Bath, BA2 7AY, United Kingdom.* [2] *Department of Biology, Syracuse University, 107 College Place Syracuse, NY 13244, USA.*

PLoS Pathogens 9(3): e1003201. doi:10.1371/journal.ppat.1003201

The two-component system (TCS) KdpD/KdpE, extensively studied for its regulatory role in potassium (K^+) transport, has more recently been identified as an adaptive regulator involved in the virulence and intracellular survival of pathogenic bacteria, including *Staphylococcus aureus,* entero-haemorrhagic *Escherichia coli*, *Salmonella typhimurium*, *Yersinia pestis*, *Francisella* species, *Photorhabdus asymbiotica* and mycobacteria. Key homeostasis requirements monitored by KdpD/KdpE and other TCSs such as PhoP/PhoQ are critical to survival in the stressful conditions encountered by pathogens during host interactions. It follows these TCSs may therefore acquire adaptive roles in response to selective pressures associated with adopting a pathogenic lifestyle. Given the central role of K^+ in virulence, we propose that KdpD/KdpE, as a regulator of a high-affinity K^+ pump, has evolved virulence-related regulatory functions. In support of this hypothesis, we review the role of KdpD/KdpE in bacterial infection, and summarize evidence that: i) KdpD/KdpE production is correlated with enhanced virulence and survival, ii) KdpE regulates a range of virulence loci through direct promoter binding, and iii) KdpD/KdpE regulation responds to virulence-related conditions including phagocytosis, exposure to microbicides, quorum sensing signals and host hormones. Furthermore, antimicrobial stress, osmotic stress and oxidative stress are associated with KdpD/KdpE activity, and the system's accessory components (which allow TCS fine-tuning or crosstalk) provide links to stress response pathways. KdpD/KdpE therefore appears to be an important adaptive TCS employed during host infection, promoting bacterial virulence and survival through mechanisms both related to and distinct from its conserved role in K^+ regulation.

Introduction

Two-component systems (TCSs) are widespread regulatory systems which enable microbes to control their cellular functions and respond appropriately to a diverse range of stimuli such as pH, osmolarity, quorum signals or nutrient availability. The two components are a histidine kinase (HK) which senses an environmental signal and a response regulator (RR) which mediates a cellular response, typically by altering expression of target genes. The genes *kdpD* and *kdpE* together encode the KdpD/KdpE TCS, which is well-studied for its regulation of the Kdp-ATPase potassium ion (K^+) pump operon *kdpFABC*. Although best studied in *Escherichia coli*, highly homologous genes are found in most other bacteria, and are assumed to function similarly in K^+ homeostasis. However, the signalling networks regulating basic bacterial physiology and bacterial virulence are sometimes intricately linked [1], and TCSs are no exception. A classic example of a TCS with pleiotropic roles in homeostasis and virulence is PhoP/PhoQ, whose regulon both mediates responses to Mg^{2+}-limited environments and governs virulence and intra-macrophage survival in a range of Gram negative species [2,3]. More recently, the GraS/GraR TCS of *Staphylococcus aureus* has also been shown to possess functional diversity – it was best known for controlling resistance to antimicrobial peptides but further investigation has revealed links to quorum sensing, stress response, cell wall metabolism, and regulation of haemolytic and fibrinogen-binding proteins [4]. Here, we review evidence from diverse and clinically-relevant bacterial species, indicating that the KdpD/KdpE TCS responds to pathogenesis-related signals, directly regulates virulence genes, and mediates stress resistance.

KdpD/KdpE and the regulation of K^+ homeostasis during pathogenesis

Regulation of K^+ homeostasis by KdpD/KdpE

K^+ uptake in bacteria occurs via different combinations of non-specific channels and specialised transport systems [5]. Constitutively-expressed systems, such as Trk, satisfy general K^+ requirements, but the Kdp-ATPase is a specialised, inducible higher-affinity K^+ pump [6]. The Kdp-ATPase itself is encoded by the structural operon *kdpFABC.* The Kdp-ATPase is widespread throughout the prokaryotes and the KdpD/KdpE TCS is found in over 1,082 bacterial and archaeal species [7]. Expression of the operon is triggered by three stimuli perceived and integrated by the HK KdpD: K^+ concentration, osmolarity, and ATP concentration [8]. Turgor pressure has also been suggested as a stimulus for KdpD/KdpE activation, although this has been a subject of debate [8]. Mutation analysis suggests that an activating stimulus causes the inhibition of the phospho-KdpE-specific

phosphatase activity of KdpD, leading to an accumulation of phospho-KdpE. This in turn binds to an operator sequence in the promoter DNA to activate transcription of *kdpFABC* [9]. Its regulation by a TCS makes Kdp the only known bacterial K^+ transport system whose expression is strongly controlled at the level of transcription [5].

Regulation of K^+ homeostasis during pathogenesis

K^+ is the single most abundant ion in the intracellular environment and its regulation is crucial for maintenance of cell turgor and for diverse processes contributing to normal homeostasis [5]. Many studies have shown that K^+ regulation is critical for bacterial virulence [10-13]. Similarly, it is an intricate aspect of host response to pathogens; in neutrophils the active transport of K^+ across the phagosomal membrane releases antimicrobial peptides, activating proteases and enabling Reactive Oxygen Species (ROS)-mediated killing of engulfed bacteria [14]. Thus, K^+ sequestration from a common limited supply may be critical to the competition between the bacterium and host. Considering the importance of K^+ regulation in virulence, it may not be surprising that genes involved in K^+ regulation and transport are critical to the survival of pathogenic bacteria. Transcriptomic evidence reveals that transcription of the *kdpD* gene is repressed at least 3-fold and in some cases up to 20-fold in *Staphylococcus aureus* in response to phagocytosis by human neutrophils (after 3 hours interaction) [15], and up-regulated in *Mycobacterium avium* during early growth in human macrophages (at 48 hours after infection) [16].

Role of KdpD/KdpE for virulence and pathogen survival

KdpD/KdpE aids bacterial survival by increasing K^+ uptake

Although the precise mechanisms of action are yet to be determined, infection models suggest that KdpD/KdpE increases the ability of some bacteria to cause disease or to survive within a host cell or animal (Table 1). For example, increased transcription of *kdpD/kdpE* was concurrent with increased survival of *S. aureus* in macrophages and deletion of the TCS resulted in attenuated survival [17,18]. In human neutrophils a *Y. pestis kdpD/kdpE* mutant was more readily killed compared to the wild-type strain [3]. A study which aimed to identify genes involved in persistent infection of the *Caenorhabditis elegans* intestine highlighted the impact of *Salmonella typhimurium kdpD* [19]. Further characterisation revealed that *kdpD* was in fact required for *S. typhimurium* infection of the nematode and also for survival in macrophage cell lines. In the nematode feeding assays, worms which had grazed on the *kdpD* mutant strain lived significantly longer than those fed on the wild-type bacteria, and in macrophages intracellular growth and cytotoxicity were reduced [19]. These observations from intracellular models are generally consistent

with the importance of K^+ scavenging in K^+ limited environments, as would be found in a phagosomal vacuole.

Table 1. Evidence supporting the role of KdpD/KdpE in bacterial virulence and survival in cell or animal models

Bacterium	Model	Link to virulence / survival	References
Staphylococcus aureus	Human blood	Knock-out (KO) decreases survival	Xue *et al.,* 2011 [17]
	Human blood	Increased transcription of *kdpD/kdpE* is concurrent with increased survival in blood. KO is attenuated	Zhao *et al.,* 2010 [18]
	Macrophage	KO decreases survival	Xue *et al.,* 2011 [17]
	Macrophage	Increased transcription of *kdpD/kdpE* is concurrent with increased survival in blood. KO is attenuated	Zhao *et al.,* 2010 [18]
	Neutrophil	*kdpD* is differentially transcribed during phagocytosis	Voyich *et al.,* 2005 [15]
Salmonella typhimurium	Nematode	KpdD/KdpE is required for colonisation of the worm. KO is attenuated	Alegado *et al.,* 2011 [19]
	Macrophage	KO decreases survival	Alegado *et al.,* 2011 [19]
Mycobacterium tuberculosis	Mouse	KO increases virulence	Parish *et al.,* 2003 [20]
Mycobacterium avium	Macrophage	*kdpD* is differentially transcribed during phagocytosis	Hou *et al.,* 2002 [16]
Yersinia pestis	Neutrophil	KO decreases survival	O'Loughlin *et al.,* 2010 [3]
Photorhabdus asymbiotica	Insect phagocyte	Transgenic expression of *P. asymbiotica* KdpD/KdpE in *Escherichia coli* increases intracellular survival	Vlisidou *et al.,* 2010 [21]
Francisella novicida	Fruit fly	Mutation of *kdpD*, *kdpE*, *kdpA*, or *kdpC* is attenuating in a competitive index assay	Moule *et al.,* 2010 [22]
Francisella tularensis	Mouse	Mutation of KdpD is attenuating for growth and survival	Weiss *et al.,* 2007 [23]
Enterohaemorrhagic *Escherichia coli* (EHEC)	HeLa cells	Deletion of *kdpE* resulted in slightly fewer lesion 'pedestals' in infected cells. Double deletion of *kdpE* and *cra* prevented pedestal formation	Njoroge *et al.,* 2012 [24]

Other KdpD/KdpE mechanisms influence bacterial virulence and survival

There are, however, several observations that don't fully fit with the K^+ requirement models. Evidence from *S. aureus* suggests that K^+ availability has little to do with KdpD/KdpE activity. Despite the fact that human blood is K^+ rich, *S. aureus kdpD/kdpE* is still up-regulated and its deletion results in attenuated survival in that environment [18]. Additionally, *S. aureus kdpD/kdpE* transcription is altered not just during phagocytosis (when it is repressed); it is enhanced during biofilm formation and in response to microbicidal neutrophil extracts [25,26], situations in which K^+ is not necessarily limited. Although, it is important to remember that it is the KdpD/KdpE phosphorylation status that is ultimately important for activity rather than the transcription level of the genes themselves. Lastly, it has been suggested that the *S. aureus* Kdp-ATPase does not even function as a predominant K^+ transporter [17]. It should be noted however that this suggestion was based on results from the deletion of only one KdpD/KdpE system when in fact some *S. aureus* strains possess two systems, with one located on the Type II SCCmec mobile genetic element [27]. Therefore, clarification of whether the strain used by Xue *et al* (NCTC 8325) carries one or more functional Kdp operons would be pertinent.

KdpE is a regulator of diverse virulence loci

As well as a regulator of the Kdp-ATPase, recent evidence supports the role of KdpE as a direct regulator of *S. aureus* virulence factors [17,18]. KdpE has been shown to bind directly to the DNA promoters of a range of virulence genes and it has been demonstrated that deletion of *kdpD/kdpE* altered the level of transcription of over 100 genes, including: (i) the surface protein gene *spa* (Staphylococcal protein A), (ii) the capsule synthesis gene *cap*, (iii) the alpha-toxin gene *hla,* (iv) the metalloproteinase aureolysin (*aur*), (v) the lipase gene *geh,* and (vi) the gamma-haemolysin gene *hlgB* [18]. Figure 1(B) depicts virulence-related regulatory targets of KdpD/KdpE in *S. aureus*. A positive regulatory effect was elicited upon the colonisation genes (*spa* and *cap*), and a negative regulatory effect was elicited upon the local invasion enzymes and toxin genes (*hla*, *aur*, *geh* and *hlgB*) [17]. *S. aureus kdpD* is most highly transcribed at low external K^+. This means that colonisation is enabled in response to low K^+ (in the external environment, for example), and once in higher K^+ conditions (in blood or cytoplasm) local pathogenesis is enabled. The *spa* gene has previously been shown to enhance virulence in mouse and macrophage models due to its anti-phagocytic role [28].

Activation of virulence genes via KdpE has also been reported for Enterohaemorrhagic *E. coli* (EHEC) strain O157:H7 [29]. The adrenergic receptor QseC enables EHEC to sense host adrenaline and noradrenaline, as well as sensing bacterial signalling molecules (Figure 1(C)). This means EHEC can exploit host signals to regulate its metabolic, virulence and stress response genes via a complex signalling cascade. In addition to its

cognate RR the QseC HK activates two additional RRs, one of which is KdpE [29]. In an *in vitro* system employing liposomes and purified proteins over 80 QseC-regulated genes were found to be activated via KdpE. Amongst its targets were the type 3 secretion system (T3SS) and its effectors (via regulation of *ler*), which are necessary genes for 'attachment and effacement' lesions of the intestinal epithelia (see Figure 1) [29]. These results show that KdpE has at least the potential to regulate critical virulence genes during infection. Further *in vitro* research has shown that KdpE directly interacts with a second transcription factor, the catabolite repressor/activator protein Cra, to regulate *ler* in a glucose-dependent manner [24]. Visualisation of infected HeLa cells revealed that deletion of *kdpE* resulted in slightly fewer lesion pedestals than wild-type, though the effect was more pronounced for the equivalent *cra* mutation. Importantly however, in a double mutant full complementation was achieved only when both proteins were expressed, indicating that both transcription factors are co-involved in regulating that aspect of EHEC virulence. Additional *in vivo* studies using a non-complemented *kdpE* knock-out strain and whole organism infection models would further help to dissect to what extent KdpE plays a direct role in EHEC virulence.

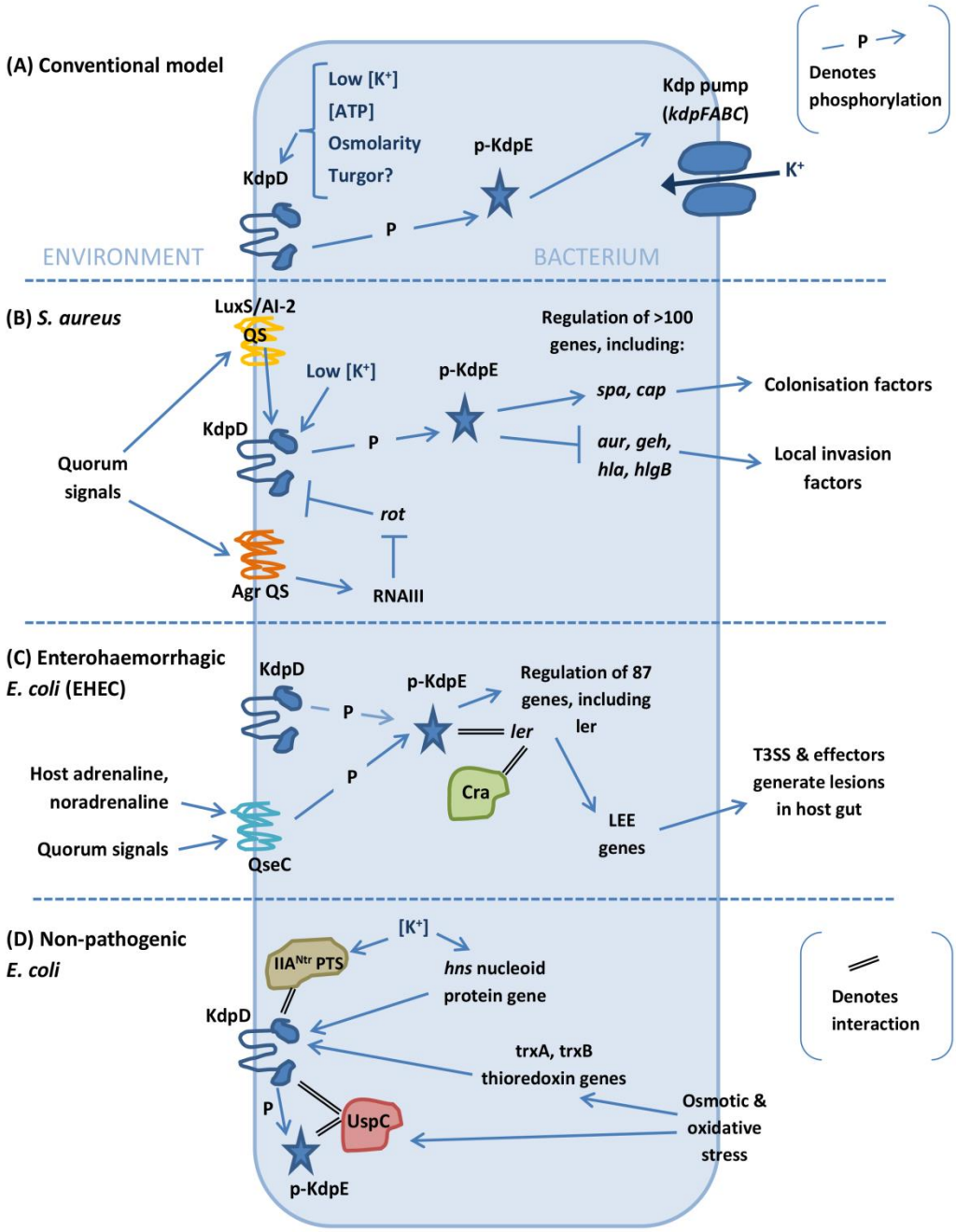

Figure 1. Schematic diagram of the varied inputs, accessory proteins, and regulatory effects of KdpD/KdpE. (A) The conventional model is that KdpD/KdpE stimulates transcription of the Kdp-ATPase in response to cytoplasmic ionic and ATP concentrations and possibly also turgor pressure [9]. (B) In *S. aureus* KdpD is affected directly or indirectly by QS systems, and KdpE regulates many downstream genes including virulence factors by directly binding to their promoters [17,18]. (C) In EHEC, KdpE can also be activated by the QseC histidine kinase which senses host adrenergic signals as well as bacterial quorum sensing (QS) signals [29]. *In vitro* its regulatory targets include the *ler* gene which controls the 'locus of enterocyte effacement' (LEE) genes. Under gluconeogenic conditions KdpE interacts with Cra to optimally regulate *ler;* both proteins bind to the promoter, perhaps through bending of the DNA [24]. The downstream regulatory cascade is integral to lesion formation in the host gut [24,29]. (D) Recently identified accessory components in non-pathogenic *E. coli* link the pathway to additional input stimuli or modulate KdpD activity [30-32].

Signal integration via the sensor kinase KdpD and the relevance for host infection

Rather than representing two distinct concepts, bacterial virulence and survival may be considered “two sides of the same coin”. Genes which promote the survival of a pathogen in its host – whether via stress response or by direct regulation of virulence genes – may be classed as virulence factors. While EHEC and *S. aureus* provide examples for the direct regulation of virulence genes by KdpE, there remains a more general implication of the importance of KdpD/KdpE in virulence mediated by stress resistance.

Stress sensing and resistance

There is a significant body of evidence supporting a link between KdpD/KdpE and the bacterial stress response, which in itself has clear relevance to survival within a host. With K^+ concentration being an activating stimulus for Kdp-ATPase expression, it is understandable that osmotic stress (salt shock) can be linked to activity of KdpD/KdpE. However, studies in several bacteria also link *kdpD/kdpE* to resistance to oxidative and antimicrobial stresses specifically. Importantly, these bacteria are all either obligate or facultative intracellular pathogens. All have been reported in some instance to be able to resist host killing [33-35] and the majority are known to spend at least part of their lifecycle in the harsh phagosomal compartment – an acidic environment containing a barrage of hydrolytic enzymes, microbicidal agents, and reactive oxygen species (ROS) including hydrogen peroxide (H_2O_2). If KdpD/KdpE does mediate the sensing of such stresses encountered in the host then the effect of knocking-out them out in those infection models would be explained. Table 2 summarises the experimental evidence where KdpD/KdpE has been implicated in stress resistance.

Table 2. Evidence that KdpD/KdpE plays a role in resisting stresses

Bacterium	Link to stress resistance	References
Salmonella typhimurium	*kdpD* KO increases sensitivity to antimicrobial stress (polymyxin B), osmotic stress (NaCl), and oxidative stress (H_2O_2). The KO mutant elicits a three-fold greater host response (production of nitric oxide) from macrophages	Alegado *et al.,* 2011 [19]
Francisella novicida	Transposon insertion mutants in *kdpD* and *kdpE*, as well as *kdpA* and *kdpC*, are more sensitive than the wild-type strain to oxidative stress (H_2O_2 and paraquat)	Moule *et al.,* 2010 [22]
Yersinia pestis	KdpD/KdpE KO results in hypersensitivity to crude neutrophil granule extracts and to five individual neutrophil microbicides. Amongst a panel of deletion mutants the effect on antimicrobial peptide resistance is second only to that of PhoP/PhoQ	O'Loughlin *et al.,* 2010 [3]
Photorhabdus asymbiotica	*P. asymbiotica* KdpD/KdpE enables *E. coli* to persist in phagocytes whereas the native KdpDE does not; the greatest amino acid divergence is in KdpD's Universal Stress Protein (Usp) domain, thought to be involved in stress sensing	Vlisidou *et al.,* 2010; Heerman and Fuchs, 2008 [21,36]
Enterohaemorrhagic *Escherichia coli* (EHEC)	KdpE is activated by the sensor kinase QseC, a receptor for adrenergic signals. Adrenergic regulation of bacterial gene expression is an underlying mechanism of stress response and cellular survival	Hughes *et al.,* 2009 [29]

Further evidence that KdpD can sense host-derived signals – including evidence for a role in stress response – was seen in *Bacillus cereus*, in which exposure to chitosan led to up-regulation of the *kdpABC* and *kdpD* genes [37]. Chitosan is an antibacterial polysaccharide, thought to induce loss of ions and cellular turgor by forming pores in bacterial membranes. This might suggest that the Kdp-ATPase was up-regulated in order to recover lost K^+. Yet two observations suggest otherwise. One is that a deletion mutant of the Kdp-ATPase structural genes actually showed no impairment of growth in conditions of either K^+-limitation or salt-stress, bringing into question the importance of Kdp for K^+ regulation in *B. cereus*. The other is that exposure to benzalkonium chloride (a disinfectant which generates leakage of intracellular ions in much the same way as chitosan) did not have the same effect of up-regulating the *B. cereus kdp* genes [38]. Taken together this suggests that ion loss alone was not being sensed, rather some other form of "antimicrobial stress" may have been. Indeed there is precedence for a TCS being directly activated by host-elicited antimicrobial peptides (AMPs) in the case of PhoP/PhoQ (Bader *et al*. 2005). It is therefore tempting to speculate that the biologically-derived

antimicrobial chitosan may be sensed by KdpD in a manner akin to the sensing of small innate immune molecules by PhoP.

Quorum sensing

As discussed earlier, in various bacteria KdpD can integrate multiple stimuli including: K^+ concentration, osmolarity, possibly turgor pressure and even host adrenergic signals. Importantly, in *S. aureus* KdpD/KdpE can also respond to population density. The two studies which showed direct regulation of *S. aureus* virulence factors also reported that KdpD/KdpE can integrate signals from two quorum sensing (QS) systems – the *luxS*/AI-2 system [18] and the Agr system [17]. Therefore KdpE-regulated *S. aureus* virulence genes are expressed appropriately according to both K^+ concentration (an indication of whether the bacterium is extra- or intracellular), and population density (indicating whether there are enough bacteria present to make a particular response appropriate, e.g. toxin production) [17]. As such, *S. aureus* uses KdpD/KdpE in an adaptive manner, utilizing its "traditional" sensor activity in an integrated fashion with input from QS systems.

Accessory components of KdpD

Accessory proteins (also known as auxiliary factors) are known to affect TCSs by: i) fine-tuning the ratio of the HK's kinase- to phosphatase-activity, ii) linking the system to other regulatory networks, or iii) enabling the sensing of additional stimuli [40,41]. Table 3 summarises accessory proteins that have been identified for KdpD and *E. coli* accessory factors are also shown in Figure 1(D). It is not clear if there is any one specific region of the KdpD protein structure that is responsible for fine-tuning sensor kinase activity through accessory protein interactions. For example, it has been suggested that the IIA^{Ntr} [41] protein (see below) interacts with the C-terminal transmitter domain of KdpD [45]. On the other hand, the N-terminus includes a conserved "KdpD" sub-domain with a regulatory ATP-binding site [42,43], and a universal stress protein (KdpD-Usp) sub-domain, which is highly variable between species. The *E. coli* universal stress protein UspC protein is known to interact with the N-terminal Usp-domain thus altering its activity [32], although not through an influence on KdpD kinase activity.

Table 3. Identification of KdpD accessory components in *E. coli* and *M. tuberculosis*

Bacterium	Component	Details	References
Escherichia coli	IIA ^{Ntr} (enzyme IIA of the Ntr phospho-transferase system)	Interacts with KdpD, stimulates auto-kinase activity and therefore Kdp pump expression. This activity is linked to glycolytic growth	Lüttman *et al.,* 2009; Njoroge *et al*., 2012 [24,30]
	trxA (thioredoxin 1), *trxB* (thioredoxin reductase)	Thioredoxins control the bacterial stress response by maintaining a reducing environment in the cell, preventing ROS damage, and signalling osmotic stress and low pH. These genes exert effects upstream of KdpD, though the precise nature of the interaction is not known. KO of either gene results in reduced expression of the Kdp pump	Sardesai and Gowrishankar, 2001; Kumar *et al*., 2004; Zeller and Klug, 2006; Ehrt and Schnappinger, 2009 [31,44-46]
	hns (H-NS nucleoid protein)	Exerts effects upstream of KdpD, though the precise mechanism of the interaction is not known. KO results in reduced expression of the Kdp pump	Sardesai and Gowrishankar, 2001 [31]
	UspC (Universal stress protein C)	Binds to the Usp sub-domain of KdpD under osmotic stress conditions, scaffolding the active KdpD/phospho-KdpE/DNA complex and stimulating expression of Kdp pump structural genes	Heerman *et al*., 2009 [32]
Mycobacterium tuberculosis	LprJ, LprF (membrane lipoproteins)	Either protein can interact specifically with KdpD (solely with the C-terminal region or while also forming a ternary complex with the N-terminal region). Appear to be involved in the phospho-relay process. Likely act as sensors or ligand-binding proteins for as-yet-unknown signals/ligands	Steyn et at., 2003; Buelow and Raivio, 2010 [41,47]

Is the Usp domain of KdpD involved in stress sensing?

A fundamental feature of Usp proteins is that they accumulate under stress conditions, and indeed UspC binds to the KdpD-Usp domain in response to osmotic stress, stimulating *kdpFABC* expression by acting as a scaffold between the active KdpD/phospho-KdpE/DNA complex [32]. This enables Kdp-ATPase expression at K^+ levels at which it would normally be repressed. It has previously been suggested that the KdpD-Usp domain might be pivotal in the sensing of additional stimuli (Alegado *et al*. 2011; Vlisidou *et al*. 2010). UspA proteins protect *E. coli* against superoxide stress and the UspA proteins of *Photorhabdus* species and *Yersinia enterocolitica* are thought to play a

role in stress sensing when invading insect hosts [32,36,48]. *Photorhabdus asymbiotica* is a facultative intracellular pathogen of insects and humans. Interestingly, when *P. asymbiotica kdpD/kdpE* was expressed in a non-pathogenic *E. coli* strain, the presence of the transgenic TCS conferred an ability to the *E. coli* strain to persist within insect phagocytic cells [21]. Although further molecular experiments would be required in order to identify the precise mechanism behind the phenomenon, this observation does show that there are differences in the functioning of the KdpD/KdpE TCSs between the two species. The greatest evolutionary divergence of the *kdpD* and *kdpE* genes from *P. asymbiotica*, *E. coli* and other bacterial species does indeed reside within the KdpD-Usp domain. Interestingly, domain swapping experiments revealed that this domain is also crucial for activation of KdpD. While the Usp-domain has a net-positive charged surface, integration of a net-negative charged surface was shown to block the activity of the protein. Therefore this domain can not only act as an interaction surface for other proteins, but also appears important for internal (de)activation of KdpD [49]. It has been suggested that binding of other Usp proteins might either alter the secondary structure of the protein or perhaps facilitate activation by shaping a more positive surface at this position. The ability of KdpD/KdpE to sense and respond to stress may thus be mediated via this Usp-binding domain, and the variability of that domain between species might contribute to differences in bacterial virulence and lifestyle.

Overview

A study of the TCSs of *M. tuberculosis* in 2003 found that deletion of *kdpD/kdpE* unexpectedly resulted in hyper-virulence in mice [20]. Although no targets of KdpD/KdpE other than the Kdp-ATPase itself had been identified at the time, the result prompted the suggestion that KdpD/KdpE deletion had de-repressed virulence genes. It is possible that several mycobacterial lipoproteins identified in a study by Steyn *et al* [47] might be targets of KdpD/KdpE regulation. Since then, a diverse set of observations in a range of species supports the role of KdpD/KdpE in promoting survival and virulence through various mechanisms distinct from K^+ regulation. In most cases it is not yet clear exactly how KdpD/KdpE impacts on virulence – it is likely that the link to stress response aids bacterial persistence within host cells. KdpD/KdpE's role in virulence is likely to be highly variable across species and may ultimately be an indicator of species-specific adaptation.

In both Gram positive and Gram negative pathogens, KdpD/KdpE functions as a previously unrecognised adaptive TCS of stimuli during host infection, integrating cues from the host (phagocytosis, host-derived antimicrobials, and adrenergic hormones) in addition to bacterial quorum sensing signals and the outside ionic concentrations. A recent review of "moonlighting" bacterial proteins focused upon glycolytic enzymes and

molecular chaperones in a range of pathogens. Just as the evidence suggests for KdpD/KdpE, this review emphasized that key metabolic proteins and molecular chaperones, essential for dealing with the bacterium's response to stress, also have unexpected functions in virulence [50]. Like key metabolic enzymes and molecular chaperones, the KdpD/KdpE TCS usually plays a conserved role in in maintaining normal cellular function. It seems that the conserved TCS KdpD/KdpE provides a further example of bacterial protein "moonlighting". It is suggested that proteins can display multi-functionality due to "biochemical" or "geographical" conditions: either through possessing additional biochemical reactions or by being located in a different cellular location (such as the pole of an asymmetric cell), or both [50]. There appear to be no reports of KdpE or KdpD being located anywhere other than the cytoplasm and cytoplasmic membrane, but evidence does suggest that the Usp domain is a prime candidate as an additional "biochemical" site. Data regarding the effects of KdpD/KdpE in pathogenesis are somewhat limited to date but come from a range of bacterial genera and experimental approaches. The evidence reveals a spectrum of Kdp function from a clearly homeostasis-based role to a highly pleiotropic one. Given its function in K^+ homeostasis, the KdpD/KdpE TCS is extremely important for bacteria in challenging environments. We argue that it is therefore likely to be a focal point for selection in relation to survival during infection. It should be noted that no additional functions have yet been ascribed to KdpD/KdpE in non-pathogenic *E. coli*; accessory components have been identified which interact with *E. coli* KdpD but these can be reasonably linked to K^+ homeostasis. Examples include: thioredoxins, which are integral in stress response pathways involving osmotic stress, the H-NS nucleoid protein which is a transcriptional repressor that can respond to K^+ concentration [51], and the IIA^{Ntr} enzyme. This enzyme has been shown to connect K^+ homeostasis with carbon starvation through direct interaction of non-phosphorylated IIA^{Ntr} with KdpD activating the kinase activity [52]. Non-pathogenic *E. coli* are not typically capable of surviving phagocytosis, and yet when expressing the KdpD/KdpE TCS from *P. asymbiotica*, *E. coli* cells did persist intracellularly [21] implying a fundamental difference between the abilities of the two systems to sense or respond to the phagocytic environment. The evidence from *F. novicida* can be adequately explained by a role in K^+ regulation; mutants in the *kdpFABC* operon (as well as those in regulatory genes) were attenuated in the fruit fly model which indicates that the Kdp-ATPase itself is important in this species [22]. Yet in *F. tularensis*, only the *kdpD* gene mutant was identified as attenuated in the mouse model; *kdpFABC* operon genes were apparently less critical than within the gene encoding the sensor kinase [23]. In EHEC, KdpE regulates K^+ uptake and osmolarity alongside important virulence genes; the EHEC QseC HK which activates KdpE has even been investigated as a potential target for novel 'anti-virulence' drugs [29,53]. KdpE interacts with Cra, which itself coordinates the *E. coli*

response to sugar availability, thereby linking metabolism to pathogenesis. It has been suggested that during its evolution EHEC has co-opted "established mechanisms for sensing the metabolites and stress cues in the environment, to induce virulence factors in a temporal and energy-efficient manner, culminating in disease" [24]. The clearest K^+ independent role in virulence so far is in *S. aureus*, in which KdpD responds to population density and KdpE actually regulates over 100 genes.

Concluding remarks and future directions

In these cases where KdpD/KdpE has been shown to regulate additional virulence genes, it is not yet clear how this has evolved. For example, did the promiscuous regulation by KdpE evolve through changes in the KdpE DNA-binding domain or has there been widespread selection for the evolution of KdpE operator sequence sites across a range of virulence loci? Furthermore, how taxonomically widespread is the expanded regulatory capacity of KdpE, and has the same mechanism occurred in each case? If specific virulence genes have evolved KdpE-responsive promoters then we may expect to see similar virulence genes under the control of KdpD/KdpE in different pathogens by virtue of horizontal gene transfer. EHEC's T3SS and lesion-causing genes were acquired on a mobile genetic element and it has been suggested that Cra and KdpE (originally regulators of non-pathogenic functions) have been "co-opted by a pathogen to regulate virulence factors encoded within a horizontally acquired [pathogenicity island]" [24].

KdpD/KdpE is positioned at a molecular hub which is fundamentally relevant to homeostasis during infection. This central position within regulatory networks controlling homeostasis, in conjunction with the radical stress associated with pathogenic host interactions is likely to explain how KdpD/KdpE has evolved a role in pathogenicity in some taxa. As such, KdpD/KdpE is likely subjected to strong selection to acquire novel functions in mediating virulence pathways. We might expect that the selection pressures, or the novel functions that result from them, would be variable across different bacteria with different hosts and infection- parameters. This taxa-specific evolutionary novelty is reflected in the phylogenetically diverse yet discontinuous nature of the data available so far. Figure 2 depicts the phylogenetic relationship between bacterial taxa where evidence supports a pleiotropic role of KdpD/KdpE. The majority of cases come from the well-studied gamma-Proteobacteria clade but there is also evidence from the more distantly related Firmicutes and Actinobacteria. The common association of KdpD/KdpE within an operon containing the structural genes KdpABC suggests that a role in K^+ homeostasis is ancestral and that KdpD/KdpE's adaptation for virulence or survival has arisen more recently and possibly multiple times. Whether K^+ regulation by KdpD/KdpE pre-dates more specific host-responsive activities or whether these evolved in parallel is a key

question with broad implications on the evolution of virulence. Ultimately, a detailed understanding (across a range of pathogenic and non-pathogenic bacteria) of KdpD/KdpE's connectivity within homeostatic response, stress response and virulence pathways will be needed to address this question.

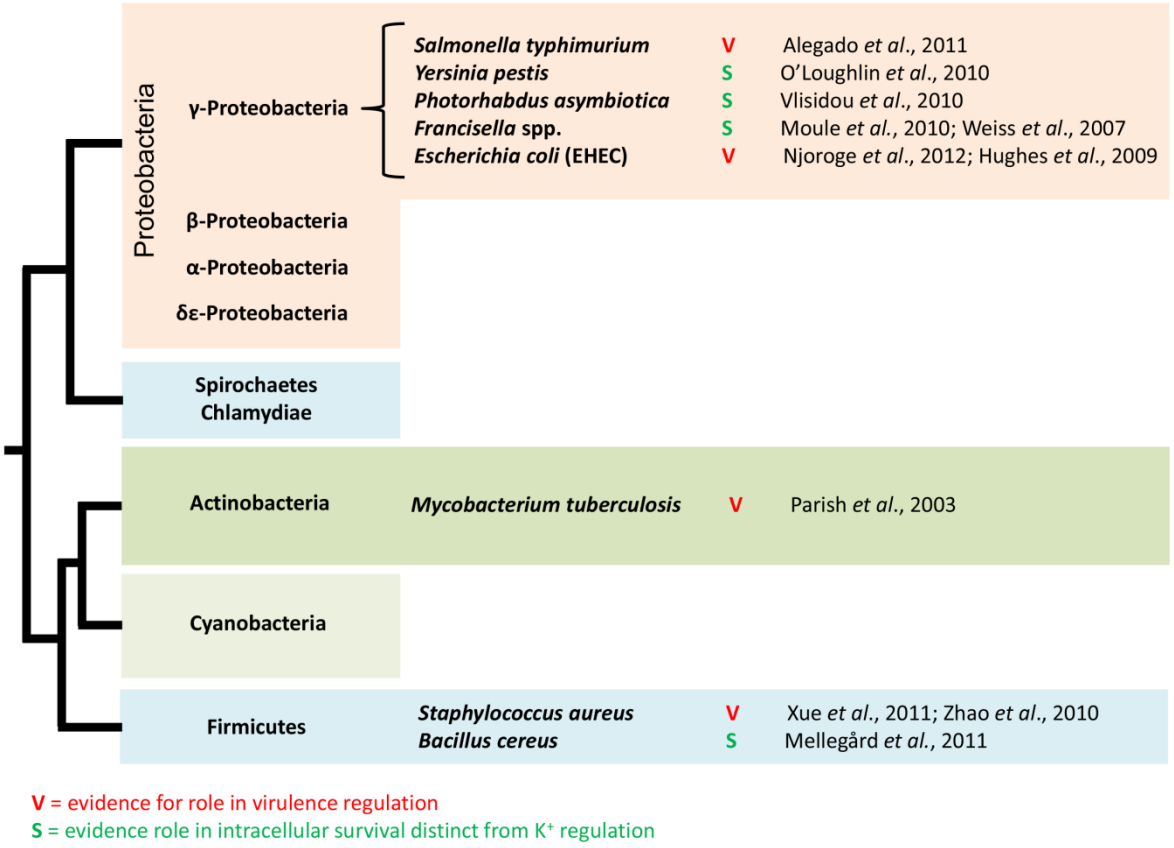

Figure 2. KdpD/KdpE virulence-related roles across bacterial taxa. Evidence supporting the role of KdpD/KdpE in virulence (V) or survival (S) is indicated across diverse bacterial species, all of which are capable of intracellular replication to some extent. The relevant references are also indicated. Phylogenetic relationships are as suggested by Battistuzzi *et al*. (2004) (not drawn to scale) [54].

The perception that Kdp serves a general homeostatic function alone means that the Kdp regulatory network has not been specifically targeted in virulence studies. The studies discussed in this review however point to a clear need for more detailed experiments, with a systematic approach across multiple taxa. Specifically, useful tools would include (i) genetic knock-outs (plus/minus complementation) of KdpD and KdpE (individually and together) and the structural genes *kdpFABC*, or (ii) combinations of transgenic and/or native TCSs and Kdp-ATPases from species observed to show different effects of KdpD/KdpE. These genetic tools could be used for transcriptomic analyses and *in vivo* studies. Transcriptomic analyses could identify networks of genes co-regulated in

response to different challenges (K^+ limitation, AMPs, oxidative or osmotic stress) or during infection of cells and whole organisms. *In vivo* studies in host organisms could examine the effects on acute virulence (measuring LD50, time to death, or host weight gain) or chronic persistence (how long bacteria can be retrieved). Ideally, it would be informative to re-investigate the species discussed in this review – and new species – using a coordinated and comparable experimental approach. To contrast with the data available so far it would be interesting to investigate species that cannot replicate intracellularly such as *Pseudomonas* spp. (gamma-Proteobacteria) or *B. cereus* (Firmicutes). Studies involving closely related species with diverse lifestyles – such as the *Burkholderia* which range from environmental organisms to obligate and opportunistic pathogens with varied host ranges – might be useful for dissecting the effects of host and lifestyle on KdpD/KdpE function.

We predict that KdpD/KdpE will continue to be demonstrated to function in K^+ homeostasis and virulence (directly or via stress response etc.) to different extents in different species. These differences are likely to correlate with whether the species in question leads a predominantly pathogenic or more environmentally-based lifestyle. In the former case, the type of host response a species encounters is also likely to be important. Finally, studies of TCSs such as PhoP/PhoQ, Cra and KdpD/KdpE suggest that other central homeostasis bacterial regulators will also prove to have various adaptive roles in virulence. The application of sophisticated systems-level studies across diverse bacterial pathogens may help to clarify this phenomenon and take us closer to understanding the regulatory breadth and complexity of pathogenesis.

References

1. Groisman EA, Mouslim C (2006) Sensing by bacterial regulatory systems in host and non-host environments. Nat Rev Microbiol 4: 705–709.

2. Groisman EA (2001) The Pleiotropic Two-Component Regulatory System PhoP-PhoQ. J Bacteriol 183: 1835–1842.

3. O'Loughlin JL, Spinner JL, Minnich SA, Kobayashi SD (2010) Yersinia pestis Two-Component Gene Regulatory Systems Promote Survival in Human Neutrophils. Infect Immun 78: 773–782.

4. Falord M, Mäder U, Hiron A, Débarbouillé M, Msadek T (2011) Investigation of the Staphylococcus aureus GraSR regulon reveals novel links to virulence, stress

response and cell wall signal transduction pathways. PloS ONE 6: e21323. doi:10.1371/journal.pone.0021323.

5. Epstein W (2003) The roles and regulation of potassium in bacteria. Prog Nucleic Acid Res Mol Biol 75: 293–320.

6. Ballal A, Basu B, Apte SKK (2007) The Kdp-ATPase system and its regulation. J Biosci 32: 559–568.

7. Heermann R, Jung K (2012) K+ Supply, Osmotic Stress, and the KdpD/KdpE Two-component System. In: Gross R, Beier D, editors. Two-component systems in bacteria. Chapter 10. Norfolk, UK: Caister Academic Press.

8. Heermann R, Jung K (2010) The complexity of the “simple” two-component system KdpD/KdpE in Escherichia coli. FEMS Microbiol Lett 304: 97–106.

9. Brandon L, Dorus S, Epstein W, Altendorf K, Jung K (2000) Modulation of KdpD phosphatase implicated in the physiological expression of the kdp ATPase of Escherichia coli. Mol Microbiol 38: 1086–1092.

10. Su J, Gong H, Lai J, Main A, Lu S (2009) The Potassium Transporter Trk and External Potassium Modulate Salmonella enterica Protein Secretion and Virulence. Infect Immun 77: 667–675.

11. Chen Y-C, Chuang Y-C, Chang C-C, Jeang C-L, Chang M-C (2004) A K+ Uptake Protein, TrkA, Is Required for Serum, Protamine, and Polymyxin B Resistance in Vibrio vulnificus. Infect Immun 72: 629–636.

12. Stingl K, Brandt S, Uhlemann E-M, Schmid R, Altendorf K, *et al*. (2006) Channel-mediated potassium uptake in Helicobacter pylori is essential for gastric colonization. EMBO J 26: 232–241.

13. Alkhuder K, Meibom KL, Dubail I, Dupuis M, Charbit A (2010) Identification of trkH, encoding a potassium uptake protein required for Francisella tularensis systemic dissemination in mice. PloS ONE 5: e8966. doi:10.1371/journal.pone.0008966.

14. Reeves EP, Lu H, Jacobs HL, Messina CGM, Bolsover S, *et al*. (2002) Killing activity of neutrophils is mediated through activation of proteases by K+ flux. Nature 416: 291–297.

15. Voyich JM, Braughton KR, Sturdevant DE, Whitney AR, Saïd-Salim B, *et al*. (2005) Insights into Mechanisms Used by Staphylococcus aureus to Avoid Destruction by Human Neutrophils. J Immunol 175: 3907–3919.

16. Hou JY, Graham JE, Clark-Curtiss JE (2002) Mycobacterium avium genes expressed during growth in human macrophages detected by selective capture of transcribed sequences (SCOTS). Infect Immun 70: 3714–3726.

17. Xue T, You Y, Hong D, Sun H, Sun B (2011) The Staphylococcus aureus KdpDE two-component system couples extracellular K+ sensing and Agr signaling to infection programming. Infect Immun 79: 2154–2167.

18. Zhao L, Xue T, Shang F, Sun H, Sun B (2010) Staphylococcus aureus AI-2 quorum sensing associates with the KdpDE two-component system to regulate capsular polysaccharide synthesis and virulence. Infect Immun 78: 3506–3515.

19. Alegado RA, Chin C-Y, Monack DM, Tan M-W (2011) The Two-Component Sensor Kinase KdpD is Required for Salmonella typhimurium Colonization of Caenorhabditis elegans and Survival in Macrophages. Cell Microbiol 13: 1618–1637.

20. Parish T, Smith DA, Kendall S, Casali N, Bancroft GJ, *et al*. (2003) Deletion of Two-Component Regulatory Systems Increases the Virulence of Mycobacterium tuberculosis. Infect Immun 71: 1134–1140.

21. Vlisidou I, Eleftherianos I, Dorus S, Yang G, ffrench-Constant RH, *et al*. (2010) The KdpD/KdpE two-component system of Photorhabdus asymbiotica promotes bacterial survival within *M. sexta* hemocytes. J Invertebr Pathol 105: 352–362.

22. Moule MG, Monack DM, Schneider DS (2010) Reciprocal Analysis of Francisella novicida Infections of a Drosophila melanogaster Model Reveal Host-Pathogen Conflicts Mediated by Reactive Oxygen and imd-Regulated Innate Immune Response. PLoS Pathog 6: e1001065. doi:10.1371/journal.ppat.1001065.

23. Weiss DS, Brotcke A, Henry T, Margolis JJ, Chan K, *et al*. (2007) In vivo negative selection screen identifies genes required for Francisella virulence. Proc Natl Acad Sci U S A 104: 6037–6042.

24. Njoroge JW, Nguyen Y, Curtis MM, Moreira CG, Sperandio V (2012) Virulence Meets Metabolism: Cra and KdpE Gene Regulation in Enterohemorrhagic Escherichia coli. mBio 3: e00280–12. doi:10.1128/mBio.00280-12.

25. Beenken KE, Dunman PM, McAleese F, Macapagal D, Murphy E, *et al*. (2004) Global Gene Expression in Staphylococcus aureus Biofilms. J Bacteriol 186: 4665–4684.

26. Palazzolo-Ballance AM, Reniere ML, Braughton KR, Sturdevant DE, Otto M, *et al*. (2008) Neutrophil microbicides induce a pathogen survival response in community-associated methicillin-resistant Staphylococcus aureus. J Immunol 180: 500–509.

27. Hanssen A-M, Ericson Sollid JU (2006) SCCmec in staphylococci: genes on the move. FEMS Immunol Med Microbiol 46: 8–20.

28. Musher D, Verbrugh H, Verhoef J (1981) Suppression of phagocytosis and chemotaxis by cell wall components of Staphylococcus aureus. J Immunol 127: 84–88.

29. Hughes DT, Clarke MB, Yamamoto K, Rasko DA, Sperandio V (2009) The QseC Adrenergic Signaling Cascade in Enterohemorrhagic *E. coli* (EHEC). PLoS Pathog 5: e1000553. doi:10.1371/journal.ppat.1000553.

30. Lüttmann D, Heermann R, Zimmer B, Hillmann A, Rampp IS, *et al*. (2009) Stimulation of the potassium sensor KdpD kinase activity by interaction with the phosphotransferase protein IIANtr in Escherichia coli. Mol Microbiol 72: 978–994.

31. Sardesai AA, Gowrishankar J (2001) trans-Acting Mutations in Loci Other than kdpDE That Affect kdp Operon Regulation in Escherichia coli: Effects of Cytoplasmic Thiol Oxidation Status and Nucleoid Protein H-NS on kdp Expression. J Bacteriol 183: 86–93.

32. Heermann R, Weber A, Mayer B, Ott M, Hauser E, *et al*. (2009) The universal stress protein UspC scaffolds the KdpD/KdpE signaling cascade of Escherichia coli under salt stress. J Mol Biol 386: 134–148.

33. Garzoni C, Francois P, Huyghe A, Couzinet S, Tapparel C, *et al*. (2007) A global view of Staphylococcus aureus whole genome expression upon internalization in human epithelial cells. BMC Genomics 8: 171–185.

34. Koziel J, Maciag-Gudowska A, Mikolajczyk T, Bzowska M, Sturdevant DE, *et al*. (2009) Phagocytosis of Staphylococcus aureus by Macrophages Exerts Cytoprotective Effects Manifested by the Upregulation of Antiapoptotic Factors. PLoS ONE 4: e5210. doi:10.1371/journal.pone.0005210.

35. Sukumaran SK, Shimada H, Prasadarao N V (2003) Entry and intracellular replication of Escherichia coli K1 in macrophages require expression of outer membrane protein A. Infect Immun 71: 5951–5961.

36. Heermann R, Fuchs T (2008) Comparative analysis of the Photorhabdus luminescens and the Yersinia enterocolitica genomes: uncovering candidate genes involved in insect pathogenicity. BMC Genomics 9: 40–61.

37. Mellegård H, Lindbäck T, Christensen BE, Kuipers OP, Granum PE (2011) Transcriptional responses of Bacillus cereus towards challenges with the polysaccharide chitosan. PloS ONE 6: e24304. doi:10.1371/journal.pone.0024304.

38. Ceragioli M, Mols M, Moezelaar R, Ghelardi E, Senesi S, *et al*. (2010) Comparative transcriptomic and phenotypic analysis of the responses of Bacillus cereus to various disinfectant treatments. Appl Environ Microbiol 76: 3352–3360.

39. Bader MW, Sanowar S, Daley ME, Schneider AR, Cho U, *et al*. (2005) Recognition of Antimicrobial Peptides by a Bacterial Sensor Kinase. Cell 122: 461–472.

40. Mitrophanov AY, Groisman EA (2008) Signal integration in bacterial two-component regulatory systems. Genes Dev 22: 2601–2611.

41. Buelow DR, Raivio TL (2010) Three (and more) component regulatory systems - auxiliary regulators of bacterial histidine kinases. Mol Microbiol 75: 547–566.

42. Jung K, Altendorf K (1998) Individual substitutions of clustered arginine residues of the sensor kinase KdpD of Escherichia coli modulate the ratio of kinase to phosphatase activity. J Biol Chem 273: 26415–26420.

43. Heermann R, Altendorf K, Jung K (2000) The hydrophilic N-terminal domain complements the membrane-anchored C-terminal domain of the sensor kinase KdpD of Escherichia coli. J Biol Chem 275: 17080–17085.

44. Kumar JK, Tabor S, Richardson CC (2004) Proteomic analysis of thioredoxin-targeted proteins in Escherichia coli. Proc Natl Acad Sci U S A 101: 3759–3764.

45. Zeller T, Klug G (2006) Thioredoxins in bacteria: functions in oxidative stress response and regulation of thioredoxin genes. Naturwissenschaften 93: 259–266.

46. Ehrt S, Schnappinger D (2009) Mycobacterial survival strategies in the phagosome: defence against host stresses. Cell Microbiol 11: 1170–1178.

47. Steyn AJC, Joseph J, Bloom BR (2003) Interaction of the sensor module of Mycobacterium tuberculosis H37Rv KdpD with members of the Lpr family. Mol Microbiol 47: 1075–1089.

48. Siegele DA (2005) Universal stress proteins in Escherichia coli. J Bacteriol 187: 6253–6254.

49. Heermann R, Lippert M-L, Jung K (2009) Domain swapping reveals that the N-terminal domain of the sensor kinase KdpD in Escherichia coli is important for signaling. BMC Microbiol 9: 133–144.

50. Henderson B, Martin A (2011) Bacterial virulence in the moonlight: multitasking bacterial moonlighting proteins are virulence determinants in infectious disease. Infect Immun 79: 3476–3491.

51. Ueguchi C, Mizuno T (1993) The Escherichia coli nucleoid protein H-NS functions directly as a transcriptional repressor. EMBO J 12: 1039–1046.

52. Lüttmann D, Göpel Y, Görke B (2012) The phosphotransferase protein EIIA(Ntr) modulates the phosphate starvation response through interaction with histidine kinase PhoR in Escherichia coli. Mol Microbiol 86: 96–110.

53. Rasko DA, Sperandio V (2010) Anti-virulence strategies to combat bacteria-mediated disease. Nat Rev Drug Discov 9: 117–128.

54. Battistuzzi F, Feijao A, Hedges SB (2004) A genomic timescale of prokaryote evolution: insights into the origin of methanogenesis, phototrophy, and the colonization of land. BMC Evol Biol 4: 44–57.

Bibliography

Alegado, R.A. *et al*., 2011. The Two-Component Sensor Kinase KdpD is Required for Salmonella typhimurium Colonization of Caenorhabditis elegans and Survival in Macrophages. *Cell Microbiol*, 13(10), pp.1618–1637.

Allwood, E.M. *et al*., 2011. Strategies for Intracellular Survival of Burkholderia pseudomallei. *Front Microbiol*, 2.

Alvarez-Venegas, R. *et al*., 2007. Origin of the Bacterial SET Domain Genes: Vertical or Horizontal? *Mol Biol Evol*, 24(2), pp.482–497.

Arnold, D.L. *et al*., 2007. Evolution of microbial virulence: the benefits of stress. *Trends Genet*, 23(6), pp.293–300.

Ashdown, L. & Koehler, J., 1990. Production of hemolysin and other extracellular enzymes by clinical isolates of Pseudomonas pseudomallei. *J Clin Microbiol*, 28(10), pp.2331–2334.

Au, C. *et al*., 2004. Effect of the insect pathogenic bacterium Photorhabdus on insect phagocytes. *Cell Microbiol*, 6(1), pp.89–95.

Auld, S.K.J.R. *et al*., 2012. Elevated haemocyte number is associated with infection and low fitness potential in wild Daphnia magna. *Funct Ecol*, 26(2), pp.434–440.

Ayala-Castro, C., Saini, A. & Outten, F.W., 2008. Fe-S Cluster Assembly Pathways in Bacteria. *Microbiol Mol Biol Rev*, 72(1), pp.110–125.

Bader, M.W. *et al*., 2005. Recognition of Antimicrobial Peptides by a Bacterial Sensor Kinase. *Cell*, 122(3), pp.461–472.

Balaji, V. *et al*., 2004. Detection of virulence attributes of Burkholderia pseudomallei. *Indian J Med Res*, 119(3), pp.101–6.

Balder, R. *et al*., 2010. Identification of Burkholderia mallei and Burkholderia pseudomallei adhesins for human respiratory epithelial cells. *BMC Microbiol*, 10, p.250.

Balls, M. *et al*., 1995. The three Rs: the way forward: the report and recommendations of ECVAM Workshop 11. *Altern Lab Anim*, 23(6), pp.838–66.

Banerjee, J. *et al*., 2006. The cytotoxic fimbrial structural subunit of Xenorhabdus nematophila is a pore-forming toxin. *J Bacteriol*, 188(22), pp.7957–62.

Bauwe, H. & Kolukisaoglu, Ü., 2003. Genetic manipulation of glycine decarboxylation. *J Exp Bot*, 54(387), pp.1523–1535.

Behrens-Kneip, S., 2010. The role of SurA factor in outer membrane protein transport and virulence. *Int J Med Microbiol*, 300(7), pp.421–8.

Biggins, J.B. *et al*., 2011. Metabolites from the induced expression of cryptic single operons found in the genome of Burkholderia pseudomallei. *J Am Chem Soc*, 133(6), pp.1638–41.

Biggins, J.B., Ternei, M.A. & Brady, S.F., 2012. Malleilactone, a polyketide synthase-derived virulence factor encoded by the cryptic secondary metabolome of Burkholderia pseudomallei group pathogens. *J Am Chem Soc*, 134(32), pp.13192–13195.

Bingle, L.E., Bailey, C.M. & Pallen, M.J., 2008. Type VI secretion: a beginner's guide. *Curr Opin Microbiol*, 11(1), pp.3–8.

Blanc, G. & Baltazard, M., 1949. Recherches sur la melioidose infection a bacille de Whitmore – etude experimentale. *Arch Inst Pasteur Maroc*, 3, pp.520–584.

Boddey, J.A. *et al*., 2007. The bacterial gene lfpA influences the potent induction of calcitonin receptor and osteoclast-related genes in Burkholderia pseudomallei-induced TRAP-positive multinucleated giant cells. *Cell Microbiol*, 9(2), pp.514–31.

Bozue, J.A. & Johnson, W., 1996. Interaction of Legionella pneumophila with Acanthamoeba castellanii: uptake by coiling phagocytosis and inhibition of phagosome-lysosome fusion. *Infect Immun*, 64(2), pp.668–73.

Brett, P J, Deshazer, D & Woods, D E, 1997. Characterization of Burkholderia pseudomallei and Burkholderia pseudomallei-like strains. *Epidemiol Infect*, 118(2), pp.137–48.

Brett, P J, DeShazer, D & Woods, Donald E, 1998. Burkholderia thailandensis sp. nov., a Burkholderia pseudomallei-like species. *Int J Syst Bacteriol*, 48 Pt 1(1 998), pp.317–20.

Brett, P J & Woods, D E, 1996. Structural and immunological characterization of Burkholderia pseudomallei O-polysaccharide-flagellin protein conjugates. *Infect Immun*, 64(7), pp.2824–8.

Burtnick, M.N. *et al*., 2011. The cluster 1 type VI secretion system is a major virulence determinant in Burkholderia pseudomallei. *Infect Immun*, 79(4), pp.1512–1525.

Bussière, F.I. *et al*., 2005. Spermine causes loss of innate immune response to Helicobacter pylori by inhibition of inducible nitric-oxide synthase translation. *J Biol Chem*, 280(4), pp.2409–12.

Butler, D., 2012. Viral research faces clampdown. *Nature*, 490(7421), p.456.

Butt, A. *et al*., 2012. Identification of Type II Toxin-antitoxin modules in Burkholderia pseudomallei. *FEMS Microbiol Lett*, 338, pp.86–94.

Cameron, S.L. & Whiting, M.F., 2008. The complete mitochondrial genome of the tobacco hornworm, Manduca sexta, (Insecta: Lepidoptera: Sphingidae), and an examination of mitochondrial gene variability within butterflies and moths. *Gene*, 408(1-2), pp.112–123.

Casadevall, A., 2005. Host as the variable: model hosts approach the immunological asymptote. *Infect Immun*, 73(7), pp.3829–32.

Casiano-Colón, A. & Marquis, R., 1988. Role of the arginine deiminase system in protecting oral bacteria and an enzymatic basis for acid tolerance. *Appl Environ Microbiol*, 54(6), pp.1318–1324.

Chan, Ying Ying & Chua, Kim Lee, 2010. Growth-related changes in intracellular spermidine and its effect on efflux pump expression and quorum sensing in Burkholderia pseudomallei. *Microbiology*, 156(Pt 4), pp.1144–54.

Chen, Y. *et al*., 2011. Regulation of Type VI Secretion System during Burkholderia pseudomallei Infection. *Infect Immun*, 79(8), pp.3064–3073.

Cheng, A.C. & Currie, B.J., 2005. Melioidosis: epidemiology, pathophysiology, and management. *Clin Microbiol Rev*, 18(2), pp.383–416.

Chieng, S., Carreto, L. & Nathan, S., 2012. Burkholderia pseudomallei transcriptional adaptation in macrophages. *BMC Genomics*, 13(1), p.328.

Chin, C.-Y., Monack, D.M. & Nathan, S., 2010. Genome wide transcriptome profiling of a murine acute melioidosis model reveals new insights into how Burkholderia pseudomallei overcomes host innate immunity. *BMC Genomics*, 11(1), p.672.

Choy, J. *et al*., 2000. Animal melioidosis in Australia. *Acta Trop*, 74(2-3), pp.153–158.

Chua, K. L., Chan, Y. Y. & Gan, Y.H., 2003. Flagella Are Virulence Determinants of Burkholderia pseudomallei. *Infect Immun*, 71(4), pp.1622–1629.

Compant, S. *et al*., 2008. Diversity and occurrence of Burkholderia spp. in the natural environment. *FEMS Microbiol Rev*, 32(4), pp.607–26.

Conejero, L. *et al*., 2011. Low-dose exposure of C57BL/6 mice to burkholderia pseudomallei mimics chronic human melioidosis. *Am J Pathol*, 179(1), pp.270–80.

Cruz-Migoni, A. *et al*., 2011. A Burkholderia pseudomallei Toxin Inhibits Helicase Activity of Translation Factor eIF4A. *Science*, 334(6057), pp.821–824.

Cuccui, J *et al*., 2007. Development of signature-tagged mutagenesis in Burkholderia pseudomallei to identify genes important in survival and pathogenesis. *Infect Immun*, 75(3), pp.1186–1195.

Cui, J. *et al*., 2010. Glutamine deamidation and dysfunction of ubiquitin/NEDD8 induced by a bacterial effector family. *Science*, 329(5996), pp.1215–8.

D'Cruze, T. *et al*., 2011. Role for the Burkholderia pseudomallei type three secretion system cluster 1 bpscN gene in virulence. *Infect Immun*, 79(9), pp.3659–3664.

Dance, D., 2000. Ecology of Burkholderia pseudomallei and the interactions between environmental Burkholderia spp. and human-animal hosts. *Acta Trop*, 74(2-3), pp.159–168.

Dance, D. a, 2000. Melioidosis as an emerging global problem. *Acta Trop*, 74(2-3), pp.115–9.

Das, P. *et al*., 2010. Modulation of the arginase pathway in the context of microbial pathogenesis: a metabolic enzyme moonlighting as an immune modulator. *PLoS Pathog*, 6(6), p.e1000899.

Day, S.R. & Sifri, C.D., 2012. Intoxication vs. infection: A decade of studying Burkholderia pseudomallei virulence in a simple infection model. *Virulence*, 3(6), pp.471–3.

Dean, P. *et al*., 2004. Hyperphagocytic haemocytes in Manduca sexta. *J Insect Physiol*, 50(11), pp.1027–36.

DeShazer, D *et al*., 2001. Identification of a Burkholderia mallei polysaccharide gene cluster by subtractive hybridization and demonstration that the encoded capsule is an essential virulence determinant. *Microb Pathog*, 30(5), pp.253–69.

DeShazer, D., 2007. Virulence of clinical and environmental isolates of Burkholderia oklahomensis and Burkholderia thailandensis in hamsters and mice. *FEMS Microbiol Lett*, 277(1), pp.64–69.

Dharakul, T. & Songsivilai, S, 1999. The many facets of melioidosis. *Trends Microbiol*, 7(4), pp.138–40.

Dorati, F., 2011. *Characterising the molecular mechanisms conferring survival and pathogenicity to the plant pathogen Pseudomonas syringae*. University of Reading.

Dowling, A.J. *et al*., 2010. Genome-Wide Analysis Reveals Loci Encoding Anti-Macrophage Factors in the Human Pathogen Burkholderia pseudomallei K96243. *PLoS One*, 5(12).

Essex-Lopresti, A.E. *et al*., 2005. A type IV pilin, PilA, Contributes To Adherence of Burkholderia pseudomallei and virulence in vivo. *Infect Immun*, 73(2), pp.1260–4.

Felgner, P.L. *et al*., 2009. A Burkholderia pseudomallei protein microarray reveals serodiagnostic and cross-reactive antigens. *Proc Natl Acad Sci U S A*, 106(32), pp.13499–13504.

Fisher, N.A. *et al*., 2012. The Madagascar hissing cockroach as a novel surrogate host for Burkholderia pseudomallei, B. mallei and B. thailandensis. *BMC Microbiol*, 12(1), p.117.

Fleming, V. *et al*., 2006. Agr interference between clinical Staphylococcus aureus strains in an insect model of virulence. *J Bacteriol*, 188(21), pp.7686–8.

Freeman, Z.N., Dorus, Steve & Waterfield, Nicholas R., 2013. The KdpD/KdpE Two-Component System: Integrating K+ Homeostasis and Virulence. *PLoS Pathogens*, 9(3), p.e1003201.

French, C.T. *et al*., 2011. Dissection of the Burkholderia intracellular life cycle using a photothermal nanoblade. *Proc Natl Acad Sci U S A*, 108(29), pp.12095–12100.

Fritz, D L *et al*., 1999. The hamster model of intraperitoneal Burkholderia mallei (glanders). *Vet Pathol*, 36(4), pp.276–91.

Fritz, D. L. *et al*., 2000. Mouse Model of Sublethal and Lethal Intraperitoneal Glanders (Burkholderia mallei). *Vet Pathol*, 37(6), pp.626–636.

Galyov, E.E., Brett, Paul J & DeShazer, David, 2010. Molecular insights into Burkholderia pseudomallei and Burkholderia mallei pathogenesis. *Annu Rev Microbiol*, 64, pp.495–517.

Gan, Y.-H. *et al*., 2002. Characterization of Burkholderia pseudomallei infection and identification of novel virulence factors using a Caenorhabditis elegans host system. *Mol Microbiol*, 44(5), pp.1185–1197.

Garsin, D.A., 2010. Ethanolamine utilization in bacterial pathogens: roles and regulation. *Nat Rev Microbiol*, 8(4), pp.290–295.

Glass, M.B., Steigerwalt, A.G., *et al*., 2006. Burkholderia oklahomensis sp. nov., a Burkholderia pseudomallei-like species formerly known as the Oklahoma strain of Pseudomonas pseudomallei. *Int J Syst Evol Microbiol*, 56(Pt 9), pp.2171–6.

Glass, M.B., Gee, J.E., *et al*., 2006. Pneumonia and septicemia caused by Burkholderia thailandensis in the United States. *J Clin Microbiol*, 44(12), pp.4601–4.

Godoy, D. *et al*., 2003. Multilocus sequence typing and evolutionary relationships among the causative agents of melioidosis and glanders, Burkholderia pseudomallei and Burkholderia mallei. *J Clin Microbiol*, 41(5), pp.2068–79.

Grant, S.G. *et al*., 1990. Differential plasmid rescue from transgenic mouse DNAs into Escherichia coli methylation-restriction mutants. *Proc Natl Acad Sci U S A*, 87(12), pp.4645–9.

Grosse-Wilde, E. *et al*., 2011. Antennal transcriptome of Manduca sexta. *Proc Natl Acad Sci U S A*, 108(18), pp.7449–7454.

Gruening, P. *et al*., 2006. Structure, regulation, and putative function of the arginine deiminase system of Streptococcus suis. *J Bacteriol*, 188(2), pp.361–369.

Harding, C.R. *et al*., 2012. Legionella pneumophila pathogenesis in the Galleria mellonella infection model. *Infect Immun*, 80(8), pp.2780–2790.

Hares, M.C. *et al*., 2008. The Yersinia pseudotuberculosis and Yersinia pestis toxin complex is active against cultured mammalian cells. *Microbiology*, 154(Pt 11), pp.3503–3517.

Harland, D.N. *et al*., 2007. ATP-binding cassette systems in Burkholderia pseudomallei and Burkholderia mallei. *BMC Genomics*, 8, p.83.

Harley, V.S. *et al*., 1998. Effects of Burkholderia pseudomallei and other Burkholderia species on eukaryotic cells in tissue culture. *Microbios*, 96(384), pp.71–93.

Hasselbring, B.M., Patel, M.K. & Schell, M.A., 2011. Dictyostelium discoideum as a model system for identification of Burkholderia pseudomallei virulence factors. *Infect Immun*, 79(5), pp.2079–2088.

Hautbergue, G.M. & Wilson, S.A., 2012. BLF1, the first Burkholderia pseudomallei toxin, connects inhibition of host protein synthesis with melioidosis. *Biochem Soc Trans*, 40(4), pp.842–845.

Hayden, H.S. *et al*., 2012. Evolution of Burkholderia pseudomallei in recurrent melioidosis. *PLoS One*, 7(5), p.e36507.

Heckly, R. & Nigg, C., 1958. Toxins of Pseudomonas pseudomallei: II. Characterization. *J Bacteriol*, 76(4), pp.427–436.

Holden, Matthew T G *et al*., 2004. Genomic plasticity of the causative agent of melioidosis, Burkholderia pseudomallei. *Proc Natl Acad Sci U S A*, 101(39), pp.14240–14245.

Horwitz, M.A., 1984. Phagocytosis of the Legionnaires' disease bacterium (Legionella pneumophila) occurs by a novel mechanism: engulfment within a pseudopod coil. *Cell*, 36(1), pp.27–33.

Hou, J.Y., Graham, J.E. & Clark-Curtiss, J.E., 2002. Mycobacterium avium genes expressed during growth in human macrophages detected by selective capture of transcribed sequences (SCOTS). *Infect Immun*, 70(7), pp.3714–26.

Hughes, D.T. *et al*., 2009. The QseC Adrenergic Signaling Cascade in Enterohemorrhagic E. coli (EHEC). *PLoS Pathog*, 5(8), p.e1000553.

Inglis, T. *et al*., 1999. Acute melioidosis outbreak in Western Australia. *Epidemiol Infect*, 123(3), pp.437–443.

Inglis, T.J. *et al*., 2003. Flagellum-mediated adhesion by Burkholderia pseudomallei precedes invasion of Acanthamoeba astronyxis. *Infect Immun*, 71(4), pp.2280–2.

Inglis, T.J. *et al*., 2000. Interaction between Burkholderia pseudomallei and Acanthamoeba species results in coiling phagocytosis, endamebic bacterial survival, and escape. *Infect Immun*, 68(3), pp.1681–6.

Jones, A.L., DeShazer, D & Woods, D E, 1997. Identification and characterization of a two-component regulatory system involved in invasion of eukaryotic cells and heavy-metal resistance in Burkholderia pseudomallei. *Infect Immun*, 65(12), pp.4972–7.

Jubelin, G. *et al*., 2009. Cycle inhibiting factors (CIFs) are a growing family of functional cyclomodulins present in invertebrate and mammal bacterial pathogens. *PLoS One*, 4(3), p.e4855.

Kanost, M.R., Jiang, H. & Yu, X.-Q., 2004. Innate immune responses of a lepidopteran insect, Manduca sexta. *Immunol Rev*, 198, pp.97–105.

Kavanagh, K. & Reeves, E.P., 2004. Exploiting the potential of insects for in vivo pathogenicity testing of microbial pathogens. *FEMS Microbiol Rev*, 28(1), pp.101–12.

Kespichayawattana, W. *et al*., 2000. Burkholderia pseudomallei Induces Cell Fusion and Actin-Associated Membrane Protrusion: a Possible Mechanism for Cell-to-Cell Spreading. *Infect Immun*, 68(9), pp.5377–5384.

Keum, Y.S. *et al*., 2009. Effects of nutrients on quorum signals and secondary metabolite productions of Burkholderia sp. O33. *J Microbiol Biotechnol*, 19(10), pp.1142–9.

Kharbov, D., Velianov, D. & Raucheva, T., 1981. Ecological aspects of Pseudomonas pseudomallei interactions with Ixodid ticks. *Acta Microbiol*, 8, pp.17–24.

Khush, R.S.R. & Lemaitre, Bruno, 2000. Genes that fight infection: what the Drosophila genome says about animal immunity. *Trends Genet*, 16(10), pp.442–449.

Kim, H Stanley *et al*., 2005. Bacterial genome adaptation to niches: divergence of the potential virulence genes in three Burkholderia species of different survival strategies. *BMC Genomics*, 6(1), p.174.

Kim, U.-J. *et al*., 1992. Stable propagation of cosmid sized human DNA inserts in an F factor based vector. *Nucleic Acids Res*, 20(5), pp.1083–1085.

Kim, Y.R. *et al*., 2003. Characterization and Pathogenic Significance of Vibrio vulnificus Antigens Preferentially Expressed in Septicemic Patients. *Infect Immun*, 71(10), pp.5461–5471.

King, J.G. & Hillyer, J.F., 2012. Infection-Induced Interaction between the Mosquito Circulatory and Immune Systems D. S. Schneider, ed. *PLoS Pathog*, 8(11), p.e1003058.

Klarsfeld, A., Goossens, P. & Cossart, P., 1994. Five Listeria monocytogenes genes preferentially expressed in infected mammalian cells: plcA, purH, purD, pyrE and an arginine ABC transporter gene, arpJ. *Mol Microbiol*, 13(4), pp.585–597.

Kleinjan, D.A. & Van Heyningen, V., 2003. Turned off by RNA. *Nat Genet*, 34(2), pp.125–6.

Langridge, G.C. *et al*., 2009. Simultaneous assay of every Salmonella Typhi gene using one million transposon mutants. *Genome Res*, 19(12), pp.2308–16.

Lazar Adler, N.R. *et al*., 2011. Autotransporters and Their Role in the Virulence of Burkholderia pseudomallei and Burkholderia mallei. *Front Microbiol*, 2, p.151.

Lazar Adler, N.R. *et al*., 2009. The molecular and cellular basis of pathogenesis in melioidosis: how does Burkholderia pseudomallei cause disease? *FEMS Microbiol Rev*, 33(6), pp.1079–99.

Leakey, A.K., Ulett, G C & Hirst, R.G., 1998. BALB/c and C57Bl/6 mice infected with virulent Burkholderia pseudomallei provide contrasting animal models for the acute and chronic forms of human melioidosis. *Microb Pathog*, 24(5), pp.269–75.

Lee, S.-H. *et al*., 2011. Complete Killing of Caenorhabditis elegans by Burkholderia pseudomallei Is Dependent on Prolonged Direct Association with the Viable Pathogen. *PLoS One*, 6(3).

Lee, Yian Hoon *et al*., 2010. Identification of tomato plant as a novel host model for Burkholderia pseudomallei. *BMC Microbiol*, 10(1), p.28.

Lemaitre, B *et al*., 1996. The dorsoventral regulatory gene cassette spätzle/Toll/cactus controls the potent antifungal response in Drosophila adults. *Cell*, 86(6), pp.973–83.

Lertpatanasuwan, N. *et al*., 1999. Arabinose Positive Burkholderia pseudomallei Infection in Humans: Case Report. *Clin Infect Dis*, 28(4), pp.927–928.

Lever, S.S. *et al*., 2003. Experimental aerogenic Burkholderia mallei (glanders) infection in the BALB/c mouse. *J Med Microbiol*, 52(Pt 12), pp.1109–1115.

Levy, A. *et al*., 2003. Invasion of Spores of the Arbuscular Mycorrhizal Fungus Gigaspora decipiens by Burkholderia spp. *Appl Environ Microbiol*, 69(10), pp.6250–6256.

Lieu, P.T. *et al*., 2001. The roles of iron in health and disease. *Mol Aspects Med*, 22(1-2), pp.1–87.

Lionakis, M.S., 2011. Drosophila and Galleria insect model hosts: new tools for the study of fungal virulence, pharmacology and immunology. *Virulence*, 2(6), pp.521–7.

Lopez, J. *et al*., 2003. Characterization of experimental equine glanders. *Microbes Infect*, 5(12), pp.1125–1131.

Ma, Y. *et al*., 2001. Drug targeting Mycobacterium tuberculosis cell wall synthesis: genetics of dTDP-rhamnose synthetic enzymes and development of a microtiter plate-based screen for inhibitors of conversion of dTDP-glucose to dTDP-rhamnose. *Antimicrob Agents Chemother*, 45(5), pp.1407–16.

Maghnouj, A. *et al*., 1998. The arcABDC gene cluster, encoding the arginine deiminase pathway of Bacillus licheniformis, and its activation by the arginine repressor argR. *J Bacteriol*, 180(24), pp.6468–6475.

Mahajan-Miklos, S., Rahme, L.G. & Ausubel, F.M., 2000. Elucidating the molecular mechanisms of bacterial virulence using non-mammalian hosts. *Mol Microbiol*, 37(5), pp.981–8.

Mahenthiralingam, E., Baldwin, A. & Dowson, C.G., 2008. Burkholderia cepacia complex bacteria: opportunistic pathogens with important natural biology. *J Appl Microbiol*, 104(6), pp.1539–51.

Manzeniuk, I.N. *et al*., 1999. [Burkholderia mallei and Burkholderia pseudomallei. Study of immuno- and pathogenesis of glanders and melioidosis. Heterologous vaccines]. *Antibiot Khimioter*, 44(6), pp.21–6.

Marsh, E.K. & May, R.C., 2012. Caenorhabditis elegans, a model organism for investigating immunity. *Appl Environ Microbiol*, 78(7), pp.2075–81.

McCormick, J.B. *et al*., 1977. Wound Infection by an Indigenous Pseudomonas pseudomallei-Like Organism Isolated from the Soil: Case Report and Epidemiologic Study. *J Infect Dis*, 135(1), pp.103–107.

Miller, W.R. *et al*., 1948. Studies on Certain Biological Characteristics of Malleomyces mallei and Malleomyces pseudomallei: II. Virulence and Infectivity for Animals. *J Bacteriol*, 55(1), pp.127–35.

Molmeret, M. *et al*., 2005. Amoebae as Training Grounds for Intracellular Bacterial Pathogens. *Appl Environ Microbiol*, 71(1), pp.20–28.

Moore, R.A. *et al*., 2004. Contribution of gene loss to the pathogenic evolution of Burkholderia pseudomallei and Burkholderia mallei. *Infect Immun*, 72(7), pp.4172–87.

Moule, M.G., Monack, D.M. & Schneider, D.S., 2010. Reciprocal Analysis of Francisella novicida Infections of a Drosophila melanogaster Model Reveal Host-Pathogen Conflicts Mediated by Reactive Oxygen and imd-Regulated Innate Immune Response. *PLoS Pathog*, 6(8), p.e1001065.

Muangman, S. *et al*., 2011. BopC is a type III secreted effector protein of Burkholderia pseudomallei. *FEMS Microbiol Lett*, 323(1), pp.75–82.

Mukhopadhyay, S. *et al*., 2010. High-redundancy draft sequencing of 15 clinical and environmental Burkholderia strains. *J Bacteriol*, 192(23), pp.6313–4.

Münch, A. *et al*., 2008. Photorhabdus luminescens genes induced upon insect infection. *BMC Genomics*, 9, p.229.

Najdenski, H., Kussovski, V. & Vesselinova, A., 2004. Experimental Burkholderia pseudomallei infection of pigs. *J Vet Med B Infect Dis Vet Public Health*, 51(5), pp.225–30.

Nardi, J.B. *et al*., 2003. Hematopoietic organs of Manduca sexta and hemocyte lineages. *Dev Genes Evol*, 213(10), pp.477–91.

Narita, M. *et al*., 1982. Pathological changes in goats experimentally inoculated with Pseudomonas pseudomallei. *Natl Inst Anim Health Q (Tokyo)*, 22(4), pp.170–179.

Nelson, M. *et al*., 2011. Development of an acute model of inhalational melioidosis in the common marmoset (Callithrix jacchus). *Int J Exp Pathol*, 92(6), pp.428–435.

Nierman, W.C. *et al*., 2004. Structural flexibility in the Burkholderia mallei genome. *Proc Natl Acad Sci U S A*, 101(39), pp.14246–51.

Norville, I.H., 2011. *The identification and characterisation of PPIases from Burkholderia pseudomallei and Burkholderia thailandensis*. University of Exeter.

Nussbaum, J.J., Hull, D.S. & Carter, M.J., 1980. Pseudomonas pseudomallei in an anopthalmic orbit. *Arch Ophthal*, 98(7), pp.1224–5.

O'Loughlin, J.L. *et al*., 2010. Yersinia pestis Two-Component Gene Regulatory Systems Promote Survival in Human Neutrophils. *Infect Immun*, 78(2), pp.773–782.

O'Quinn, A.L., Wiegand, E.M. & Jeddeloh, J.A., 2001. Burkholderia pseudomallei kills the nematode Caenorhabditis elegans using an endotoxin-mediated paralysis. *Cell Microbiol*, 3(6), pp.381–93.

Ooi, S.-K. *et al*., 2012. Burkholderia pseudomallei kills Caenorhabditis elegans through virulence mechanisms distinct from intestinal lumen colonization. *Virulence*, 3(6), pp.485–96.

Pauchet, Y. *et al*., 2010. Pyrosequencing the Manduca sexta larval midgut transcriptome: messages for digestion, detoxification and defence. *Insect Mol Biol*, 19(1), pp.61–75.

Pilátová, M. & Dionne, M.S., 2012. Burkholderia thailandensis Is Virulent in Drosophila melanogaster. *PLoS One*, 7(11), p.e49745.

Pilatz, S. *et al*., 2006. Identification of Burkholderia pseudomallei genes required for the intracellular life cycle and in vivo virulence. *Infect Immun*, 74(6), pp.3576–86.

Price, E.P. *et al*., 2012. Development and validation of Burkholderia pseudomallei-specific real-time PCR assays for clinical, environmental or forensic detection applications. *PLoS One*, 7(5), p.e37723.

Price, E.P. *et al*., 2010. Within-host evolution of Burkholderia pseudomallei in four cases of acute melioidosis. *PLoS Pathog*, 6(1), p.e1000725.

Propst, K.L. *et al*., 2010. A Burkholderia pseudomallei deltapurM mutant is avirulent in immunocompetent and immunodeficient animals: candidate strain for exclusion from select-agent lists. *Infect Immun*, 78(7), pp.3136–3143.

Ramarao, N., Nielsen-Leroux, C. & Lereclus, D., 2012. The Insect Galleria mellonella as a Powerful Infection Model to Investigate Bacterial Pathogenesis. *J Vis Exp*, (70).

Ramel, C. *et al*., 2012. Regulation of biosynthesis of syringolin A, a Pseudomonas syringae virulence factor targeting the host proteasome. *Mol Plant Microbe Interact*, 25(9), pp.1198–208.

Ramli, N.S.K. *et al*., 2012. The effect of environmental conditions on biofilm formation of Burkholderia pseudomallei clinical isolates. *PLoS One*, 7(9), p.e44104.

Reckseidler-Zenteno, S.L. *et al*., 2010. Characterization of the type III capsular polysaccharide produced by Burkholderia pseudomallei. *J Med Microbiol*, 59(12), pp.1403–1414.

Reynolds, S E, Nottingham, S.F. & Stephens, A.E., 1985. Food and water economy and itsrelation to growth in 5th-instar larvae of the Tobacco Hornworm, Manduca-Sexta. *J Insect Physiol*, 31(2), pp.119–127.

Rowbotham, T., 1980. Preliminary report on the pathogenicity of Legionella pneumophila for freshwater and soil amoebae. *J Clin Pathol*, 33(12), pp.1179–1183.

Sadd, B.M. & Schmid-Hempel, P., 2006. Insect immunity shows specificity in protection upon secondary pathogen exposure. *Curr Biol*, 16(12), pp.1206–10.

Saenz, H.L. & Dehio, C., 2005. Signature-tagged mutagenesis: technical advances in a negative selection method for virulence gene identification. *Curr Opin Microbiol*, 8(5), pp.612–9.

Sargent, F., 2007. The twin-arginine transport system: moving folded proteins across membranes. *Biochem Soc Trans*, 35(Pt 5), pp.835–47.

Van Schaik, E. *et al*., 2008. Development of novel animal infection models for the study of acute and chronic Burkholderia pseudomallei pulmonary infections. *Microbes Infect*, 10(12-13), pp.1291–9.

Schell, M.A. *et al*., 2007. Type VI secretion is a major virulence determinant in Burkholderia mallei. *Mol Microbiol*, 64(6), pp.1466–85.

Schell, M.A., Lipscomb, L. & DeShazer, David, 2008. Comparative genomics and an insect model rapidly identify novel virulence genes of Burkholderia mallei. *J Bacteriol*, 190(7), pp.2306–13.

Schwager, S. *et al*., 2012. Identification of Burkholderia cenocepacia H111 virulence factors using non-mammalian infection hosts. *Infect Immun*, 80(11), pp.143–53.

Shalom, G., Shaw, J.G. & Thomas, M.S., 2007. In vivo expression technology identifies a type VI secretion system locus in Burkholderia pseudomallei that is induced upon invasion of macrophages. *Microbiology*, 153(Pt 8), pp.2689–99.

Sim, B.M.Q. *et al*., 2010. Genomic acquisition of a capsular polysaccharide virulence cluster by non-pathogenic Burkholderia isolates. *Genome Biol*, 11(8), p.R89.

Sim, S.H. *et al*., 2008. The core and accessory genomes of Burkholderia pseudomallei: implications for human melioidosis. *PLoS Pathog*, 4(10), p.e1000178.

Simon, R., Priefer, U. & Pühler, A., 1983. A Broad Host Range Mobilization System for In Vivo Genetic Engineering: Transposon Mutagenesis in Gram Negative Bacteria. *Nat Biotech*, 1(9), pp.784–791.

Smith, M.D. *et al*., 1997. Arabinose assimilation defines a nonvirulent biotype of Burkholderia pseudomallei. *Infect Immun*, 65(10), pp.4319–21.

Soffler, C. *et al*., 2012. Development and characterization of a caprine aerosol infection model of melioidosis. *PLoS One*, 7(8), p.e43207.

Song, H. *et al*., 2009. Simple sequence repeat (SSR)-based gene diversity in Burkholderia pseudomallei and Burkholderia mallei. *Mol Cells*, 27(2), pp.237–41.

Srikumar, S. & Fuchs, T.M., 2011. Ethanolamine utilization contributes to proliferation of Salmonella enterica serovar Typhimurium in food and in nematodes. *Appl Environ Microbiol*, 77(1), pp.281–290.

Stephens, J.M., 1962. Bactericidal Activity of the Blood of Actively Immunized Wax Moth Larvae. *Can J Microbiol*, 8(4), pp.491–499.

Stevens, J.M., Galyov, E.E. & Stevens, M.P., 2006. Actin-dependent movement of bacterial pathogens. *Nat Rev Microbiol*, 4(2), pp.91–101.

Stevens, M.P. *et al*., 2003. A Burkholderia pseudomallei type III secreted protein, BopE, facilitates bacterial invasion of epithelial cells and exhibits guanine nucleotide exchange factor activity. *J Bacteriol*, 185(16), pp.4992–6.

Stevens, M.P. *et al*., 2002. An Inv/Mxi-Spa-like type III protein secretion system in Burkholderia pseudomallei modulates intracellular behaviour of the pathogen. *Mol Microbiol*, 46(3), pp.649–59.

Stevens, M.P. *et al*., 2005. Identification of a bacterial factor required for actin-based motility of Burkholderia pseudomallei. *Mol Microbiol*, 56(1), pp.40–53.

Stevenson, L.G. *et al*., 2007. Rhomboid protease AarA mediates quorum-sensing in Providencia stuartii by activating TatA of the twin-arginine translocase. *Proc Natl Acad Sci U S A*, 104(3), pp.1003–8.

Stone, R., 2007. Infectious disease. Racing to defuse a bacterial time bomb. *Science*, 317(5841), pp.1022–4.

Strand, M.R., 2008. The insect cellular immune response. *Insect Sci*, 15(1), pp.1–14.

Suparak, S. *et al*., 2005. Multinucleated giant cell formation and apoptosis in infected host cells is mediated by Burkholderia pseudomallei type III secretion protein BipB. *J Bacteriol*, 187(18), pp.6556–60.

Suputtamongkol, Y *et al*., 1994. The epidemiology of melioidosis in Ubon Ratchatani, northeast Thailand. *Int J Epidemiol*, 23(5), pp.1082–90.

Swanson, M.S. & Hammer, B.K., 2000. Legionella pneumophila pathogesesis: a fateful journey from amoebae to macrophages. *Annu Rev Microbiol*, 54, pp.567–613.

Tayeb, L.A. *et al*., 2008. Comparative phylogenies of Burkholderia, Ralstonia, Comamonas, Brevundimonas and related organisms derived from rpoB, gyrB and rrs gene sequences. *Res Microbiol*, 159(3), pp.169–77.

Titball, Richard W *et al*., 2008. Burkholderia pseudomallei: animal models of infection. *Trans R Soc Trop Med Hyg*, 102 Suppl , pp.S111–6.

Torres-Cruz, J. & Van der Woude, M.W., 2003. Slipped-strand mispairing can function as a phase variation mechanism in Escherichia coli. *J Bacteriol*, 185(23), pp.6990–6994.

Tuanyok, A. *et al*., 2006. Genome-wide expression analysis of Burkholderia pseudomallei infection in a hamster model of acute melioidosis. *Infect Immun*, 74(10), pp.5465–76.

Uehlinger, S. *et al*., 2009. Identification of specific and universal virulence factors in Burkholderia cenocepacia strains by using multiple infection hosts. *Infect Immun*, 77(9), pp.4102–10.

Ulett, Glen C *et al*., 2005. A model of immunity to Burkholderia pseudomallei: unique responses following immunization and acute lethal infection. *Microbes Infect*, 7(11-12), pp.1263–75.

Ulrich, R.L. & DeShazer, David, 2004. Type III secretion: a virulence factor delivery system essential for the pathogenicity of Burkholderia mallei. *Infect Immun*, 72(2), pp.1150–4.

Utaisincharoen, P. *et al*., 2001. Burkholderia pseudomallei interferes with inducible nitric oxide synthase (iNOS) production: a possible mechanism of evading macrophage killing. *Microbiol Immunol*, 45(4), pp.307–13.

Vasil, M.L., Tomaras, A.P. & Pritchard, A.E., 2012. Identification and evaluation of twin-arginine translocase inhibitors. *Antimicrob Agents Chemother*, 56(12), pp.6223–34.

Velapatiño, B. *et al*., 2012. Identification of differentially expressed proteins from Burkholderia pseudomallei isolated during primary and relapsing melioidosis. *Microbes Infect*, 14(4), pp.335–340.

Vial, L. *et al*., 2010. Phase variation has a role in Burkholderia ambifaria niche adaptation. *ISME J*, 4(1), pp.49–60.

Vial, L. *et al*., 2011. The various lifestyles of the Burkholderia cepacia complex species: a tribute to adaptation. *Environ Microbiol*, 13(1), pp.1–12.

Vlisidou, I. *et al*., 2009. Drosophila embryos as model systems for monitoring bacterial infection in real time. *PLoS Pathog*, 5(7), p.e1000518.

Vlisidou, I. *et al*., 2010. The KdpD/KdpE two-component system of Photorhabdus asymbiotica promotes bacterial survival within M. sexta hemocytes. *J Invertebr Pathol*, 105(3), pp.352–362.

Vogel, Heiko *et al*., 2011. A comprehensive transcriptome and immune-gene repertoire of the lepidopteran model host Galleria mellonella. *BMC Genomics*, 12(1), p.308.

Voyich, J.M. *et al*., 2005. Insights into Mechanisms Used by Staphylococcus aureus to Avoid Destruction by Human Neutrophils. *J Immunol*, 175(6), pp.3907–3919.

Wand, M. *et al*., 2011. Macrophage and Galleria mellonella infection models reflect the virulence of naturally occurring isolates of B. pseudomallei, B. thailandensis and B. oklahomensis. *BMC Microbiol*, 11(1).

Warawa, J. & Woods, Donald E., 2005. Type III secretion system cluster 3 is required for maximal virulence of Burkholderia pseudomallei in a hamster infection model. *FEMS Microbiol Lett*, 242(1), pp.101–108.

Waterfield, N *et al*., 2005. Potentiation and cellular phenotypes of the insecticidal Toxin complexes of Photorhabdus bacteria. *Cell Microbiol*, 7(3), pp.373–82.

Waterfield, N R *et al*., 2001. The tc genes of Photorhabdus: a growing family. *Trends Microbiol*, 9(4), pp.185–91.

Waterfield, Nicholas *et al*., 2001. Oral toxicity of Photorhabdus luminescens W14 toxin complexes in Escherichia coli. *Appl Environ Microbiol*, 67(11), pp.5017–24.

Waterfield, Nicholas R *et al*., 2003. The insecticidal toxin makes caterpillars floppy 2 (Mcf2) shows similarity to HrmA, an avirulence protein from a plant pathogen. *FEMS Microbiol Lett*, 229(2), pp.265–270.

Waterfield, Nicholas R. *et al*., 2008. Rapid Virulence Annotation (RVA): identification of virulence factors using a bacterial genome library and multiple invertebrate hosts. *Proc Natl Acad Sci U S A*, 105(41), pp.15967–15972.

Watts, K.M. & Hunstad, D. a, 2008. Components of SurA required for outer membrane biogenesis in uropathogenic Escherichia coli. *PLoS One*, 3(10), p.e3359.

Whitmore, A., 1913. An Account of a Glanders-like Disease occurring in Rangoon. *J Hyg (Lond)*, 13(1), pp.1–34.

Wiersinga, W.J. *et al*., 2006. Melioidosis: insights into the pathogenicity of Burkholderia pseudomallei. *Nat Rev Microbiol*, 4(4), pp.272–82.

Wiersinga, W.J., Currie, B.J. & Peacock, S.J., 2012. Melioidosis. *N Engl J Med*, 367(11), pp.1035–44.

Woods, D E, Jones, A.L. & Hill, P.J., 1993. Interaction of insulin with Pseudomonas pseudomallei. *Infect Immun*, 61(10), pp.4045–50.

Wuthiekanun, V *et al*., 2006. Development of antibodies to Burkholderia pseudomallei during childhood in melioidosis-endemic northeast Thailand. *Am J Trop Med Hyg*, 74(6), pp.1074–5.

Xue, T. *et al*., 2011. The Staphylococcus aureus KdpDE two-component system couples extracellular K+ sensing and Agr signaling to infection programming. *Infect Immun*, 79(6), pp.2154–2167.

Yang, Guowei *et al*., 2012. Pdl1 is a putative lipase that enhances Photorhabdus toxin complex secretion. *PLoS Pathog*, 8(5), p.e1002692.

Yao, Q. *et al*., 2009. A bacterial type III effector family uses the papain-like hydrolytic activity to arrest the host cell cycle. *Proc Natl Acad Sci U S A*, 106(10), pp.3716–3721.

Yao, Q. *et al*., 2012. Structural mechanism of ubiquitin and NEDD8 deamidation catalyzed by bacterial effectors that induce macrophage-specific apoptosis. *Proc Natl Acad Sci U S A*, 109(50), pp.20395–400.

Yap, E.H. *et al*., 1995. Comparison of Pseudomonas pseudomallei from humans, animals, soil and water by restriction endonuclease analysis. *Singapore Med J*, 36(1), pp.60–2.

Yeager, J.J. *et al*., 2012. Natural history of inhalation melioidosis in rhesus macaques (Macaca mulatta) and African green monkeys (Chlorocebus aethiops). *Infect Immun*, 80(9), pp.3332–40.

Yu, Yiting *et al*., 2006. Genomic patterns of pathogen evolution revealed by comparison of Burkholderia pseudomallei, the causative agent of melioidosis, to avirulent Burkholderia thailandensis. *BMC Microbiol*, 6(1), p.46.

Zhang, J., Quigley, N.B. & Gross, D.C., 1997. Analysis of the syrP gene, which regulates syringomycin synthesis by Pseudomonas syringae pv . syringae. *Appl Environ Microbiol*, 63(7), pp.2771–8.

Zhao, L. *et al*., 2010. Staphylococcus aureus AI-2 quorum sensing associates with the KdpDE two-component system to regulate capsular polysaccharide synthesis and virulence. *Infect Immun*, 78(8), pp.3506–3515.

Zou, Z. *et al*., 2008. Pyrosequence analysis of expressed sequence tags for Manduca sexta hemolymph proteins involved in immune responses. *Insect Biochem Mol Biol*, 38(6), pp.677–82.